
The University Of Sheffield.

# Lithium Enhances Osteogenic Responses to Fluid Shear Stress

**Liam A. Boyle**

**A thesis submitted in partial fulfilment of the requirements for the degree of Doctor of Philosophy**

**The University of Sheffield**

**Faculty of Engineering**

**Department of Materials Science and Engineering**

**September 2019**

# Abstract

Bone is a dynamic tissue that is continuously remodelling itself in response to the mechanical loading that it is placed under. The cells within the bone sense the mechanical loads and respond in an appropriate manner. This can be through increasing bone resorption or increasing bone deposition in response to decreased or increased loading respectively.

Cells themselves have a number of mechanisms thought to be involved in sensing mechanical loads and transforming them into biochemical signals in a process known as mechanotransduction. One such mechanism thought to be involved is the primary cilium. The primary cilium is a hair-like organelle that protrudes from the surface of the majority of cells during interphase. It is theorised that the bending of this organelle in response to fluid shear stress (FSS) results in the activation of downstream signalling pathways. Primary cilia have been shown to regulate their mechanosensitivity through altering their length, becoming shorter and less sensitive in response to continuous loads. Lithium chloride has been shown to elongate primary cilia and could therefore have the potential to increase osteogenic responses to FSS. The aim of this thesis was to examine the effect of lithium chloride on mechanoinduced osteogenesis.

An *in vitro* FSS stimulus was optimised to stimulate osteogenic responses in hES-MP and MLO-A5 cells. The effects of LiCl on primary cilia length and osteogenesis was than evaluated at a range of concentrations and durations. Continuous 1 mM LiCl was found to increase osteogenesis in both cell lines. Intermittent treatment with 1 mM LiCl was found to increase cilia length without affecting cilia prevalence or osteogenesis. Cells treated with LiCl were then stimulated, where they showed increased osteogenic responses to FSS in both monolayer culture and 3D culture. LiCl was also found to decrease

cAMP but increase $Ca^{2+}$ responses to FSS. These results demonstrate that LiCl increases mechanically induced osteogenic responses *in vitro*.

# Acknowledgements

I would like to thank my supervisor Dr. Gwendolen Reilly for providing me the opportunity to undertake my PhD. I am especially grateful for the input and encouragement throughout my undergraduate research project that inspired me to pursue this project and for the continual support and freedom you gave me to explore my ideas. Thank you to the University of Sheffield for my studentship and EPSRC for funding this, and providing me a job after.

My PhD would not have been the same without all the great friends that surrounded me throughout. Rob and Hossein, thank you for keeping me sane and making endless media changes more fun with chats about F1, Peaky Blinders or more often than not, just nonsense. Also for your continual support throughout, with great scientific advice and keeping the lab running with ingenuous fixes and infinite supplies of stock solutions and tip boxes. Julie, thank you for making sure the lab didn't fall apart and for always being keen for a cuppa. A big thanks to Luke and Claudi for their great help and advice on doing "good science" and for all the trips to the pub. Carlos, thank you for the great rides in the Peaks and introducing me to Jupyter Notebook and Holoviews, it was invaluable when making all my graphs. I'd also like to thank all the current and past people in the lab and office for all their help.

A special thanks to my Mum Sarah, for everything you have done for me. You have always supported and encouraged me to be adventurous and inquisitive which inspired my interest in science and led to where I am today. I'd also like to thank my brothers Jamie and Marcus, for all your support and for always being there for me. Finally, I would like to thank Mehri, you have been the best partner and friend I could imagine. Our coffee breaks and lunches together kept me going through the day and your encouragement and support, whether through your great broccoli salad or your proof reading and cutting down of my long sentences and yes, this is one of them, kept me going through the long nights. I wouldn't have got this finished without you.

# Outputs

## Publications

Alberto Sensini, Chiara Gualandi, Maria Letizia Focarete, Juri Belcari, Andrea Zucchelli, **Liam A Boyle**, Gwendolen C Reilly, Alexander P Kao, Gianluca Tozzi, Luca Cristofolini. "Multiscale hierarchical bioresorbable scaffolds for the regeneration of tendons and ligaments." *Biofabrication*, vol. 11, no. 3, 2019.

Alberto Sensini, Chiara Gualandi, Andrea Zucchelli, **Liam A Boyle**, Alexander P Kao, Gwendolen C Reilly, Gianluca Tozzi, Luca Cristofolini, Maria Letizia Focarete. "Tendon fascicle-inspired nanofibrous scaffold of polylactic acid/collagen with enhanced 3D-structure and biomechanical properties." *Scientific reports*, vol. 8, no. 1, 2018.

## Oral presentations

*European Society of Biomechanics*: "The Effects Of Unidirectional And Oscillating Fluid Flow On Osteogenic Progenitors Cells On Porous Scaffolds", July 2016, Lyon, France.

*Advances in Cell and Tissue Culture*: "Primary cilia elongation and its effects on mechanosensitivity", July 2017, Manchester, UK.

*Biomaterials and Tissue Engineering*: "Primary cilia elongation and enhanced mechanosensitivity with lithium chloride treatment", December 2017, Leeds, UK.

*8$^{th}$ World Congress of Biomechanics*: "Manipulation of primary cilia mechanotransduction", July 2018, Dublin, Ireland.

*Nanomaterials for Biosensors and Biomedical Applications*: "Primary cilia elongation enhances mechanosensitivity in 3D constructs", July 2019, Riga, Latvia.

*European Society of Biomechanics*: "Primary cilia elongation enhances mechanosensitivity", July 2019. Vienna, Austria.

## Poster presentations

*Engineering Research Symposium*: "The effect of primary cilia elongation on mechanosensitivity", June 2017, Sheffield, UK.

*Tissue and Cell Engineering Society*: "Primary cilia mediated mechanotransduction in differentiating osteoblasts", July 2018, Keele, UK.

*Biomaterials and Tissue Engineering*: "Manipulation of primary cilia mechanotransduction in a 3D construct", December 2018, Sheffield, UK.

## Awards

Two travel grants awarded from University of Sheffield Learned Society Fund (£450 in 2016 and £450 in 2019)

European Society of Biomechanics Travel Award 2019 (€400).

# List of Figures

# Contents

# Abbreviations

| | |
|---|---|
| **11$\beta$-HSD** | 11$\beta$-hydroxysteroid dehydrogenase |
| **2D** | two-dimensional |
| **3D** | three-dimensional |
| **AA-2P** | ascorbic acid 2-phosphate |
| **AC** | adenylyl cyclase |
| **Akt** | protein kinase B |
| **ALP** | alkaline phosphatase |
| **ANOVA** | analysis of variance |
| **APC** | adenomatous polyposis coli |
| **ARS** | alizarin red S |
| **ATP** | adenosine triphosphate |
| **BGP** | $\beta$-glycerophosphate |
| **BM** | basal media |
| **BMD** | bone mineral density |
| **BMP** | bone morphogenetic protein 2 |
| **BMU** | basic multicellular unit |
| **BRONJ** | bisphosphonate-related osteonecrosis of the jaw |
| **BSP** | bone sialoprotein |
| **CAB** | cell assay buffer |
| **cAMP** | 3',5'-cyclic adenosine monophosphate |
| **CDB** | cell digestion buffer |
| **CK1A** | casein kinase 1A |
| **$CO_2$** | carbon dioxide |
| **COL-1$\alpha$1** | collagen type 1 $\alpha$ 1 |
| **COX-1** | cyclooxygenase-1 |
| **COX-2** | cyclooxygenase-2 |
| **CRE** | cAMP response element |
| **CREB** | cAMP response element-binding protein |

| | |
|---|---|
| **DAAM** | disheveled-associated activator of morphogenesis |
| **DAPI** | 4', 6-diamidino-2- phenylindole dihydrochloride |
| **Dex** | dexamethasone |
| **di$H_2O$** | deionized water |
| **DMSO** | dimethyl sulfoxide |
| **DNA** | deoxyribonucleic acid |
| **DR80** | direct red 80 |
| **dsDNA** | double-stranded deoxyribonucleic acid |
| **Dsh** | dishevelled |
| **DW** | dexamethasone withdrawn media |
| **ECM** | extracellular matrix |
| **EDTA** | ethylenediaminetetraacetic acid |
| **ELISA** | enzyme-linked immunosorbent assay |
| **EM** | expansion media |
| **FBS** | fetal bovine serum |
| **Fluo-4** | Fluo-4 acetoxymethyl ester |
| **FSS** | fluid shear stress |
| **Fzd** | Fused |
| **GSK3-$\beta$** | glycogen synthase kinase 3 $\beta$ |
| **H&L** | heavy and light chain |
| **HBSS** | hanks balanced salt solution |
| **HEPES** | 4-(2-hydroxyethyl)-1-piperazineethanesulfonic acid |
| **hES-MP** | human embryonic stem-cell derived mesenchymal progenitors 002.5 |
| **hFGF** | human basic fibroblastic growth factor |
| **HIPE** | high internal phase emulsion |
| **HRP** | horseradish peroxidase |
| **HRT** | hormone replacement therapy |
| **IFT** | intraflagellar transport |
| **IGF** | insulin-like growth factor |
| **IgG** | immunogloblin G |
| **IL-1** | interleukin-1 |
| **IMPase** | inositol monophosphatase |
| **$IP_3$** | inositol 1,4,5-trisphosphate |
| **IPP** | inositol polyphosphate 1-phosphatase |
| **IQR** | interquartile range |
| **JNK** | c-Jun N-terminal kinase |
| **LiCl** | lithium chloride |
| **LRP** | low-density lipoprotein receptor-related protein |

| | |
|---|---|
| **MC3T3-E1** | mouse calvaria 3T3 clone-E1 |
| **M-CSF** | macrophage colony stimulating factor |
| **MDL** | MDL-12330A hydrochloride |
| **miRNA** | micro ribonucleic acid |
| **MLO-A5** | murine long bone osteocyte A5 |
| **MLO-Y4** | murine long bone osteocyte Y4 |
| **mRNA** | messenger ribonucleic acid |
| **MSC** | mesenchymal stem cells |
| **NO** | nitric oxide |
| **OCN** | osteocain |
| **OIM** | osteogenesis induction media |
| **OPG** | osteoprotegrin |
| **OPN** | osteopontin |
| **PBS** | dulbeco's phosphate buffered saline |
| **PBST** | dulbeco's phosphate buffered saline with 0.1 vol/vol% TWEEN® 20 |
| **PC** | polycystin |
| **PCL** | polycaprolactone |
| **PDMS** | polydimethylsiloxane |
| **PEG** | polyethylene glycol |
| **PGA** | polyglycolide |
| **$PGE_2$** | prostaglandin $E_2$ |
| **PI3K** | phosphoinositide 3-kinase |
| **$PIP_2$** | Phosphatidylinositol 4,5-bisphosphate |
| **PK** | protein kinase |
| **PKA** | protein kinase A |
| **PLA** | polylactic acid |
| **pNP** | para-nitrophenol |
| **pNPP** | para-nitrophenol phosphate |
| **PP2a** | protein phosphatase 2A |
| **PTH** | parathyroid hormone |
| **PU** | polyurethane |
| **RANK** | receptor activator of nuclear factor kappa-B |
| **RANKL** | receptor activator of nuclear factor kappa-B ligand |
| **ROCK** | Rho-associated protein kinase |
| **RPM** | revolutions per minute |
| **RR** | resazurin reduction |
| **RUNX2** | runt-related transcription factor 2 |
| **SD** | standard deviation |

| | |
|---|---|
| **SERMs** | selective oestrogen receptor modulators |
| **siRNA** | small interfering ribonucleic acid |
| **SM** | supplemented media |
| **SuFu** | suppressor of fused |
| **TGF** | transforming growth factor |
| **TMB** | 3,3',5,5'-tetramethylbenzidine |
| **TNF-α** | tumor necrosis factor α |
| **TRP** | transient receptor potential |
| **Wnt** | wingless/integrated |
| **α-MEM** | α-minimum essential medium |

# 1. Introduction

Bone is a dynamic tissue widely known to be responsive to mechanical stimulation. The ability of one's bones to sense and adapt to these stimuli through bone remodelling is important, not only in maintaining the health and strength of bones themselves, but also for one's overall wellbeing. This relationships between mechanical stimuli, bone formation and resorption are finely tuned to give bones the required strength to prevent mechanical failure whilst keeping the use of material, and therefore bone mass, to a minimum. Understanding the mechanisms behind how bone responds to mechanical stimulation could aid in the understanding and treatment of bone diseases such as osteoporosis or even aid in the healing of bone fractures. Furthermore, a better understanding of the mechanobiology of bone could aid in the design and implementation of bone tissue engineered constructs with superior ossteointegration. The study of mechanobiology and mechanotransduction is therefore of high interest in a number of research fields.

# 2. Background

## 2.1 Bone structure and physiology

### 2.1.1 Bone function and anatomy

Bone is a highly organised, dynamic tissue that performs several roles within the body: Bones protect vital organs, provide support, facilitate movement through acting as levers and providing anchorage for muscles, act as a mineral reservoir for minerals such as calcium and phosphorus and produce blood cells and store energy in the form of lipid filled yellow marrow [1, 2]. In adults, bone tissue is comprised of two types of osseous tissue, cortical bone and cancellous bone (also known as compact bone and trabecular or spongy bone, respectively). Cortical bone comprises around 80% of an adult skeleton whereas cancellous bone comprises only 20% [3]. Cortical bone is much denser than cancellous bone, with a typically porosity lower than 5% compared to 50-90% for cancellous bone, making its compressive strength around twenty times higher [4]. The porous structure of cancellous bone is formed of interconnected trabecular plates and rods which are filled with bone marrow and blood vessels [5].

### 2.1.2 Bone macrostructure

Bones can vary greatly in shape and size and can be classified by their shape into five categories; flat, short, long, sesamoid and irregular. From these five categories flat and long bones can be thought of as the two main categories. Flat bones such as those found in the skull, scapula and sternum are composed of a layer of cancellous bone sandwiched between an exterior of cortical bone. Long bones such as those found in the femur, tibia and humerus consist of

three regions, the epiphysis, diaphysis and metaphysis. The epiphysis forms the ends of the bones and is predominantly a core of cancellous bone with a shell of cortical bone. The diaphysis is the shaft of the bone; it is formed from a hollow tube of cortical bone with the cavity (known as the medullary cavity) filled with bone marrow. The metaphysis is the region of bone that grows during childhood and is otherwise known as the epiphyseal plate. It sits between the epiphysis and diaphysis of the bone at both the proximal and distal ends.

Bones also have an exterior sheath of fibrous connective tissue called the periosteum. The periosteum is formed of two layers; the outer layer is formed of dense, irregular collagenous tissue and the inner layer is formed of a single layer of bone cells. The periosteum covers the whole surface of the bone except at joints where the bones are covered by articular cartilage. The interior surface of bone is also lined by a membranous sheath termed the endosteum [6, 7].

### 2.1.3 Bone micro and nano structure

Bone is a composite material composed of one third organic and two thirds inorganic matter that forms a mineralised matrix containing cells. The organic matter provides the tensile strength for the bone and allows some degree of flexibility. The inorganic matter gives bones their compressive strength. The cells within the bone deposit and resorb the matrix to maintain its health and strength. The inorganic matter of bone is comprised of around 85% hydroxyapatite, 10% carbonated apatite, which can contain ion substitutes of potassium, fluoride and sodium. The organic matter of bone is comprised of various large proteins such a type I collagen; which accounts for around 90% of the total protein within bone [8]. In addition to type I collagen, trace amounts of type III and type V collagen are also present [9]. Other non-collagenous proteins, such as proteoglycans, glycosaminoglycans and glycoproteins are also present in bone and make up around 10% of the total bone. These proteins typically have a high affinity to calcium ions; which is due to their glutamic and aspartic acid residues [10].

Osteopontin, osteonectin, osteocalcin and alkaline phosphatase (ALP) are some examples of the non-collagenous proteins that are present in bone. Osteopontin is a sialoprotein that is involved in bone remodelling and the attachment

of cells to the bone matrix and has been shown to be an early indicator of osteoblast differentiation [11, 12]. Osteonectin is a glycoprotein involved in mineralisation and it has a high binding affinity to calcium, collagen and hydroxyapatite. Osteocalcin is a matrix gla protein specifically produced by osteoblasts that also has a high binding affinity to calcium [12, 13]. It is thought that osteocalcin plays a role in bone remodelling and control of mineralisation through its inhibition [12, 13].

There are multiple types of the ALP enzyme present throughout the body. Within bone tissue non-specific ALP is secreted by osteoblasts and it promotes the formation of hydroxyapatite crystals within the bone matrix [14]. ALP activity is also known to increase as cells develop along the osteogenic lineage and is a specific marker for differentiated bone-forming osteoblasts [15]. It is therefore commonly used *in vitro* as an early marker of osteogenic differentiation of stem cells [16]. Despite this the exact mechanisms of its involvement in bone formation is unknown.

The structural components of bone like many other tissues are arranged in a hierarchical structure from the nano to the macro scale (Figure 2.1). The nanostructure consists of the collagen molecules that form mineralised fibrils and in turn fibers. The microstructure consists of trabeculae and concentric layers of bone called lamellae which in turn form osteons. The macroscale consists of the cortical and cancellous bone [17].

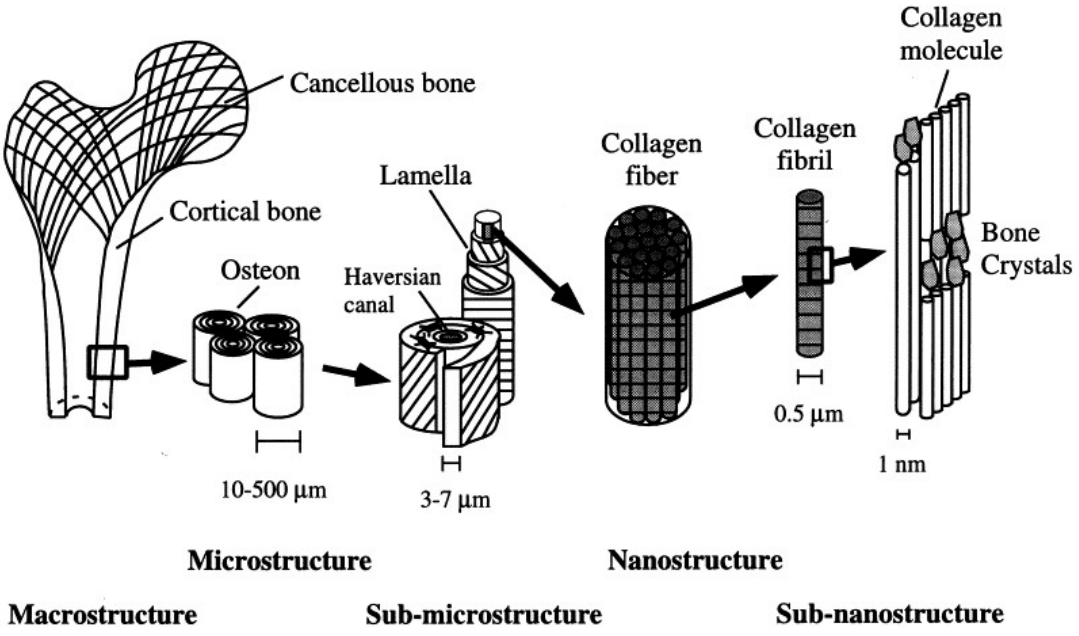


**Figure 2.1:** Hierarchical structure of bone. Figure taken from [15].

### 2.1.4 Cell biology of bone

Within bones there are four different types of cells each with a specific function: osteoblasts, osteocytes, osteoclasts and osteogenic progenitor cells [5]. Osteogenic progenitor cells are a progenitor cell that arise from mesenchymal stem cells present in the bone marrow. They are able to differentiate into osteoblasts and therefore give rise to bone formation [18]. However, they can ultimately also terminally differentiate into osteocytes or some may undergo apoptosis or become bone lining osteoblasts [19]. Osteogenic progenitor cells are therefore able to form all bone cells except osteoclasts which are derived from haematopoietic stem cells.

Osteoclasts are multinucleated cells that resorb bone matrix through excretion of acids and enzymes. They are formed from monocyte progenitors derived from haematopoietic stem cells that fuse together to become a multinucleated osteoclast [20]. Osteoclasts have a short lifespan of around 15-20 days before they undergo apoptosis, which means they must be constantly replaced from haematopoietic stem cells [21].

Osteogenic differentiation of osteogenic progenitors can occur by two distinct pathways, either directly via intermembranous ossification or indirectly via endochondral ossification [22]. In direct differentiation, osteogenic progenitors will directly differentiate into osteoblasts during intermembranous ossification. In indirect differentiation, osteogenic progenitors will first differentiate into chondrocytes where they will initially proliferate before becoming hypertrophic. When these cells become hypertrophic, osteogenic differentiation is triggered and the cells differentiate into osteoblasts [5, 19].

Osteoblasts are responsible for the deposition of new bone and when completely encased in deposited bone matrix become osteocytes [2]. Inactive osteoblasts line the surface of bone and are known as bone lining cells. These cells form part of an intracellular communication network (along with active osteoblasts and osteocytes), which is hypothesised to be one mechanism responsible for directing and sensing the need for new bone formation [23]. When osteoblasts become osteocytes, they undergo many phenotypic changes: They become smaller and more stellate in shape as more bone is deposited around them until they are encased in newly deposited bone, where the remaining space in which they reside becoming known as a lacuna. Osteocytes have a high number of cytoplasmic processes and they form gap junctions with the

processes of other osteocytes, osteoblasts or bone lining cells. These processes also become embedded in newly deposited bone and the resulting channels in which they lie become known as canaliculi. This interconnectivity is thought to play a role in the way bone senses and responds to mechanical stimuli [23]. Current theories hypothesise that the interstitial fluid that surrounds the osteocytes flows from regions of high to low pressure under bone deformation. This applies a shear stress to the cells, which in turn stimulates osteocytes to produce signalling molecules that regulate bone formation and resorption. These fluid shear forces can also occur within the bone marrow itself and can act upon both bone lining osteoblasts but also the osteogenic progenitors within the bone marrow [24, 25].

## 2.2 Bone remodelling

Bone continually remodels itself throughout one's lifetime and it is an essential physiological process in the maintenance of bone strength and mineral homoeostasis [26]. Remodelling occurs through the resorption of fractured or micro-damaged old bone and immature woven bone followed by deposition of new bone often creating changes in the bone architecture in response to applied loading forces. In a typical healthy individual approximately 5% of cortical bone and 20% of trabecular bone is remodelled in this process each year [27]. Throughout childhood bone deposition outweighs bone resorption resulting in increased bone density. This balance continues until approximately 30 years of age where peak bone density is reached [28, 29]. After this point bone deposition and resorption are balanced maintaining this peak bone mass for approximately 20 years until bone density begins to decrease through increases in bone resorption [27].

Old bone is resorbed by osteoclasts and new bone matrix is deposited by osteoblasts. These cells perform this remodelling process together by assembling into what is known as a basic multicellular unit (BMU). A BMU is composed of a group of osteoclasts ahead of a group of osteoblasts contained within supporting connective tissue and accompanied by a blood supply. The osteoclasts at the front of the BMU resorb bone, this is followed by deposition of new bone matrix by the trailing osteoblasts. The BMU can advance at up to $40\,\mu m\,d^{-1}$ in cortical bone and up to $11\,\mu m\,d^{-1}$ in trabecular bone [30, 31]. These differences are due to the way bone is resorbed, in cortical bone the

BMU forms and fills tunnels whereas in trabecular bone trenches are created and filled on the surface of the bone (Figure 2.2) [5, 32]. Bone remodelling

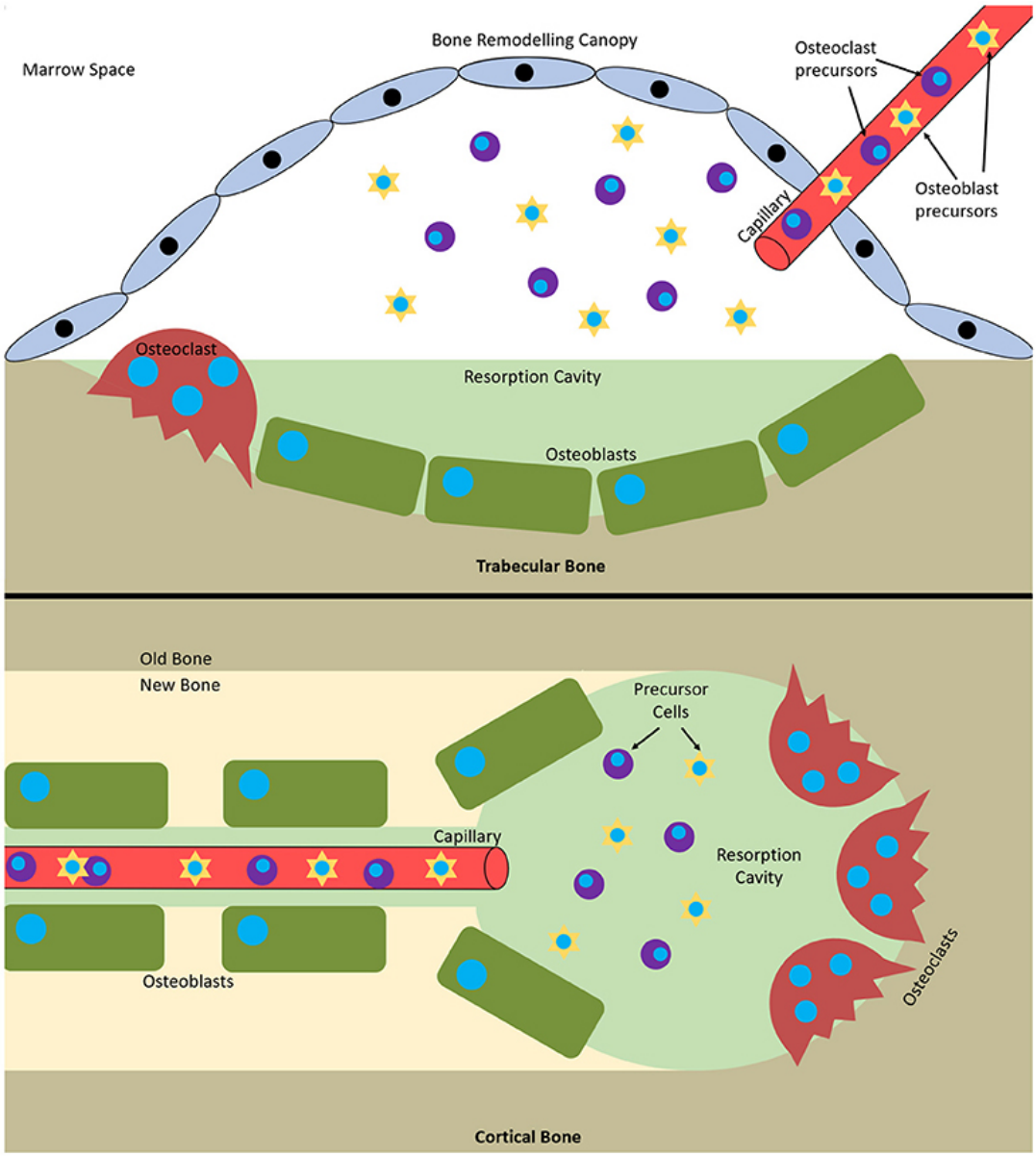


**Figure 2.2:** Basic multicellular units in trabecular (top) and cortical (bottom) bone. In trabecular bone BMUs initiate underneath a canopy of bone lining osteoblasts. In cortical bone BMUs initiate within the Haversian canals. Figure taken from [33].

follows a tightly controlled sequence of phases; quiescence, activation, resorption, reversal and formation. Quiescence is the inactive state of bone where no remodelling is occurring. Activation begins with the detachment of bone lining osteoblasts from the bone surface and the recruitment of mononuclear osteoclast precursors which are supplied by the local blood supply in the area of remodelling. These mononuclear cells attach to the bone surface where they mature and fuse to form multi-nucleated osteoclasts. The maturation of these

mononuclear cells is controlled by the release of macrophage colony stimulating factor (M-CSF) and receptor activator of nuclear factor kappa-B ligand (RANKL) by osteocytes and osteoblasts which initiate osteoclastogenesis. This formation can also be inhibited by osteoprotegrin (OPG) which can antagonise the binding of RANKL to receptor activator of nuclear factor kappa-B (RANK).

Once osteoclasts are formed resorption of the bone matrix occurs and can continue for 2 to 4 weeks. Osteoclasts themselves are short lived, with an average lifespan of around 10 days. Therefore, a supply of new mononuclear precursors from the bone marrow are required in order for new osteoclasts to form and resorption to continue after the apoptosis of old osteoclasts. After the bone is resorbed the reversal phase occurs. This phase is not well understood but involves the colonisation of the resorbed bone surface by a population of mononucleated reversal cells which prepare the degraded bone surface for new bone deposition. During both bone resorption and the reversal phase many cytokines are released from the degraded bone matrix including, bone morphogenetic protein 2 (BMP)s, insulin-like growth factor (IGF)s, human basic fibroblastic growth factor (hFGF)s and transforming growth factor (TGF)-$\beta$. The release of these cytokines promotes the migration of osteogenic progenitor cells and undifferentiated osteoblasts to the BMU and also stimulates their proliferation, differentiation and the beginning of new bone matrix deposition [26, 34–38].

After the bone is prepared by the reversal phase osteoblasts begin to replace the resorbed bone during this process osteoblast morphology changes and they become flatter. A cementing substance is initially secreted by the osteoblasts after which collagenous matrix is deposited. This collagenous matrix is then mineralised by the osteoblasts through the secretion of membrane-bound vesicles which increase the concentration of calcium and phosphorous ions at the mineralisation front. As deposition progresses some osteoblasts become embedded in the new matrix, differentiating into new osteocytes, some osteoblasts will apoptose and others will remain on the bone surface and become new bone lining osteoblasts. The lifespan of osteoblasts is therefore much more varied and can be anything from a few days to 100 days (Figure 2.3) [27, 39].

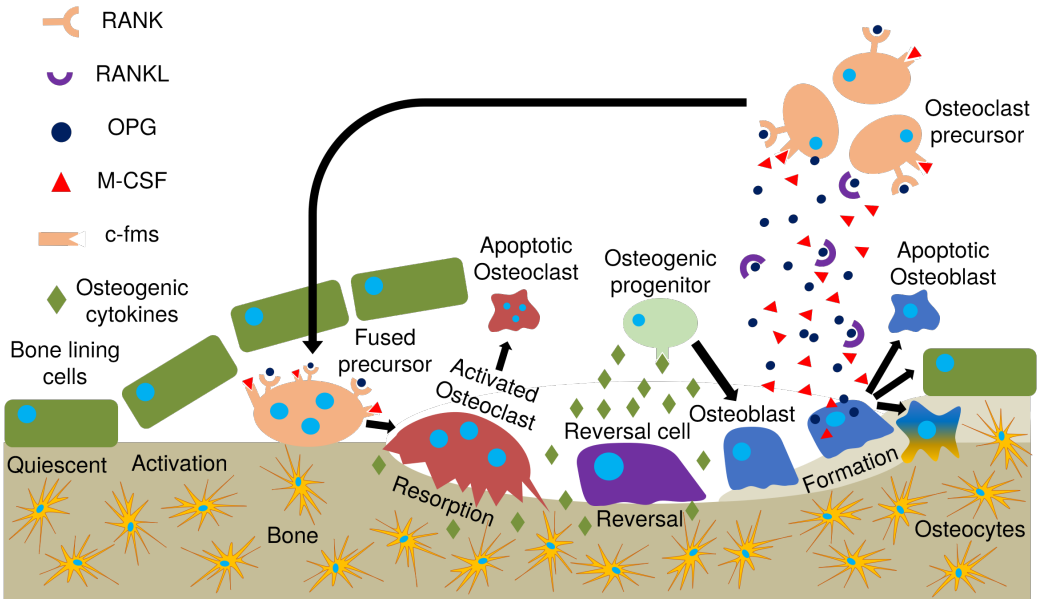


**Figure 2.3:** Illustration of the five stages of bone remodelling, quiescence, activation, resorption, reversal and formation. Formation and activation of osteoclasts are controlled through the RANK/RANKL/OPG pathway. Resorption and the reversal phase release osteogenic cytokines from the bone including BMPs, IGFs, hFGFs and TGF-$\beta$ which are involved in controlling proliferation and differentiation of osteogenic progenitor cells.

## 2.3 Osteoporosis

Osteoporosis is a bone disorder characterised by reduced bone mineral density (BMD), impaired microarchitecture and decreased bone mass and strength resulting in an increase in bone fragility and an increased propensity of fragility fractures (Figure 2.4) [40]. An estimated 22 million women and 5.5 million men have osteoporosis in Europe with around 3.5 million people affected within the UK alone [41]. An individual is classified as having osteoporosis when their BMD lies more than 2.5 standard deviations below the mean for a typical young adult i.e. a T score less than -2.5, typically assessed by dual x-ray absorptiometry of the femoral neck. Osteoporosis can be further classified into primary or secondary, with primary further divided into type I and type II [40]. Primary type I, or postmenopausal osteoporosis is the most common form of osteoporosis and is linked to the decline in oestrogen production in postmenopausal women. Primary type II, or senile osteoporosis affects both men and women and is associated with ageing. Secondary osteoporosis can be caused by several comorbid diseases but can also be caused due to the adverse effects of medications. Most commonly this can include diseases such as Cushing's syndrome, rheumatoid arthritis and hypogonadism and adverse effects from glucocorticoids [42–44].

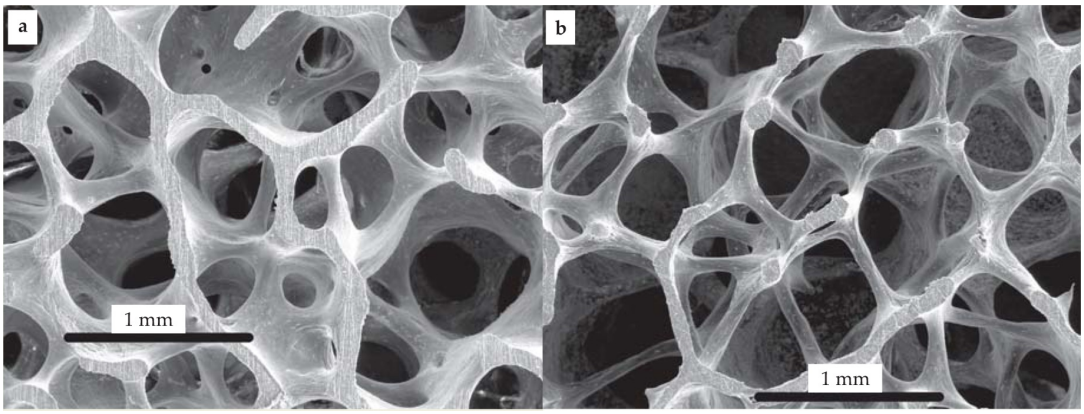


**Figure 2.4:** Trabecular bone of (A) a 21-year old male and (B) a 65-year old post menopausal female. Image adapted and reprinted with the kind permission of Dr. James Weaver and printed in [45].

Osteoporosis manifests itself through fractures, however defining a fracture as on osteoporotic fracture is not straightforward. For example, although the incidence of fractures increases with age these may not be due to osteoporosis since the incidence of falls also rises with age. Therefore, an important aspect of classifying an osteoporotic fracture is to consider whether a similar trauma would have caused a fracture in a healthy individual or whether the fracture site is associated with low BMD. It is estimated that 20% of men and 50% of women will have an osteoporotic fracture after the age of 50. These fractures can result in temporary or permanent loss of mobility, greatly reduce the quality of life and in hip and spinal fractures up to 20% of cases result in fatality within a year [46]. In addition, these fractures and the subsequent health and social care costs create a significant economic burden. In the UK alone the health and social care costs of treating osteoporotic fractures exceeds £4.5 billion per year and this is forecast to increase by 30.2% by 2030 [47].

As a baseline treatment for osteoporosis patients are recommended to make lifestyle changes, such as reduction of alcohol consumption, cessation of smoking and increased physical exercise. In addition, vitamin D and calcium supplements may be given if nutritional intake is inadequate. Therapies for osteoporosis typically employ bone anabolic drugs that stimulate bone deposition or anti-resorptive drugs which aim to slow the resorption of bone. Bisphosphonates are an anti-resorptive drug that promote osteoclast apoptosis and are typically the first-line therapy employed. Despite their low cost and long-time success in reducing bone resorption, they can cause gastrointestinal side effects when taken orally and influenza like side effects when administered

intravenously. Osteoporosis is asymptomatic until fractures present and this can mask the importance of medicating especially when it can result in such side effects. This may account for patient non-compliance or discontinuation of treatment which occurs in around 30% of patients [48]. Furthermore, recent research has recognised bisphosphonate-related osteonecrosis of the jaw (BRONJ) as a potential complication to bisphosphonate treatment [49]. Although this risk is higher in patients treated with bisphosphonates for cancer, it has been estimated 7.8% of patients treated for osteoporosis may be affected [50]. Long-term use of bisphosphonates has also been associated with atypical femur fractures due to suppression of bone remodelling [51].

Hormonal therapies for osteoporosis include hormone replacement therapy (HRT), selective oestrogen receptor modulators (SERMs) and parathyroid hormone (PTH). HRT involves the administration of oestrogen alone or in combination with progesterone and in addition to reducing the risk of fracture, HRT also reduces the symptoms of menopause. Despite this, HRT is typically reserved for high-risk postmenopausal women after other treatment therapies have been ruled out. This is due to the increased risk of stroke, breast cancer, venous thromboembolism and heart disease associated with the use of this treatment [52].

SERMs exhibit both antagonistic and agonistic properties on oestrogenic pathways, decreasing bone resorption and bone turnover rates [53]. Similarly to HRT, SERMs increase the risk of stroke, cardiovascular disease and venous thromboembolism [54]. Additionally, there is currently limited clinical data on the effectiveness of SERMs in reducing fracture risk compared to other treatment options, therefore SERMs are typically a second-line treatment option.

PTH treatment is one of the few osteoporosis treatments that are anabolic. Recombinant PTH is administered via daily injections and stimulates new bone formation on the bone surface increasing BMD and reducing fracture risk [55]. Additionally, bone quality is also improved with cortical thickening and increased trabecular bone connectivity [56]. Due to the high costs and the need for daily injections, PTH treatment is typically reserved for high-risk patients and is contraindicated for patients with Paget's disease, primary or metastatic bone malignancy, hyperparathyroidism and hypercalcaemic disorders [57]. In comparison to other treatment options PTH shows less severe side effects, most commonly dizziness, headaches, fatigue nausea and cramps. However,

currently treatment is limited to a maximum of two years due to long term concerns with the development of osteosarcoma which has been shown to occur in rats [58].

Bisphosphonates still remain the first-line treatment for osteoporosis. Despite other treatments showing promise in reducing fracture risk many of the alternative treatment options are expensive, increase the risk of developing other diseases or can only be used for a limited duration. However, there is increasing concern with the safety of bisphosphonate treatment due to newly associated risks with BRONJ and atypical femur fractures. Alternative therapies would therefore be beneficial.

## 2.4 Mechanical forces in bone

Mechanical forces in bone can be generated by our weight due to gravity, impacts from movement and also from muscle contractions. These forces result in deformation of bone which can in turn generate matrix strain and fluid shear stress.

### 2.4.1 Strain

When bone deforms due to loading it induces strain within the bone matrix but also in the cells within the bone. Physiological strains that induce bone remodelling and deposition were first postulated to range between 0.03% and 0.15% by Frost et al. in 1987 [59]. When strains fall below this range bone resorption occurs and above this range bone damage and even fracture can occur. More recently these numbers have been confirmed experimentally *in vivo* [60, 61]. Although these numbers appear to be correct *in vivo*, *in vitro* cells require much greater strains in the range of 1% and 10% in order to induce osteogenic responses [62, 63]. These strains are of such a high magnitude that if these strains were to be applied *in vivo* it would result in bone fracture. This suggests that bone cells *in vitro* may not be directly sensing these matrix strains but instead may be detecting other forces within the bone such as interstitial fluid flow or may be detecting microstructural strains within the bone such as strains near lacunae, which are thought to be greater [64].

### 2.4.2 Fluid shear

The flow of fluid through the extracellular matrix of tissues such as bone is known as interstitial fluid flow. Interstitial fluid flow forms an integral part in microcirculation and is important for the transportation of proteins and other molecules through the inerstitium [65]. In addition to this role, it also provides mechanical cues, in the form of fluid shear stress, to cells within the interstitial environment. Within bone interstitial fluid occupies the space surrounding blood vessels within the Volkmann and Haversian canals and also within the lacuna-canalicular network. The flow of interstitial fluid can be driven by a number of factors, including hydrostatic and osmotic pressure differences between blood vessels, interstitium and the lymphatic system, but also by blood pressure changes due to movement and the mechanical loading that movement itself applies [24, 65].

Within bone one of the major drivers of interstitial fluid flow is the hydrostatic pressure drop between the bone marrow and the periosteum [24, 66]. This pressure drop causes fluid to flow outward radially from the bone marrow and since bone does not contain a lymphatic system within the bone marrow the fluid flows through interconnected channels of the bone to the lymphatic system at the periosteal surface. Interstitial fluid flow can also be induced through muscle contractions during exercise [67–69]. When muscles contract the pressure within the bone marrow can be temporarily increased due to occlusion of the veins that exit the marrow. After the muscle relaxes and blood can again exit the marrow, it can cause a decrease in marrow pressure a draw new interstitial fluid into the marrow, creating a pulsatile pressure wave. In addition to muscle contractions during exercise inducing interstitial fluid flow, the resultant mechanical loading and deformation of the bone can also induce flow. Deformation of the bone creates pressure gradients across the bone causing fluid to flow through the lacuna-canalicular network. Flow rates of the same magnitude to that caused by hydrostatic pressure drops between the bone marrow and periosteum can be induced by as little as 75 microstrain [70]. Considering strains due to mechanical loading are typically in the millistrain magnitude, the fluid flow induced by mechanical loading is much more substantial and therefore likely to be a more potent mechanical stimulus [71].

All cells within bone are likely to be subjected to some level of interstitial fluid flow and therefore fluid shear stress. Osteocytes are likely to be subjected to

the highest magnitude of fluid shear stress due to the small spaces and narrow channels of the lacunae and canaliculi in which they reside. Weinbaum et al., estimated the fluid shear stress that is applied to osteocytic processes in the canaliculi during loading to be in the order of 0.8-3 Pa [72]. Osteoblasts and osteogenic progenitor cells are likely to be subjected to lower magnitudes of fluid shear stress due to the more open porosity environments in which they reside. Estimation of the fluid shear stress which osteoblasts and osteogenic progenitors are subjected to are more complicated due to the fact the geometries in which they reside are continually remodelling and the mechanical properties of newly deposited osteoid is not definitively known. Despite this, many authors appear to be in agreement that the fluid shear stress levels osteoblasts and osteogenic progenitors are subjected to are lower and different to that subjected to osteocytes [73, 74].

## 2.5 Bone mechanobiology

Mechanical loading is essential for bone health and plays an active role in directing bone deposition and resorption. This is evident when loading of bone is removed, for example through extended periods of bed rest or limb paralysis, but also when loading levels are increased, for example in the playing arm of a tennis player where bone density is greater than in the non-playing arm [75–77]. In order for bone to remodel in response to mechanical loading, there must be a shift in the current resorption and deposition levels. Since new bone is deposited predominantly along the loading stress lines, this suggest there must be some local sensing and regulation, due to mechanical stimuli, that regulates bone formation and resorption [78]. The mechanism by which cells detect and convert mechanical forces into biochemical signals is called mechanotransduction [79].

As previously discussed, the intracellular communication network formed by osteogenic progenitors, osteoblasts and osteocytes is thought to play a role in the control of bone homeostasis and adaptation. However, it is unclear what role each cell type plays in this network. Experimental evidence has shown that all three cell types can be sensitive to mechanical stimuli and that each cell type can respond differently to different mechanical stimuli [80–82]. For example, 15 minutes of pulsating fluid flow has been shown to increase prostaglandin G/H synthase-2 messenger ribonucleic acid (mRNA) expression

in osteocytes but not in osteoblasts, whereas 6 hours of intermittent hydrostatic compression has been shown to stimulate prostaglandin $E_2$ ($PGE_2$) production in both osteoblasts and osteocytes [80, 81]. In addition to their ability to sense mechanical stimuli, the distribution and abundance of osteocytes within the bone matrix (around 90% of all bone cells), places them in an ideal location to sense any local mechanical loading throughout the bone. This has resulted in the consensus that osteocytes are the primary mechanosensor within bone. Despite this, primary osteocytes are not widely studied due to difficulties extracting them from within the lacunae of bone and culturing them for long periods. Therefore, osteocyte-like cell lines such as murine long bone osteocyte Y4 (MLO-Y4) and murine long bone osteocyte A5 (MLO-A5) are typically used [62].

There are many physical triggers that could provide the stimuli to the mechanosensitive cells, such as matrix strain, interstitial fluid flow and hydraulic pressure. It is unclear if one of these mechanisms or an interplay between them all is the physical stimulus that triggers a response. However fluid flow induced shear stress has become the most studied mechanism. Experimental evidence has confirmed the idea that interstitial fluid flows in response to local bone deformation through the following of tracers through the lacuna-canalicular network during bone loading [83]. In addition, bone cells in culture have been shown to be responsive to fluid shear within a range of shear values and loading frequencies expected to occur *in vivo* (1-3 Pa at 1-3 Hz) [84, 85]. Fluid flow both *in vitro* and *in vivo* not only induces a shear stress on cells but also creates streaming potentials and increased chemotransport. By altering flow rate while also altering fluid viscosity, fluid transport and therefore chemotransport can be altered without also changing the applied fluid shear. This has shown that streaming potentials and chemotransport have little to no effect as a stimulus in comparison to fluid shear [86].

The exact mechanisms behind how bone cells translate these mechanical stimuli into biochemical responses are also not fully understood. However, force induced changes in structures such as integrin complexes, mechanosensitive ion channels, cell-cell adhesions, glycocalyx and primary cilia are all potential sensory elements (Figure 2.5). As in other mechanosensitive cells, the cytoskeleton is thought to play a role in the mechanotransduction and biochemical response. This is through the interaction of the cytoskeleton and extracellular matrix (ECM), through transmembrane cell surface receptors, known as integrins [87]. In osteoblasts, actin disruption and mutant adhesion

proteins have been shown to inhibit various signal pathways induced by fluid shear, highlighting the importance of the cytoskeleton and integrins in mechanotransduction [88]. In addition, gene expression of cytoskeletal and integrin related molecules have been shown to be upregulated by the application of fluid shear [89]. These results suggest the cytoskeleton rearranges its structure to increase cell adhesion with the ECM, increasing the expression of integrin related molecules that aid in the transfer of mechanical stimuli into the cells.

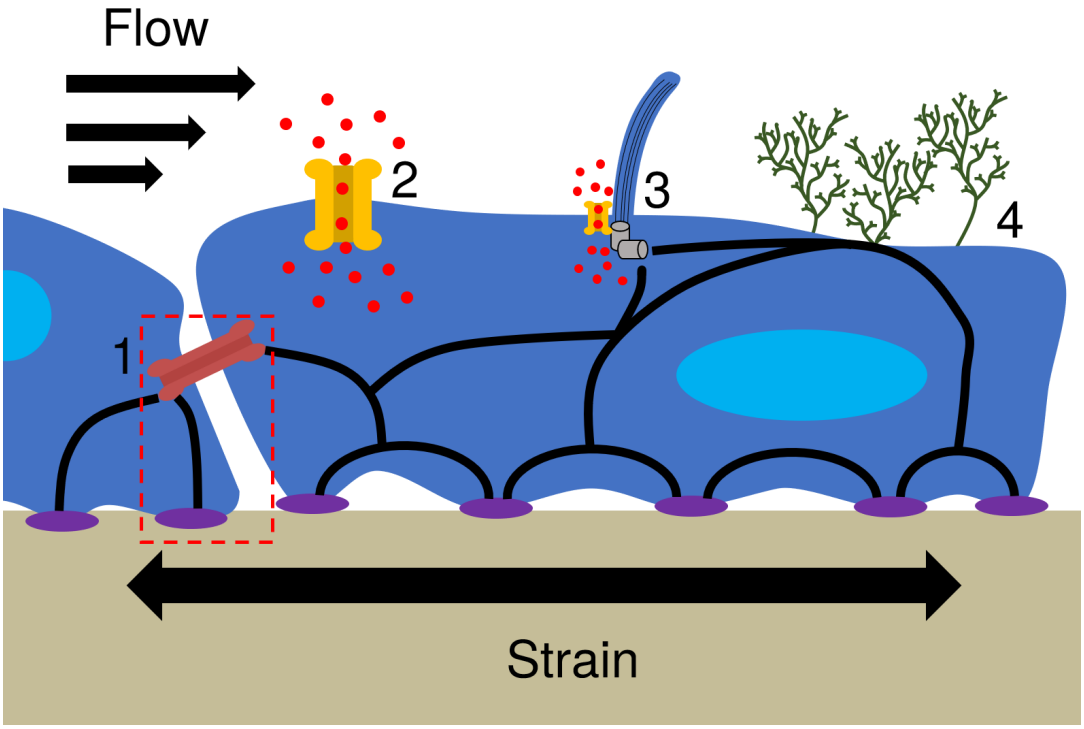


**Figure 2.5:** Mechanosensory structures in bone cells. (1) Cytoskeleton, integrins and cell-cell adhesion complexes. (2) Mechanosensitive sensitive ion channels. (3) The primary cilium. (4) The glycocalyx.

A second mechanism theorised involves the activation of mechanosensitive ion channels resulting in an influx/efflux of ions into or out of the cell [90]. Mechanosensitive ion channels can be activated or inactivated by mechanical forces and can respond to stretch, curvature or other deformation that causes tension in the cell membrane [91]. There are large number of mechanosensitive ion channels with the most commonly studied falling into the TREK, TRAAK or TRP families. These channels are known to be present in osteogenic cells [92, 93]. These mechanosensitive ion channels can be located throughout the cell membrane but have also been found to be localised to the primary cilium membrane [94].

The primary cilium is another popular cellular feature thought to play a role in mechanotransduction. It was once believed that primary cilia were a vestigial organelle that no longer play any role in the cell. However, more recently the primary cilium has been implicated in a number of biological responses such as sonic hedgehog signalling, an important signalling pathway in embryonic development [95], control of left-right axis determination during embryonic development [96] and polycystic kidney disease [97] and will be discussed further later in this chapter.

Absence or damage to any of these key functional or structural components can have major clinical implications. Duchenne muscular dystrophy is caused by mutations in the dystrophin gene causing disruption in force transmission between the cytoskeleton and ECM resulting in muscle degeneration [98]. Abnormalities in mechanosensitive ion channels can result in neuronal and muscular degeneration, cardiac arrhythmias, hypertension and polycystic kidney disease [99–103]. Previous research on the role primary cilia play in these diseases have found both chemosensory and mechanosensory roles in response to fluid flow.

## 2.6 Primary cilia

Primary cilia are solitary, immotile, hair-like protrusions that emanate from the cell surface of most mammalian cells [104], including bone cells [105], during arrested cell growth. The length of a typical cilium can range in length from 1-10 µm, varying between cell types and culture conditions [106]. Not all cells that are known to express primary cilia generate one and spatial confinement, one key regulator of cilia genesis, is thought to control this [107]. Primary cilia themselves have been linked to a number of signalling pathways and cellular processes such as polycystin, hedgehog and wingless/integrated (Wnt) signalling [108–110]. Defects of primary cilia can therefore cause a wide range of diseases termed ciliopathies.

### 2.6.1 Primary cilia structure

The ciliary skeleton or axoneme, extends from the basal body and consists of nine microtubule doublets. In contrast to motile cilia, primary cilia do not contain a central doublet and have hence been termed 9+0 cilia (Figure 2.6)

[111]. Primary cilia also lack elements of motile cilia involved in cilia motility such as the outer and inner dynein arms [110]. The axoneme of the primary cilia is surrounded by the ciliary membrane which is an extension of the cell membrane. The ciliary membrane is separated from the cell membrane by the ciliary necklace and in some cells also the ciliary pocket. These regions form a barrier to the movement of proteins and lipids into and out of the primary cilia, allowing the primary cilia to have a unique membrane composition [89]. The membranes of primary cilia contain a high density of receptor proteins and calcium channel proteins, with many of these proteins being specific to the primary cilia itself [112, 113]. The localisation of these proteins further supports the sensory role of primary cilia.

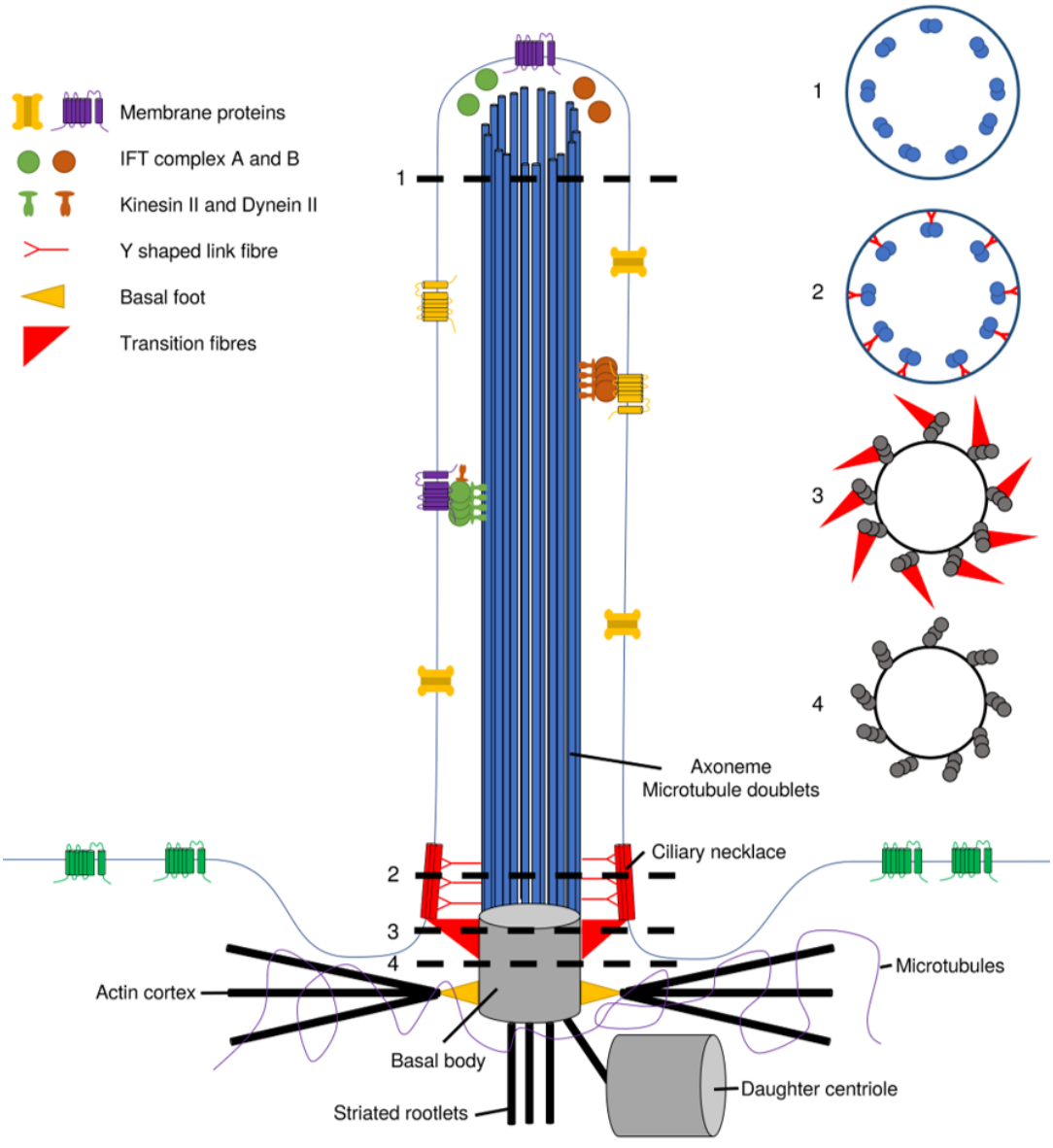


**Figure 2.6:** A Schematic illustration of a primary cilium including transverse sections of the cilium at different points along its axis.

Primary cilia do not contain the necessary machinery to synthesise these proteins, thus they must be transported from the cell cytoplasm into the cilia. This role is performed by the intraflagellar transport (IFT) system, which is itself formed from many proteins that aid in the trafficking of proteins towards the distal ends of the cilia and back again [114]. The IFT system is formed of protein modules, known as IFT trains, particles or rafts which travel along the axoneme of the cilium. IFT particles are assembled at the base of the cilium in the transition zone [115]. The IFT particles carry the protein cargoes in the anterograde direction, from the base to the distal end of the cilium powered by the kinesin-2 motor-complex [116]. At the cilium tip kinesin-2 is inactivated and protein cargoes are released. The IFT particles return to the cilium base by retrograde IFT powered by dynein-2 [117]. These retrograde particles may also contain protein cargoes; however, proteins can also be transported out of the cilium by ectosomes and vesicle shedding [118].

### 2.6.2 Ciliogenesis

Primary cilia form from the mother centriole in a process termed ciliogenesis. Due to this, ciliogenesis is intrinsically linked to the cell cycle as centriole duplication requires resorption of the primary cilia [119]. Cilium formation occurs several hours after mitosis in vitro and typically occurs in G1/G0 phase [120, 121]. Once cilia form it can take several days before they reach their full length, after which if cells do not remain quiescent primary cilia are resorbed upon the cells entering either S-phase or G2/M-phase [104, 120, 121].

After mitosis the mother centriole migrates from the mitotic spindle and docks at the actin-rich cell cortex. During migration to the cell cortex the centriole associates with membrane vesicles and upon docking these vesicles subsequently fuse to the cell membrane establishing the primary cilia membrane and the basal body [122, 123]. The axoneme is formed by nucleation of axonemal microtubules from the basal body that begin to protrude beneath the primary cilia membrane extension. The transition zone is the most proximal region of the cilium and contains the ciliary necklace, which along with the transition fibres form a functional barrier that separates the ciliary membrane from the plasma membrane [124]. Protein synthesis does not occur within the primary cilium itself so all proteins required for elongation of the cilium must be actively imported and transported to the tip of the cilium [125, 126]. This

process is known as intraflagellar transport (IFT), is bidirectional and involves the movement of protein complexes along the axoneme via a molecular motor-driven process. Once the primary cilium is formed there is still continuous turnover of tubulin at the ciliary tip, with disassembly of microtubules and new tubulin being incorporated [127]. This continuous turnover is balanced such that the cilium does not elongate further or shorten.

### 2.6.3 Primary cilia mediated mechanotransduction

Primary cilia were first noted for their mechanosensitivity in kidney epithelial cells, where they are thought to act as urine flow sensors [128]. The degree of cilium bending correlates with the applied fluid shear magnitude similar to a cantilever beam [128]. This has been mathematically modelled by Schwartz et al. where it was shown that cilium bending increases strain on the convex side of the cilium [129]. In renal tubules primary cilia are bent by the flow of urine and it is theorised that this deflection is detected by a heterodimeric complex containing polycystin (PC)-1 and PC-2 [114]. However, this is not universally accepted and others have suggested that PC-1/2 are not activated by cilia deflection. Upon deflection the membrane strain causes these mechanosensitive ion channels to undergo a conformation change allowing the passage of $Ca^{2+}$ into the cell triggering a local increase in $Ca^{2+}$ concentration and subsequent activation of downstream signalling cascades [114, 130]. Direct stimulation of primary cilia by micropipette to induce primary cilia bending has also resulted in increases in intracellular calcium. This direct stimulation of primary cilia rather than applying fluid flow to the whole cell removed the influence other cellular mechanotransducers may have played and verified the role of the primary cilia.

In addition to their role in kidneys primary cilia have been shown to play an important role in bone mechanotransduction as well as other tissues. Primary cilia are present on bone cells both *in vivo* and *in vitro*. Furthermore, primary cilia have been shown to bend in response to sub-physiological flow in a similar manor to that of kidney cells. Primary cilia are required for many osteogenic mechanoresponses to occur. When primary cilia are removed through chloral hydrate treatment, fluid flow induced increases in osteopontin (OPN) no longer occur. However, these cells are still able to upregulate OPN expression in response to vitamin D administration. This demonstrated that removal of primary cilia did not itself inhibit OPN gene expression. Removal

of primary cilia through either chloral hydrate treatment or small interfering ribonucleic acid (siRNA) targeting of IFT88 (an IFT protein required for ciliogenesis) has been shown to abrogate other fluid flow induced responses in bone cells, including $PGE_2$, matrix mineralisation, cyclooxygenase-2 (COX-2) and 3',5'-cyclic adenosine monophosphate (cAMP) signalling further demonstrating the role primary cilia play as a mechanotransducer in bone [131–133].

Although primary cilia act as mechanosensors in multiple tissues, the mechanism by which this occurs has been shown to differ. In kidney cells, primary cilia bending has been shown to be responsible for $Ca^{2+}$ signalling responses [114, 130]. In addition to kidney cells this calcium dependent mechanism also occurs in cholangiocytes in the liver [134]. The influx of extracellular $Ca^{2+}$ across the cell membrane has been shown to be required for whole cell calcium signalling to occur. The bending force induced by fluid flow is theorised to induce conformational changes in PC1, which in turn activates PC2, a $Ca^{2+}$ channel that forms a complex with PC1 in the primary cilia membrane. The resulting influx of $Ca^{2+}$ then triggers intracellular $Ca^{2+}$ release and subsequently various cellular functions, including cell growth, apoptosis and gene expression. Additionally, after fluid flow is ceased the intracellular tail of PC1 is proteolytically cleaved, where it translocates to the nucleus to function as a transcription factor [135]. Another $Ca^{2+}$ channel, transient receptor potential (TRP)V4 has also been found to be essential in regulating responses to fluid flow in kidney cells where it co-localizes and interacts with PC2 [136]. However, a recent paper by Delling et al. found that $Ca^{2+}$ signalling does not originate in the primary cilia and that the mechanosensory role primary cilia play, if any, must be through some other pathway [137]. This has been refuted by others, where it has been suggested that the contrasting results may be due to Delling et al. not subjected the cells to long enough stimuli durations that other groups have required to detect peak calcium flux [138].

Although bone cells show a similar increase in intracellular $Ca^{2+}$ in response to fluid flow, this response still occurs in the absence of primary cilia [131]. Furthermore, when $Ca^{2+}$ channels are inhibited by gadolinium chloride intracellular $Ca^{2+}$ still increases in response to fluid flow. This demonstrates that calcium signalling in bone cells is not dependant on the influx of extracellular $Ca^{2+}$ as in kidney cells. Other studies have also shown primary cilia mediated mechanosensing in bone cells is $Ca^{2+}$ independent [131, 139]. An alternative signalling pathway that has been shown to occur in bone cells upon fluid flow stimuli is cAMP. Kwon et al. found osteocytes subjected to fluid flow

showed a decrease in cAMP after 2 min which led to an increase in COX-2 gene expression. This cAMP response to fluid flow has also been shown to be abrogated through removal of primary cilia, demonstrating cAMP to be cilia mediated [140]. Furthermore, upon downregulation of adenylyl cyclase (AC)6, an andenylyl cyclase isoform that has been shown to be specific to primary cilia, flow mediated cAMP responses have been shown to be disrupted similarly to if primary cilia are removed altogether [140]. After the initial decrease in cAMP in response to fluid flow, intracellular cAMP levels then increase [133].

AC is the sole enzyme that synthesizes cAMP from adenosine triphosphate (ATP) and there are numerous isoforms, many of which have been shown to localize to the primary cilia microdomain [133, 140, 141]. Different AC isoforms can be either inhibited by (AC5 and AC6), stimulated by (AC1, AC3 and AC8) or insensitive to (AC2, AC4, and AC7) $Ca^{2+}$ [142]. Most notably, both AC3 - a $Ca^{2+}$ stimulated isoform and AC6 - a $Ca^{2+}$ inhibited isoform, localise to the primary cilia membrane and this may explain the initial decrease and subsequent increase in cAMP in response to fluid flow. This interplay between $Ca^{2+}$ and cAMP signalling in response to fluid flow has been shown to be required for the initial decrease in cAMP. When $Ca^{2+}$ channels were blocked with gadolinium chloride in osteocytes the cAMP decrease was no longer observed. Furthermore, the decrease was shown to be independent of intracellular $Ca^{2+}$ release, indicating $Ca^{2+}$ influx was required to trigger the decrease. The importance of this interplay between $Ca^{2+}$ and ACs was further highlighted by Moore et al. where osteocytes were transfected with AC3/6 and TRPV4 plasmids that do not interact with $Ca^{2+}$. Adverse cAMP responses were observed in response to fluid flow and expression of COX-2 was downregulated [143].

### 2.6.4 Primary cilia mediated signalling

In addition to their role in mechanotransduction, primary cilia also play an important role in a number of extracellular signalling pathways. Wnt, hedgehog and IGF signalling have all been shown to utilise mechanisms involving the primary cilium.

#### Insulin like growth factor signalling

IGF-1 is a hormone similar in structure to insulin and has anabolic effects in a number of tissues including bone [144]. The link between IGF-1 and primary

cilia was first demonstrated by Zhu et al, in preadipocyte cells, where IGF-1 was found to play an important role in the induction of adipogenic differentiation [145]. When primary cilia were removed, cells had reduced sensitivity to insulin and reduced expression of adipogenic genes. It was also found that a small fraction of the cellular IGF-1R localised to the primary cilia and it was proposed that this compartmentalisation enhanced the receptor sensitivity to insulin. This was similarly found to occur in bone marrow derived stem cells undergoing adipogenic differentiation [146]. Further research by Wang et al. suggested IGF-1R signalling relies on the formation of a protein complex at the base of the cilium [147]. In addition to adipogenic differentiation primary cilia mediated IGF signalling has been implicated in cell cycle progression [148]. Activation of IGF-1R localised to primary cilia in retinal pigment epithelium and in fibroblasts accelerates primary cilia resorption and cell cycle progression from $G_1$ phase to S phase [148].

### Hedgehog signalling

The importance of primary cilia in hedgehog signalling was first discovered through genetic screening in mice that identified genes required for both primary cilia formation and normal hedgehog signalling [149]. The hedgehog family of proteins, consisting of Sonic, Desert and Indian in mammals, play roles in controlling cell growth, survival and fate and in embryonic development are responsible for patterning tissues [150]. Since the discovery of this link numerous mutations that result in primary cilia and hedgehog signalling disruption have been discovered [151]. In the absence of hedgehog, patched-1 is localised to the primary cilium membrane where it suppresses smoothened activity and excludes it from the cilium (Figure 2.7) [152]. In this inactivated state, Gli is sequestered and suppressed by suppressor of fused (SuFu). Upon binding of hedgehog patched-1 is internalised and degraded resulting in translocation of smoothened into the primary cilium and its activation. The activation of smoothened represses SuFu halting suppression of Gli resulting in the formation of Gli activator which is transported out of the cilium to the nucleus where it modifies target gene transcription [153–156]. IFT plays an important role in the trafficking of these signalling intermediaries into and out of the cilium [157, 158]. Therefore, IFT protein function is also essential for the correct functioning of hedgehog signalling.

The Primary cilium can act as a positive or negative regulator of the hedgehog signalling pathway [158, 159]. Ciliary defects can have wide ranging effects

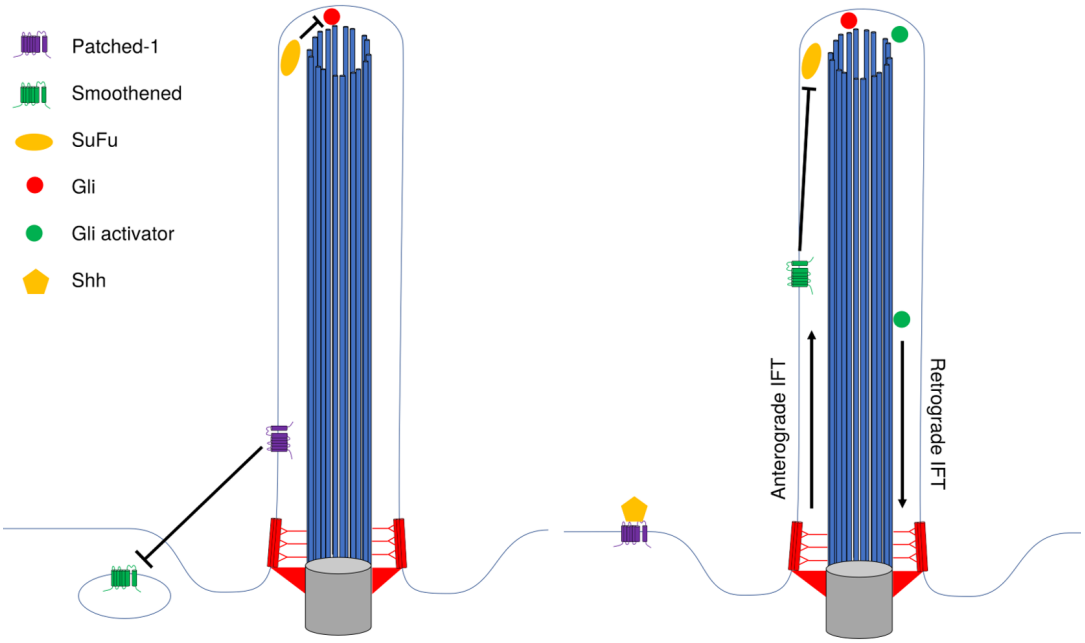


**Figure 2.7:** A Schematic illustration of Hedgehog signalling. (Left) In the unstimulated state, patched-1 is localised to the cilium and suppresses smoothened activity. In this inactive state Gli is sequestered and suppressed by SuFu. (Right) In the stimulated state, patched-1 is internalised and degraded resulting in the transolcation of smoothened which in turn suppresses SuFu halting the suppression of Gli. This results in the formation of Gli activator which is transported out of the cilium to the nucleus where it can modify target gene transcription.

including defects in neural tube formation, structural heart defects, polydactyl, coloboma and lung hypoplasia [149, 160–163]. In addition, there is increasing evidence that cilia-mediated hedgehog signalling may play a role in cancer progression. In some forms of cancer where hedgehog signalling is upregulated a large proportion of the cells lack primary cilia compared to the surrounding normal tissue cells [164]. This can either inhibit or promote cancer progression dependent upon whether the tumours are driven by activation of Gli or activation of smoothened [165, 166].

### Wnt signalling

Wnt signalling consists of two pathways, canonical and non-canonical. Canonical Wnt signalling involves $\beta$-catenin and is therefore also referred to as $\beta$-catenin dependant Wnt signalling. Non-canonical Wnt signalling functions independently of $\beta$-catenin and is functionally more complex. It is largely accepted that the primary cilium plays a role in both of these pathways. However, some studies have disputed this role in canonical Wnt signalling [164, 167].

The activation of both pathways begins with Wnt binding to Fused (Fzd) and a co-receptor of Fzd (Figure 2.8) [168, 169]. In the case of non-canonical Wnt signalling this co-receptor is not well-defined, in canonical Wnt signalling this co-receptor is low-density lipoprotein receptor-related protein (LRP)5/6 [170]. The activation of the Wnt receptor complex leads to interaction of Fzd with dishevelled (Dsh) in the cytoplasm [171]. It is at this point that Wnt signalling branches into the distinct canonical or non-canonical pathways.

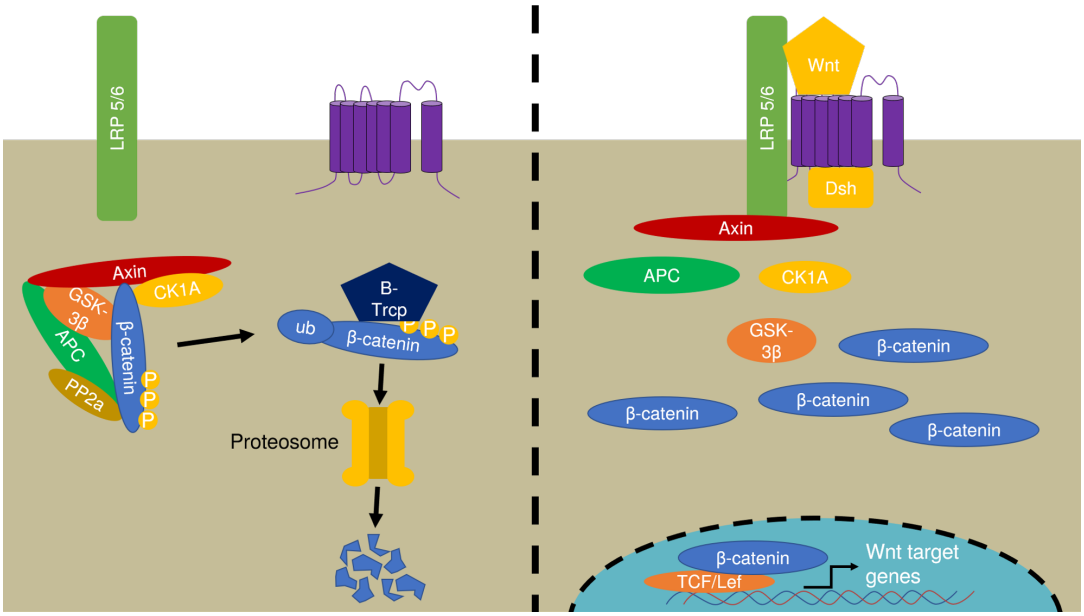


**Figure 2.8:** A Schematic illustration of canonical Wnt signalling. (Left) In the unstimulated state, cytoplasmic $\beta$-catenin is targeted for ubiquitination by a destruction complex. (Right) In the activated state Wnt binds to its receptor complex, activating Dsh. Axin translocates to the tail of LRP5/6 disrupting the $\beta$-catenin destruction complex through the inhibition of glycogen synthase kinase 3 $\beta$ (GSK3-$\beta$). This results in the accumulation of stabilised $\beta$-catenin in the cytoplasm, which subsequently translocates to the nucleus where it functions as a transcriptional co-activator.

In the absence of Wnt signalling, cytoplasmic $\beta$-catenin is targeted for ubiquitination by a destruction complex formed of axin, adenomatous polyposis coli (APC), protein phosphatase 2A (PP2a), GSK3-$\beta$ and casein kinase 1A (CK1A) through phosphorylation by GSK3-$\beta$ and CK1A [172, 173]. Upon Wnt binding to its receptor complex, the activation of Dsh results in the translocation of axin to the tail of LRP5/6 disrupting the $\beta$-catenin destruction complex through the inhibition of GSK3-$\beta$ [174, 175]. Due to the inactivation of this complex $\beta$-catenin is no longer targeted for ubiquitination. This results in the accumulation of stabilised $\beta$-catenin in the cytoplasm, which subsequently translocates

to the nucleus where it functions as a transcriptional co-activator [176]. Many osteogenic genes are targets of $\beta$-catenin transcriptional co-activation including OPG, BMP, COX-2 and activation of canonical Wnt has been reported to result in increased bone formation [177–180]. In addition, canonical Wnt signalling suppresses RANKL expression in osteoblasts, this in combination with the upregulation of OPG can result in decreased osteoclastogenesis and bone resorption [181].

In non-canonical Wnt signalling the binding of Wnt and recruitment of Dsh activates Rho and Rac (Figure 2.9). Activation of Rho occurs through complex formation of Dsh with disheveled-associated activator of morphogenesis (DAAM)1, which subsequently leads to activation of Rho-associated protein kinase (ROCK), a key regulator of the actin cytoskeleton and its arrangement [182, 183]. Activation of Rac is independent of DAAM1 and results in the activation of c-Jun N-terminal kinase (JNK) [184]. The activity of Wnt signalling downstream of JNK is poorly understood but it is thought to also play roles in cytoskeleton regulation [185].

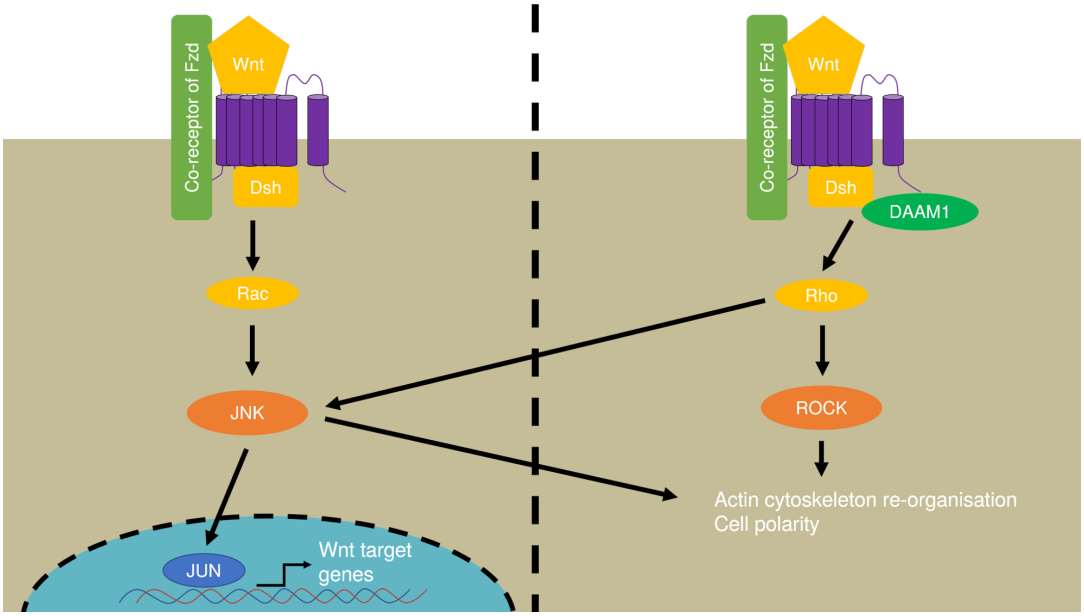


**Figure 2.9:** A Schematic illustration of non-canonical Wnt signalling. (Left) DAAM1 independent non-canonical Wnt signalling through Rac. (Right) DAAM1 dependent non-canonical Wnt signalling through Rho.

The primary cilium plays an essential role in non-canonical Wnt signalling, specifically in planar cell polarity as the process is dependent upon migration of the basal body to the apical surface of the cell [186]. Defects in proteins regulating the migration of the basal body and ciliogenesis can therefore lead

to neural tube, inner ear and gastrulation defects. The ciliary protein, inversin acts as a switch between the two different Wnt signalling cascades [187]. In the canonical Wnt pathway inversin targets Dsh for degradation, resulting in reduced disruption of the $\beta$-catenin destruction complex, preventing $\beta$-catenin accumulation. The primary cilium can further control Wnt signalling through jouberin [188]. Jouberin facilitates the translocation of $\beta$-catenin into the nucleus, however upon sequestration of jouberin in the primary cilium translocation of $\beta$-catenin is disrupted and Wnt signalling is inhibited.

### 2.6.5 Primary cilia length regulation

Primary cilia have a highly conserved basic morphology. However, *in vivo* distinct cell types bear cilia with different mean lengths suggesting there is some biological control of their length [189]. Primary cilia length regulation has primarily been determined through genetic and human disease studies that have focused on the molecular components that are required for their correct formation. These studies have identified the involvement of molecules that play a role in the levels of soluble tubulin and the organization of the actin cytoskeleton [190, 191]. Regulation of primary cilia length is one mechanism by which cells can modulate mechanosensitivity and cilia-mediated signalling.

Regulation of cilia length is a dynamic process that is balanced through the continuous assembly and disassembly of ciliary axonemal subunits at the ciliary tip [127]. The regulation of cilia length via assembly and disassembly forms the basis of the "balance-point" model. IFT proteins transport the required axonemal subunits to the ciliary tip and if this process is "switched off", it results in a constant rate of resorption of the primary cilia [192]. This rate of resorption suggests that the disassembly rate of cilia is independent of their length [127]. In order for cilia to maintain a constant length, the rates of assembly and disassembly must therefore be equal if the amount of IFT does not alter [193]. Furthermore, if cilia disassembly is independent of its length then this suggests the mechanisms involved must act upon the assembly process of the primary cilium. The actual mechanism by which cilium length is regulated remains elusive, despite the large and growing list of involved genes and potential signalling pathways.

The "balance-point" model is likely to be an oversimplification of a more complex regulation mechanism. In some instances, primary cilia have been

shown to decrease in length with increases in both anteroegrade and retrograde IFT [194]. This is due to disrupted cargo loading of anterograde IFT particles resulting in the transportation of cargo-less IFT particles. The increase in cargo-less particles reaching the ciliary tip results in increased ciliary disassembly due to greater availability of empty cargo binding sites for disassembly products. There are therefore at least two mechanisms able to regulate primary cilia length, IFT velocity and cargo loading of IFT particles.

In addition to genetic defects an increasing amount of evidence has shown that both chemical and mechanical stimuli can affect the architecture and length of cilia. Several studies have shown that mechanical stimulation can cause cilia length to decrease in a variety of different cell types from kidney cells to osteoblasts [104, 195]. Besschetnova et al. demonstrated that this decrease in cilia length due to mechanical loading may be due to decreases in cAMP levels and increases in intracellular $Ca^{2+}$ acting through a protein kinase A (PKA))-dependant increase in anterograde IFT [195]. This response was also shown to be dependent upon PC1 and PC2, two mechanosensitive proteins present in the ciliary membrane that have been shown to play a role in mechanosensitivity of many cell types [196–198]. Additionally, it was also found that cilia elongation could be induced through activation of AC with forskolin: which subsequently increases cAMP, or inhibition of $Ca^{2+}$ by treatment with $Gd^{3+}$. This response of cilium to cAMP and $Ca^{2+}$ creates a negative feedback loop where decreases in cAMP and increases in $Ca^{2+}$, due to mechanical stimulation, causes a decrease in cilia length. This decrease in length has been shown to result in reduced mechanosensitivity, thought to be due to the decreased lever length [199]. This reduction causes a larger force to be required to bend the cilia and activate signalling cascades. With the removal of the stimuli and the return of the pre-stimulated $Ca^{2+}$ and cAMP levels, cilia length and mechanosensivity is restored. The theory that cilia length is regulated by its assembly rate was also supported by the study by Besschetnova et al, where the anterograde IFT velocity was shown to increase when the cells were treated with forskolin or $Gd^{3+}$ treatment without effecting the retrograde IFT rate [195].

### 2.6.6 Chemical and biological manipulation of primary cilia

Several chemical agents have been shown to alter cilia length which may be useful in studying the role of cilia, both modelling ciliopathies and studying their treatments and in beneficially altering mechanoresponses *in vivo* and *in vitro*. Primary cilia can be removed, shortened or lengthened with a variety of both chemical and biological methods.

For complete cilia removal chloral hydrate is commonly used which acts by disrupting the cilium-basal body junction and causing microtubule disassembly [200]. However, this chemical has fallen out of use due to its unspecific effects on the cell cytoskeleton and the introduction of siRNA techniques [131]. siRNA techniques prevent primary cilia from forming through knocking down genes essential in ciliogenesis. Cells are typically transfected with plasmids containing siRNA sequences against IFT88 or IFT20 [201, 202].

Cilia length can be reduced with the CDK5 inhibitors R-roscovitine or S-CR8. Both of these chemicals have been shown to result in sustained cilia length reductions even after their withdrawal in jck mice [203]. The chemicals were not shown to affect the velocities of either anterograde or retrograde IFT suggesting CDK5 and its direct target CRMP2 may play a role in cilia length regulation by altering microtubule dynamics. CRMP2 has been shown by recent studies to be a critical protein in microtubule assembly, axon and ultimately primary cilia formation [204].

For cilia elongation, many chemical agents have been shown to be effective. Fenoldopam, a dopamine D1-like receptor agonist has recently been shown to elongate primary cilia through an AC-cAMP mechanism [205–207]. Similarly, forskolin, a commonly used drug used to directly activate AC increasing cAMP, has also been shown to increase the length of primary cilia. This supports the previous studies suggesting cAMP levels regulate cilia length. Lithium, through the use of lithium chloride (LiCl) and other lithium salts, has also been shown to induce cilia elongation both *in vivo* and *in vitro* [208–211]. The mechanism by which lithium induces cilia elongation is unclear. Nakakura et al proposed lithium induces cilia elongation through an increase in acetylated $\alpha$-tubulin triggered by inhibition of GSK3-$\beta$ by LiCl [208]. Another study also showed LiCl inhibition of GSK3-$\beta$ was involved in cilia elongation and additionally showed two other GSK3-$\beta$ inhibitors also induced cilia elongation

[212]. However, other studies have shown that cilia elongation induced by LiCl is not dependent on GSK3-$\beta$ inhibition and that other GSK3-$\beta$ inhibitors do not effect cilia length, instead suggesting the increase in cilia length is due to an inhibition of AC and a reduction of cAMP [209, 210]. This contradicts the previously mentioned research that increases in cAMP results in cilia elongation. The interaction between AC, cAMP and cilia length is clearly complex and these conflicting results highlight the potential of other feedback mechanisms that may play a role in cilia length regulation. Clearly further research in this area is required to pinpoint the mechanisms behind cilium length regulation.

### 2.6.7 Lithium

Lithium salts including lithium chloride have been used to treat bipolar disorder since the 1970s where they have been shown to reduce suicidal tendencies [213]. The therapeutic range of lithium has been shown to be narrow with therapeutic serum concentrations typically between 0.8-1.2 mM, with mild toxicity presenting in humans at levels between 1.5-2.5 mM and moderate to severe symptoms presenting at serum concentrations greater than 2.5 mM with continuous treatment [214, 215].

Lithium's pharmacological actions are caused by the inhibition of magnesium dependent enzymes due to competition from lithium ions [216]. Lithium and magnesium have similar ionic radii and ionic potentials allowing them to compete for the same binding sites on biomolecules. Due to this lithium affects the activity of many enzymes and therefore pathways within cells. This includes muscarinic and $\beta$-adrenergic receptor coupling to G proteins, inositol monophosphatase (IMPase), AC, bisphosphate 3-prime-nucleotidase and GSK3-$\beta$ [217–221]. Many of these enzymes are themselves involved in a large range of biological processes and pathways, for example GSK3-$\beta$ alone has a predicted 256 proteins that it directly interacts with [222]. The three main enzymes that have been studied with regards to lithium's affects are IMPase, GSK3-$\beta$ and AC.

GSK3-$\beta$ can be inhibited by lithium in a number of ways, the first is through direct inhibition through competing with magnesium, secondly through increasing its inhibitory phosphorylation and finally through inhibiting its transcription (Figure 2.10) [223, 224]. The exact mechanism by which lithium promotes the phosphorylation of GSK3-$\beta$ is not fully understood. However,

activation of phosphoinositide 3-kinase (PI3K) and inhibition of PP2a, an enzyme that dephosphorylates both GSK3-$\beta$ and protein kinase B (Akt) (which in turn phosphorylates GSK3-$\beta$), are known to be involved. Inhibition of GSK3-$\beta$ by lithium activates pathways that would be inhibited by its activity. One major pathway that GSK3-$\beta$ is involved in is Wnt signalling, where it marks $\beta$-catenin for ubiquitination. Lithium inhibits this activity resulting in the accumulation of $\beta$-catenin, effectively mimicking Wnt signalling [225].

Lithium directly inhibits IMPase through competing with magnesium for at least two binding sites. In addition to IMPase, lithium inhibits another enzyme involved in the inositol phosphate signalling pathway, inositol polyphosphate 1-phosphatase (IPP) by direct competition with magnesium (Figure 2.10). The inhibition of these enzymes results in the depletion of inositol and subsequent reduction in Phosphatidylinositol 4,5-bisphosphate ($PIP_2$) and inositol 1,4,5-trisphosphate ($IP_3$) [226]. $IP_3$ is a second messenger that binds to receptors on the endoplasmic reticulum, inducing the release of internal $Ca^{2+}$ stores which activates downstream $Ca^{2+}$ dependent kinases, such as protein kinase (PK)C. In osteoblasts PKC can enhance proliferation and suppress differentiation, although this pathway is also regulated by Wnt signalling [227]. The effect lithium has on proliferation and differentiation in bone cells may therefore depend on the degree of $IP_3$ inhibition and Wnt signalling activation.

Lithium directly inhibits AC through competing with magnesium on the magnesium binding site on AC itself or on the G-protein which activates it (Figure 2.10) [219]. cAMP is a ubiquitous second messenger that is synthesised by AC, the inhibition of AC by lithium therefore reduces cAMP levels. cAMP activates PKA which regulates the activity of a multitude of enzymes through phosphorylation [228]. In addition, PKA regulates gene transcription through phosphorylation of the transcription factor cAMP response element-binding protein (CREB) [229]. Genes that are upregulated by CREB contain a cAMP response element (CRE) in the promoter region of the gene. In bone BMP2, a gene which is important in osteoblast differentiation and bone formation, contains a CRE in its promoter region and is known to be stimulated by CREB [230].

**Lithium's effects on osteogenesis and mechanosensitivity**

As previously mentioned, lithium treatment has been shown to increase cilium length in tissues *in vivo*, but it has also been shown to increase bone mineral

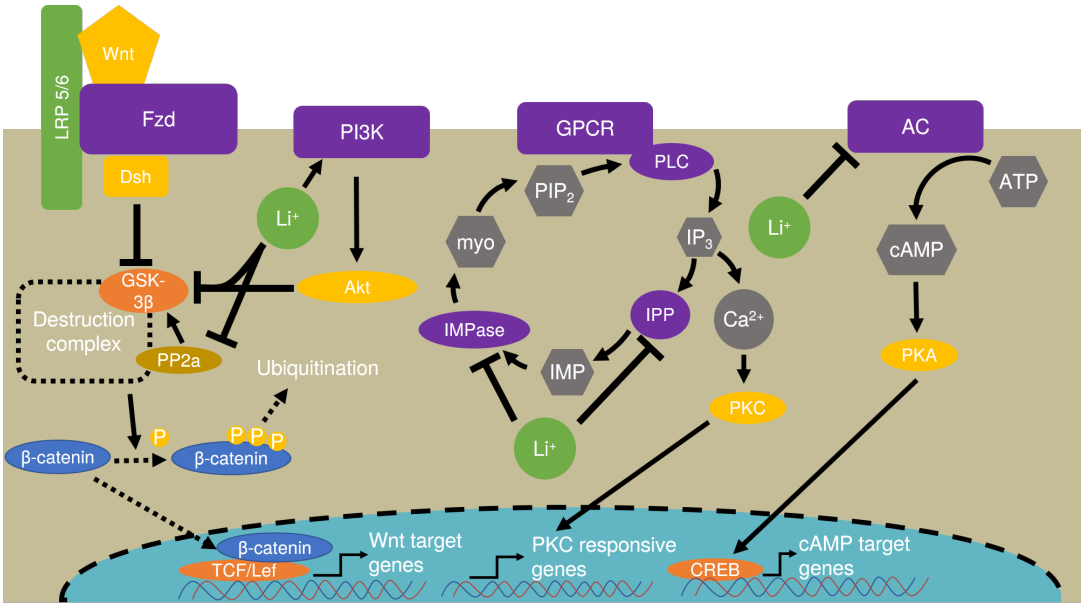


**Figure 2.10:** A Schematic illustration of lithium responsive signal transduction pathways.

density in patients treated with lithium for psychiatric disorders [231]. *In vivo* studies have shown GSK3-$\beta$ inhibition causes increases in osteogenesis and reduced bone turnover [232–234]. Since inhibition of GSK3-$\beta$ upregulates Wnt/$\beta$-catenin signalling, which is a well-known regulator of bone metabolism, it is not surprising that lithium treatment increases bone formation [225]. However, it is not known if this is the whole story, if cilia elongation is linked to GSK3-$\beta$ inhibition, this increase in osteogenesis may also be linked to the increase in cilia length and a subsequent increase in mechanosensitivity in bone cells. Cilia length has been shown to effect mechanosensitivity with increases in length showing increases in mechanosensitivity and vice versa. A study by Spasic et al has shown increases in osteogenic gene expression in mechanically stimulated, LiCl treated cells compared to only mechanically stimulated cells [205]. Therefore, it is possible the increase in bone production found with lithium treatment may be due to both direct inhibition of GSK3-$\beta$ and an increase in mechanosensitivity due to cilia elongation.

## 2.7 *In vitro* mechanical stimulation

Bone cells have been shown to be responsive to a number of different mechanical stimuli in vitro. A great deal of research has looked at various loading durations, magnitudes and frequencies yet an optimum loading stimulus is still unknown. In *in vitro* culture the use of fluid flow induced shear stress is a popular method

and more recently the use of magnetic particles attached to various elements of the cell have seen increased use. Both of these methods can be used to apply stimuli to cells in a controlled manner. Fluid flow induced shear stress is thought to be a major influencing stimulus experienced by bone cells *in vivo*, caused by the interstitial fluid flow through the lacunocanalicular network. To apply shear stress to cells *in vitro* a number of methods can be employed. The simplest systems include orbital shakers and rocking "see-saw" platforms with slightly more complex systems such as parallel plate flow chambers also being commonly used. For three-dimensional (3D) culture a range of different bioreactors can be employed to apply fluid shear.

### 2.7.1 Parallel-plate flow chamber

Parallel plate flow chambers can be built in-house out of glass slides and polydimethylsiloxane (PDMS) or can be obtained from a range of manufacturers. Parallel plate flow chambers apply well-defined, uniform and predictable laminar flow allowing modelling of the shear forces experienced by the cells. This flow can also be oscillatory, pulsatile or unidirectional [235–237]. Oscillatory flow is often used as it is thought to be more representative of the in vitro environment. Shear stress can be applied at a physiologically relevant range of 0.001-3 Pa [238]. Due to the pump driven nature of parallel plate flow chambers, in addition to fluid shear hydrostatic pressure is also applied to the cells within the chamber. This can be reduced through the use of "push-pull" pump systems to reduce the pressure build-up within the device.

The culture surface of the chamber can be modified with micro-patterning to modify cell attachment and alter their morphology. For example, an osteocyte network in a parallel plate flow chamber was built by Lu et al. through modifying the surface chemistry of the chamber and applying micro-contact printing [237]. This technique could therefore be useful for investigating signalling in osteocyte networks in response to various fluid flow regimes.

Imaging of cells within parallel plate flow chambers can be performed *in situ* during the application of flow. This has made them a popular choice for studying cell signalling in response to fluid flow applications. Typically, other short term responses can also be analysed, such as gene expression and cytokine release. However, parallel plate flow chambers are rarely used in longer term experiments that may look at matrix deposition. This is due to

common problems such as bubble formation in the channels and blocking of the channels with deposited extracellular matrix.

### 2.7.2 Rocking platforms and orbital shakers

Orbital shakers and rocking platforms produce a less well-defined fluid flow which can be unidirectional or oscillatory for orbital shakers and only oscillatory for rocker platforms. The simplicity, high throughput of samples and ability to culture for longer time periods compared to parallel plate flow chambers makes them a favourable method for long-term responses to fluid flow stimulation. Although the fluid flow is less well-defined in rocker platforms the shear stress induced by rocking has been modelled through the use of a lubrication-based model [83]. This has been further characterised with a finite element model which was validated with PIV measurements [239]. Both see-saw and orbital shakers are only able to create low magnitudes of fluid shear stress (FSS) (<1 Pa). The FSS magnitude is also not even throughout the surface of the well plate. In both systems FSS is higher at the edge of the well plate compared to the centre.

Despite the low magnitude FSS that can be applied, studies implementing these methods have found osteogenic cells do respond to these low levels. Delaine-Smith et al. found osteogenic progenitor cells subjected to rocking increased ALP activity and matrix mineralisation [240]. Lim et al. found osteogenic progenitor cells subjected to orbital shaking increased matrix mineralisation [241]. Well plate stimulation methods have also been used to create conditioned media from stimulated cells which can be applied to separate cells to investigate the osteogenic effects of factors released in response to loading [242].

### 2.7.3 Magnetic bead stimulation

Techniques that allow forces to be directly transmitted to cells and even directly to specific regions of individual cells are another method used for the stimulation of cells. One such method to achieve this direct manipulation of cells is through the use of magnetic particles and magnetic field bioreactors. The magnetic particles can be attached to regions of cells and by altering a magnetic field the particles can be manipulated to stimulate the cells. Previous studies have shown that using magnetic particles to directly manipulate inte-

grin receptors results in a range of responses in osteoblasts, including changes in MAP kinase activity and increases in intracellular calcium [243, 244]. Typically, these studies have focused on short term culture due to internalisation of particles. However, this internalisation of particles does not produce any measurable toxicity with the use of coated particles [245]. Magnetite (iron oxide) is typically used as the base for magnetic particles and it is known to naturally occur in a number of regions within the human body [246]. Commonly coatings of dextran or polyethylene glycol (PEG) are also applied as they have been shown to reduce possible cytotoxic effects of nano sized particles [247]. This biocompatibility of coated magnetic particles has resulted in their approval for human clinical use. Therefore, it is clear that magnetic particles can be used for longer culture periods. Indeed, a study conducted by Cartmell et al. has shown that mechanical stimulation of osteoblasts with RGD coated magnetic particles is possible for extended periods of time and that this stimulation increases mineralisation [248]. In addition to dextran and PEG coatings magnetic particles can also be functionalised with proteins or peptides to allow specific targeting of the particles to regions of the cell such as integrins or ion channels, where this targeted stimulation has been shown to stimulate bone cells [249].

### 2.7.4 Perfusion flow bioreactors

For applying FSS to cells in a 3D environment basic apparatus such as placing scaffolds in a well plate on an orbital shaker or rocking platform or placing scaffolds inside a spinner flask are commonly used. However, the FSS that this applies is not defined and may only be applied to the surface of the scaffold [250]. Therefore, perfusion flow bioreactors are more commonly used. Perfusion flow bioreactors force fluid through the entire scaffold giving a more homogeneous microenvironment throughout the scaffold. Approximations of shear stress magnitude within the scaffold can be made through the use of cylindrical pore models. For this porosity of the scaffold must be known and all pores are assumed to be the same size and cylindrical. This model is therefore an oversimplification for the majority of scaffold designs and alternative methods of estimate FSS should be employed such as through computational modelling.

Similarly to parallel plate flow chambers, perfusion flow bioreactors also apply hydrostatic pressure to the cells, which again can be reduced through, push-pull designs. The fluid flow within the scaffold also causes it to deform,

resulting in scaffold strain which can be detected by cells on the scaffold. In addition, FSS forces can also be transmitted to deposited matrix within the scaffold resulting in matrix stain. Furthermore, the deformation of the scaffold itself can also cause fluid flow itself. This is similar to how interstitial fluid flow is caused by bone deformation *in vivo*. Clearly the mechanical microenvironment within scaffolds is more complex than the mechanical environment in monolayer culture.

## 2.8 Bone tissue engineering

Large bone defects that will not heal without interventions are known as critical-sized bone defects. Critical-sized bone defects can be caused by comminuted fractures and bone tumour resection and require bone grafts to fill the defects and facilitate bone healing. Bone is the second most transplanted tissue after blood with an estimated 2.2 million grafts performed each year [251]. Autologous bone grafts can be taken from the metaphysis adjacent to the reconstruction site or when larger grafts are required, from the iliac crest. Autologous bone grafts contain native cells and growth factors and therefore result in osteogenic, osteoinductive and angiogenic grafts that promote bone healing upon implantation [252, 253]. However autologous grafts can result in donor site morbidity and prolonged pain for the patient and are also limited by the amount of tissue that can be harvested. Alternatively, allogeneic bone can be used from other human donors after decellularisation of the donor bone. Allografts allow larger defects to be filled and tissue is more readily available. However, due to the decellularisation, homologous bone grafts do not vascularise as well as autologous grafts and therefore the bone defect often takes longer to heal [254]. Additionally, disease transmission and immune rejection are also a concern. Another alternative is the use of xenogeneic grafts from bone harvested from another species. Xenografts are processed similarly to allografts and therefore have the same advantages and disadvantages, although immune responses can be more severe in xenografts [255].

None of the currently used bone grafts are ideal and have drawbacks in terms of osteogenic and angiogenic potentials, donor site morbidity, size and shape restrictions, patient safety, availability, shelf life and cost. Bone tissue engineering is an emerging field that aims to create bone grafts with more beneficial characteristics that address these limitations. The basic concept of

bone tissue engineering involves the harvest of cells from a patient which are then expanded, seeded onto a scaffold and implanted into the defect site where they are resorbed over time [256].

Scaffolds used in bone tissue engineering can be formed of biological materials such as collagen or chitosan or synthetic materials such as ceramics, metals and polymers [257]. Ceramics and metals have high mechanical strength and both have been shown to be osteoinductive through their use in dental and orthopaedic applications. However, ceramics can be vulnerable to fracture and neither material is biodegradable. Furthermore, due to their higher stiffness compared to bone they can result in poor osseointegration with the surrounding bone. Polymers used in bone tissue engineering can be synthetic or natural and biodegradable or non-biodegradable. Synthetic polymers typically used include polylactic acid (PLA), polycaprolactone (PCL), polyurethane (PU) and polyglycolide (PGA) [257]. Natural polymers include proteins such as collagen, silk and keratin and polysaccharides such as chitin and cellulose. Collagen scaffolds tend to have excellent osseoinduction and osseointegration due to being a natural component of bone matrix. Despite this, collagen scaffolds provide poor structural support and this typically applies to other polymers that can be employed. To tailor mechanical properties and biological activity these materials can be combined into composites of different polymers or polymer/ceramic/metal.

Different cell types can be used for bone tissue engineering. Bone marrow or adipose derived stem cells are one option. These stem cells are able to differentiate into osteogenic, chondrogenic or adipogenic lineage cells [258]. The lineage to which the cells differentiate can be controlled through biochemical or physical cues or a combination of the two [259–261]. Since the cells are derived from the patient's own cells there are no issues with immune rejection as with autografts. Additionally, the harvest of bone marrow or adipose derived stem cells results in less donor site morbidity than the harvest of bone for an autograft. Despite these positives, currently this approach would necessitate two operations, one to harvest the cells and one to implant the tissue engineered construct. Additionally, the cell expansion process is time consuming and expensive. This may improve in the future with cell banks and improvements in culture methods and automated cell culture.

Scaffolds can be seeded with cells and directly implanted or can be initially cultured *in vitro* to allow time for cells to deposit matrix onto the scaffold before

implantation. In monolayer culture cells are typically cultured statically with no issues of nutrient or oxygen availability. However, in tissue engineered constructs nutrient and oxygen availability can become an issue in larger scaffolds and can result in necrosis at the core of the scaffold [262]. To overcome this, bioreactors that introduce some form of fluid flow can be employed. Bioreactors can range in complexity from a basic culture vessel placed on an orbital shaker, to bespoke perfusion flow systems and even bioreactors that apply mechanical loading to the scaffolds [263]. In addition to the increased mass transport provided by dynamic culture the fluid flow itself can be implemented in other useful ways. Cell seeding can be improved through dynamic seeding, improving the distribution of cells throughout the scaffold. Additionally, the fluid shear stress created can mechanically stimulate the cells in a similar manner to the interstitial fluid flow within bone itself. The combination of fluid shear and increased mass transport can therefore improve cell distribution, proliferation, differentiation and matrix deposition [264–266]. Perfusion flow systems typically perform better than other bioreactor systems in terms of cell distribution, growth and matrix deposition [263]. However, there is currently no consensus on the optimal culture and flow regime to be employed, for example flow duration and magnitude. To optimise bioreactor culture for bone tissue engineering, bioreactor designs that allow for higher throughput and evenly distribute flow throughout scaffolds are needed. Additionally, knowledge in the area of bone mechanotransduction may help to design and improve flow regimes and subsequent cellular responses in bioreactors used for bone tissue engineering.

# 3. Project aims and objectives

The overall aim of the work presented in this thesis was to investigate the effects of lithium chloride on primary cilia length and prevalence, osteogenesis and mechanostimulated osteogenic responses in osteogenic progenitor and osteoblast cells. It was hypothesised that lithium chloride would enhance mechanosensitivity and therefore result in enhanced osteogenic responses to fluid shear stress. In order to achieve this aim, the project was divided into the following objectives:

1. Investigate the effects of lithium chloride on osteogenesis and primary cilia length and prevalence.
2. Develop a protocol to mechanically stimulate cells with fluid shear stress that induces osteogenic responses.
3. Measure the osteogenic responses to fluid shear stress when cells have been treated with lithium chloride compared to untreated controls.
4. Measure cAMP and $Ca^{2+}$ responses to fluid shear when cells have been treated with lithium chloride.

# 4. Materials and methods

## 4.1 Materials

All reagents were purchased from Sigma-Aldrich (UK) unless otherwise stated. Tissue culture plastic was purchased from Thermo Fischer Scientific (UK).

## 4.2 Methods

The plate reader used in all measurements was a Tecan Infinite® 200 PRO

### 4.2.1 Cell lines

#### hES-MP 002.5

Human embryonic stem-cell derived mesenchymal progenitors 002.5 (hES-MP) cells were purchased from Cellartis (Sweden). They are a multi-potent mesenchymal progenitor cell line derived from Cellartis' SA002.5 embryonic stem cell line. They are able to differentiate into several mesodermal lineages including osteogenic lineages. They have a high resemblance to adult human mesenchymal stem cells.

#### MC3T3-E1

Mouse calvaria 3T3 clone-E1 (MC3T3-E1) cells are a clonal osteoblast precursor cell line established from new-born C57BL/6 mice using standard 3T3 passaging [267]. However, although originally established as a clonal cell line, prolonged passaging resulted in a phenotypically heterogeneous population.

In 1999 Wang *et al.* isolated 52 subclones from this heterogeneous population and selected 10 of these based on their ability to produce or not produce mineralised matrix [268]. Although having been used extensively, the subclone used in studies is commonly not reported giving no indication of whether a phenotypically heterogeneous population was used or a subclone. Differences between findings using MC3T3-E1s may therefore, be due to differences in the populations used. The MC3T3-E1s used here were subclone 4, which exhibit high levels of mineralised matrix production.

**MLO-A5**

Murine long bone osteocyte A5 (MLO-A5) cells are a post-osteoblast/pre-osteocyte cell line established from osteocalcin promotor-driven immortalizing T-antigen transgenic mice [269]. They rapidly produce sheets of mineralised extracellular matrix and express high levels of alkaline phosphatase (ALP), osteocain (OCN) and bone sialoprotein (BSP), typical of the post-osteoblast phenotype [270].

### 4.2.2 Culture media preparation

The media composition used for each cell line is presented in Section 4.1. All media used were based on basal media (BM) which was the simplest formulation used. BM consisted of $\alpha$-minimum essential medium ($\alpha$-MEM) (Lonza, UK) with 10 vol/vol% fetal bovine serum (FBS), 100 U ml$^{-1}$ penicillin, 100 µg ml$^{-1}$ and 2 mM L-glutamine. Cells were passaged in their respective expansion media (EM), which was BM supplemented with human basic fibroblastic growth factor (hFGF) for hES-MPs and BM for all other cell lines used. Media used to promote osteogenic matrix formation is referred to as either supplemented media (SM) or osteogenesis induction media (OIM). Both of these media contained ascorbic acid 2-phosphate (AA-2P) and $\beta$-glycerophosphate (BGP), however, OIM contained dexamethasone (Dex), a corticosteroid, to stimulate osteogenic differentiation.

**Table 4.1:** Media compositions used for each cell line

| Cell Line | Media Type | hFGF | AA-2P | BGP | Dex |
|---|---|---|---|---|---|
| **hES-MP**<br>**MLO-A5**<br>**MC3T3-E1** | BM | 0 | 0 | 0 | 0 |
| **hES-MP** | EM | 4 | 0 | 0 | 0 |
| **MLO-A5**<br>**MC3T3-E1** | EM | 0 | 0 | 0 | 0 |
| **hES-MP** | OIM | 0 | 50 | 5 | 100 |
| **MC3T3-E1** | OIM | 0 | 50 | 5 | 10 |
| **hES-MP**<br>**MLO-A5** | SM | 0 | 50 | 5 | 0 |

### 4.2.3 General cell culture

All cells were cultured following aseptic technique and incubated in a humidified 5% carbon dioxide ($CO_2$) environment at 37 °C.

#### Passaging of cells

Cells were rinsed with Dulbeco's phosphate buffered saline (PBS) twice before adding 1 ml of trypsin-ethylenediaminetetraacetic acid (EDTA) per 25 $cm^3$ of flask area. Flasks were then incubated for 5 min at 37 °C to detach the cells. The flasks were checked under the microscope to ensure the cells had detached and the trypsin was inhibited by adding 2 ml of BM per 1 ml of trypsin-EDTA. This solution was then centrifuged for 5 min at 200 × g. The supernatant was removed and the cell pellet re-suspended in a known volume of BM. A known volume of the cell suspension was mixed with a known volume of Trypan Blue®, placed in a haemocytometer and live cells counted. At this point cells were either cryopreserved, passaged into new flasks at a density of 6,600 cells $cm^{-3}$ or used in experiments.

#### Cryopreservation of cells

After cells were detached and counted, they were adjusted to $1 \times 10^6$ cells $ml^{-1}$ in freezing medium (10 vol/vol% dimethyl sulfoxide (DMSO) in FBS). The cells were aliquoted into 1 ml cryo vials and frozen at a rate of –1 °C $min^{-1}$ in an isopropanol jacketed freezing container in a –80 °C freezer. Once frozen the cells were transferred to liquid nitrogen for long term storage.
Cells were thawed by warming briefly in a water bath before immediately transferring the defrosted cells into 10 ml of BM and centrifuging at 200 × g for 5 min. The supernatant was removed and the cells re-suspended in BM and transferred into new flasks at 6,600 cells $cm^{-3}$.

### 4.2.4 3D Culture

#### Polyurethane scaffold preparation

Polyurethane (PU) foam (Caligen Foam Ltd) was cut into 4 mm × 5 mm (diameter × height) cylinders using a biopsy punch to create a long cylinder and cutting to the correct length with a scalpel. The cut scaffolds were submerged in

a 0.1 w/v% gelatin solution and autoclaved at 121°C for 30 minutes to sterilise the scaffolds and coat the surface with gelatin.

#### Polyurethane scaffold seeding

Prior to seeding, the gelatin was aspirated from the polyurethane (PU) scaffolds before soaking them in BM for 1 hour. To seed the scaffolds, the BM was aspirated and 20 µL of seeding suspension was distributed throughout the scaffold. 1,200 cells $mm^{-3}$ and 600 cells $mm^{-3}$ were seeded per scaffold for hES-MPs and MLO-A5s respectively. Cells were left to attach for 1 hour before submerging in BM. The following day, scaffolds were transferred to new well plates with serum free media with the relevant supplements for or each cell type. Media was changed every 2-3 days.

### 4.2.5 Resazurin reduction assay

Cell viability was assessed by measuring the metabolic activity of cells through the use of resazurin reduction (RR) assays. Metabolically active cells reduce the weakly fluorescent resazurin sodium salt to the highly orange fluorescent resorufin. The intensity of the fluorescence therefore correlates with metabolic activity [271].
The stock solution (1 mM resazurin sodium salt in deionized water (di$H_2O$)) was diluted to make a 0.1 mM working solutions (10 vol/vol% resazurin stock solution in BM). Media was removed from the wells and replaced with a known volume of the resazurin working solution and incubated for 4 h. When performing a RR on scaffolds the scaffolds were first transferred to new well plates to ensure only the metabolic activity of cells attached to the scaffolds were measured. After 4 h, 200 µl was transferred in triplicate to a 96-well plate and read on a plate reader at $\lambda_{ex}$: 540 nm and $\lambda_{em}$: 590 nm. Wells or scaffolds were then washed twice with PBS and fresh media added.

### 4.2.6 Prostaglandin E2 quantification

Prostaglandin $E_2$ ($PGE_2$) is a lipid metabolite derived from arachidonic acid through cyclooxygenase-1 (COX-1) and cyclooxygenase-2 (COX-2) activity. It plays an important role in regulating bone metabolism, although its mode of action and whether it is primarily an anabolic or catabolic stimulant of bone

metabolism is still widely debated. However, $PGE_2$ has been shown to be essential in early responses to mechanical stimulation *in vivo*, where its inhibition at the time of mechanical stimulation prevents osteogenic responses [272]. *in vitro*, $PGE_2$ is released into the culture medium in response to mechanical stimulation. Therefore, to measure the amount of $PGE_2$ released in response to mechanical stimulation an enzyme-linked immunosorbent assay (ELISA) was performed on cell culture supernatants. Media was changed 1 h before mechanical stimulation and 2 h after stimulation the culture media supernatant was taken and centrifuged at 200 × g to remove particulates. A commercially available $PGE_2$ ELISA kit (R&D systems, UK) was used following the manufacturer's instructions. The optical density of each well was measured at $\lambda_{abs}$: 450 nm. The absorbance at 570 nm was subtracted from the absorbance at 450 nm to correct for optical aberrations in the plate. To determine the concentration of $PGE_2$ in the samples, a four-parameter logistic curve, fit to the absorbance of the known standards was used.

### 4.2.7 Cell digestion

Cells were digested to produce lysates for ALP activity and deoxyribonucleic acid (DNA) assays. Media was removed from wells and washed twice with PBS. Cell digestion buffer (CDB) was made by diluting cell assay buffer (CAB) (1.5 M Tris-HCL, 1 mM $ZnCl_2$ and 1 mM $MgCl_2$ in di$H_2O$) in di$H_2O$ (10 vol/vol%) and adding 1 vol/vol% Triton-X100. In two-dimensional (2D) culture 1 ml CDB was added to each well followed by 30 min incubation. In three-dimensional (3D) culture the scaffolds were transferred to 1.5 ml tubes and 1 ml of CDB added followed by 30 min incubation. The well plates or tubes were then freeze-thawed three times (–80 °C 10 min, 37 °C 15 min). After the last thaw, wells were scraped and the lysates transferred to 1.5 ml tubes. All samples were vortexed and then centrifuged at 6700 × g for 5 minutes to remove cell debris. If not used immediately, samples were stored at –80 °C.

### 4.2.8 Alkaline phosphatase activity

ALP is an enzyme synthesised by a range of cells within the body including those of an osteogenic lineage. ALP catalyses the hydrolysis of phosphomonoesters, releasing inorganic phosphate [273]. Although its precise function in bone formation is unknown, it is thought to be involved in the early stages of osteogenesis. Due to this, it is widely used as an early marker of osteogene-

sis. To measure ALP activity a Pierce™ para-nitrophenol phosphate (pNPP) substrate kit (Thermo Scientific, UK) was used. One 5 mg pNPP tablet was dissolved per 5 mL of diethanolamine buffer (20 vol/vol% in di$H_2O$) to form the substrate solution. 20 µl of cell lysate (Section 4.2.7) was added to a 96-well plate in triplicate. 180 µl of the substrate solution was added and the optical density of each well was measured at $\lambda_{abs}$: 405 nm once a minute for 30 min at 25 °C. The molar absorption coefficient was calculated from a standard curve of known concentrations of para-nitrophenol (pNP) using the Lambert-Beer law. ALP activity, expressed as nmol pNP min$^{-}$1 was calculated from the molar absorption coefficient.

### 4.2.9 DNA quantification

DNA was quantified from the same cell lysates as used in the ALP activity assay. This allowed the ALP activity to be normalised to the amount of DNA in each sample. A Quant-iT® high sensitivity double-stranded deoxyribonucleic acid (dsDNA) assay kit was used to quantify the amount of DNA in each cell lysate. 10 µL of the cell lysate was added in triplicate to a 96-well plate. The Quant-iT® reagent was diluted in the Quant-iT® assay buffer (0.5 vol/vol%) and 90 µl of this solution was then added to each well. The plate was incubated for 10 min at room temperature to allow the reagent and DNA to conjugate. The fluorescence was measured using a plate reader at $\lambda_{ex}$: 485 nm and $\lambda_{em}$: 535 nm.

### 4.2.10 Cell fixation

To fix samples for antibody, alizarin red S (ARS) and direct red 80 (DR80) staining media was removed from each well followed by two washes in PBS. The samples were then submerged in 3.7 vol/vol% formaldehyde for 20 min in 2D and 30 min in 3D. The formaldehyde was removed and the samples washed twice in PBS and used immediately or submerged in PBS for short term storage at 5 °C.

### 4.2.11 Alizarin red S staining

ARS is commonly used to stain calcium in biological samples by forming a non-water-soluble ARS-calcium complex salt [274, 275]. ARS staining was therefore used to measure the amount of mineralised matrix produced by the

cells. ARS was dissolved in di$H_2O$ at 1 weight/vol% and buffered to pH 4.1 with 0.1 M ammonium hydroxide. The buffered ARS solution was then filtered through a 0.45 µm filter to remove any undissolved particles. The PBS was removed from the fixed samples followed by two washes in di$H_2O$. The samples were submerged in ARS solution and left for 30 min for the ARS to form water insoluble ARS-calcium complex. The stain was removed and the samples washed with gently running di$H_2O$ until the water remained clear to remove excess ARS that had not formed complexes. 1 mL of 5 vol/vol% perchloric acid was then added followed by 15 min of orbital shaking at 100 revolutions per minute (RPM) to destain the ARS from the ARS-calcium complexes. 150 µL of the destained sample solution was added in triplicate to a 96-well plate and the optical density was measured at $\lambda_(\text{abs})$: 405 nm in a plate reader. The concentration of ARS was calculated from a standard curve fit to the absorbance of known concentrations of serially diluted ARS in destain solution.

### 4.2.12 Direct red 80 staining

Direct red 80 (DR80), commonly referred to as Sirius Red, is a sulphonated strongly acidic azo dye. It binds to collagen through strong interactions of its acidic sulphonic groups with the basic amino acids of collagen molecules [276, 277]. DR80 staining was therefore performed to measure the amount of collagen produced by the cells. DR80 was dissolved in saturated picric acid (1 weight/vol%) and filtered through a 0.45 µm filter to remove any undissolved particles. The PBS was removed from the previously fixed samples followed by two washes in di$H_2O$. The samples were submerged in DR80 solution and left for 30 min. The stain was removed and the samples rinsed with gently running di$H_2O$ until the water remained clear to remove any remaining unbound DR80. A destain solution was made by mixing 0.2 M sodium hydroxide and methanol in equal volumes. 1 ml of the destain solution was then added followed by 15 min of orbital shaking at 100 RPM. 150 µL of the destained sample solution was added in triplicate to a 96-well plate and the optical density was measured at $\lambda_(\text{abs})$: 405 nm in a plate reader. The concentration of DR80 was calculated from a standard curve fit to the absorbance of known concentrations of serially diluted DR80 in destain solution.

### 4.2.13 Fluorescence microscopy staining

To image primary cilia and cell nuclei, antibody staining and 4', 6-diamidino-2-phenylindole dihydrochloride (DAPI) staining was performed. PBS was removed from previously fixed samples and samples were submerged in 0.1 vol/vol% Triton X-100 for 10 min to permeabilise the cells. The samples were washed twice with PBS and a blocking solution of 5 vol/vol% goat serum in dulbeco's phosphate buffered saline with 0.1 vol/vol% TWEEN® 20 (PBST) applied for 1 h at room temperature to block non-specific binding of the antibodies, followed by two washes in PBS. Between each of the following steps 3 PBS washes of 5 min each were performed. All antibodies were diluted in PBST with 5 vol/vol% goat serum to reduce non-specific protein-protein interactions. $1\,\mu g\,mL^{-1}$ of anti-acetylated $\alpha$-tubulin clone 6-11B-1 produced in mouse (Sigma Aldrich - T7451, UK) was applied for 24 h at 5 °C. Goat anti-mouse immunogloblin G (IgG) heavy and light chain (H&L) conjugated to Alexa Fluor® 488(Abcam - ab150113, UK) was applied for 1 h at room temperature. Finally, DAPI ($1\,\mu g\,mL^{-1}$ in PBST only) was applied for 15 min at room temperature. Once stained samples were imaged using either a Nikon Eclipse Ti microscope (Nikon Instruments Europe BV, Netherlands) a Zeiss LSM510 Meta confocal microscope (Carl Zeiss AG, Germany) or a Zeiss Z.1 light-sheet microscope (Carl Zeiss AG, Germany).

### 4.2.14 Light-sheet microscopy

Light-sheet imaging was performed using a Zeiss Z.1 light-sheet microscope (Carl Zeiss AG, Germany). Samples were mounted in 0.8 vol/vol% agarose in di$H_2O$ inside a 1 mL syringe. To mount the samples, agarose was heated to 70°C in a heating block to melt it. The end of a syringe was removed by cutting it with a scalpel. The melted agarose was aspirated into the syringe and the sample to be mounted placed within the syringe in the agarose. Once the agarose had cooled the syringe was placed in the accompanied syringe holder and inserted into the sample chamber filled with di$H_2O$. The samples were positioned and focused using the infra-red camera. Samples were illuminated via two 10×/0.2 objectives (Carl Zeiss AG, Germany) positioned perpendicular to a W Plan-Apochromat 20×/1.0 UV-VIS detection objective (Carl Zeiss AG, Germany) as shown in Figure 4.1. 405 nm (20 mW), 488 nm (50 mW) and 561 nm (20 mW) lasers were used to excite the samples for fluorescence imaging at blue, green and red wavelengths respectively. Samples could be moved in the x, y and z-axis and rotated around the centre of the field of view or around the central drive axis. For the 20×/1.0 objective images were acquired at a

pixel resolution of 92 × 92 nm and a z step-size of 385 nm.

### 4.2.15 Statistical analysis

All statistical analysis was performed using Graphpad Prism v7.0. Datasets were tested for normality (D'Agostini-Pearson omnibus normality test) and normally distributed datasets were analysed with either a student's t-test for comparing two populations, or for comparing more than two populations, by a one or two-way analysis of variance (ANOVA) followed by Tukey's post-hoc multiple comparisons, depending on whether a response was affected by one or two factors. Datasets that were not normally distributed were analysed by a Mann-Whitney test for the comparison of two populations, or by a Kruskal-Wallis test followed by Dunn's multiple comparison test for the comparison of more than two populations. Differences were considered significant when $p<0.05$ with notable significant differences indicated on graphs by *. Unless otherwise stated in the figure legend graphs are presented as mean ± standard deviation (SD). Experiments were repeated three times in triplicate for each condition unless stated otherwise in the figure legend where the total number of replicates (n) is stated.

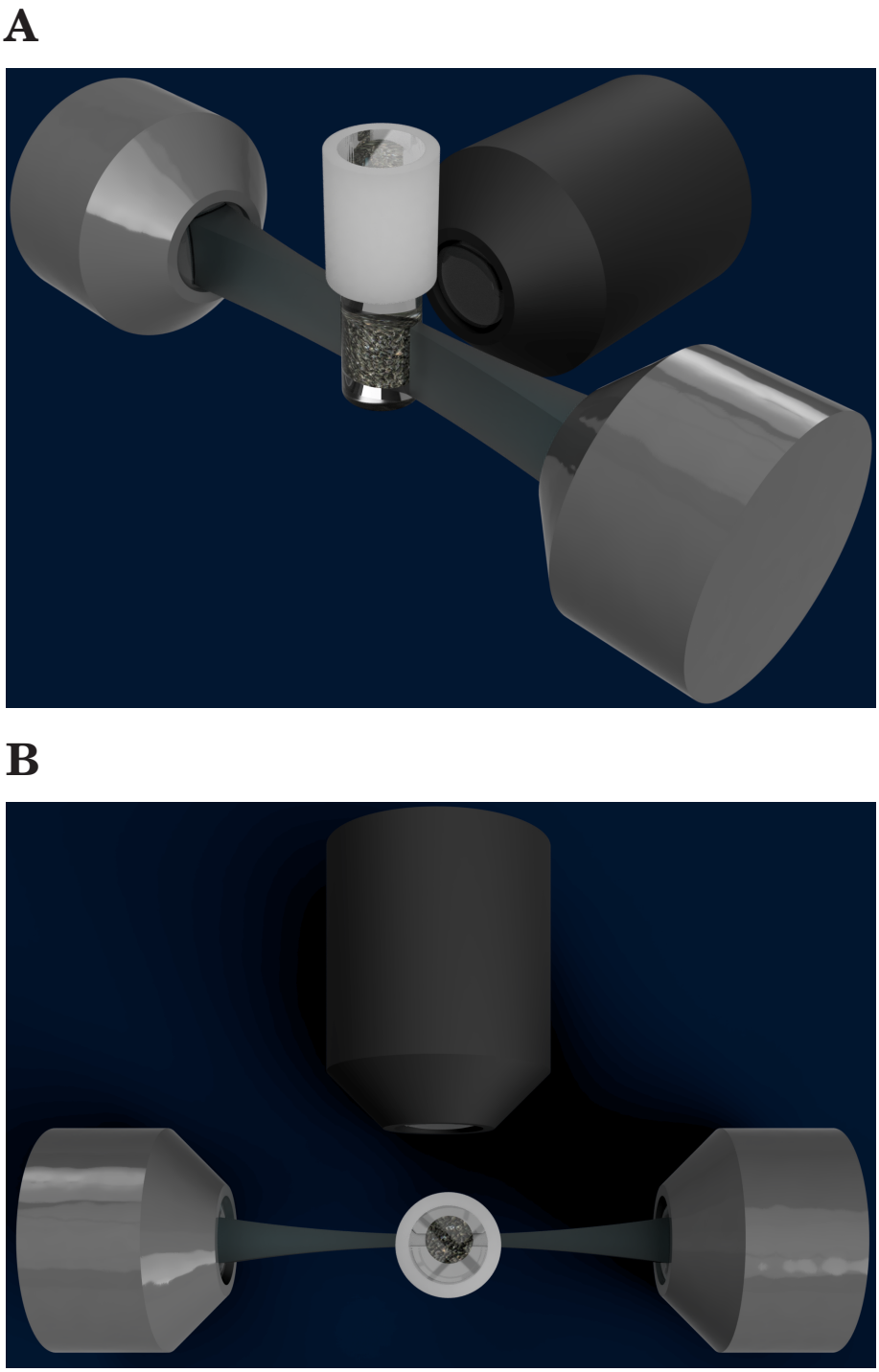


**Figure 4.1:** (A) Illustration of light-sheet microscope set-up showing the illumination objectives, detection objective and a PU scaffold embedded in an agarose gel held in a 1 mL syringe. (B) Top view of the planar illumination light-sheet illustrating the most tightly focused midpoint thickness of the light-sheet which becomes less tightly focused moving away from this central point.

# 5. Lithium accelerates osteogenesis and elongates primary cilia

## 5.1 Introduction

Lithium is most commonly used in the treatment of psychiatric disorders such as bipolar disorder, due to its mood stabilising and neuroprotective effects [278–280]. It is commonly administered as a salt such as lithium carbonate lithium orotate or lithium chloride. A number of case-control studies have reported a reduction in fracture risk with lithium use in psychiatric patients, including reduced risk of osteoporotic fractures [281–283]. However, psychiatric disorders are often themselves associated with increased fracture risk and these studies do not fully account for the association between the treatment of the underlying mental disorder on the risk of fractures and the reduction in fracture risk due to lithium itself [284]. This is complicated by the fact that pharmacological alternatives to lithium, such as selective serotonin reuptake inhibitors, may actually increase fracture risk [284–286]. This led to studies directly investigating the effects of lithium on osteogenesis or bone mineral density itself, with conflicting results reported in the literature [287–291]. Specifically, studies involving mice found increased osteogenesis and bone mineral density with lithium treatment [289, 290] and a study in chickens found lower bone stiffness without affecting bone volume or trabecular number and thickness [288]. In humans, Cohen et al. found no differences in bone mineral density between short-term and long-term lithium treatment groups [287]. However, Zamani et al. found lithium treatment increased bone mineral density, although this was only significant in women, with the authors concluding the increase in bone mineral density may be due to a decrease in bone turnover. In addition, *in vitro*, Satija et al. found lithium treatment upregulated osteogenic gene expression in mesenchymal stem cells (MSC)s [231,291].

Lithium's pharmacological actions are complex and multifaceted, affecting a number of different biological pathways, as discussed in detail in chapter 2.6.7. Lithium typically exerts its effects through competing with $Mg^{2+}$ for metal-binding sites on enzymes resulting in their subsequent inhibition and subsequent alteration of complex and interconnected signalling cascades. The main pathways affected by lithium are wingless/integrated (Wnt)/$\beta$-catenin, through glycogen synthase kinase 3 $\beta$ (GSK3-$\beta$) inhibition, 3',5'-cyclic adenosine monophosphate (cAMP), through adenylyl cyclase (AC) inhibition and $Ca^{2+}$ signalling through inositol depletion. These pathways have all been implicated in osteogenic differentiation of stem cells, stimulation of osteogenesis itself and mechanotransduction pathways including length regulation of the primary cilium. It is therefore possible that lithium's effects on osteogenesis *in vivo* could be a result of its actions on osteogenesis itself, mechanotransduction or a combination of the two. Activation of Wnt/$\beta$-catenin signalling has been shown to result in increased osteogenesis and play an important role in mechanotransduction in osteocytes [180, 292–297]. However, $Ca^{2+}$ and cAMP signalling play an important role in both osteogenesis and mechanotransduction, therefore, lithium's inhibitory effects on these pathways may be detrimental.

Primary cilia are thought to play an important role in mechanotransduction in bone. Through regulating their sensitivity, primary cilia can control osteogenic responses to mechanical loading. One way primary cilia may alter their sensitivity to mechanical stimuli is through regulation of their length, shortening in response to a continuous or high magnitude stimulus and elongating after the stimulus is removed [195]. This results in a negative feedback loop, where a decrease in length results in a decrease in sensitivity requiring a greater magnitude of stimulus to generate the same biological response. This suggests that increasing primary cilia length may increase mechanosensitivity and therefore, also increase osteogenic responses to the current level of mechanical loading. Lithium has been shown to elongate primary cilia in a range of different cell types [208–211]. This elongatory effect may therefore be another potential mechanism behind how lithium could increase osteogenesis.

Due to the conflicting results in studies assessing the effects of lithium on osteogenesis clearly further investigation is required. This chapter therefore explores the effects of lithium on osteogenic differentiation, matrix production and its effects on primary cilia length and prevalence.

## 5.2 Aims and objectives

The aim of this chapter was to explore the osteogenic response of progenitor and osteoblast cells to lithium chloride (LiCl) and the effects of LiCl on primary cilia length and prevalence. This was performed in order to develop a relevant protocol for investigating the effects of lithium on mechanotransduction. The experiments were performed in monolayer initially in order to establish a smaller range of concentrations to apply to a 3D culture system. Since monolayer culture can provide misleading data that is not representative of *in vivo* cell behaviour, 3D culture was performed to evaluate LiCl's effects in an environment that more closely reflects the *in vivo* environment. In addition, one hypothesis was that LiCl would stimulate matrix formation for bone tissue engineering applications. An industrially sourced PU foam was chosen due to its previous use in bone tissue engineering studies [298, 299]. In this chapter the following objectives were addressed:

- Assess the effect of LiCl on the indicators of osteogenesis, ALP and collagen and mineralised matrix production in monolayer culture.
- Assess the effect of LiCl in a 3D culture system on indicators of osteogenesis, ALP and collagen and mineralised matrix production in order to evaluate LiCl's effects in a culture environment more reflective of the *in vivo* environment and its potential for use in bone tissue engineering.
- Examine the response of primary cilia prevalence and length to LiCl treatment in monolayer culture and PU scaffolds.

## 5.3 Methods

The following materials and methods are specific to the work presented in this chapter. General details can be found in chapter 4.

### 5.3.1 Application of lithium chloride

Serum-free and serum-containing stock solutions were made by dissolving LiCl salt directly in serum-free BM and sterile filtering. For the serum containing stock solution, 10 vol/vol% FBS was added. The final concentration of both stock solutions was 100 mM once the appropriate supplements had been added. To create working solutions the stock solution was serially diluted in serum-

free or serum-containing BM as appropriate giving final concentrations of 100, 50, 20, 10, 1 and 0.1 mM once the appropriate supplements had been added. Three LiCl treatment regimens were used, continuous, intermittent and single (Figure 5.1). For assessing the effects of LiCl on cilia prevalence and length a single treatment of 10, 1 or 0.1 mM LiCl was applied for 24 hours before fixing and staining the samples (Figure 5.2).

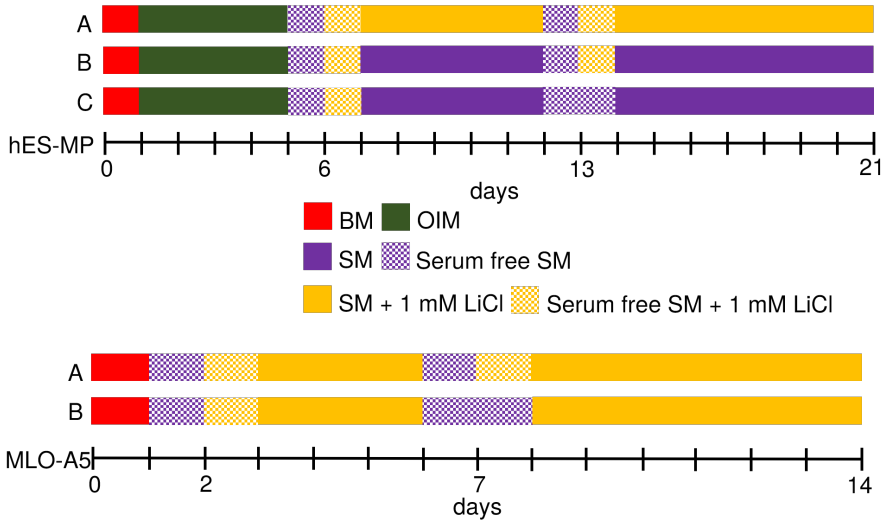


**Figure 5.1:** LiCl treatment regime timelines used in assessing LiCl's osteogenic effects in monolayer culture. (A) Continuous treatment, (B) intermittent treatment and (C) single treatment.

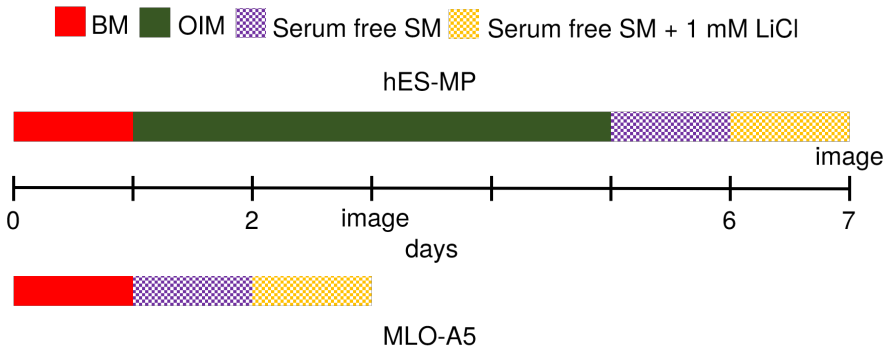


**Figure 5.2:** LiCl treatment regime timelines used to asses LiCl's effects on primary cilia prevalence and length.

### 5.3.2 Primary cilia measurement

After samples were fixed and stained following the protocols in Section 4.2.10 "Cell fixation" and section 4.2.13 "Fluorescence microscopy staining" the samples were imaged using a fluorescent, confocal or light-sheet microscope. A

Nikon Eclipse Ti microscope (Nikon Instruments, Netherlands) in conjunction with a Nikon Intensilight CHGFI fluorescence unit was used to count the number of ciliated cells in monolayer. An Upright LSM510 Meta confocal microscope (Carl Zeiss AG, Germany) was used to measure primary cilia length in monolayer. A Zeiss Z.1 light-sheet microscope (Carl Zeiss AG, Germany) was used for both primary cilia prevalence and length measurements. To measure the number of cells with primary cilia, three fields of view (838 µm x 707 µm) per sample were imaged and analysed. The number of ciliated cells was determined by counting the number of nuclei and the number of those nuclei with primary cilia present. The length of primary cilia in monolayer was determined by measuring the length of each primary cilium in a maximum intensity projection and the number of z-stack slices over which the primary cilium appears and applying Pythagoras theorem (Figure 5.3). When imaging scaffolds, as the plane of illumination within the light-sheet microscope is not an even width within the whole field of view, the axial resolution is greatest in the centre. Due to this and the greater lateral resolution, primary cilia length was measured by positioning each cilium centrally within the field of view and orientating it so as to position the cilia longitudinally in the x-y axis. ImageJ was used for all measurements except primary cilia length in 3D which was measured using the ZEN 2 (Blue Edition) software packaged with the light-sheet microscope.

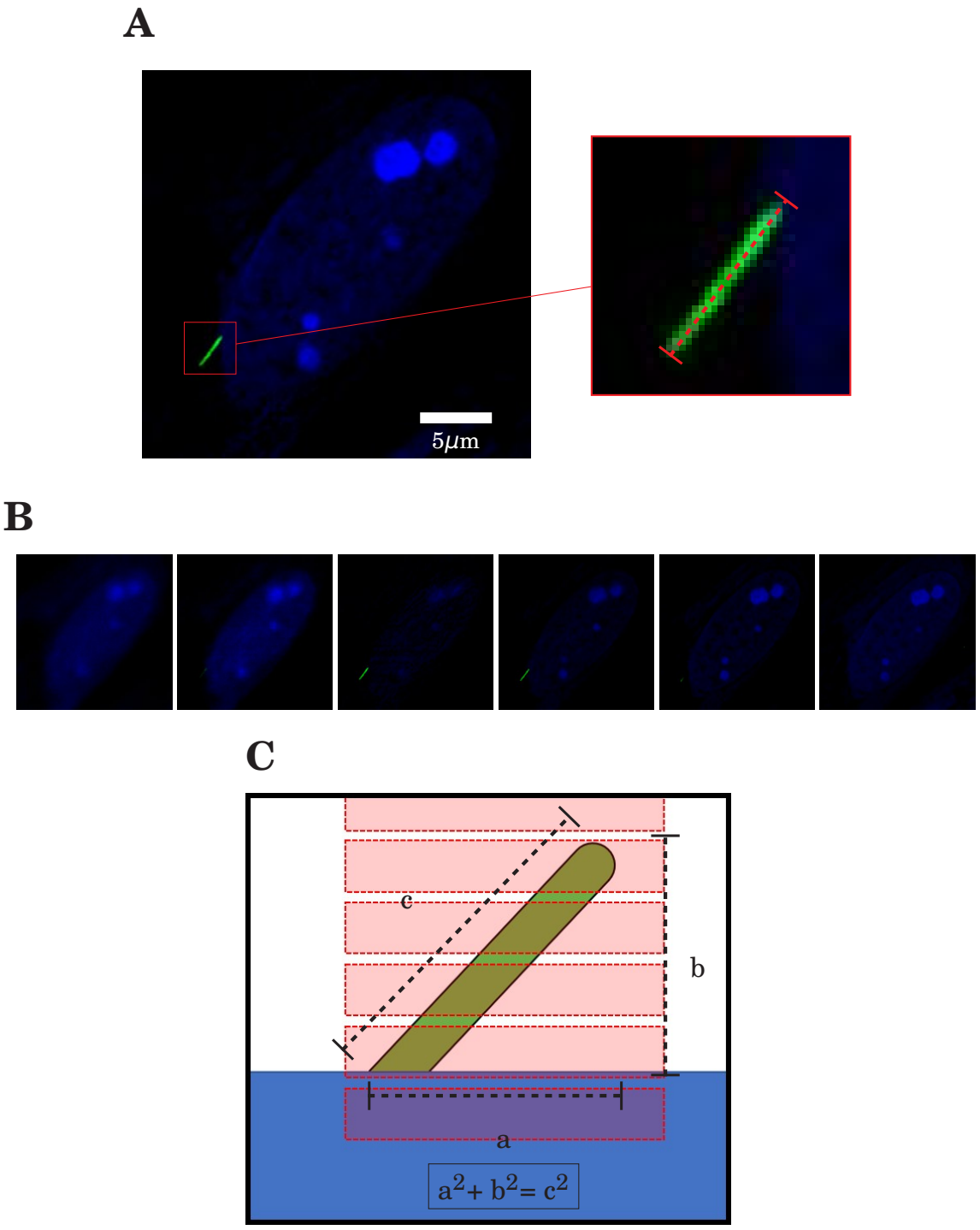


**Figure 5.3:** Primary cilia length measurement with confocal microscopy. (A) A maximum intensity projection of cell nucleus and primary cilium. The primary cilium is measured from its base to its tip as shown in the cropped image (2.7 µm). (B) Sequential optical sections of 0.4 µm thickness. The primary cilium is not visible in the first or last optical sections, and is therefore only visible in 4 sections, giving a height of 1.6 µm (0.4 µm × 4 = 1.6 µm). (C) Illustration of primary cilium protruding from a cell. Red dashed boxes indicate an optical section. a is the maximum intensity projection measurement, b the number of optical sections multiplied by their thickness and c the actual cilium length, which here is 3.13 µm ($\sqrt{2.7^2 + 1.6^2} = 3.13$ ).

## 5.4 Results

### 5.4.1 Continuous lithium chloride exposure is cytotoxic at 10 mM and above

#### Lithium chloride cytotoxicity in hES-MP cells

When used therapeutically lithium is administered daily to keep blood serum levels within a tight range, around 1 mM. Above this level cytotoxic effects become apparent rapidly. However, *in vitro*, lithium has been used at concentrations up to 100 mM with no reported cytotoxicity in some instances. Therefore, the cytotoxicity of lithium was first evaluated in both hES-MP and MLO-A5 cells in monolayer and 3D culture to evaluate if there were any differences in cytotoxicity between osteogenic progenitors and post-osteoblasts/pre-osteocytes in monolayer or 3D culture.

In hES-MP cells, at concentrations at or below the therapeutic concentration of 1 mM, no significant differences in metabolic activity compared to the untreated control were found over the 21 days of culture in monolayer or 3D (Figures 5.4 - 5.5). Cytotoxicity was observed at all concentrations evaluated above 1 mM. In monolayer culture, at 10 mM and above, cytotoxicity was observed after only 24 hours of LiCl treatment (day 7), with significantly lower metabolic activity found compared to the untreated control. However, on day 7 in 3D culture metabolic activity was only lower in 50 mM LiCl treated cells. Metabolic activity reduced significantly between day 7 and 21 in 10 mM and above LiCl treated cells in both monolayer and 3D culture. There was no change in metabolic activity in 10 mM LiCl treated cells in monolayer between day 7 and 14, but there was a significant reduction between day 14 and 21.

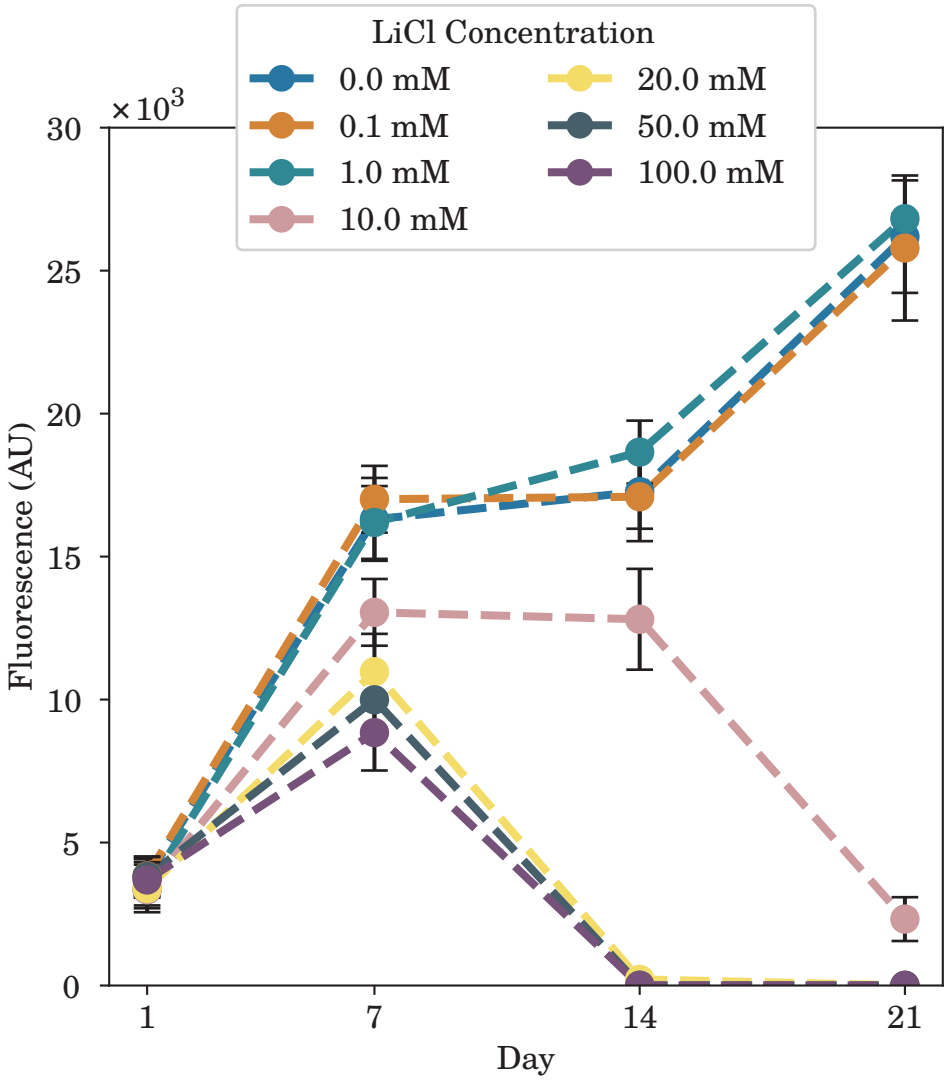


**Figure 5.4:** Effect of continuous LiCl exposure applied from day 6 on hES-MP metabolic activity over 21 days of monolayer culture. Cytotoxicity was observed at concentrations of 10 mM and above. Data represents mean ± SD n=9. Fluorescence was measured at $\lambda_{ex}$: 540 nm and $\lambda_{em}$: 590 nm.

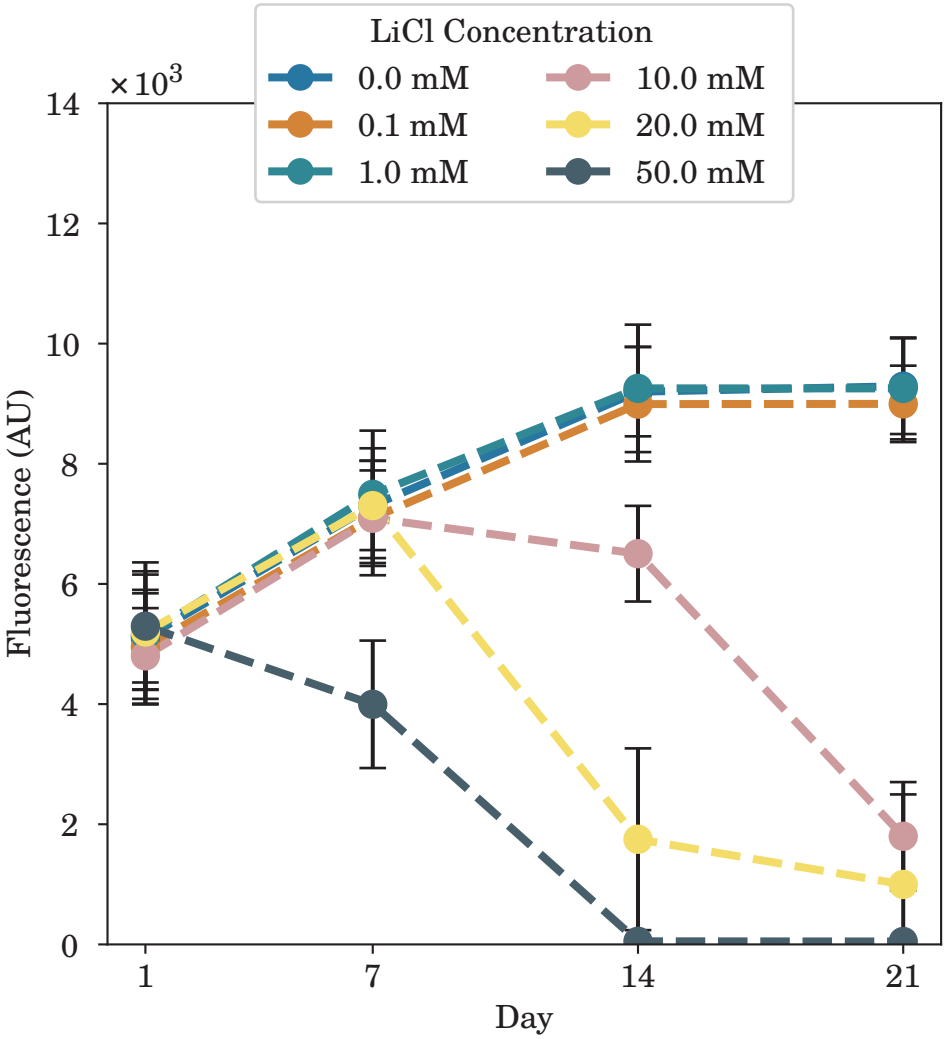


**Figure 5.5:** Effect of continuous LiCl exposures applied from day 6 on hES-MP metabolic activity over 21 days of 3D culture. Cytotoxicity was observed at concentrations of 10 mM and above. Data represents mean ± SD n=9. Fluorescence was measured at $\lambda_{ex}$: 540 nm and $\lambda_{em}$: 590 nm.

### Lithium chloride cytotoxicity in MLO-A5 cells

One replicate of the following results were performed by Ingvar Kiricenko during his INSIGNEO summer project under my guidance.
Similarly to hES-MP cells, in MLO-A5 cells no significant differences in metabolic activity were observed in 0.1 or 1 mM LiCl treated cells over the 14 day culture period in monolayer or 3D culture (Figures 5.6 - 5.7). However,

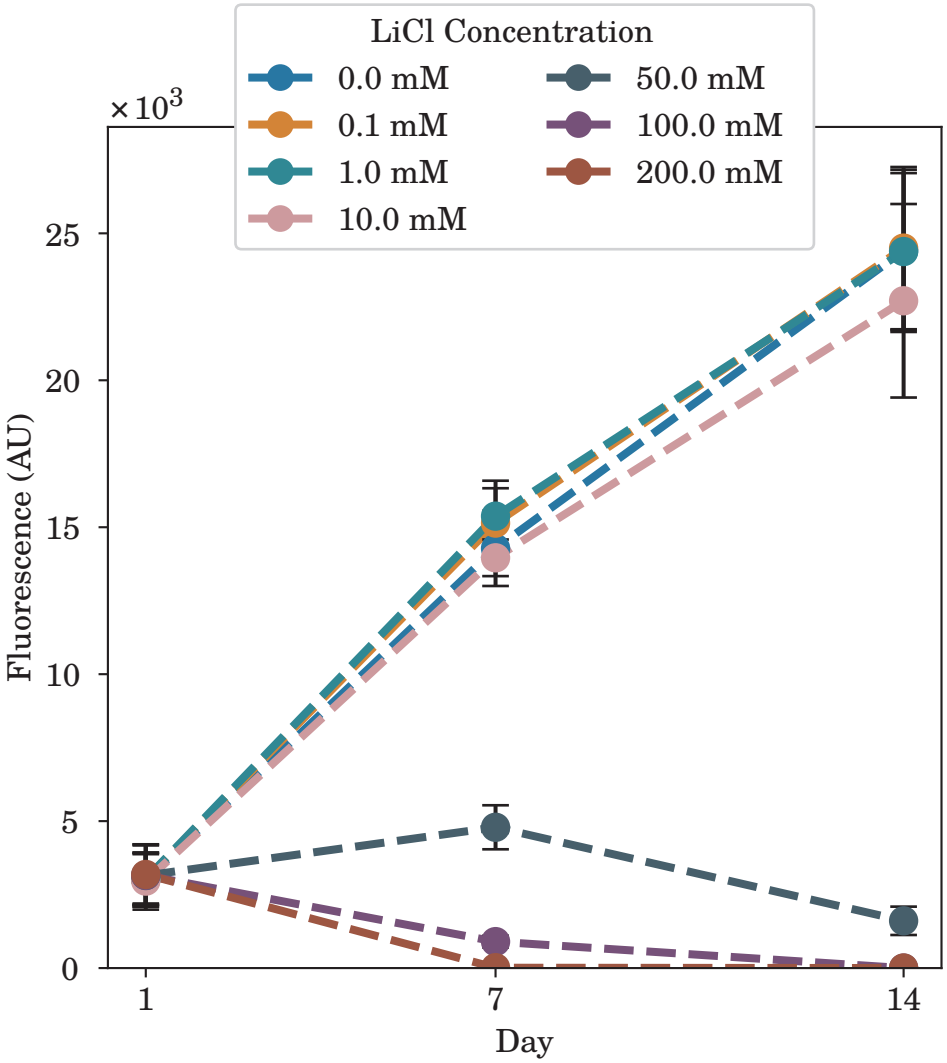


**Figure 5.6:** Effect of continuous LiCl exposure applied from day 2 on MLO-A5 metabolic activity over 14 days of monolayer culture. Cytotoxicity was observed at concentrations of 20 mM and above. Data represents mean ± SD n=9. Fluorescence was measured at $\lambda_{ex}$: 540 nm and $\lambda_{em}$: 590 nm.

in monolayer culture 10 mM LiCl treatment also had no significant effect over 14 days. At 50 mM LiCl and above, metabolic activity significantly reduced over 14 day in both monolayer and 3D culture. In 3D culture, after an initial increase in metabolic activity between day 1 and 5, 10 mM LiCl treated cell's

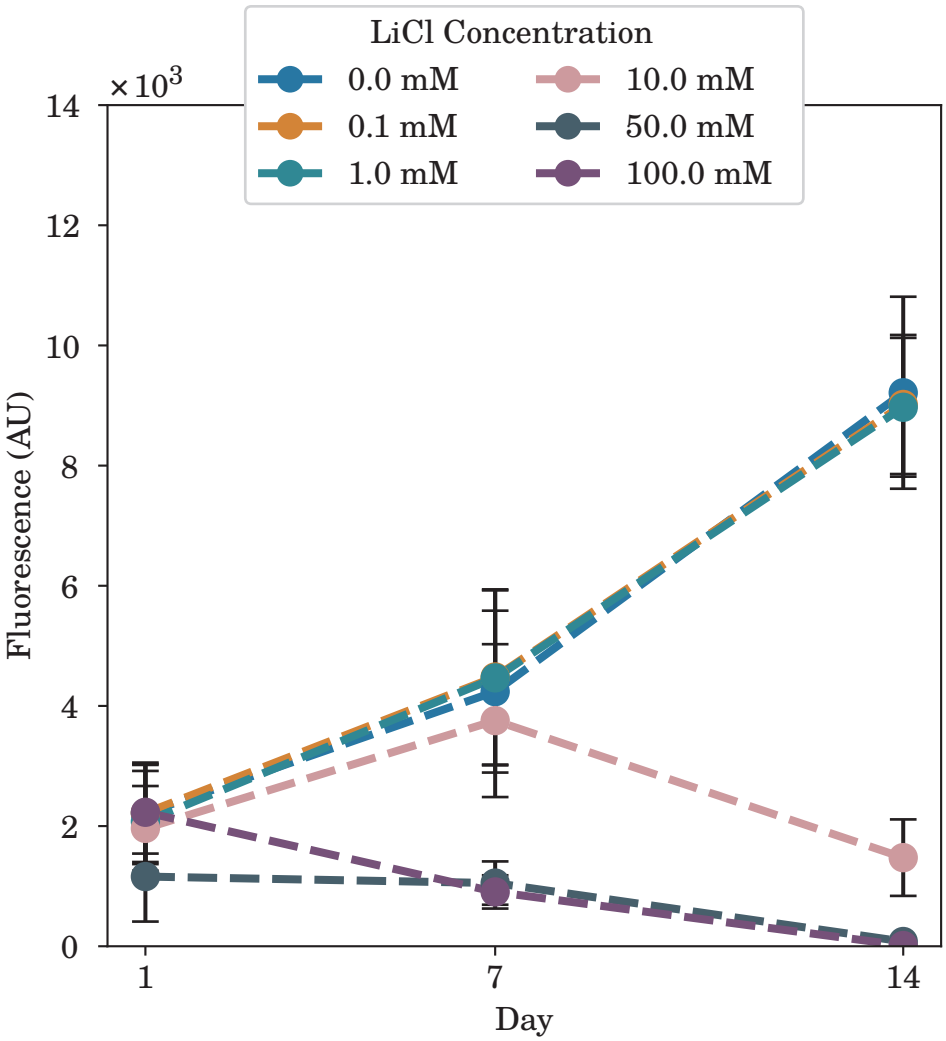


**Figure 5.7:** Effect of continuous LiCl exposure applied from day 2 on MLO-A5 metabolic activity over 14 days of 3D culture. Cytotoxicity was observed at concentrations of 10 mM and above. Data represents mean ± SD n=9. Fluorescence was measured at $\lambda_{ex}$: 540 nm and $\lambda_{em}$: 590 nm.

metabolic activity decreased back to day 1 levels.

### 5.4.2 Continuous lithium chloride treatment stimulates osteogenesis

#### Osteogenic effects of lithium chloride in hES-MP cells

ALP activity, an early marker of osteogenesis, was higher with continuous 1 mM LiCl treatment in both monolayer and 3D culture of hES-MP cells compared to the untreated control (Figures 5.8 - 5.9). This was found for both total ALP activity and normalised ALP activity. Total DNA showed similar results to the day 14 RR results. 20, 50 and 100 mM LiCl treated groups had significantly lower DNA levels compared to the untreated control. However, 10 mM LiCl treated cells were not significantly different to the untreated control, as was found in the RR assay. 0.1 mM LiCl treatment did not affect ALP activity or total DNA in monolayer or 3D culture. In addition to increasing early markers of osteogenesis, 1 mM LiCl treatment also resulted in an increase in matrix mineralisation, as shown by ARS in both monolayer and 3D culture (Figures 5.10 - 5.11). Despite the increase in matrix mineralisation at 1 mM LiCl, there was no increase found in collagen production in either monolayer or 3D culture. In fact, in monolayer culture there was a significant reduction in the amount of collagen produced after 21 days compared to the untreated control and although not statistically significant, the amount of collagen produced in 3D culture was also found to be lower. Both total matrix mineralisation and collagen production were found to be significantly lower compared to the untreated control in monolayer and 3D culture at 10 mM and above, except for matrix mineralisation in 3D culture, which although lower was not statistically different. 0.1 mM LiCl treatment did not affect matrix mineralisation or collagen production in monolayer or 3D culture.

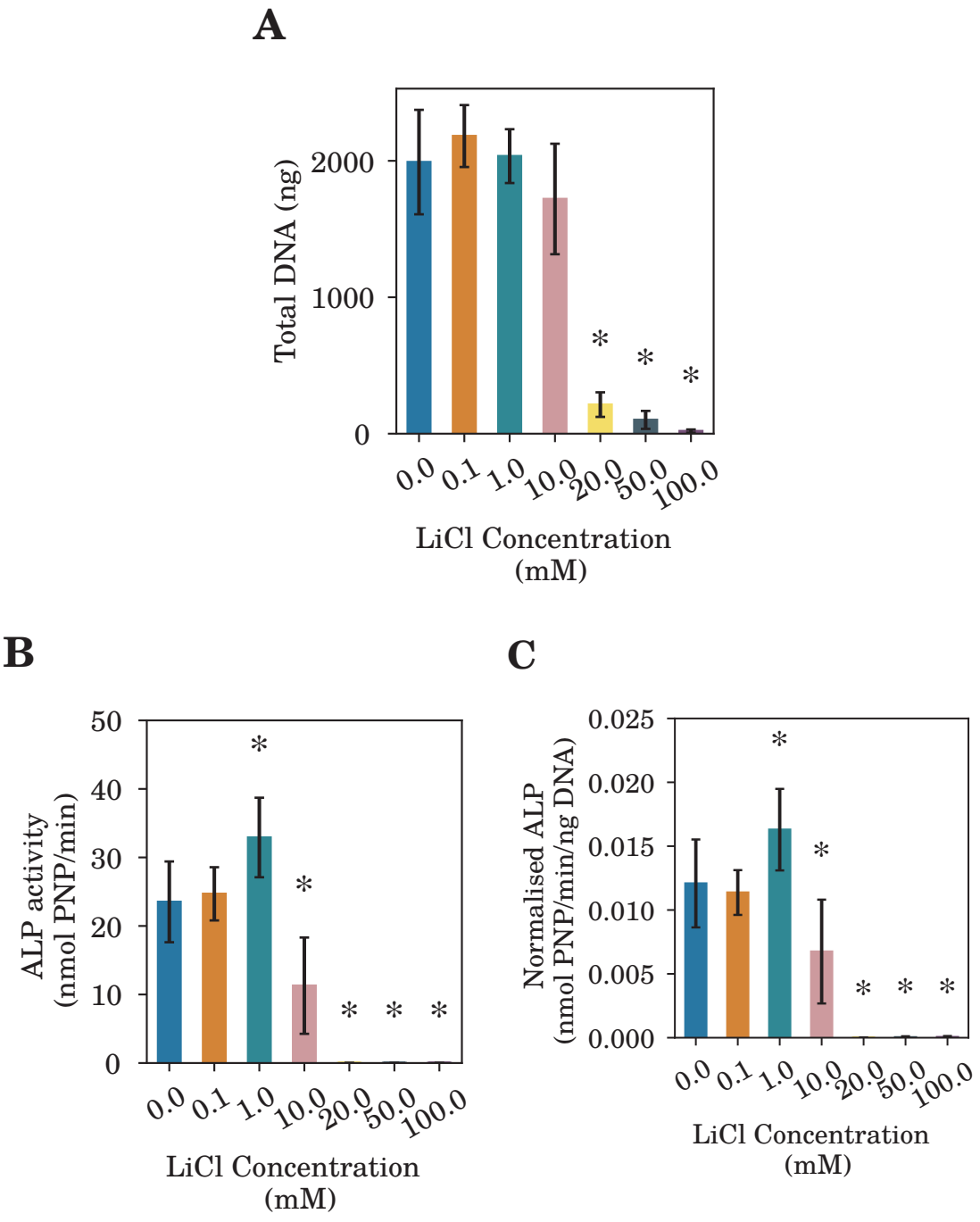


**Figure 5.8:** Effect of continuous LiCl exposure applied from day 6 on hES-MP day 14 cell number and ALP activity in monolayer culture. (A) Total DNA. (B) ALP activity. (C) ALP activity normalised to total DNA. Data represents mean ±SD n=9.

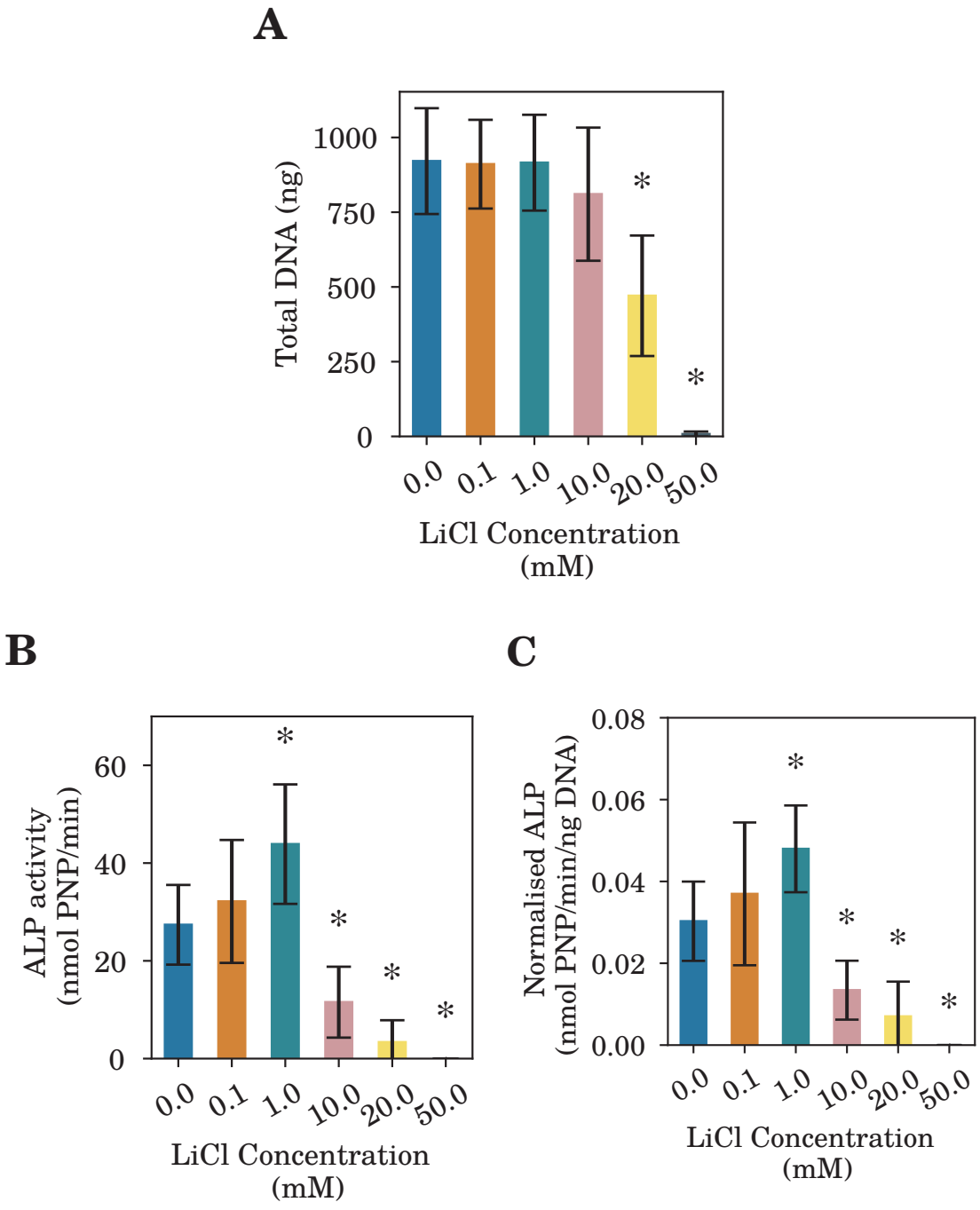


**Figure 5.9:** Effect of continuous LiCl exposure applied from day 6 on hES-MP day 14 cell number and ALP activity in 3D culture. (A) Total DNA. (B) ALP activity. (C) ALP activity normalised to total DNA. Data represents mean ±SD n=9.

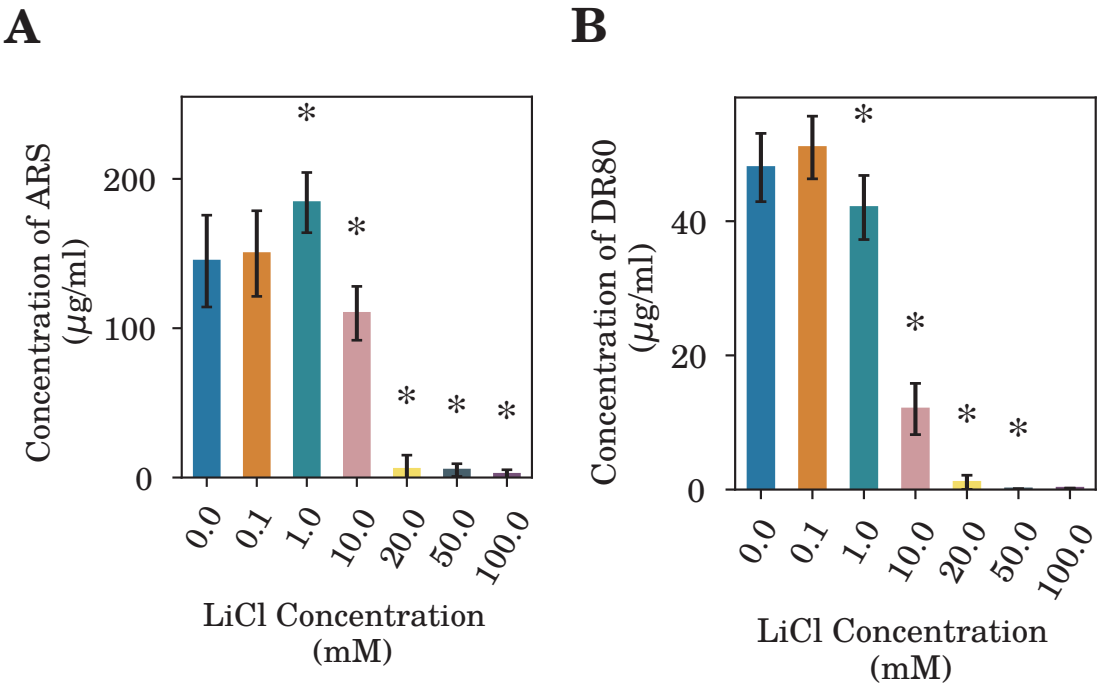


**Figure 5.10:** Effect of continuous LiCl exposure applied from day 6 on hES-MP matrix formation in monolayer culture. (A) Day 21 matrix calcium quantified by ARS. (B) Day 21 matrix collagen quantified by DR80. Data represents mean ±SD n=9.

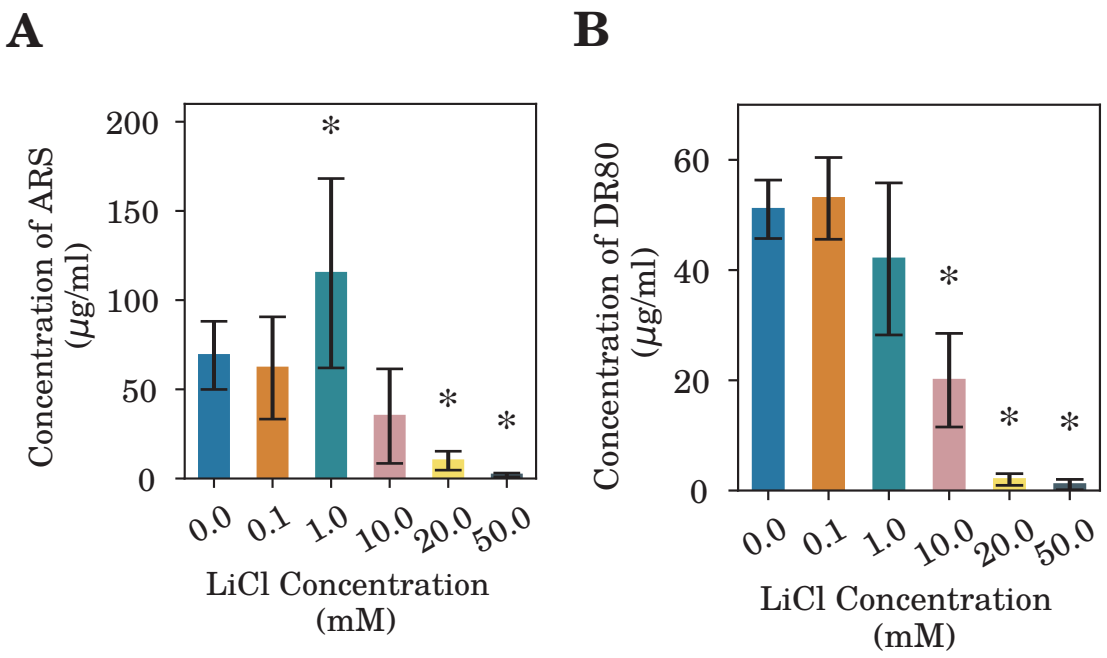


**Figure 5.11:** Effect of continuous LiCl exposure applied from day 6 on hES-MP matrix formation in 3D culture. (A) Day 21 matrix calcium quantified by ARS. Matrix calcium formation was higher in the 1 mM LiCl treated cells and lower in the 50 mM and above LiCl treated cells. (B) Day 21 matrix collagen quantified by DR80. Collagen matrix formation was lower in the 10 mM and above LiCl treated cells compared to the control. Data represents mean ±SD n=9.

**Osteogenic effects of lithium chloride in MLO-A5 cells**

One replicate of the following 3D culture results were performed by Ingvar Kiricenko during his INSIGNEO summer project under my guidance.
In MLO-A5 cells, ALP activity and total DNA was not affected by 0.1 or 10 mM LiCl treatment in monolayer or 3D culture (Figures 5.12 - 5.13). 1 mM LiCl treatment resulted in a significant increase in total ALP activity and normalised ALP activity in both monolayer and 3D culture. LiCl treatment with 10 mM and above resulted in a significant decrease in ALP activity and total DNA in both monolayer and 3D culture. Similarly to ALP activity mineralised matrix production was also significantly increased compared to the untreated control with 1 mM LiCl treatment in both monolayer and 3D culture (Figures 5.14 - 5.15) . In monolayer culture, both 0.1 and 1 mM LiCl treatment increased collagen production compared to the untreated control. At 50 mM and above, LiCl treatment resulted in no matrix mineralisation and very little collagen production in both monolayer and 3D culture. In 3D culture 10 mM LiCl treatment also resulted in a decrease in matrix mineralisation and total collagen production. However, in monolayer culture there was no significant effect.

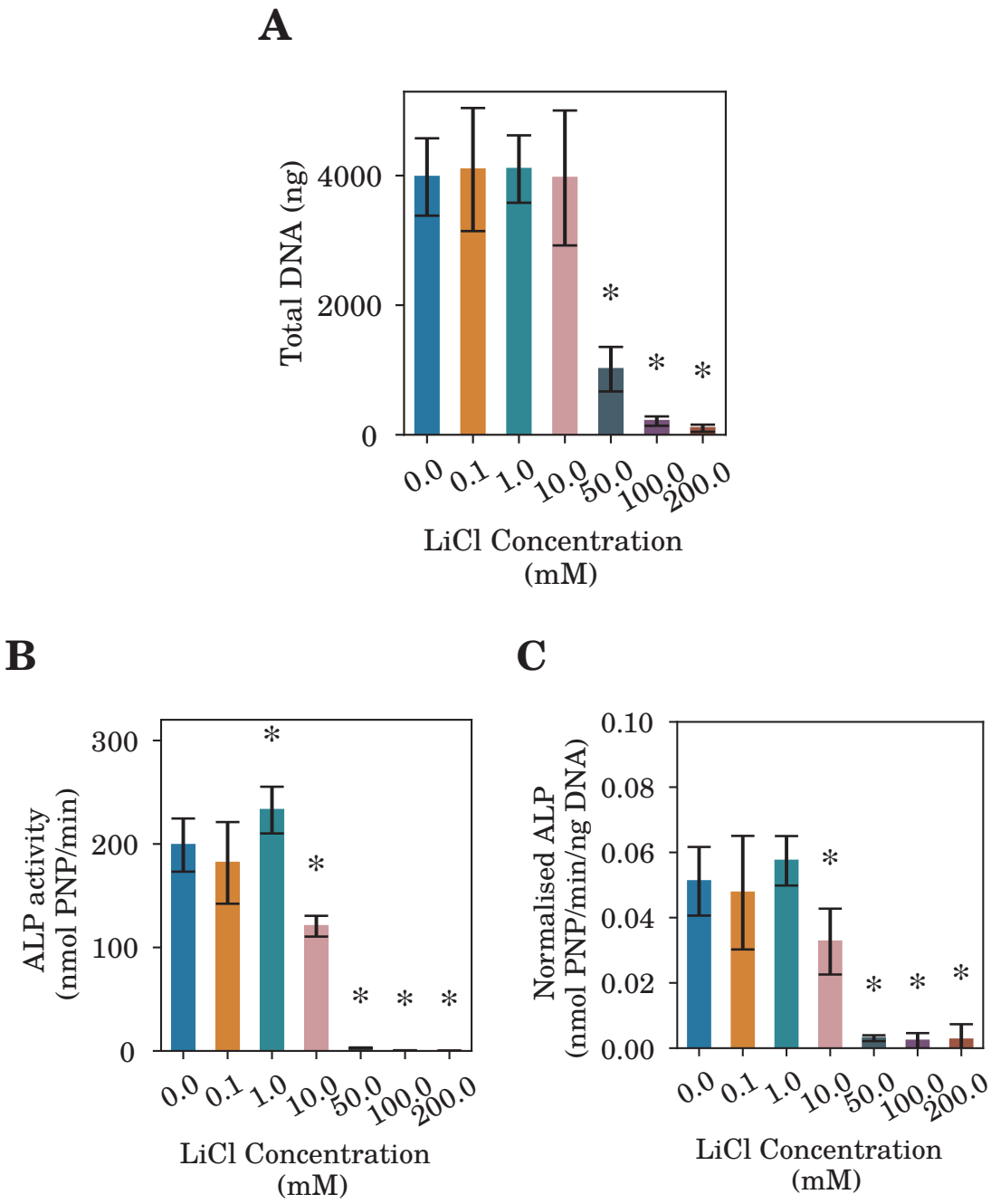


**Figure 5.12:** Effect of continuous LiCl exposure on MLO-A5 day 7 cell number and ALP activity in monolayer culture. (A) Total DNA. (B) ALP activity. (C) ALP activity normalised to total DNA. Data represents mean ±SD, n=9, * = $p<0.05$ compared to the untreated control.

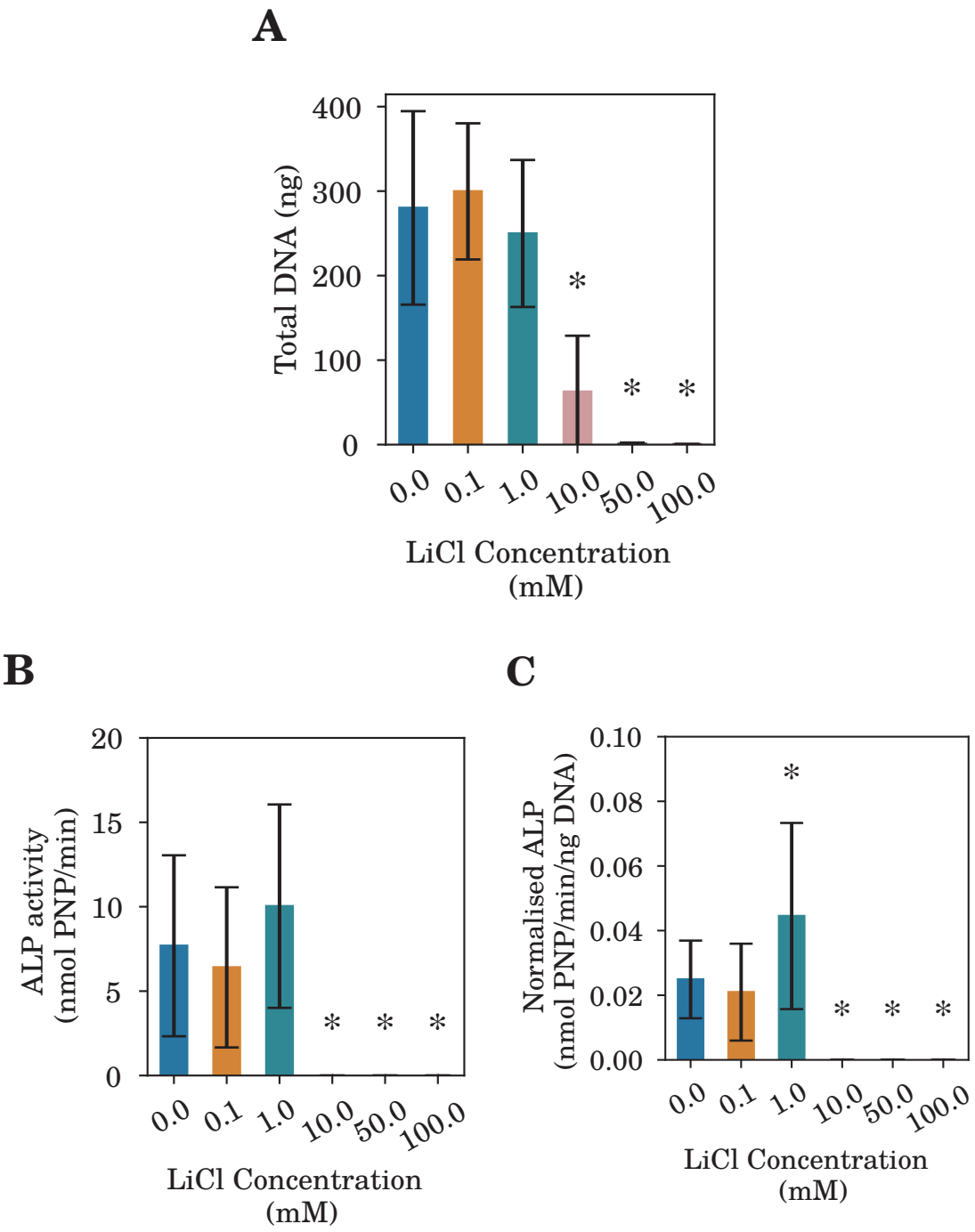


**Figure 5.13:** Effect of continuous LiCl exposure on MLO-A5 day 7 cell number and ALP activity in 3D culture. (A) Total DNA. (B) ALP activity. (C) ALP activity normalised to total DNA. Data represents mean ±SD n=9, * = $p<0.05$ compared to the untreated control.

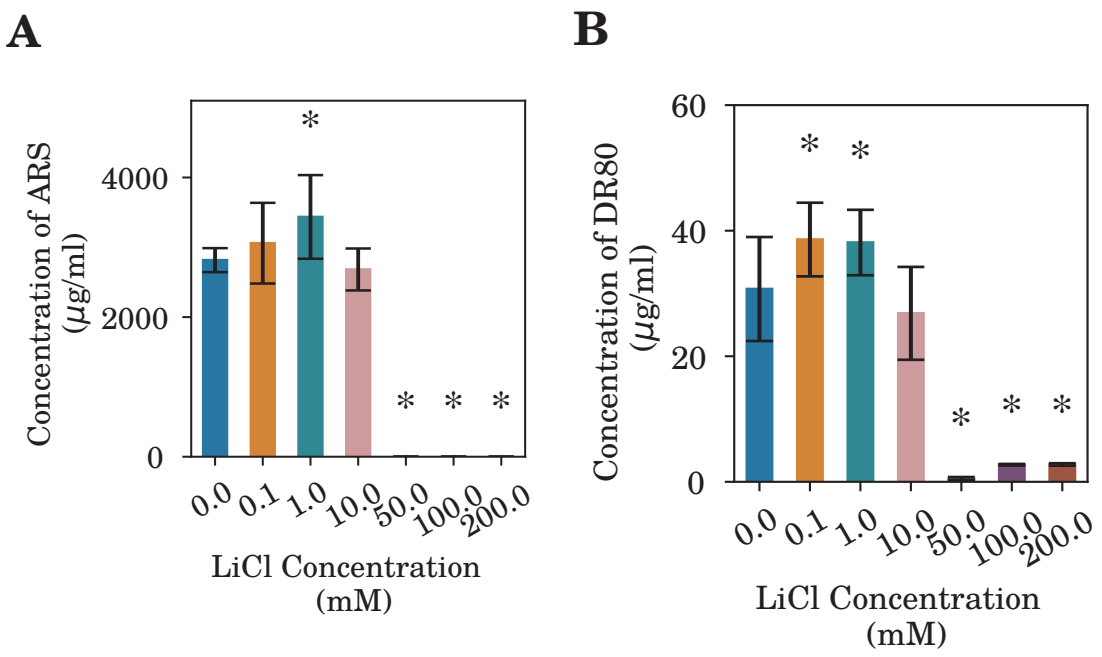


**Figure 5.14:** Effect of continuous LiCl exposure on MLO-A5 matrix formation in monolayer culture. (A) Day 14 matrix calcium quantified by ARS. (B) Day 14 matrix collagen quantified by DR80. Data represents mean ±SD n=9, * = p<0.05 compared to the untreated control.

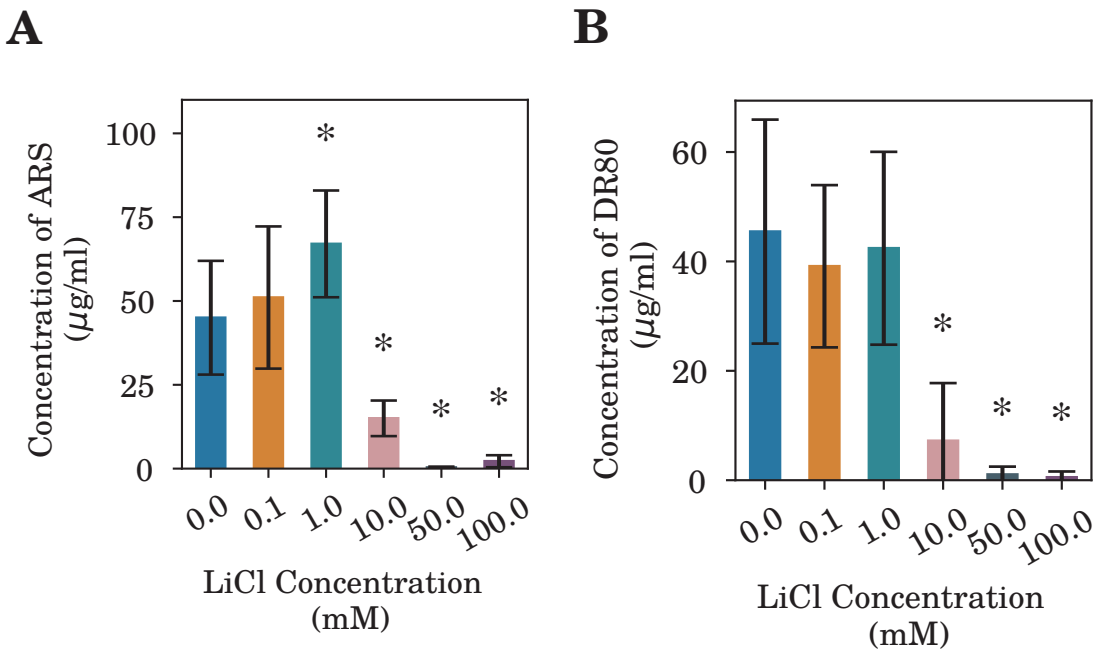


**Figure 5.15:** Effect of continuous LiCl exposure on MLO-A5 matrix formation in 3D culture. (A) Day 14 matrix calcium quantified by ARS. (B) Day 14 matrix collagen quantified by DR80. Data represents mean ±SD n=9, * = p<0.05 compared to the untreated control.

### 5.4.3 Short term lithium treatment does not stimulate osteogenesis

In order to assess if lithium treatment alters mechanoinduced osteogenic responses, a LiCl treatment regime that did not affect osteogenesis in static conditions was required. Therefore, shorter term LiCl treatments were assessed for their osteogenic effects.

#### Short term lithium chloride treatment in hES-MP cells cultured in 2D

In monolayer culture of hES-MP cells were treated with LiCl for 24 h on day 6 (single treatment) only or day 6 and day 13 (intermittent treatment) of culture. 50 mM LiCl treatment resulted in minimally detectable metabolic activity indicating cell death. However, the reduction in metabolic activity over the 21 day culture period occurred at a slower rate, taking 21 days compared to 14 days for metabolic activity to reduce to near zero levels with both a single dose (Figure 5.16) and double dose (Figure 5.17). 20 mM LiCl treatment resulted in lower metabolic activity by day 21 in both single and double dose treatment regimens compared to the untreated control. In addition, both single and double dose 20 mM LiCl treatments had significantly lower metabolic activity on day 21 of culture compared to the untreated control.
With both single dose and intermittent treatment regimens 1 mM LiCl or lower had no effect on ALP activity or total DNA (Figure 5.18). Although day 14 metabolic activity was only significantly lower with intermittent treatment in 20 mM LiCl treated cells, total DNA was significantly lower in both single dose and intermittent treatment regimens compared to the untreated control. 20 mM LiCl treatment decreased total DNA and ALP activity compared to the untreated control with both single dose and intermittent treatment. Matrix mineralisation and total collagen production was decreased in both single dose and intermittent treatment groups when treated with 20 mM LiCl and above (Figure 5.19). At 10 mM, only intermittent LiCl treatment significantly reduced matrix mineralisation compared to the untreated control. However, both single dose and intermittent treatment at 10 mM LiCl significantly reduced collagen production. At 1 mM or below, LiCl treatment did not affect either matrix mineralisation or total collagen production in either single dose or intermittent treatment.

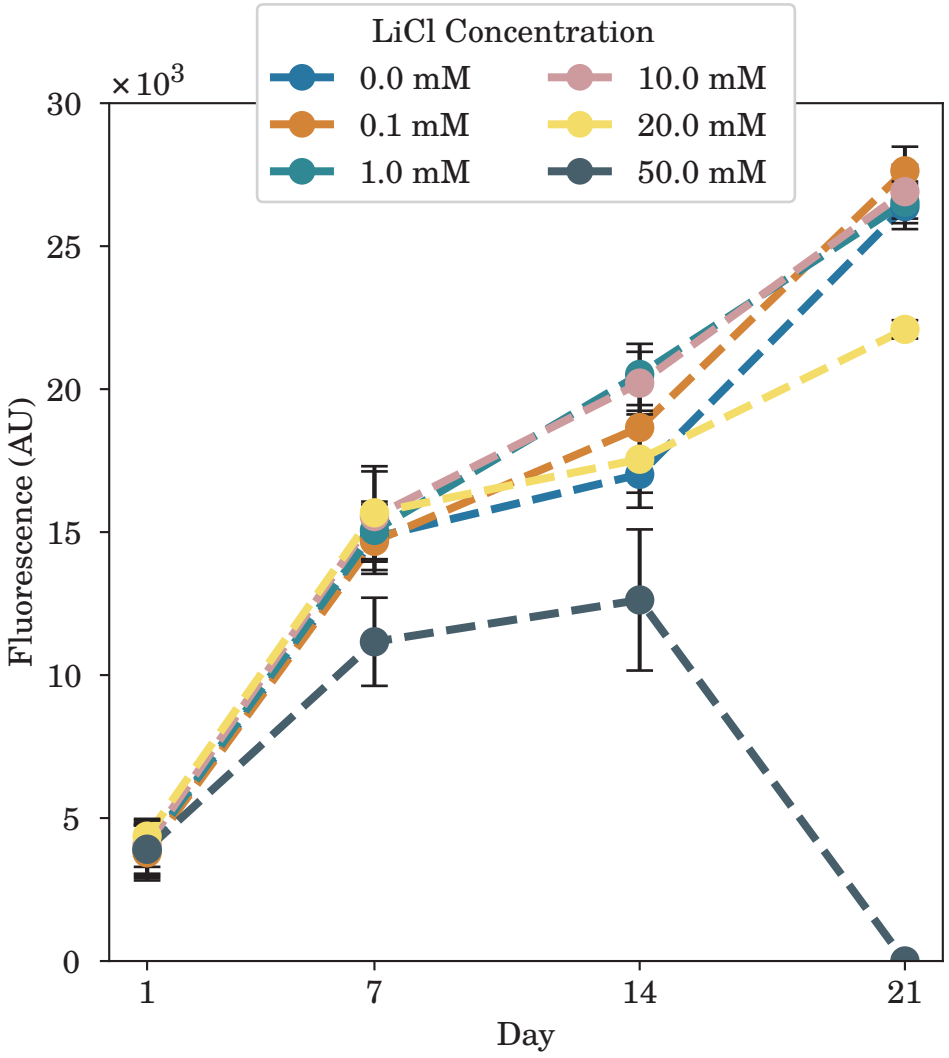


**Figure 5.16:** Effect of a single LiCl exposure on hES-MP metabolic activity over 21 days of culture monolayer culture. Data represents mean ±SD n=9. Fluorescence was measured at $\lambda_{ex}$: 540 nm and $\lambda_{em}$: 590 nm.

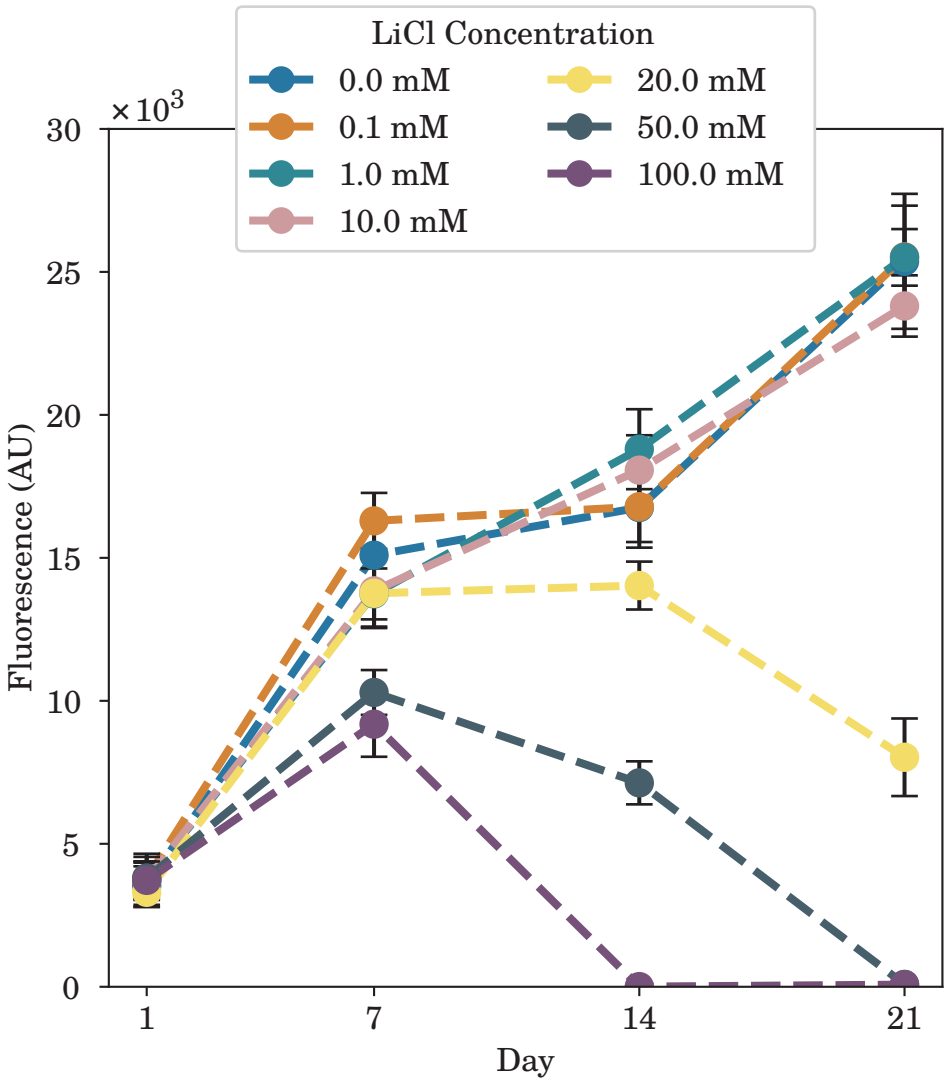


**Figure 5.17:** Effect of intermittent LiCl exposure on hES-MP metabolic activity over 21 days of monolayer culture. Data represents mean ±SD n=9. Fluorescence was measured at $\lambda_{ex}$: 540 nm and $\lambda_{em}$: 590 nm.

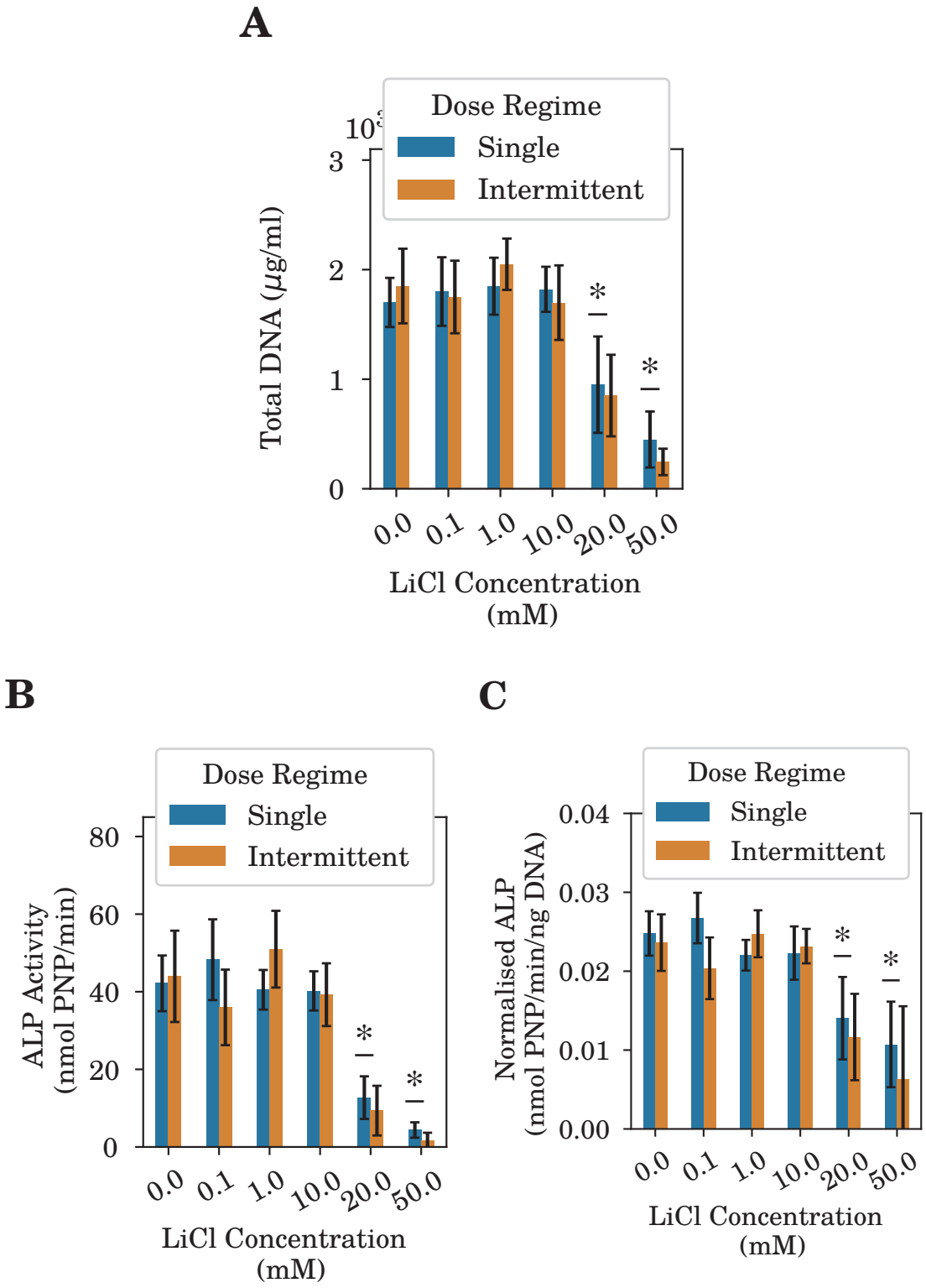


**Figure 5.18:** Effects of a single and intermittent LiCl exposure on hES-MP day 14 cell number and ALP activity. (A) Total DNA. (B) ALP activity. (C) ALP activity normalised to total DNA. Data represents mean ±SD n=9, * = $p<0.05$ compared to the untreated control.

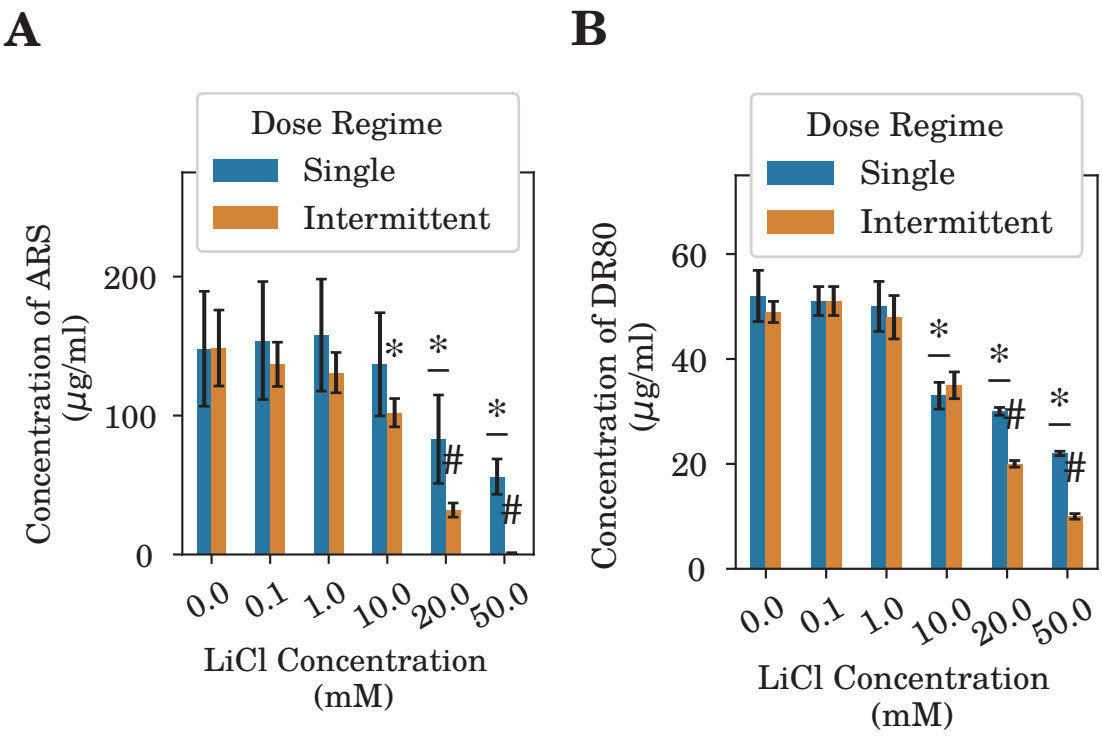


**Figure 5.19:** Effects of a single and intermittent LiCl exposure on hES-MP matrix formation. (A) Day 21 matrix calcium quantified by ARS. (B) Day 21 matrix collagen quantified by DR80. Data represents mean ±SD n=9. * = $p<0.05$ compared to the untreated control. # = $p<0.05$ compared to the single treatment regime.

### Short term lithium chloride treatment in hES-MP cells cultured in 3D

In 3D culture of hES-MP cells 24 h treatments of LiCl were applied on day 4, 12 and 17. Intermittent LiCl treatment had no significant effects on metabolic activity at any time point compared to the untreated control (Figure 5.20). However, 10 mM was the only concentration to show no significant increase in metabolic activity between day 7 and 21. There were no significant differences in total DNA or ALP activity on day 14 (Figure 5.21). There were also no significant differences in day 21 matrix mineralisation or total collagen production (Figure 5.22).

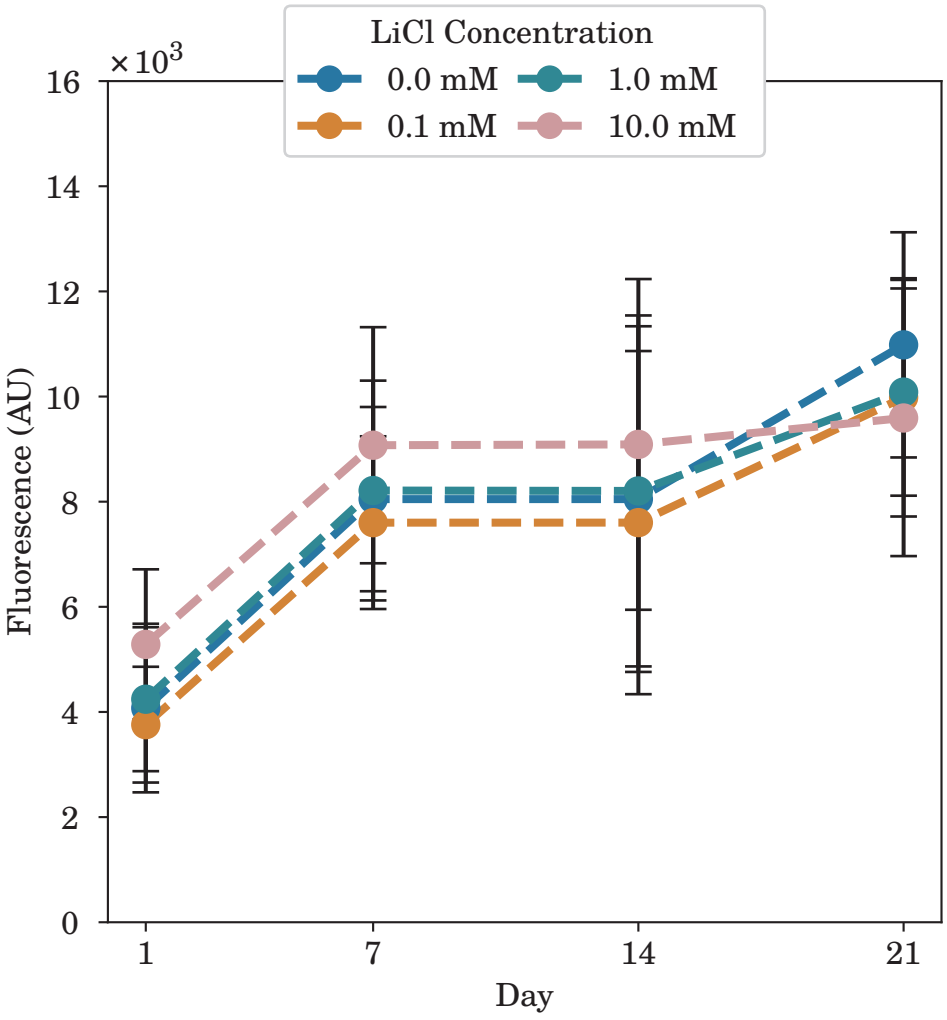


**Figure 5.20:** Effect of three 24 hour LiCl exposures on hES-MP metabolic activity over 21 days of culture. Data represents mean ±SD n=9. Fluorescence was measured at $\lambda_{ex}$: 540 nm and $\lambda_{em}$: 590 nm.

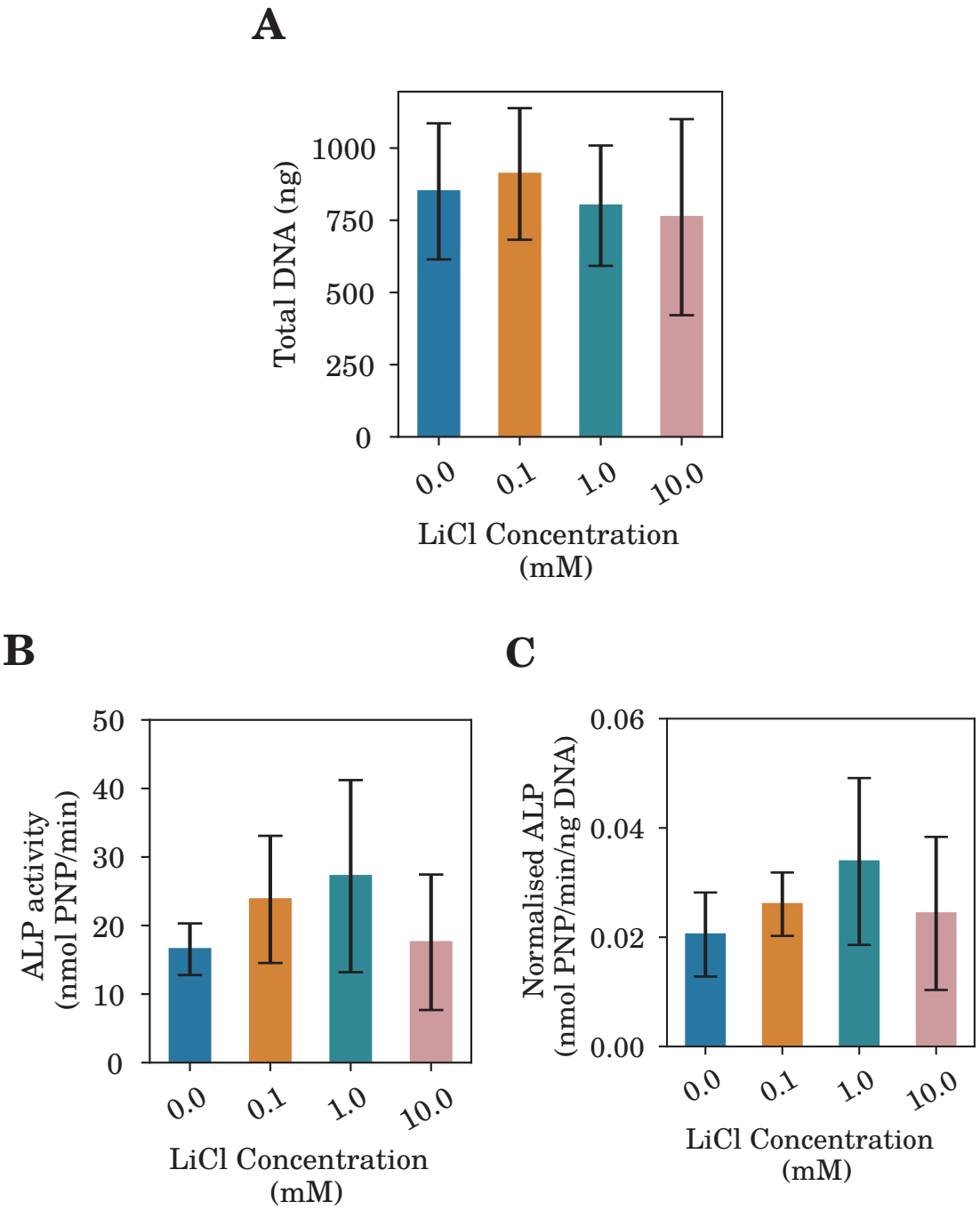


**Figure 5.21:** Effect of three 24 hour LiCl exposures on hES-MP day 14 cell number and ALP activity. (A) Total DNA. (B) ALP activity. (C) ALP activity normalised to total DNA. Data represents mean ±SD n=9.

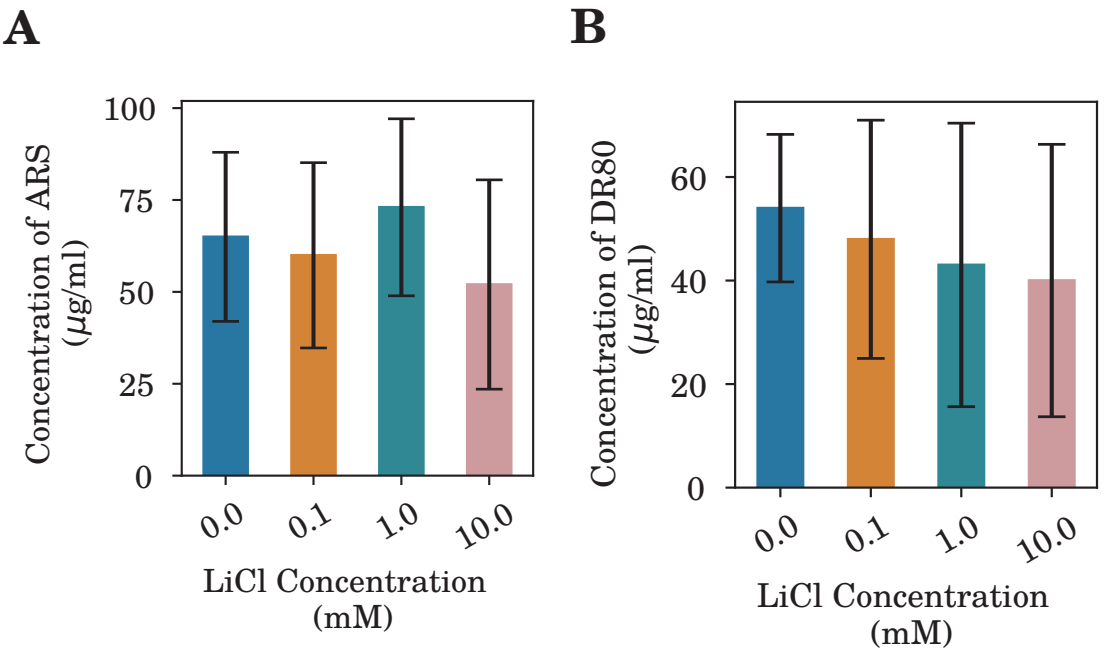


**Figure 5.22:** Effect of three 24 hour LiCl exposures on hES-MP matrix formation. (A) Day 21 matrix calcium quantified by ARS. (B) Day 21 matrix collagen quantified by DR80. Data represents mean ±SD n=9.

**Short term lithium chloride treatment in MLO-A5 cells cultured in 2D**

Repeats of the following results were performed by Ingvar Kiricenko during his INSIGNEO summer project under my guidance.

LiCl was applied for 24 h on day 2 and 7 for intermittent treatment of MLO-A5 cells. On day 7 only 100 mM LiCl treatment resulted in a decrease in metabolic activity compared to day 1, which remained at near zero levels on day 14 (Figure 5.23). Although metabolic activity increased from day 1 to 7 in both 20 and 50 mM LiCl treated cells, their metabolic activity was significantly lower than the untreated control.

Although day 7 metabolic activity was lower in 50 mM LiCl treated cells, day 14 total DNA was not significantly different to the untreated control (Figure 5.24). At concentrations below 50 mM there were also no significant effects on total DNA. Both 50 and 100 mM LiCl treatment significantly decreased total DNA levels and ALP activity. Although, 10 and 50 mM LiCl treatment significantly decreased total ALP activity, when normalised to total DNA this was no longer significant. 1 mM LiCl treatment and below had no significant effect on ALP activity. Interestingly, although both 10 and 50 mM LiCl treatment decreased total ALP activity, they both increased matrix mineralisation compared to the untreated control (Figure 5.25). Additionally, although 50 mM LiCl treatment decreased ALP activity, matrix mineralisation and total collagen production were not affected. Treatment with 1 mM LiCl and below had no effect on matrix mineralisation or total collagen production.

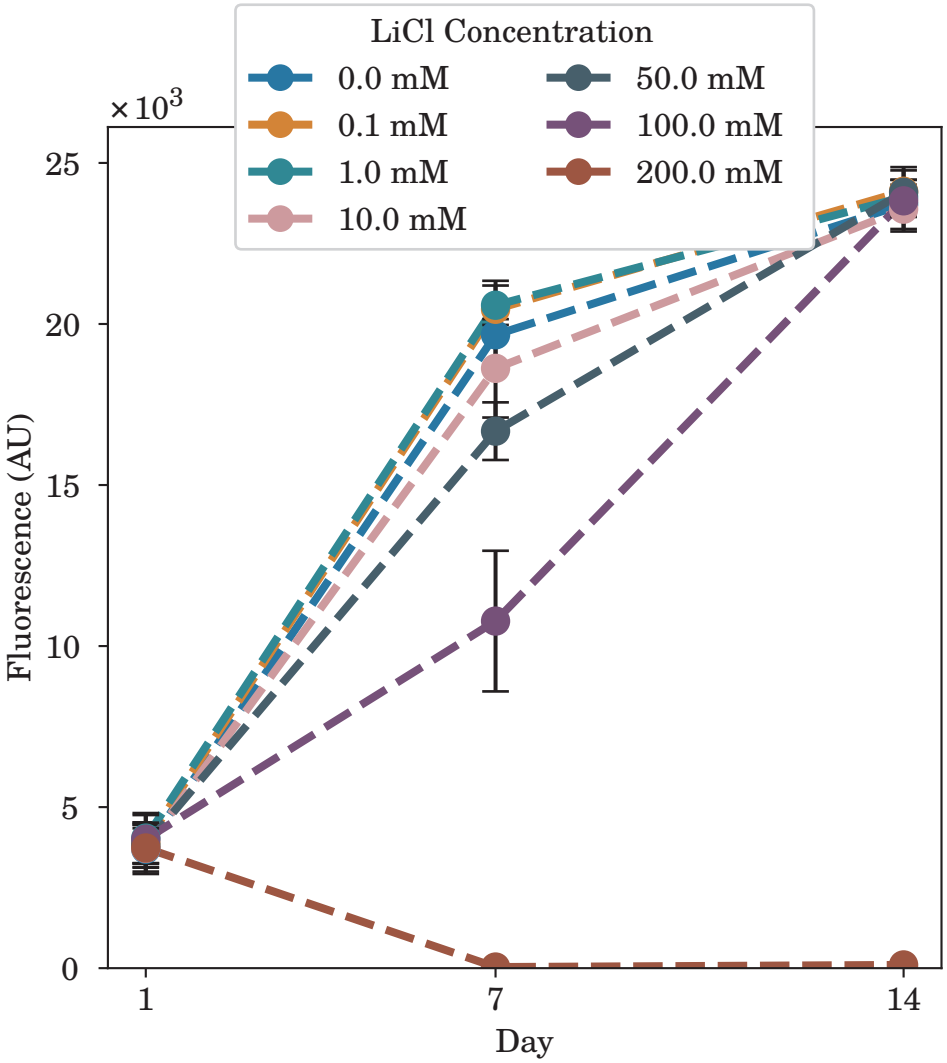


**Figure 5.23:** Effect of intermittent LiCl exposure on MLO-A5 metabolic activity over 14 days of monolayer culture. Cytotoxicity was observed at concentrations of 100 mM and above. Data represents mean ±SD n=9. Fluorescence was measured at $\lambda_{ex}$: 540 nm and $\lambda_{em}$: 590 nm.

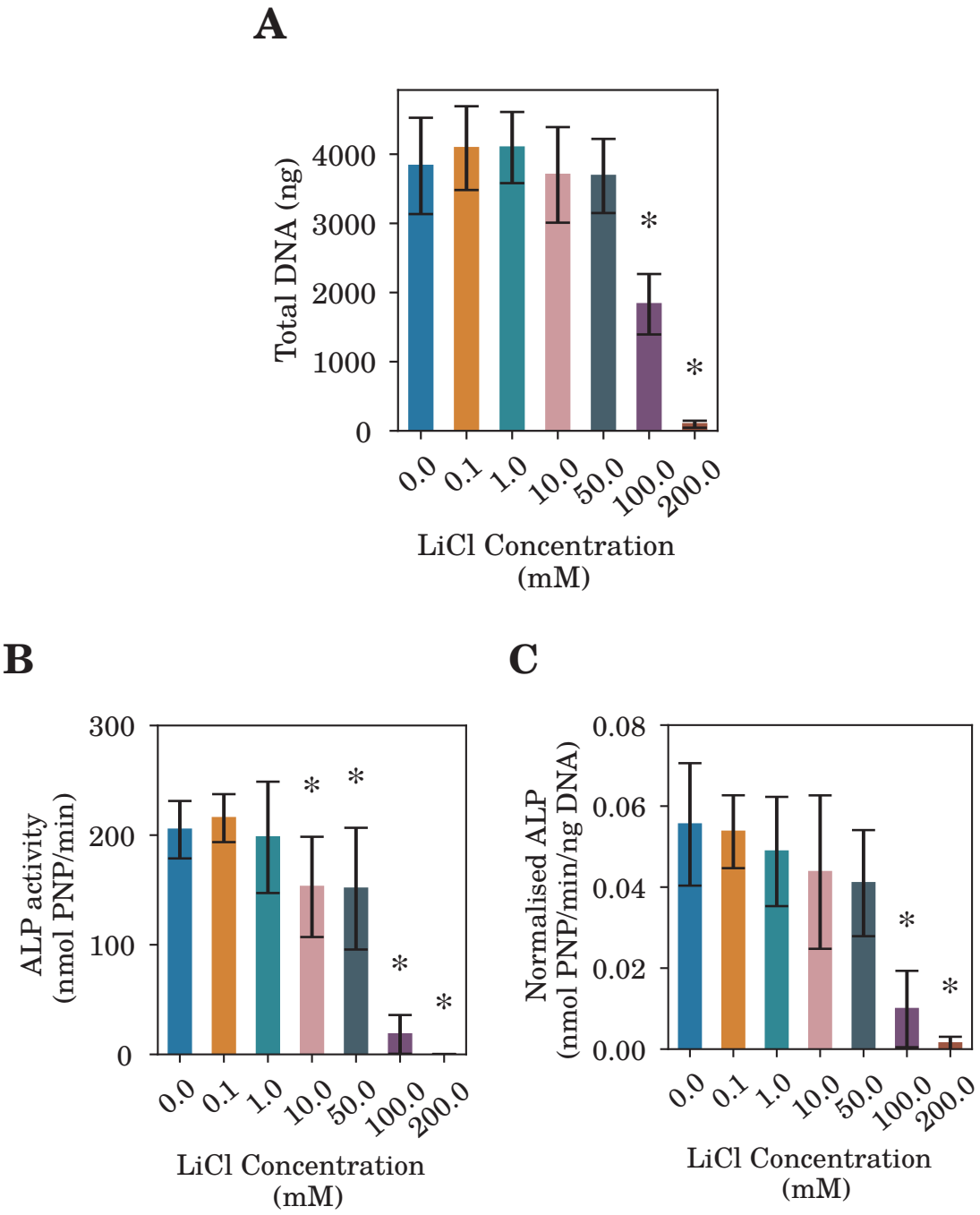


**Figure 5.24:** Effect of intermittent LiCl exposure on MLO-A5 day 7 cell number and ALP activity in monolayer culture. (A) Total DNA. (B) ALP activity. (C) ALP activity normalised to total DNA. Data represents mean ±SD n=9. * = $p<0.05$ compared to the untreated control.

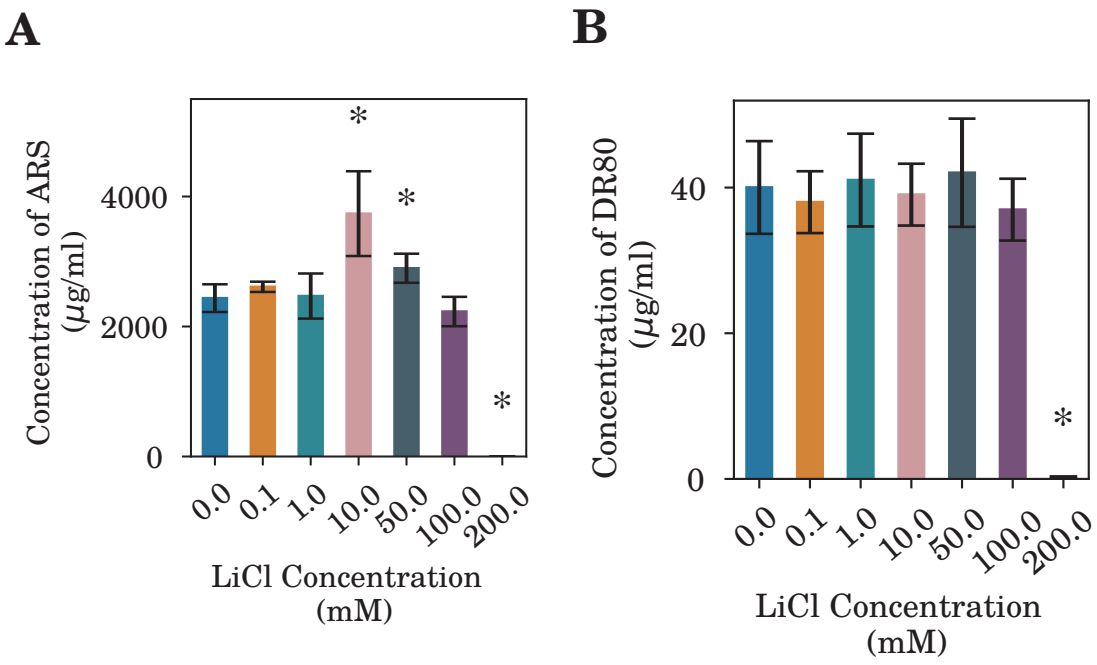


**Figure 5.25:** Effect of intermittent LiCl exposure on MLO-A5 matrix formation in monolayer culture. (A) Day 14 matrix calcium quantified by ARS. (B) Day 14 matrix collagen quantified by DR80. Data represents mean ±SD n=9. * = $p<0.05$ compared to the untreated control..

**Short term lithium chloride treatment in MLO-A5 cells cultured in 3D**

Repeats of the following results were performed by Ingvar Kiricenko during his INSIGNEO summer project under my guidance.
In 3D culture intermittent LiCl treatment was applied for 24 h on day 2 and 7 of culture. 0.1 and 1 mM LiCl treatment had no effect on metabolic activity over the 14 day culture period (Figure 5.26). 10 mM LiCl treatment resulted

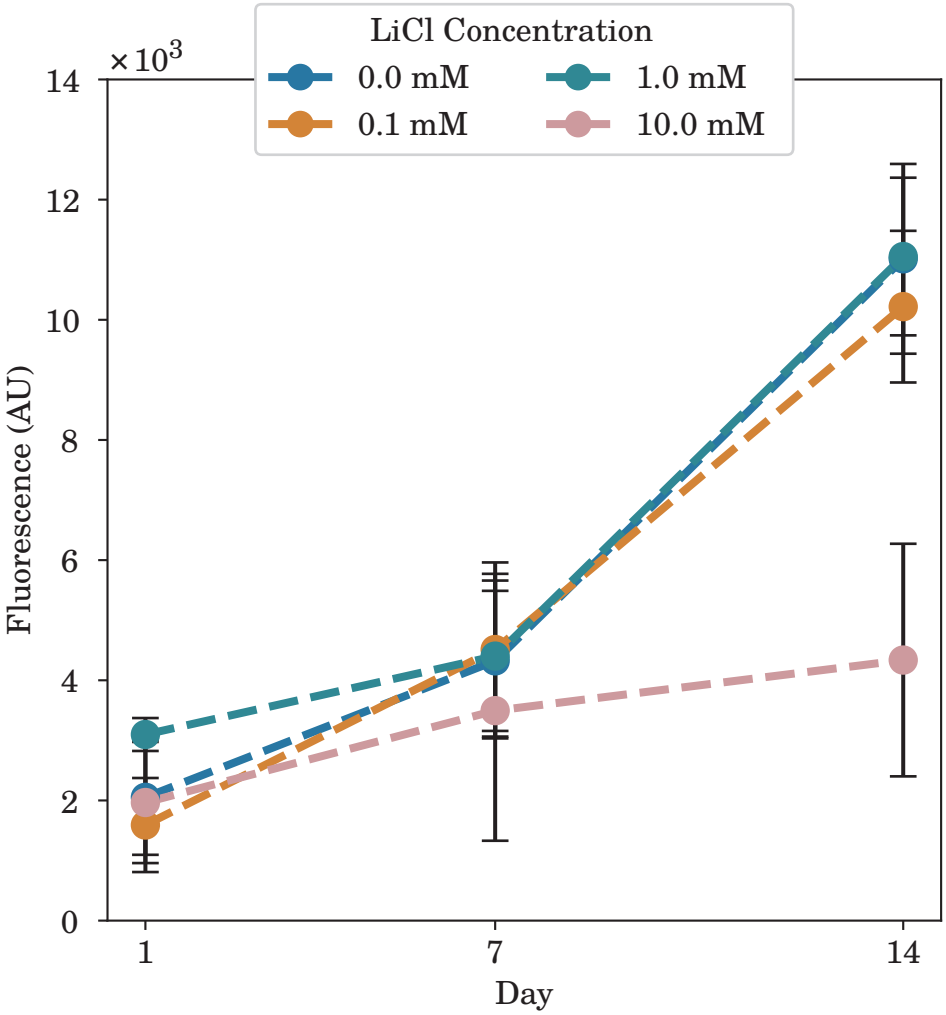


**Figure 5.26:** Effect of intermittent LiCl exposure on MLO-A5 metabolic activity over 14 days of 3D culture. Cytotoxicity was observed at concentrations of 10 mM and above. Data represents mean ±SD n=9. Fluorescence was measured at $\lambda_{ex}$: 540 nm and $\lambda_{em}$: 590 nm.

in significantly lower metabolic activity on day 14 of culture compared to the untreated control. 10 mM LiCl treatment decreased day 7 total DNA and total ALP activity (Figure 5.27). However, when ALP activity was normalised to total DNA this was no longer significant. No other concentration tested had an effect on ALP activity or total DNA. Intermittent LiCl did not affect matrix

mineralisation at any of the concentrations tested (Figure 5.28). Only 10 mM LiCl treatment had a significant effect on total collagen production, causing a decrease in collagen compared to the untreated control.

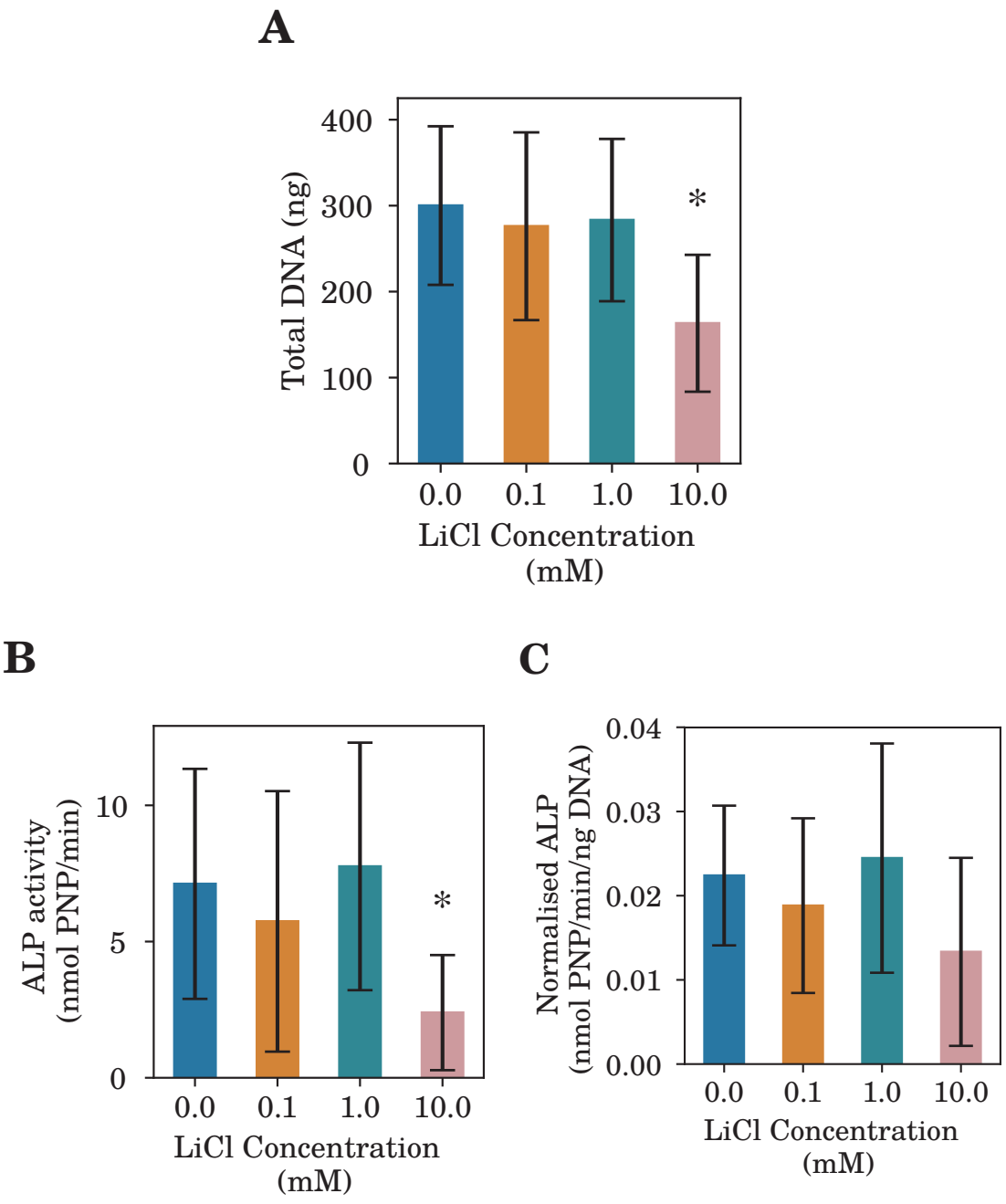


**Figure 5.27:** Effect of intermittent LiCl exposure on MLO-A5 day 7 cell number and ALP activity in 3D culture. (A) Total DNA. (B) ALP activity. (C) ALP activity normalised to total DNA. Data represents mean ±SD n=9. * = $p<0.05$ compared to the untreated control.

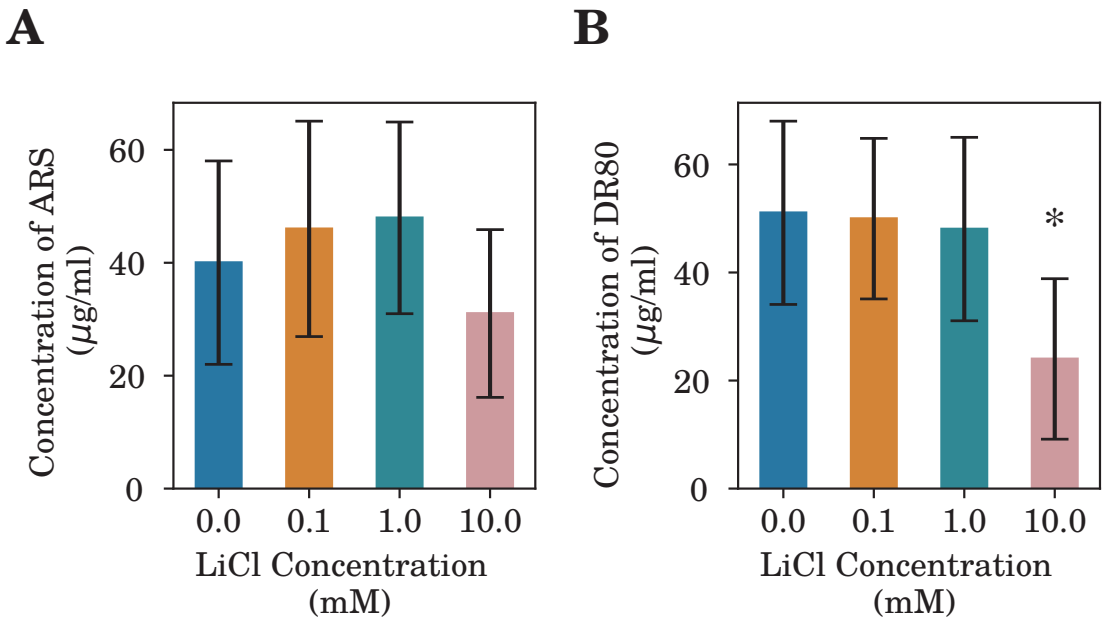


**Figure 5.28:** Effect of intermittent LiCl exposure on MLO-A5 matrix formation in 3D culture. (A) Day 14 matrix calcium quantified by ARS. (B) Day 14 matrix collagen quantified by DR80. Data represents mean ±SD n=9. * = $p<0.05$ compared to the untreated control.

### 5.4.4 1 mM lithium chloride does not induce osteogenic differentiation

The previously reported experiments using hES-MP cells have all been performed with media containing Dex for the first 5 days of culture. Dex itself stimulates osteogenic differentiation, therefore, to assess the effects of lithium on osteogenic differentiation 1 mM LiCl was applied either continuously or intermittently in hES-MP cells cultured without Dex (SM) and compared with culture with Dex to day 5 (dexamethasone withdrawn media (DW)). hES-MP cells cultured in SM showed a significantly greater increase in metabolic activity over 21 days compared to hES-MP cells cultured in DW ($p \leq 0.05$) (Figure 5.29). On day 7 of culture cells cultured in SM media and continuously treated with LiCl had significantly higher metabolic activity compared to the untreated control cultured in SM ($p \leq 0.05$). There were no other significant differences between groups in SM cultured cells at any other time point. In DW cultured cells, there were no significant differences between treatment groups on any day except day 21, where continuous LiCl treated cells had a higher metabolic activity compared to the untreated control ($p \leq 0.05$). Similarly to the RR results LiCl had no effect on day 14 total DNA levels in either media type (Figure 5.30). ALP activity was significantly lower in hES-MP cells cultured in SM compared to DW. In hES-MP cells cultured in SM LiCl had no effect on ALP activity. However, as previously shown continuous LiCl treatment significantly increased ALP activity in DW cultured cells. Total collagen production was not significantly different between SM and DW culture. Continuous, but not intermittent LiCl treatment significantly reduced total collagen production compared to the untreated control (Figure 5.31). In SM cultured hES-MP cells LiCl had no effect on total collagen production with either continuous or intermittent treatment. Matrix mineralisation was significantly lower in hES-MP cells cultured in SM compared to DW. In DW cultured hES-MP cells continuous, but not intermittent LiCl treatment significantly increased matrix mineralisation compared to the control. In SM cultured hES-MP cells LiCl treatment had no effect on matrix mineralisation with either continuous or intermittent treatment.

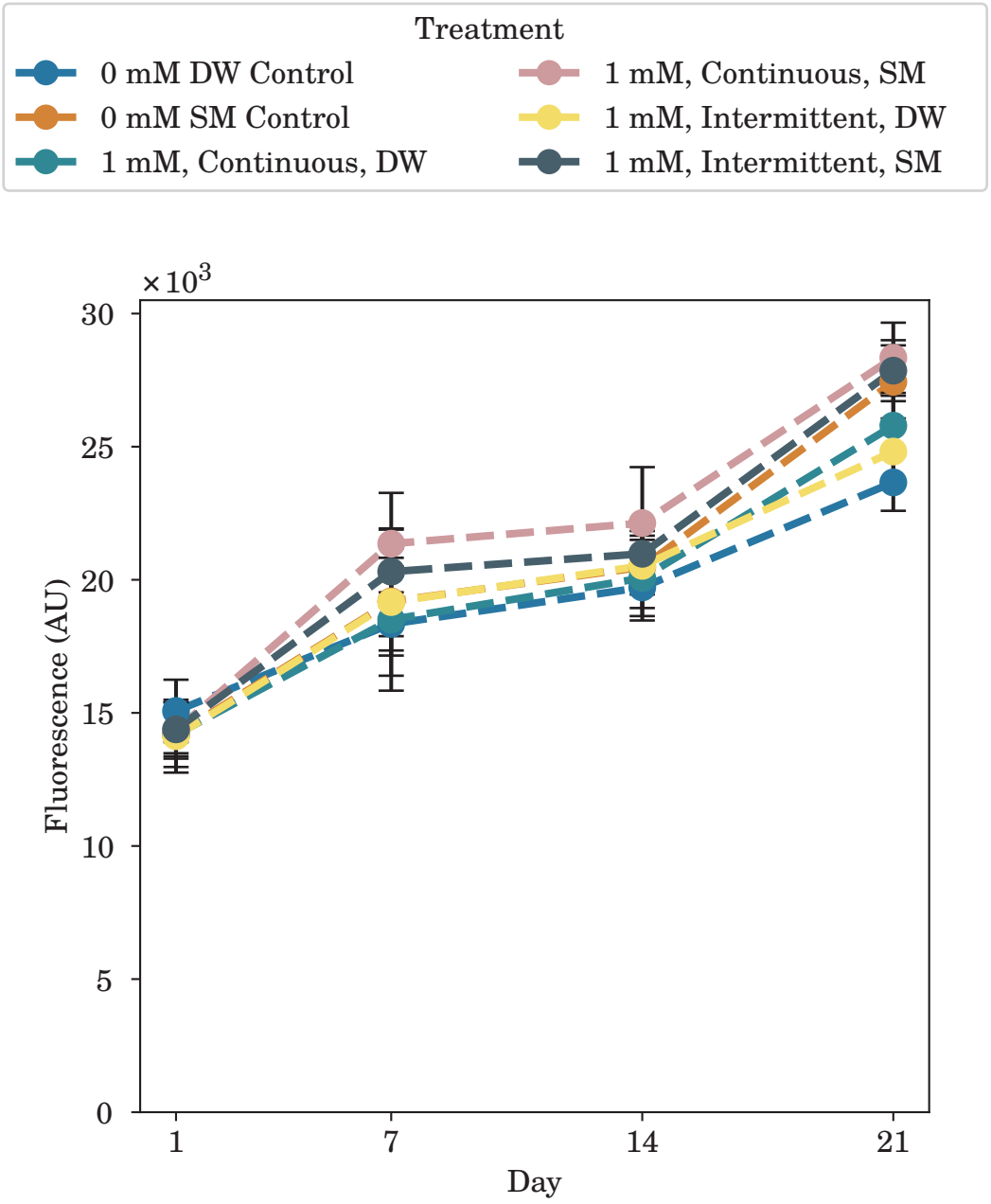


**Figure 5.29:** Comparison of the effects of intermittent and continuous LiCl exposure on hES-MP metabolic activity in SM or DW monolayer culture. Data represents mean ±SD n=9. Fluorescence was measured at $\lambda_{ex}$: 540 nm and $\lambda_{em}$: 590 nm.

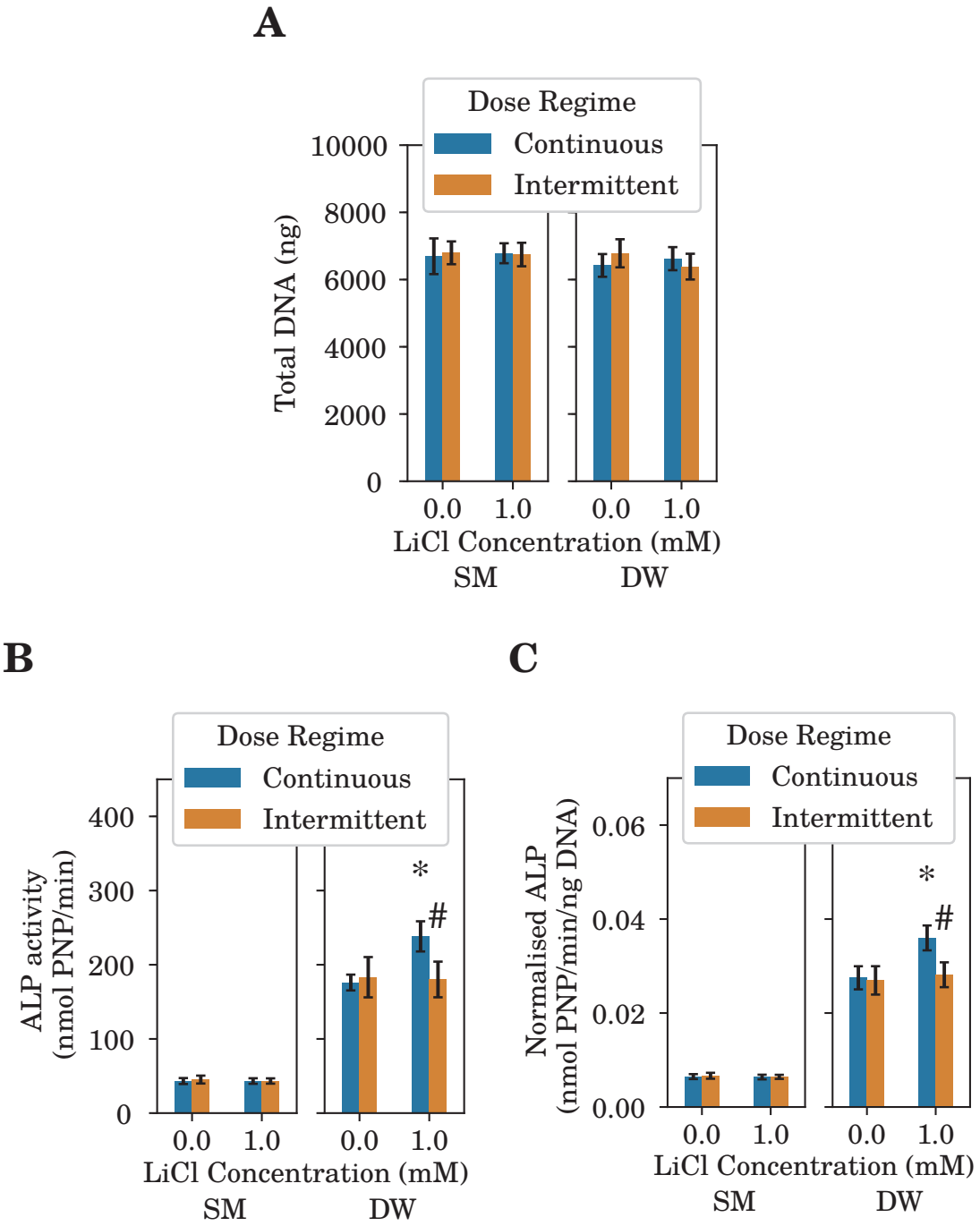


**Figure 5.30:** Comparison of the effects of intermittent and continuous LiCl exposure on hES-MP ALP activity in SM and DW monolayer culture. (A) Total DNA. (B) ALP activity. (C) ALP activity normalised to total DNA. Data represents mean ±SD n=9. * = $p<0.05$ compared to the untreated control. # = $p<0.05$ compared to the continuous treatment regime.

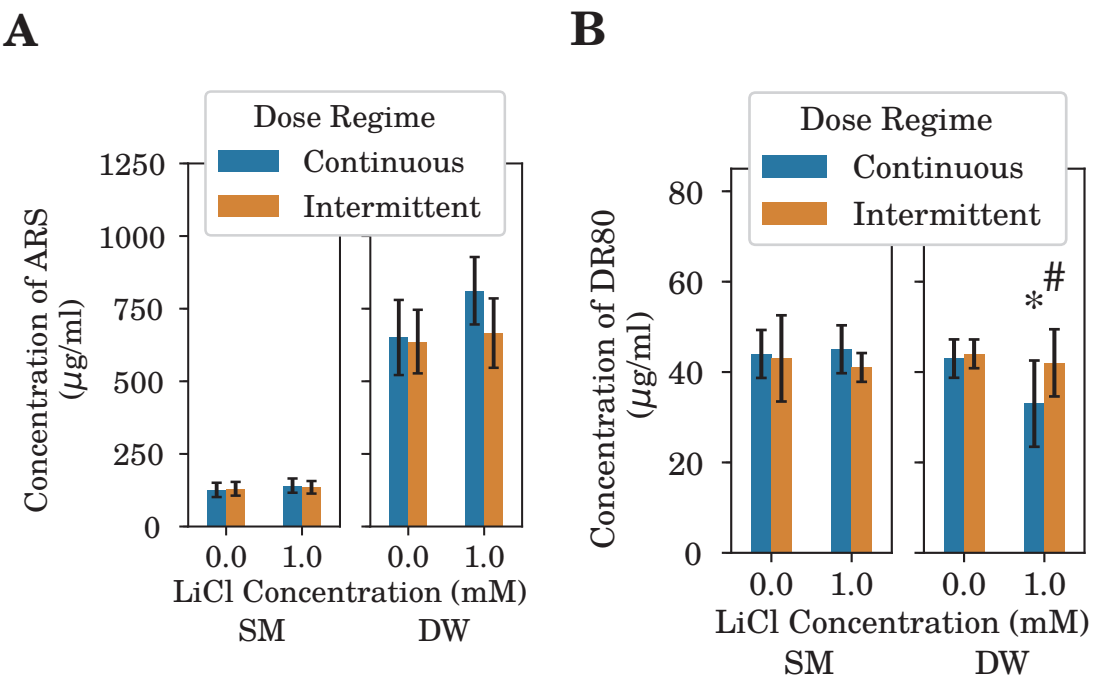


**Figure 5.31:** Comparison of the effects of intermittent and continuous LiCl exposure on hES-MP matrix formation in SM and DW monolayer culture. (A) Day 14 matrix calcium quantified by ARS. (B) Day 14 matrix collagen quantified by DR80. Data represents mean ±SD n=9. * = $p<0.05$ compared to the untreated control. # = $p<0.05$ compared to the continuous treatment regime.

### 5.4.5 1 mM lithium chloride induces primary cilia elongation

In addition to lithium's direct effects on osteogenesis, lithium treatment has also been shown to elongate primary cilia. Since primary cilia are thought to be mechanosensitive with their length regulating their sensitivity, Lithium induced primary cilia elongation could also affect osteogenesis by altering mechanosensitivity. Therefore, the effects of lithium treatment on primary cilia length and prevalence was evaluated. Cells were cultured in LiCl or vehicle control for 24 h and immunocytochemistry used to image primary cilia in order to assess the number of ciliated cells and any changes in primary cilia length.

#### hES-MP primary cilia length and prevalence in monolayer culture

In hES-MP cells in monolayer culture, only 10 mM LiCl treatment had an effect on the number of ciliated cells, showing a reduction of 33 % compared to the untreated control (Figures 5.34A & 5.32). Both 1 and 10 mM LiCl treatment significantly increased primary cilia length by 42 % and 53 % respectively, compared to the untreated control (Figures 5.34B & 5.33).

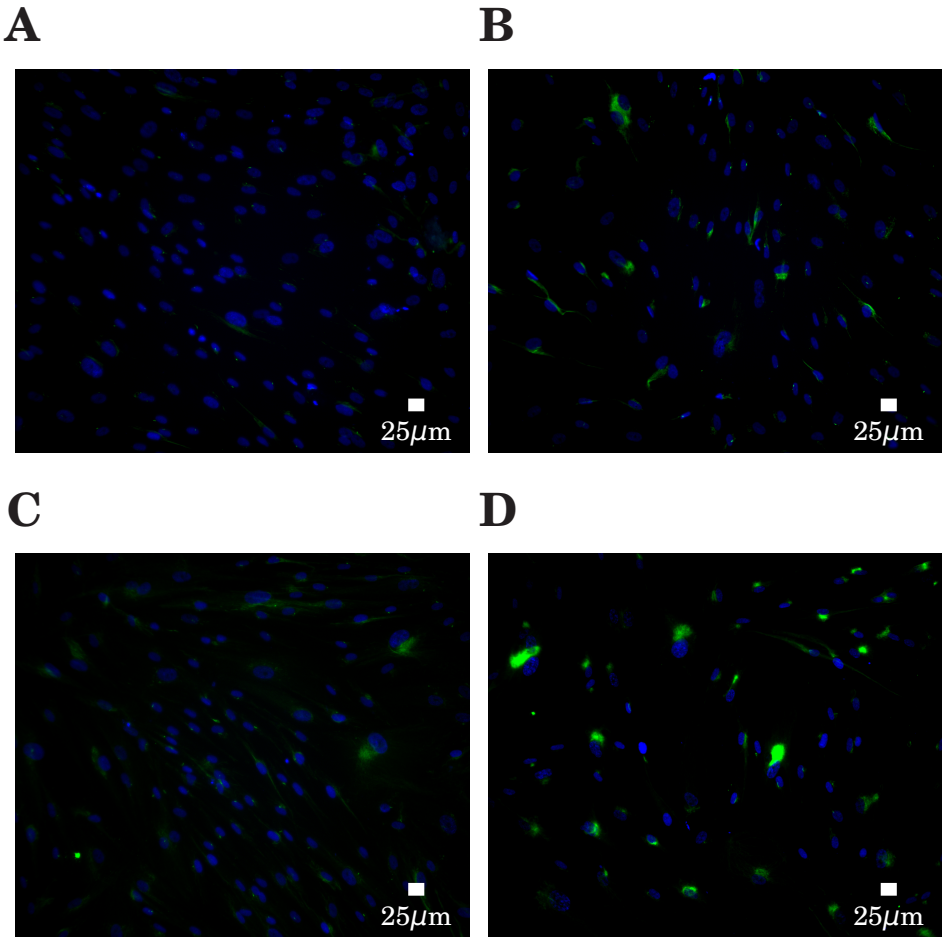


**Figure 5.32:** Fluorescent images representative of ciliated hES-MP cells after LiCl treatment in monolayer. hES-MP cells cultured for 7 days were labelled with anti-acetylated a-tubulin antibody (green) and DAPI (blue) to view the primary cilia and nuclei respectively. (A) untreated control, (B) 0.1 mM LiCl, (C) 1 mM LiCl and (D) 10 mM LiCl.

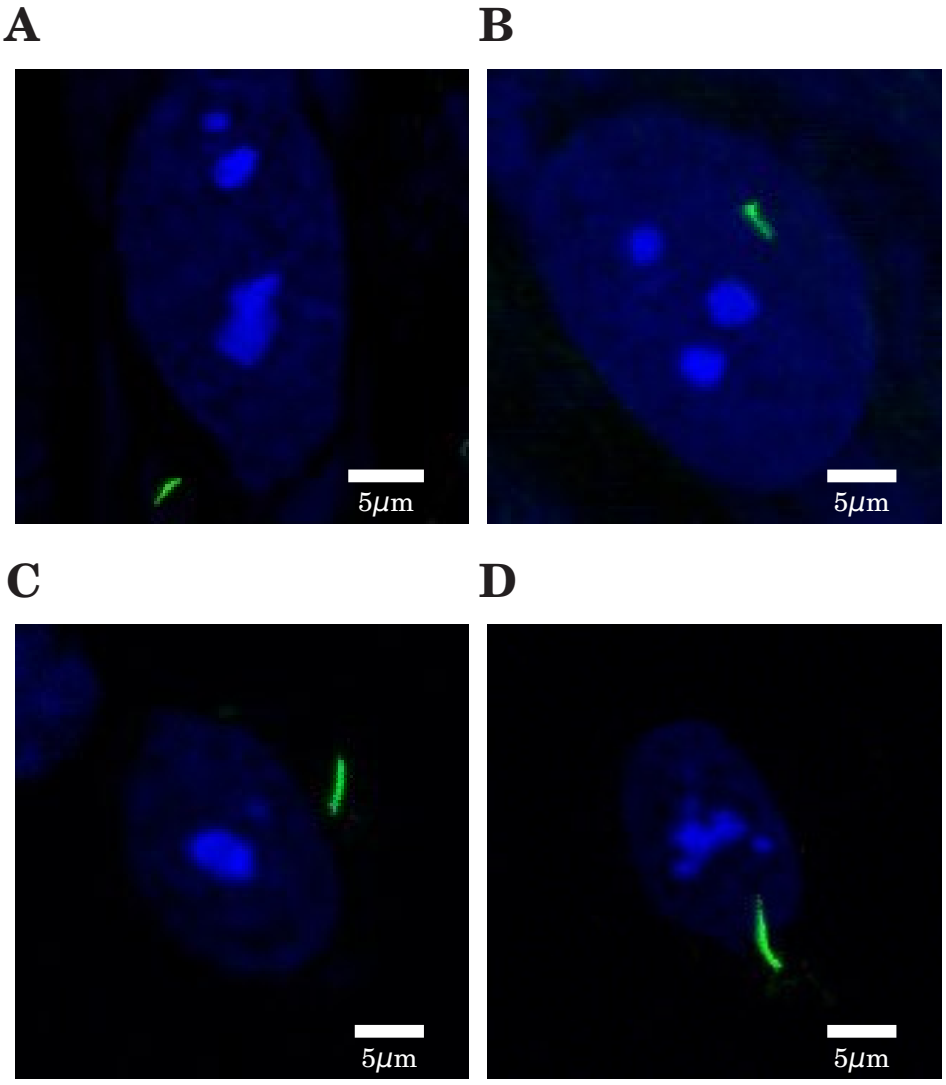


**Figure 5.33:** Fluorescent images representative of hES-MP primary cilia after LiCl treatment in monolayer. hES-MP cells cultured for 7 days were labelled with anti-acetylated a-tubulin antibody (green) and DAPI (blue) to view the primary cilia and nuclei respectively. (A) untreated control, (B) 0.1 mM LiCl, (C) 1 mM LiCl and (D) 10 mM LiCl.

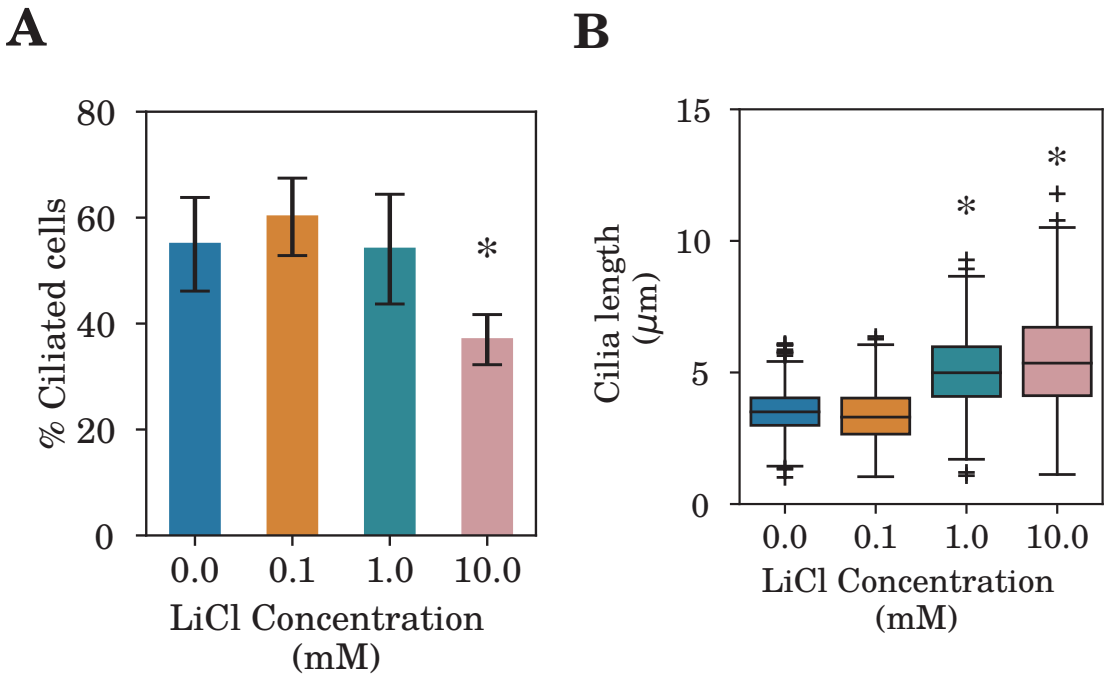


**Figure 5.34:** Effect of LiCl exposure on hES-MP primary cilia prevalence and length in monolayer. (A) Percentage of hES-MPs that bear a primary cilium. Data represents mean ±SD n≥450.(B) Box and whisker plot of primary cilia length. The central line indicates the median, the box the 25$^{th}$ to 75$^{th}$ percentile and the whiskers the upper/lower quartile ±1.5×interquartile range (IQR). + indicates outliers n ≥100. Statistical significance was assessed using Mann Whitney U test. * = $p<0.05$ compared to the untreated control.

### hES-MP primary cilia length and prevalence in 3D culture

In 3D culture only the effects of 1 mM LiCl treatment on primary cilia prevalence and length was evaluated, as this concentration was found to increase length without affecting prevalence in monolayer culture. As in monolayer culture primary cilia prevalence was not affected by 1 mM LiCl treatment (Figures 5.37A & 5.35). Primary cilia prevalence was also similar at 55 % ± 8.8 % in monolayer culture and 53 % ± 12.4 % in 3D culture in the untreated control groups. Primary cilia length was 63 % shorter in 3D culture compared to monolayer culture, at a median length of 1.3 µm and 3.5 µm respectively for the untreated control groups. 1 mM LiCl treatment significantly increased primary cilia length by 66 % (Figures 5.37B & 5.36).

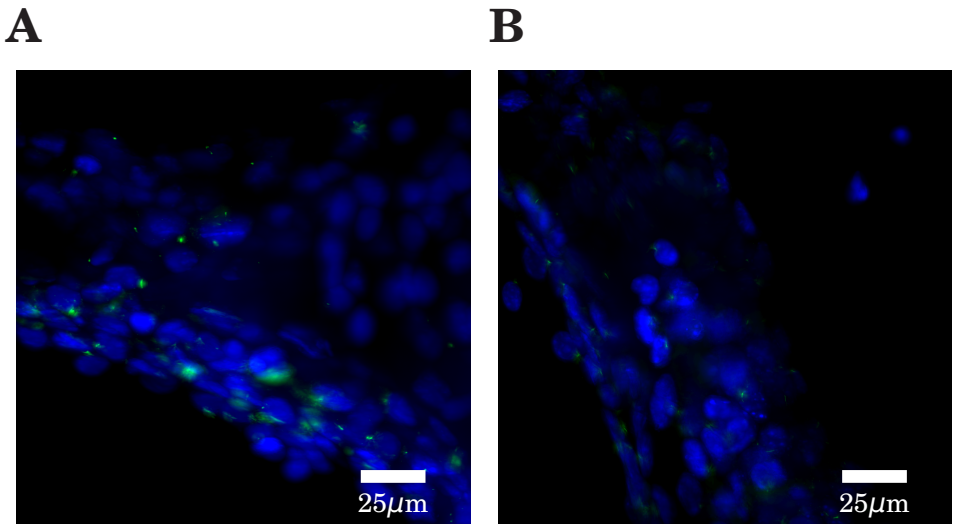


**Figure 5.35:** Fluorescent images representative of ciliated hES-MP cells after LiCl treatment in 3D. hES-MP cells cultured for 5 days were labelled with anti-acetylated a-tubulin antibody (green) and DAPI (blue) to view the primary cilia and nuclei respectively. (A) untreated control and (B) 1 mM LiCl.

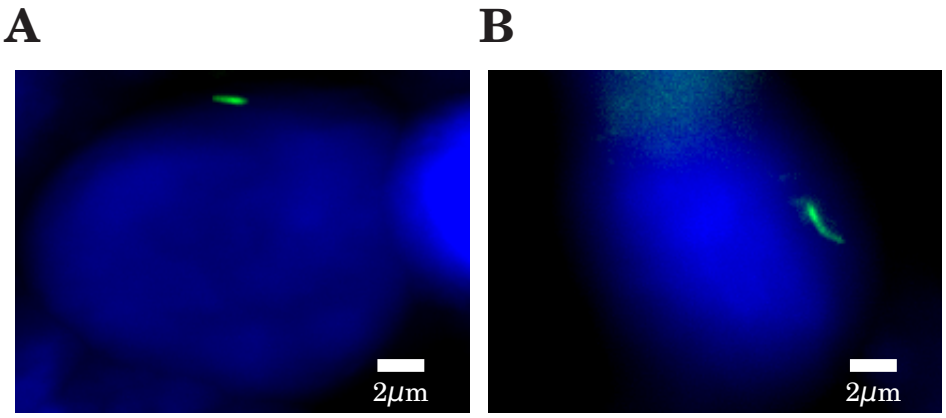


**Figure 5.36:** Fluorescent images representative of untreated (A) and 1 mM (B) LiCl treated hES-MP cell's primary cilium in 3D. hES-MP cells cultured for 7 days were labelled with anti-acetylated a-tubulin antibody (green) and DAPI (blue) to view the primary cilia and nuclei respectively.

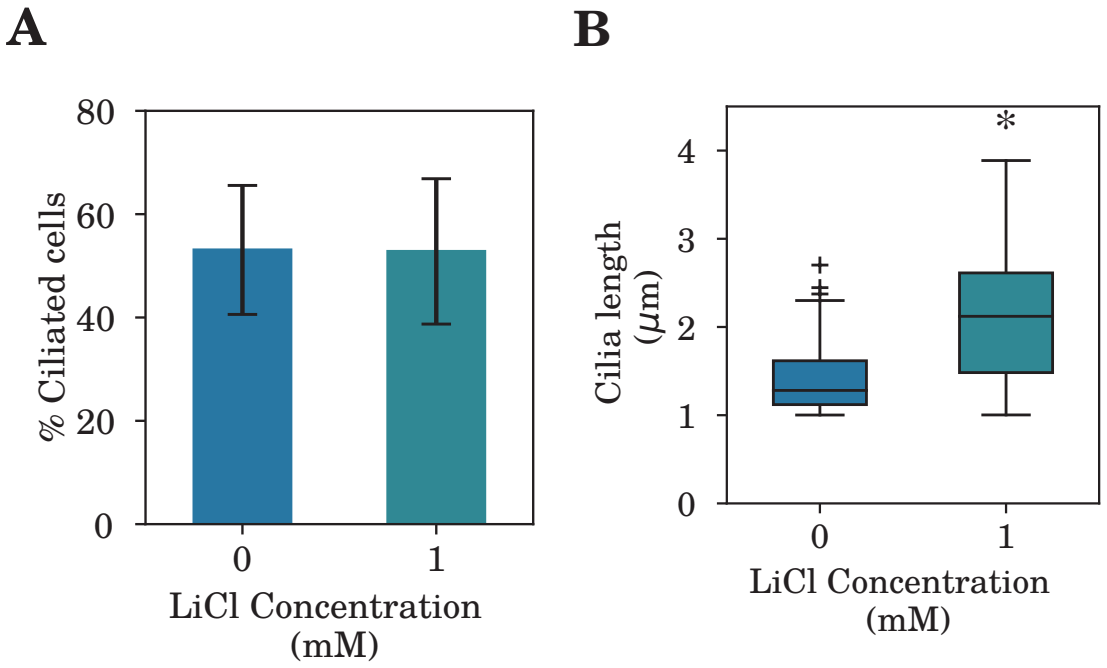


**Figure 5.37:** Effect of LiCl exposure on hES-MP primary cilia prevalence and length in 3D. (A) Percentage of hES-MPs that bear a primary cilium. Data represents mean ±SD n≥500. (B) Box and whisker plot of primary cilia length. The central line indicates the median, the box the 25$^{th}$ to 75$^{th}$ percentile and the whiskers the upper/lower quartile ±1.5×IQR. + indicates outliers n ≥100. Statistical significance was assessed using Mann Whitney U test. * = $p<0.05$ compared to the untreated control.

### MLO-A5 primary cilia length and prevalence in monolayer culture

In MLO-A5 cells in monolayer culture, 1 mM LiCl treatment did not affect primary cilia prevalence (Figures 5.40A & 5.38). Primary cilia prevalence was similar to that found in hES-MP cells at 61 % ± 15 % compared to 55 % ± 8.8 % in hES-MP cells in the untreated controls. Primary cilia of the untreated control were 52 % shorter in MLO-A5 cells compared to hES-MP cells. 1 mM LiCl treatment increased primary cilia length by 96 % compared to the untreated control (Figures 5.40B & 5.39).

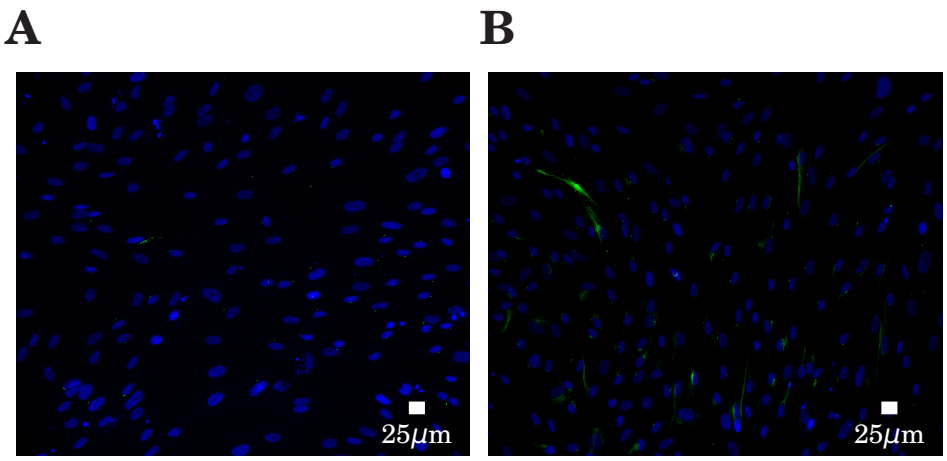


**Figure 5.38:** Fluorescent images representative of ciliated MLO-A5 cells after LiCl treatment in monolayer. MLO-A5 cells cultured for 3 days were labelled with anti-acetylated a-tubulin antibody (green) and DAPI (blue) to view the primary cilia and nuclei respectively. (A) untreated control and (B) 1 mM LiCl.

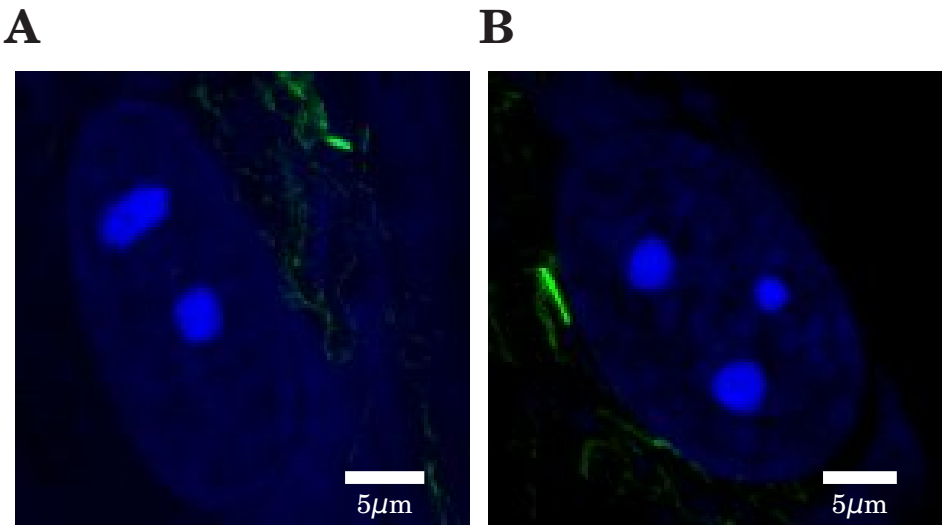


**Figure 5.39:** Fluorescent images representative of untreated (A) and 1 mM (B) LiCl treated MLO-A5 cell's primary cilium in monolayer. MLO-A5 cells cultured for 3 days were labelled with anti-acetylated $\alpha$-tubulin antibody (green) and DAPI (blue) to view the primary cilia and nuclei respectively.

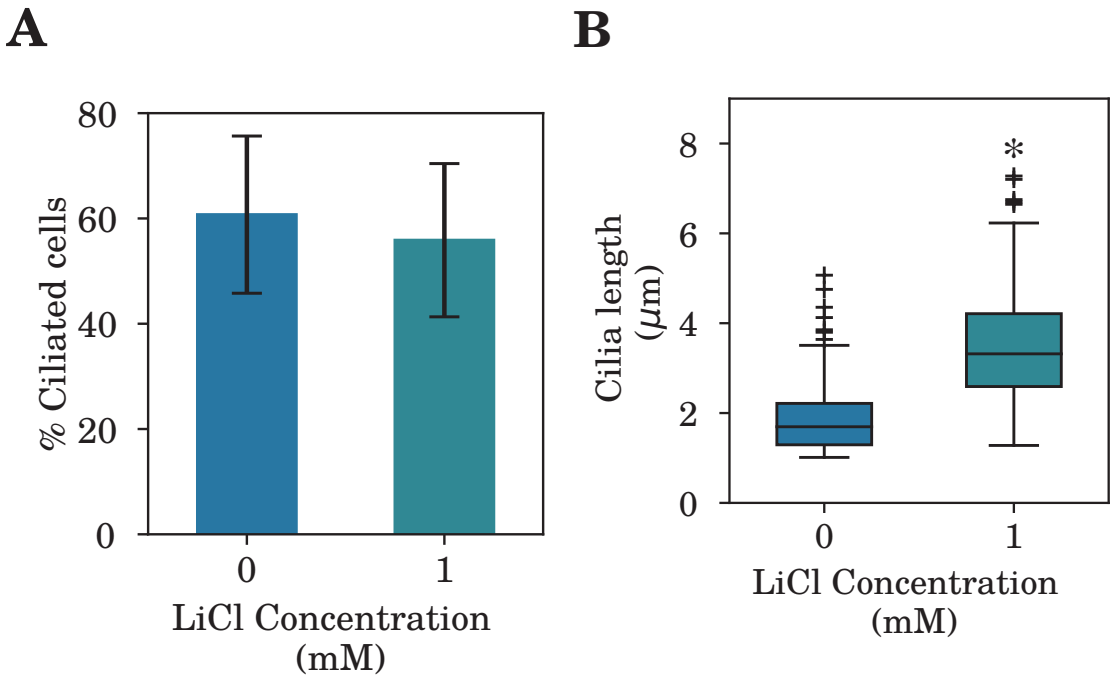


**Figure 5.40:** Effect of LiCl exposure on MLO-A5 primary cilia prevalence and length. (A) Percentage of MLO-A5s that bear a primary cilium. Data represents mean ±SD n≥500. (B) Box and whisker plot of primary cilia length. The central line indicates the median, the box the 25$^{th}$ to 75$^{th}$ percentile and the whiskers the upper/lower quartile ±1.5×IQR. + indicates outliers n ≥100. Statistical significance was assessed using Mann Whitney U test. * = $p<0.05$ compared to the untreated control.

### MLO-A5 primary cilia length and prevalence in 3D culture

In MLO-A5 cells in 3D culture, 1 mM LiCl treatment did not affect primary cilia prevalence (Figures 5.43A & 5.41). Primary cilia prevalence was significantly lower to that found in MLO-A5 cells in monolayer culture at 27 % ± 8.3 % compared to 61 % ± 15 % in monolayer culture in the untreated controls. Primary cilia of the untreated control were 37 % shorter in 3D culture compared to monolayer culture. 1 mM LiCl treatment had a less pronounced effect on primary cilia length in MLO-A5 3D culture only increasing primary cilia length by 12 % compared to the untreated control (Figures 5.43B & 5.42).

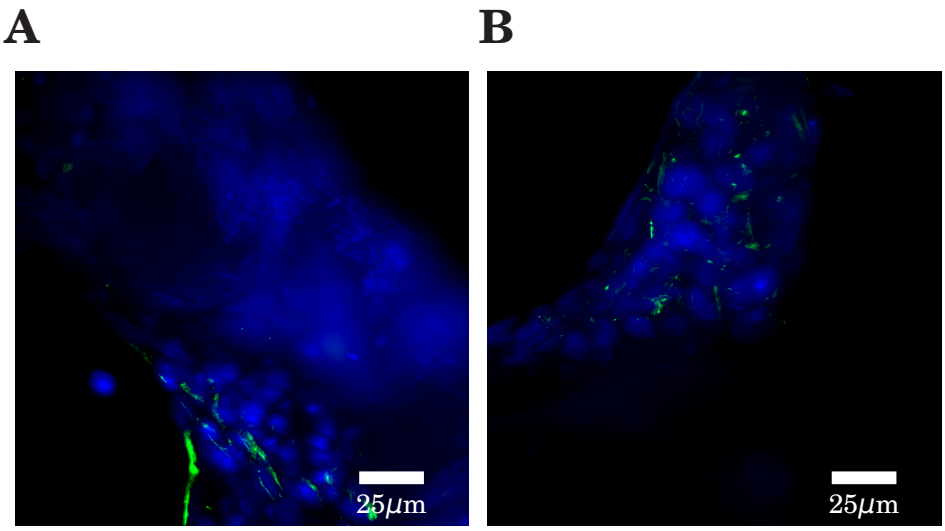


**Figure 5.41:** Fluorescent images representative of ciliated MLO-A5 cells after LiCl treatment in 3D. MLO-A5 cells cultured for 3 days were labelled with anti-acetylated a-tubulin antibody (green) and DAPI (blue) to view the primary cilia and nuclei respectively. (A) untreated control and (B) 1 mM LiCl.

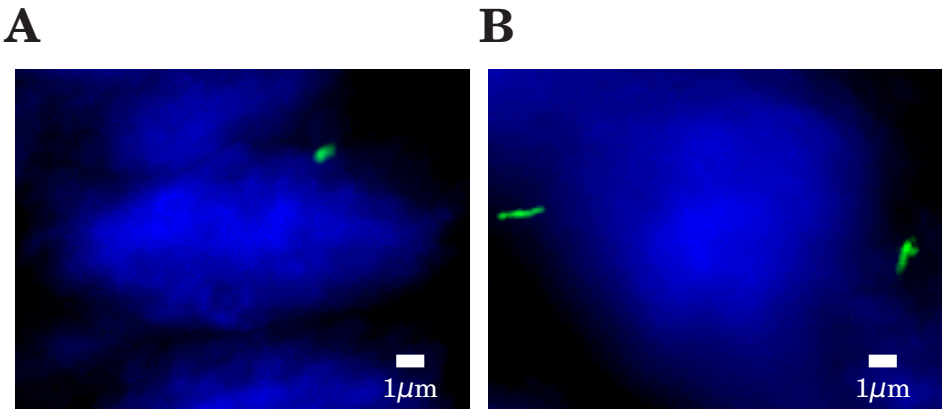


**Figure 5.42:** Fluorescent images representative of untreated (A) and 1 mM (B) LiCl treated MLO-A5 cell's primary cilium in 3D. MLO-A5 cells cultured for 3 days were labelled with anti-acetylated $\alpha$-tubulin antibody (green) and DAPI (blue) to view the primary cilia and nuclei respectively.

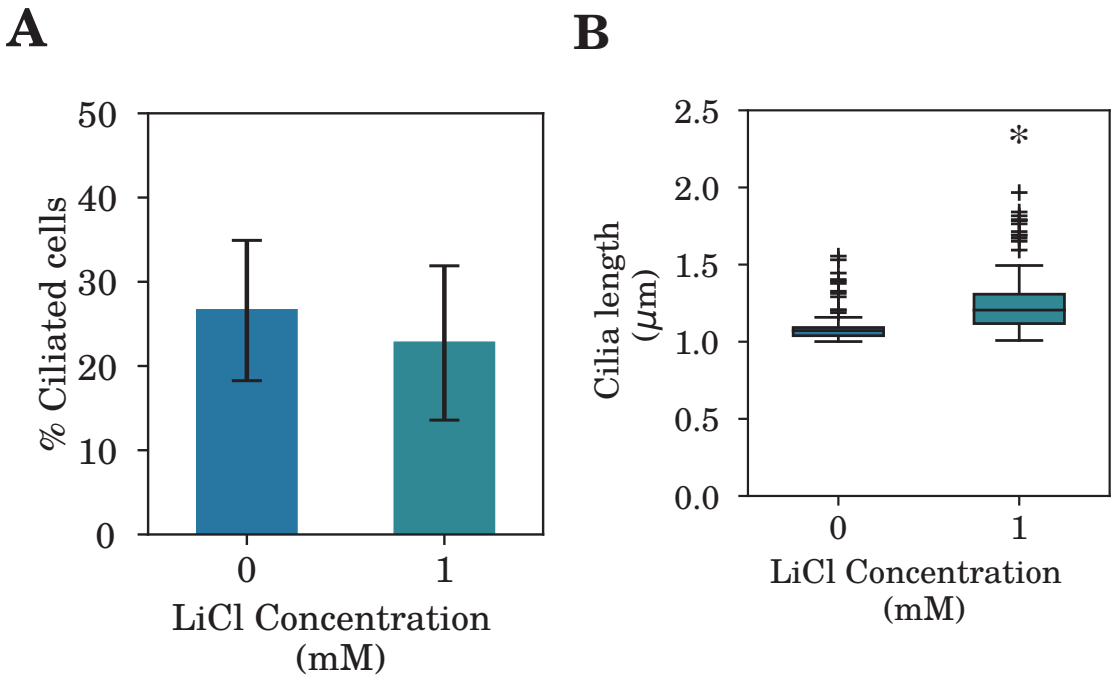


**Figure 5.43:** Effect of LiCl exposure on MLO-A5 primary cilia prevalence and length. (A) Percentage of MLO-A5s that bear a primary cilium. Data represents mean ±SD n≥400. (B) Box and whisker plot of primary cilia length. The central line indicates the median, the box the $25^{th}$ to $75^{th}$ percentile and the whiskers the upper/lower quartile ±1.5×IQR. + indicates outliers n ≥100. Statistical significance was assessed using Mann Whitney U test. * = $p<0.05$ compared to the untreated control.

## 5.5 Discussion

This chapter investigated the response of osteogenic progenitors (hES-MP) and post-osteoblast/pre-osteocyte (MLO-A5) cell lines to LiCl treatment. The reported osteogenic effects of lithium have been conflicting, therefore a range of concentrations, including the therapeutically relevant concentration 1 mM, were tested for cytotoxicity and osteogenic effects. Lithium has also been reported to elongate primary cilia in a number of different cell types. The length of primary cilia has been shown to regulate the sensitivity of cells to mechanical stimulation. Therefore, since bone is a mechanically sensitive organ that upregulates bone deposition in response to increases in load, enhanced sensitivity to mechanical stimulation through elongation of primary cilia may be one mechanism behind any positive effect lithium has on osteogenesis. In order to assess if primary cilia elongation could be involved in any increased osteogenesic response to mechanical stimulation, LiCl treatment regimens were evaluated in conjunction with assessing LiCl's effects on primary cilia prevalence and length. This was performed in order to assess whether primary cilia were elongated at the same concentrations that would be used to assess the effects of lithium mechanoinduced osteogenesis.

Lithium, administered as lithium carbonate, lithium orotate or lithium chloride, is most commonly used in the treatment of psychiatric disorders such as bipolar disorder [278–280]. In the treatment of psychiatric disorders, the blood serum concentration of lithium is tightly controlled, with therapeutic effects typically seen at concentrations between 0.8-1.2 mM [214, 215]. The tight control of serum concentrations is due to mild toxicity presenting at levels between 1.5-2.5 mM and chronic toxicity presenting at serum concentrations greater than 2.5 mM with continuous treatment [300]. Here in both monolayer and 3D culture of hES-MP cells, continuous LiCl treatment showed cytotoxicity at concentrations of 10 mM and above in both monolayer and 3D culture. In MLO-A5 cells, cytotoxicity was observed at 50 mM LiCl and above in monolayer culture and 10 mM LiCl and above in 3D culture. These concentrations are higher than the toxicity levels reported *in vivo* [300]. However, they are comparable to the toxicity levels found *in vitro*, which have been reported to range between 20 mM and 50 mM [301–303]. Although, Ou et al used 100 mM LiCl with no cytotoxicity reported when applied for between 7 and 12 h in synoviocytes [209]. This reduced exposure time may explain the tolerance of the cells to this higher concentration. Similarly, hES-MP and MLO-A5 cells cultured in monolayer had a greater tolerance to higher LiCl concentrations

with shorter exposures in intermittent treatments. MLO-A5 cells were also more tolerant to higher LiCl concentrations in monolayer culture compared to hES-MP cells, with toxicity presenting at 50 mM and 10 mM respectively with continuous treatment. Since lithium does not passively transport into or out of cells, these differences may be due to different transport rates into and out of the cells between hES-MP and MLO-A5 cells. A higher transport of lithium out of, or lower transport into MLO-A5 cells would result in lithium being less toxic [304]. Alternatively, as lithium affects multiple pathways, the differences observed may be due to differences in these pathways between stem cells and mature bone cells or even between human and mouse cells.

Activation of the Wnt/$\beta$-catenin signalling pathway through inhibition of GSK3-$\beta$ is one of the mechanisms by which lithium affects cells [305]. Wnt/$\beta$-catenin signalling, known as canonical Wnt signalling, plays an important role in the development and maintenance of a number of tissues and is known to be involved in stem cell self-renewal, osteogenic differentiation and osteogenesis itself [180, 306, 307]. Lithium treatment is therefore likely to affect these cellular functions. Wnt/$\beta$-catenin signalling occurs through Wnt binding to frizzled inducing complex formation with the co-receptor low-density lipoprotein receptor-related protein (LRP)5/6 [308]. This leads to intracellular dishevelled (Dsh) binding and activation which in turn inhibits the axin, adenomatous polyposis coli (APC), GSK3-$\beta$ complex [309]. The inhibition of the axin, APC, GSK3-$\beta$ complex prevents GSK3-$\beta$ phosphorylating $\beta$-catenin resulting in $\beta$-catenin accumulation in the cytosol and its subsequent translocation into the nucleus where it can mediate transcriptional activity through binding with transcription factors, altering gene expression [310].

In haematopoietic and mesenchymal stem cells, lithium has been shown to promote proliferation [303, 311, 312]. This increase in proliferation with LiCl treatment was not seen here in the dose response studies where hES-MP cells were cultured in DW media. However, when comparing the effects of LiCl on osteogenesis in SM and DW media, a greater increase in metabolic activity between day 1 and day 7 was observed in cells cultured in SM and continuously treated with 1 mM LiCl compared to the untreated control. This greater increase in metabolic activity indicates a greater increase in cell number and therefore greater proliferation. However, this increase in proliferation was not observed in hES-MP cells cultured intermittently in LiCl. Zhang et al. demonstrated that the pathway through which lithium promoted stem cell proliferation was through its inhibitory effects on GSK3-$\beta$ and the subsequent

accumulation of $\beta$-catenin and Wnt pathway activation [303]. Interestingly, Dex has also been shown to affect proliferation through GSK3-$\beta$, where Smith et al. showed Dex inhibited cell cycle progression, reducing proliferation through GSK3-$\beta$ activation and direct degradation of c-Myc [313].

This inhibitory effect of Dex on proliferation was also observed here, with reduced cell metabolic activity over the 21 day culture of hES-MP cells in DW compared to SM. Since Dex was withdrawn on day 5 of culture and metabolic activity was not significantly lower until day 21, this suggests the inhibitory effects of Dex either persist or take an extended culture period to become apparent. LiCl inhibition of GSK3-$\beta$ has been shown to counteract the inhibitory effects of Dex on cell proliferation [313, 314]. This was observed here where continuous 1 mM LiCl treatment of DW cultured hES-MP cells resulted in a greater metabolic activity on day 21 compared to the untreated DW control, indicating an increase in proliferation over the 21 days of culture. Continuous 1 mM LiCl treatment in DW cultured cells also partially counteracted the inhibitory effects of Dex on cell proliferation. Day 21 metabolic activity of both intermittent and untreated controls were significantly lower compared to all SM cultured groups but the continuous treatment group was not significantly different. It should be noted that LiCl was not applied to cells until after Dex withdrawal, unlike the studies by Smith, et al. and Ohnaka, et al. where LiCl was applied in combination with Dex to counteract its inhibitory effects on cell proliferation. Therefore, the LiCl applied here may not be directly counteracting the activity of Dex.

In addition to promoting proliferation, LiCl has also been shown to promote osteogenic markers *in vitro* and *in vivo* [231, 287–291, 315]. In order to evaluate if lithium may promote osteogenesis in stem cells or mature bone cells, the effects of continuous LiCl treatment at 1 mM were evaluated. In addition, concentrations above and below this concentration were evaluated for their potential use in promoting osteogenesis in a tissue engineering capacity. These higher LiCl concentrations were tested as with *in vitro* use the LiCl concentration is not limited by toxicity on different cells within the body. *In vitro*, studies investigating LiCl's effects on osteogenic differentiation or osteogenesis have typically been performed in monolayer culture and focused on osteogenic gene expression. The extended culture periods performed here, allowed evaluation of matrix formation further building on these previous studies. Furthermore, the inclusion of 3D culture was used to assess its suitability in stimulating osteogenesis for tissue engineering applications.

Unsurprisingly, at the concentrations that were found to be cytotoxic, all osteogenic markers were reduced compared to the untreated controls in both hES-MP and MLO-A5 cells and in both monolayer and 3D culture. In other studies, these higher concentrations have been shown to stimulate osteogenic differentiation [315,316]. Li et al. reported both 50 and 100 mM LiCl promoted proliferation and stimulated increases in osteogenic gene expression [316]. However, Bain et al. reported 100 mM LiCl to be cytotoxic, but both 10 and 25 mM promoted osteogenic gene expression with no negative effects on cell viability or proliferation [315].

Although higher concentrations were cytotoxic and therefore did not promote osteogenic differentiation, continuous 1 mM LiCl consistently promoted osteogenesis here. ALP activity was up-regulated in hES-MP cells in both monolayer and 3D culture and MLO-A5 cells in 3D culture. Matrix mineralisation in both hES-MP and MLO-A5 cells in monolayer and 3D culture was also up-regulated. Similarly, Satija et al. also reported higher concentrations to be cytotoxic and detrimental to osteogenic markers but found 5 mM LiCl promoted ALP activity and osteogenic gene expression in MSCs [291]. In contrast, De Boer et al. found that although 4 mM LiCl treatment enhanced proliferation, it actually had no effect on ALP activity in MSCs [312]. The difference between these two studies may be due to the duration of LiCl exposure. Satija et al. cultured MSCs in LiCl for 7 days before ALP levels were measured, compared to 4 days for De Boer et al. Although MSCs were not used here, hES-MP cells have similar characteristics and would therefore likely behave in a similar manner. The duration of LiCl exposure used here was slightly longer at 8 days and an increase in day 14 ALP activity was observed. This suggests that the short duration of culture used by De Boer et al. may not have been long enough for osteogenic differentiation to have progressed sufficiently for ALP levels to be affected. Although the MLO-A5 cells were only cultured in LiCl for 5 days before ALP levels were evaluated, they are a mature post-osteoblast/pre-osteocyte cell line with inherently high levels of ALP activity and do not need to undergo osteogenic differentiation for ALP activity levels to increase. After exposure times of up to 48 h and 72 h for hES-MP and MLO-A5 cells respectively, no increases in any of the osteogenic markers were observed. This gives further evidence that prolonged LiCl exposure may be needed to increase osteogenesis.

The results presented here also suggest 1 mM LiCl itself may not induce osteogenic differentiation and requires the use of Dex. To investigate LiCl

induced osteogenic differentiation hES-MP cells were cultured without Dex, since Dex itself induces differentiation [317]. Without Dex no changes in ALP activity or matrix production were observed with continuous 1 mM LiCl treatment. LiCl itself therefore did not induce osteogenic induction but did synergistically increase osteogenic markers when used on stem cells stimulated by Dex to differentiate. Additionally, since this same treatment regime (continuous 1 mM LiCl in SM) promoted increases in matrix production in MLO-A5s, which are mature bone cells, these results suggest 1 mM LiCl treatment alone only promotes osteogenic responses in osteogenically differentiating cells or in mature bone cells and does not induce osteogenic differentiation itself. In contrast Tang et al. investigated LiCl effects on osteogenic differentiation, concluding that LiCl does induce osteogenic differentiation. However, the MSCs were cultured with Dex and therefore, their conclusion that LiCl induces osteogenic differentiation may be inaccurate [318].

A number of case-control studies investigating fracture risk in osteoporotic psychiatric patients have shown lithium treatment can reduce fracture risk [281–283]. A study by Zamani et al. found lithium treatment in patients increased bone mineral density in the spine, femoral neck and trochanter [231]. Additionally, an *in vivo* study of mice fed lithium rich diets by Clement-Lacroix et al. also found increases in bone mineral density due to lithium [289]. Similarly to the *in vivo* studies, continuous lithium treatment applied at a therapeutically relevant concentration (1 mM) increased osteogenesis. One mechanism by which lithium acts is though inhibition of GSK3-$\beta$. The $K_i$ for lithium on GSK3-$\beta$ has been shown to be 2 mM in isolated GSK3-$\beta$, which would suggest that the increase in osteogenic markers with continuous 1 mM lithium exposure would not be due to inhibition of GSK3-$\beta$ [319]. Other *in vitro* studies investigating the osteogenic effects of lithium have typically used 5 mM LiCl or above and would therefore be above this threshold [291, 315, 318]. However, the $K_i$ has been shown to be greatly dependent upon the free $Mg^{2+}$ concentration and at $Mg^{2+}$ levels found within cells; the $K_i$ is reduced to 0.8 mM LiCl [320, 321]. As the 1 mM LiCl concentration used here is above this threshold, GSK3-$\beta$ inhibition could be a mechanism behind the increase in osteogenic markers and proliferation and would also be relevant to the anabolic actions on bone seen *in vivo*. Together this suggests lithium, or alternative drugs that target GSK3-$\beta$ or the canonical Wnt signalling pathway could be used therapeutically as an anabolic agent for bone.

Although continuous LiCl treatment increased osteogenic markers in hES-MP

cells at a therapeutically relevant concentration, it also required the use of Dex to have this effect. When used therapeutically LiCl is not typically used in combination with steroids. Therefore, the observation of other studies that bone mineral density increases with lithium treatment may not be due to increased bone stem cell differentiation. Increased stem cell proliferation may however play a part, since this was observed without the use of Dex. Continuous 1 mM LiCl treatment did however increase matrix production in MLO-A5 cells which were not cultured with Dex. Therefore, the increase in bone mineral density observed with LiCl treatment *in vivo* could be due to increased matrix production from osteoblasts and not from any increased osteogenic differentiation of stem cells. However, both increased stem cell proliferation and increased matrix production from osteoblasts would be beneficial in increasing bone health in osteoporotic patients, improving fracture healing and in bone tissue engineering. Studies have highlighted the potential benefits of short-term systemic lithium administration to improve bone fracture healing through increased stem cell proliferation and matrix production. In an *in vivo* study by Vachhani et al., ovariectomised rats subjected to femoral diaphyseal fracture were administered lithium [322]. This resulted in a 50% higher maximum yield torque compared to the control and better periosteal and mineralized callus bridging. Another similar study by Wang et al. found that rats subjected to an osteotomy and distraction showed greater bone mineral density and better continuity in the regenerated bone mass in the distraction gaps in rats administered lithium compared to the controls [323].

In addition to lithium's systemic administration, lithium could also be administered locally, potentially avoiding or reducing side effects. Administration of lithium to enhance matrix production locally would be beneficial in fracture treatment, hip implants and other bone tissue engineering applications. Furthermore, although the LiCl concentrations above 1 mM applied here were not found to be osteogenic, other studies have found higher concentrations up to 20 mM to be more osteogenic than lower concentrations [318, 324]. Although it would not be possible to apply these concentrations systemically, local application of concentrations at this higher range could be possible without inducing toxicity or severe side effects. Lithium could be administered locally through injection or through incorporating lithium into implantable materials that subsequently elute it into the local area. Li et al. for example, incorporated lithium into porous gelatin/hydroxyapatite nanospheres and implanted them into rabbit femoral heads where they were found to improve new bone formation at the defect site [325]. However, the study did not evaluate the

concentration of lithium eluted. A similar study by Khan et al. incorporated lithium into bioactive glass scaffolds and implanted them into rabbit femoral head defects [326]. Scaffolds incorporating lithium also showed increased new bone formation and better scaffold integration compared to the control bioactive glass scaffolds.

To avoid administration of lithium and introducing it into the body, lithium could be used in the pre-treatment of bone tissue engineered scaffolds to promote matrix production in scaffolds before implantation. This would take advantage of the positive effects of lithium on matrix production whilst avoiding any potential toxicity of lithium within the body. The increases in matrix production with continuous 1 mM LiCl found here highlight this potential use. For implant use, an alternative stem cell source to hES-MP cells would be required, such as the patient's own MSCs. Additionally, the PU scaffold used here would also not be suitable for implantation and would therefore also require an alternative scaffold. However, these results do demonstrate a proof of concept for using lithium *in vitro* to improve matrix production in tissue engineered bone constructs.

Although continuous LiCl treatment was found to be osteogenic, intermittent 0.1 and 1 mM LiCl treatment in hES-MP and MLO-A5 cells and 10 mM in hES-MP cells was not found to be osteogenic in static conditions and did not affect cell viability. Intermittent 0.1, 1 and 10 mM LiCl treatment could therefore be used in hES-MP cells and 1 mM in MLO-A5 cells to investigate the mechanoinduced osteogenic effects of LiCl.

To investigate whether primary cilia elongation could be a potential method by which lithium treatment increases osteogenesis *in vivo*, primary cilia length and prevelance was also evaluated. *In vitro* studies utilising osteogenic cell types have shown primary cilia elongation at physiological ($\leq$1 mM)and supraphysiological (>1 mM) concentrations of lithium [205, 327, 328]. At the physiologically relevant concentrations, primary cilia elongation varies between 46% (0.5 mM LiCl [205]) and 80% (1 mM LiCl [328]). At the physiologically relevant concentrations tested here, 0.1 mM had no effect on primary cilia length in hES-MP cells cultured in monolayer. 1 mM LiCl increased primary cilia length by 42% in hES-MP cells and 96% in MLO-A5 cells. The lack of primary cilia elongation with 0.1 mM LiCl treatment is likely due to the concentration being below the threshold at which it has an effect. Since Spasic et al. found 0.5 mM LiCl did elongate primary cilia, this threshold is likely to

be somewhere between 0.1 and 0.5 mM. Due to having no effect on primary cilia length in hES-MP cells in monolayer culture, 0.1 mM LiCl treatment was not used in any further primary cilia elongation experiments. At 1 mM LiCl, the increases observed in hES-MP (42%) and MLO-A5 cells (96%) are similar to the 46% and 80% elongation found at physiologically relevant concentrations by Spasic et al. and Oliazadeh et al. Although there have been no *in vivo* studies investigating the effects of lithium on primary cilia length in bone cells, there have been studies in other cell types that have shown lithium can increase primary cilia length *in vivo*. One such study by Thompson et al. found Wistar rats administered dietary lithium resulted in a 19% increase in primary cilia length in chondrocytes [210]. The lack of *in vivo* studies investigating cilia elongation in osteogenic cells is likely due to the difficulties in imaging the organelle *in vivo*. Taken with the fact primary cilia elongation does occur *in vivo* in other cells and that hES-MP and MLO-A5 cells were elongated with the physiologically relevant concentrations of LiCl used here, it is certainly possible that primary cilia of osteogenic cells would also elongate *in vivo* with lithium treatment.

At supraphysiological concentrations of LiCl, Oliazadeh et al. and Shi et al. observed primary cilia elongation of 166% (10 mM) and 139% (5 mM) respectively. Although 10 mM LiCl also elongated hES-MP primary cilia to a greater extent than 1 mM LiCl, it was only a modest increase (53%) in elongation compared to that found by Oliazadeh et al. and Shi et al. Although elongation did not increase as much with higher concentrations as was found by Oliazadeh et al., primary cilia elongation still increased in a dose dependant manner. The differences in elongation may be due to different sensitivities of the cells used in each of the experiments. This is supported by the fact that 1 mM LiCl increased hES-MP and MLO-A5 cell primary cilia by different extents (42% compared to 96% respectively). Alternatively, the difference may be due to 10 mM LiCl being cytotoxic to hES-MP cells. As although with short-term treatment (as was used when elongating primary cilia), 10 mM LiCl was not found to affect cell viability, but with continuous treatment it did and could therefore, still be having a negative effect on the cells. This may prevent primary cilia elongation to the extent seen by Oliazadeh et al. Further evidence was seen with the reduction in the number of ciliated cells. LiCl treatment did not affect the number of ciliated cells at any other concentration used and was not reduced by the 10 mM LiCl treatment used by Oliazadeg et al. The reduction in the number of ciliated cells is therefore likely due to the toxicity of LiCl rather than it having a specific effect on ciliogenesis.

The previously discussed studies were all performed in monolayer culture and to the authors knowledge no 3D *in vitro* studies have been performed assessing the effects of LiCl on primary cilia length in osteogenic cells. Interestingly, in 3D culture the primary cilia of both hES-MP and MLO-A5 cells were shorter, by 63% and 37% respectively. The greater reduction in length with 3D culture in hES-MP cells compared to MLO-A5 cells is likely due to the primary cilia being longer in monolayer hES-MP culture and therefore, could have a greater decrease in length. Primary cilia have also been shown to be shorter in 3D culture compared to monolayer culture in a study by Zhang et al., where MSCs were roughly 39% shorter when cultured on a 3D structured surface compared to when cultured on glass coverslips [329]. Similarly to the results presented here, the materials of the monolayer and 3D surfaces used by Zhang et al. were different. It is therefore possible that instead of, or in addition to the change to a 3D environment having an effect on cilia length, the actual material itself may be affecting primary cilia length. Interestingly, the study by Zhang et al. went further and evaluated the effects of different surface topographies of the same material on primary cilia length and found primary cilia were longer on surfaces with a submicron topography compared to a micron topography. In addition to primary cilia length, the number of ciliated cells were also found to be lower in micron topography scaffolds compared to submicron and glass coverslips. Primary cilia prevalence was only found to be lower in MLO-A5 cells cultured in 3D compared to monolayer and not in hES-MP cells. From this it is clear that surface topography and therefore 3D culture compared to monolayer culture can alter primary cilia length and prevalence. These changes could be caused by a variety of factors known to be different in 3D culture compared to monolayer culture.

One of the major differences in 3D culture compared to monolayer culture is cell attachment, which regulates many fundamental cellular behaviours such as, differentiation and proliferation [330,331]. Since primary cilia are only present during $G_1$ and $G_0$ phases of the cell-cycle, changes in cell proliferation can have an effect on primary cilia prevalence [332]. It would therefore be logical that a decrease in proliferation rate would result in an increase in primary cilia prevalence. However, counter-intuitively the opposite was found here and 3D culture of MLO-A5 cells resulted in a decrease in proliferation rate and a decrease in primary cilia prevalence. Additionally, although hES-MP cell proliferation was also lower in 3D compared to monolayer culture, primary cilia prevalence was not affected. These results suggest proliferation rate does

not have an effect on primary cilia prevalence. Since not all cells that have exited the cell division cycle generate a primary cilium, cilia prevalence must be affected by more than just the rate of proliferation [333].

In relation to proliferation, the level of confluence is also known to influence primary cilia prevalence [334]. It is difficult to compare confluence levels between monolayer and 3D cultures and the idea of "confluence" may not be relevant to 3D culture. However, in monolayer at "confluence" cell-cell contact and spatial confinement of cells is at its maximum. Of these, spatial confinement has been shown to play a role in ciliogenesis and could therefore be a mechanism behind why "confluence" results in a higher cilia prevalence [333]. In MLO-A5 cells in 3D culture primary cilia prevalence was measured on day 3 of culture compared to day 7 of culture in hES-MP cells. Although MLO-A5 cells both grow and deposit matrix faster than hES-MP cells, due to the earlier timepoint of the measurement the MLO-A5 cells would have proliferated less and deposited little matrix. This would likely result in a lower level of spatial confinement compared to the hES-MP cells and may explain the lower primary cilia prevalence observed.

Interestingly, the lengths of primary cilia in 3D culture were closer to the lengths found in bone *in vivo* compared to those of monolayer culture [335]. Shorter primary cilia *in vivo* compared to monolayer culture have also been observed in other cell types such as chondrocytes [210]. In a study by Coughlin et al. primary cilia were measured in cells within the trabeculae and within bone marrow, where primary cilia were found to be longer in both osteoblasts and osteocytes (1.65 µm) within the bone compared to the cells within the marrow (1.46 µm). The pericellular space between osteocytes and the lacunar wall has been reported to be between 0.1 µm-2.7 µm with a typical space of 1 µm which suggests that this spatial constraint is what limits primary cilia length in osteocytes [335–338]. However, the cells within bone marrow have no such spatial constraint. Additionally, the 3D cultured hES-MP and MLO-A5 cells would not be under these same spatial constraints and they also had similarly short primary cilia lengths of 1.1 µm and 1.3 µm for MLO-A5 and hES-MP cells respectively. It is therefore likely that primary cilia lengths are not shorter *in vivo* and in 3D culture compared to monolayer culture due to spatial constraints but instead may be due to differences between the "2D" and 3D environment.

## 5.6 Summary

To summarise, a LiCl treatment regime that did not alter osteogenesis in static conditions was developed in monolayer and in 3D culture. Continuous doses of 1 mM LiCl was found to promote osteogenic markers and was therefore excluded from use. However, when used intermittently 1 mM LiCl did not alter osteogenesis. This same treatment regime was also found to increase primary cilia length without affecting primary cilia prevelance. Since primary cilia length is thought to be one mechanism by which cells regulate their mechanosensitivity. This LiCl induced primary cilia elongation could be one mechanism behind any LiCl induced changes in mechanotransduction.

# 6. Response of bone and bone precursor cells to fluid shear

## 6.1 Introduction

Mechanical loading is well known to stimulate osteogenic responses in osteogenic cells both *in vivo* and *in vitro*. *In vivo* this functions to stimulate bone remodelling to ensure the demands of its mechanical environment are met. Within bone itself, osteogenic cells such as osteoblasts, osteocytes and bone precursor cells are all subjected to mechanical stimuli. Mature osteocytes are thought to mainly have a mechanosensory role within bone and do not actively produce bone matrix. Osteoblasts are produced from bone precursor cells and although their main role is the production of bone matrix, osteoblasts and their precursors have also been shown to be mechanosensitive. It is therefore likely that all three of these cell types play an important part in mechanosensation and adaptation within bone.

Bone cells are subjected to a number of different mechanical stimuli from compression to fluid shear stress (FSS). *In vitro* FSS is a commonly used mechanical stimulus used to study the response of osteogenic cells to mechanical stimuli. However, these studies are typically short-term studies that evaluate cell signalling, such as calcium signalling or upregulation of genes such as runt-related transcription factor 2 (RUNX2), ALP and COX-2. These short-term studies are suitable for evaluating osteocyte responses to FSS, since they themselves do not actively produce bone matrix. However, since these studies only evaluate initial responses, it is not always clear whether these would translate into long-term osteogenic responses such as osteogenesis in osteoblasts or their precursors. Osteogenesis itself takes multiple weeks to occur and therefore requires longer term studies.

Assessment of osteogenesis in response to mechanical stimuli *in vitro* requires a device that allows application of fluid flow in combination with long-term culture of cells. This excludes parallel plate flow chambers, one of the most commonly used methods to apply FSS, as they become blocked with long-term matrix production. Two devices that can be used to apply FSS and allow long term culture are rocking platforms and orbital shakers. Both of these devices allow the use of standard well plates, are high throughput. However, only rocking platforms can apply oscillatory fluid flow which is thought to more closely replicate that of the FSS stimulus that occurs *in vivo*. The FSS produced by rocking platforms (<0.1 Pa) is likely lower than that which bone cells are subjected to *in vivo*, which has been theorised to range between 0.3-25 Pa [339, 340]. Despite this, previous studies have shown bone cells to be sensitive to this low-level stimulus [132, 240]. Furthermore, since the use of low-level stimuli is unlikely to saturate mechanoresponses, rocking platforms may be useful when assessing the effects of treatments aimed at increasing mechanosensitivity.

## 6.2 Aims and objectives

The aim of this chapter was to explore the mechanoresponse of osteogenic progenitor and osteoblast cells to low-level FSS. This was performed in order to develop an optimised mechanical loading regime that could be used to investigate the effects of lithium on mechanotransduction. The following objectives were addressed in order to achieve this:

- Evaluate the effect of rocking frequency on three cell lines (MLO-A5, MC3T3-E1 and hES-MP) that have previously been shown to be mechanosensitive.
- Evaluate the effect seeding density has on osteogenic responses to FSS.
- Evaluate the effects culture conditions, in particular temperature and $CO_2$ concentrations have on osteogenic responses to FSS.
- Evaluate the effect the duration of Dex exposure has on osteogenic responses to FSS in hES-MP cells.
- Evaluate the effect of serum batch variability on osteogenic responses to FSS in hES-MP cells.

## 6.3 Methods

### 6.3.1 Application of fluid shear stress

Oscillatory FSS was generated in circular 6-well plates through the use of either a Stuart SSL4 see-saw rocker (Stuart, UK) or an IKA 2D digital see-saw rocker (IKA, UK). The use of a see-saw rocker and circular wells has previously been implemented by Delaine-Smith et al. to stimulate osteogenic responses in hES-MP and MLO-A5 cells [132, 240]. The choice of circular wells compared to square wells is not optimum as the shear stress on the bottom surface in circular wells is not evenly distributed as it would be in square wells. However, as previous studies utilised circular wells, circular wells were also used here to allow cross-comparison. Initially a Stuart SSL4 rocker was utilised following the same method used by Delaine-Smith et al. Well plates with 2 ml of media were placed on the rocking platform and subjected to either 0.75 Hz or 1 Hz. Since the Stuart rocking platform was not suitable for use in an incubator an IKA rocking platform was also used to stimulate cells. The IKA rocking platform had a lower maximum tilt angle of 5° compared to the 7° of the Stuart rocking platform. Therefore instead of 1 Hz a higher frequency of 1.33 Hz was chosen to match the FSS generated by the rocking platform used by Delaine-Smith et al. (0.05 Pa. The characteristic FSS magnitude ($\tau$), defined as the FSS at the centre of the well when the plate is horizontal, was calculated using a model developed by Zhou et al. (Equation 6.1) where $\mu$ is the fluid viscosity ($1 \times 10^{-3}$ Pa s, $\theta_{\max}$ is the maximum tilt angle of the platform (radians), sigma is the ratio of the fluid depth (2.08 mm) to diameter (35 mm) in the well and T is the time for one cycle (seconds). The manufacturers stated maximum angle of 7° (0.122 rad) was used for the Stuart rocker and the IKA rocker was set at its maximum 5° (0.087 rad) tilt angle. The characteristic FSS was calculated using these manufacturer stated tilt angles for each rocker frequency used (Table 6.1).

$$|\tau| = \frac{\pi\mu\theta_{\max}}{2\delta^2 \mathrm{T}} \tag{6.1}$$

#### MLO-A5 rocking

MLO-A5 cells are a fast-growing post-osteoblast/pre-osteocyte cell line. The doubling rate of the batch of cells initially used was greater than the doubling rate reported by Kato et al. and also appeared greater compared to the growth

**Table 6.1:** Theoretical characteristic FSS ($\tau$) generated by see-saw rockers

| Rocker | Frequency (Hz) | $\lvert\tau\rvert$ (Pa) |
|---|---|---|
| **Stuart SSL4** | 0.75 | 0.04 |
| | 1 | 0.05 |
| **IKA 2D Digital** | 0.75 | 0.03 |
| | 1.33 | 0.05 |

rate of the MLO-A5 cell used by Delaine-Smith et al. [269]. This resulted in cell detachment and death during long term experiments when cells were seeded at 1,000 cells $cm^{-2}$, as used by Delaine-Smith et al. Therefore, the seeding density was lowered to 50 cells $cm^{-2}$ which prevented this. Additionally, a new batch of cells was purchased from Kerafast (Boston, USA) and experiments were repeated at 1,000 cells $cm^{-2}$. Cells were cultured in 6-well plates in 2 mL of media and subjected to rocking at room temperature on a Stuart rocker or in an incubator on an IKA rocker, static cells were also placed at room temperature for 1 hour for room temperature experiments. Cells were rocked for 1 hour per day, 5 days per week, from day 3 at 0.75 Hz or 1 Hz on a Stuart rocker and 0.75 Hz or 1.33 Hz on an IKA rocker.

### hES-MP rocking

hES-MP cells were seeded at 1,000 or 10,000 cells $cm^{-2}$ in a 6 well plate to assess the effect of seeding density on mechanically induced osteogenic responses. Cells were cultured in one of three different batches of FBS and BM was changed to OIM on day 1 of culture. On day 5 of culture Dex was either withdrawn from the media for the remainder of culture (DW) or Dex was not withdrawn. Rocking was performed for 1, 2 or 3 hours per day, 5 days per week, from day 7 at 1 Hz or 1.33 Hz on an IKA rocker at room temperature or in an incubator.

### MC3T3-E1 rocking

MC3T3-E1 cells are another osteogenic cell line that have previously been shown to be sensitive to mechanical stimuli [86, 341, 342]. Cells were seeded at 200,000 cells per well in a 6 well plate in 2 mL of media and subjected to rocking in an incubator on an IKA rocker. Rocking was performed for 1 hour per day 5 days per week from day 7 at 0.75 Hz or 1.33 Hz.

### 6.3.2 Rocker characterisation

An inertial measurement unit (OPAL, APDM Inc., Portland, Oregon USA) was used to measure rocking platform movement to characterise the rocking platform's cycle frequency. The inertial measurement unit was located in the same position as where well plates were placed for rocking experiments and firmly secured to the platform. The signals were recorded for 5 cycles once the rocker had been running for 30 seconds at a sampling frequency of 128 samples $s^{-1}$. The acquired acceleration data was low pass filtered using a $4^{th}$ order Butterworth filter with a cut-off frequency of 5Hz and any DC offset was removed. The tilt angle of the rocker was calculated using Equation 6.2 where a is the acceleration and g is acceleration due to gravity taken as $9.807\,m\,s^{-2}$. The tilt angle was plotted and the mean frequency of the rocker was calculated using the built in Matlab function "meanfreq". Mean peak tilt angle was calculated by averaging peak tilt angle from each half cycle.

$$\theta = \sin^{-}1\left(\frac{a}{-}\right) \tag{6.2}$$

The calculated angles over the rocking period were then used to calculate the characteristic wall shear stress and the wall shear stress at three points in the well plate over the rocking cycle using another model developed by Zhou et al. (Equation 6.1, 6.3) [83].

$$|\tau| = \frac{2\pi\mu\theta_{max}x(2R-x)}{T(h_0\cot\theta + R - x)^2\sin^2\theta}\cos\frac{2\pi t}{T} \tag{6.3}$$

## 6.4 Results

### 6.4.1 Rocker platform cycle characterisation

The Stuart rocking platform cycle did not conform with the set frequency, with measurements showing a mean frequency of 0.89 Hz (14% higher) and 1.21 Hz (21% higher) when set at 0.75 Hz and 1 Hz respectively (Figure 6.1). Additionally, the mean peak tilt angle was also found to be higher at 9.13° and 10.2° respectively. This resulted in 1.2% (0.051 Pa) and 2.4% (0.077 Pa) higher characteristic FSS than that calculated using the set values for "0.75 Hz" and "1 Hz" respectively. The IKA rocking platform showed more reliable values, with measurements showing a mean frequency of 0.79 Hz (3.4% higher) and

1.38 Hz (4.9% higher) when set at 0.75 Hz and 1.33 Hz respectively. The mean peak angles also deviated less from the set values at 5.5° and 5.9° when set at 5° for 0.75 Hz and 1.33 Hz respectively. These deviations resulted in 0.2% (0.03 Pa) and 1% (0.077 Pa) higher characteristic FSS than that calculated using the set values for "0.75 Hz" and "1.33 Hz" respectively.

The FSS at 3 points parallel to the fluid movement along the centre of the base of the well were calculated ($\frac{x}{R}$ = 1, 0.75, 0.5, where x is the distance from the well edge and R is the diameter). The FSS varied between points in the well becoming higher the nearer to the edge of the well (Figure 6.2). The FSS varied in a sinusoidal manner at the centre of the well ($\frac{x}{R}$ = 1) but deviated from a typical sinusoidal wave at $\frac{x}{R}$ = 0.75 and 0.5. This was particularly evident with the Stuart rocking platform at $\frac{x}{R}$ = 0.5 where the FSS had an initial peak of 0.07 Pa or 0.2 Pa followed by a second peak of 0.05 Pa or 0.12 Pa for 0.75 Hz and 1 Hz cycles respectively. Peak FSS levels with the IKA rocking platform only varied slightly between positions in the well and between each peak.

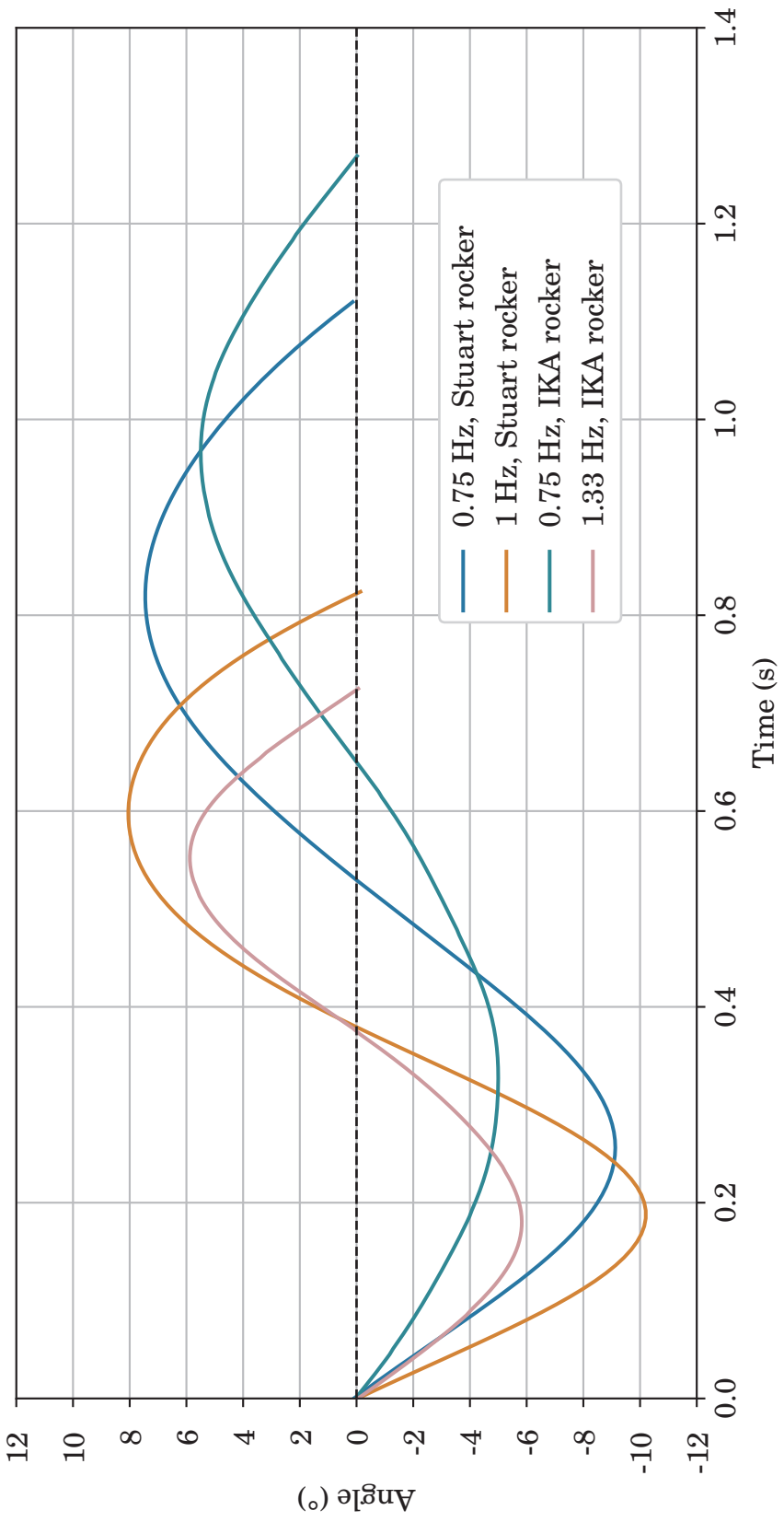


**Figure 6.1:** Stuart and IKA rocker platform cycles at different frequencies recorded with an inertial measurement unit.

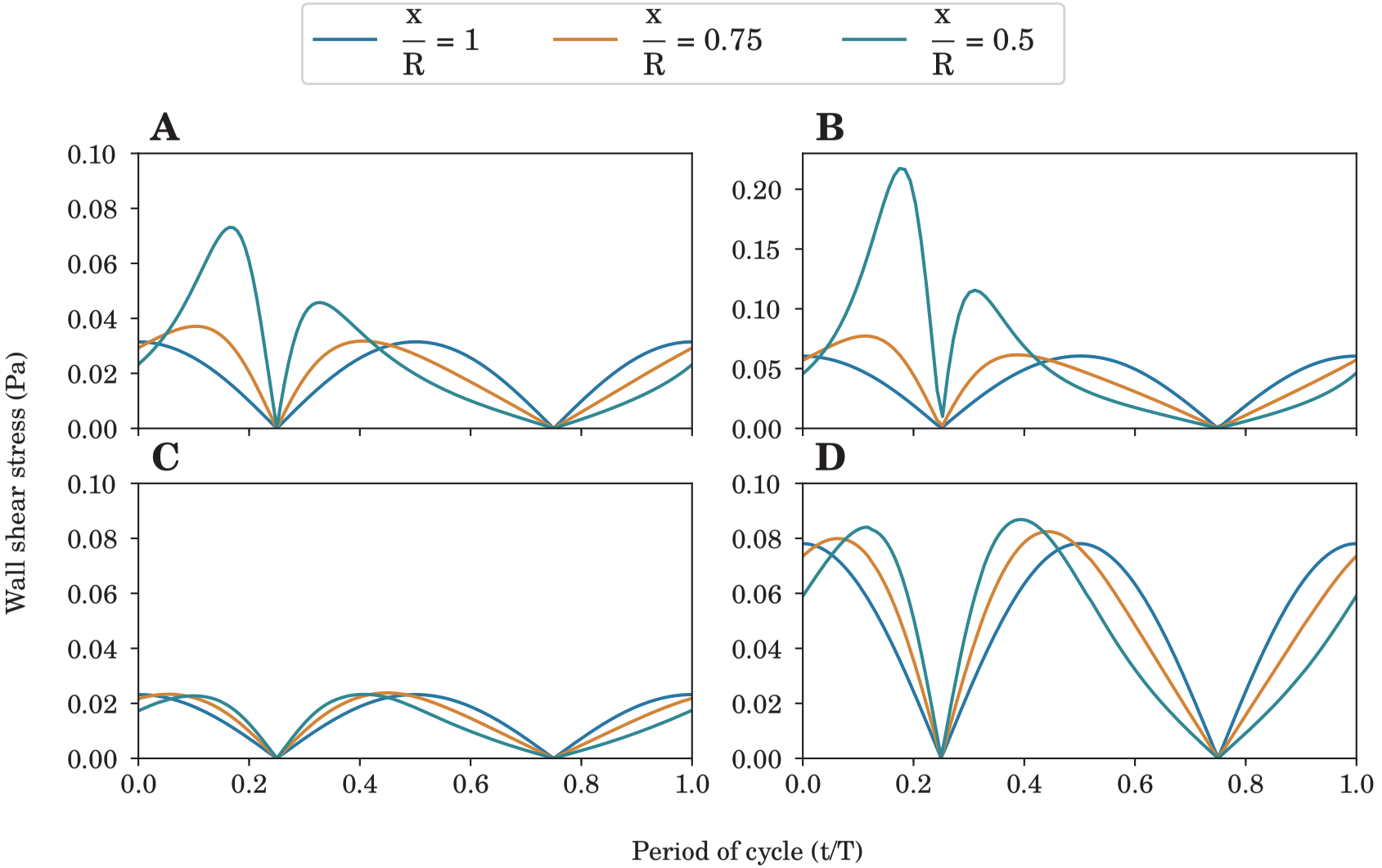


**Figure 6.2:** Fluid shear stress profiles at the bottom of a 6-well plate for one cycle on an IKA rocker at three different locations. $\frac{x}{R}$ = 1, 0.75 or 0.5, where x is the distance from the edge of the well and R is the radius of the well. (A) 0.75 Hz Stuart rocker. (B) 1 Hz Stuart rocker. (C) 0.75 Hz IKA rocker. (D) 1.33 Hz IKA rocker.

### 6.4.2 Rocker culture of MLO-A5

Initial rocking experiments were performed with a Stuart rocking platform. However, after its rocking cycle was shown to be unreliable further experiments were performed with an IKA rocking platform that had the added benefit of being rated for use in an incubator.

#### Influence of seeding density on osteogenic responses to FSS

Seeding density had no significant effect on cell growth rate at room temperature or when stimulated in an incubator. Both low and high seeding densities had similar increases in metabolic activity over 14 days at each temperature (Figure 6.3, 6.4). There were also no significant differences in metabolic activity between static and rocked groups at either seeding density at either temperature. Both metabolic activity and total DNA levels were higher when cells were seeded at a higher seeding density compared to the lower seeding density.

Both static and rocked groups had similar levels of ALP activity suggesting FSS had no effect on ALP activity (Figure 6.5, 6.6).

Both DR80 and ARS staining showed patchy staining spread across the bottom surface of the wells at low seeding density at both temperatures (Figure 6.7, 6.8). ARS staining was more intense and covered a greater area in the cells stimulated in an incubator compared to at room temperature. Areas of staining corresponded with colonies of confluent cells. There were no visual differences between staining of rocked groups compared to static groups in terms of staining intensity or staining distribution in cells seeded at low-density. This was further confirmed quantitatively, with no differences between groups when samples were destained. At high seeding density, both ARS and DR80 staining was more evenly distributed on the bottom surface of the wells. There were no visual differences in terms of distribution and staining intensity between static and rocked groups in cells stimulated at room temperature. However, when stimulated in an incubator ARS staining was more intense in cells subjected to 1.33 Hz and when destained was also quantitatively higher than the statically cultured cells. There were no consistently observable differences in staining distribution between static or rocked cells or between each rocking frequency.

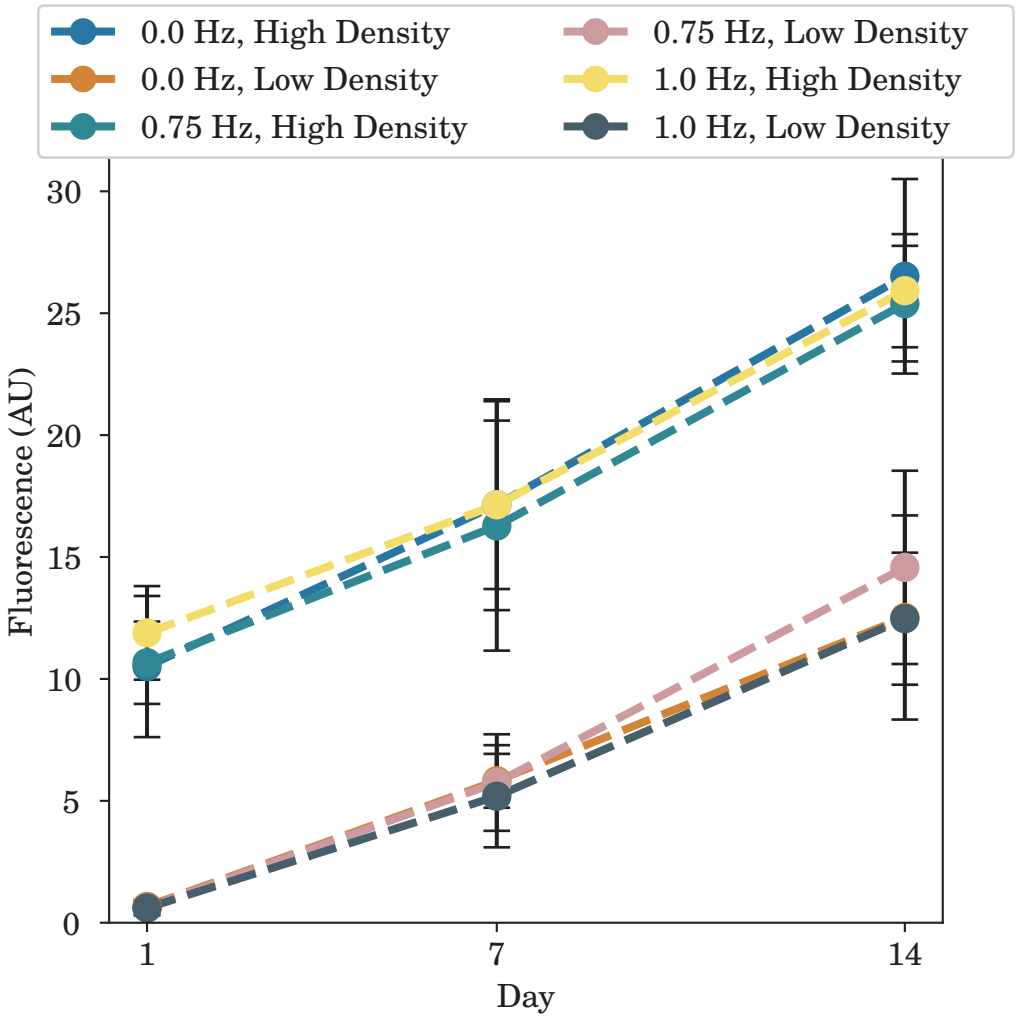


**Figure 6.3:** Effect of FSS on MLO-A5 metabolic activity over 14 days of monolayer culture at a high and low seeding density. Cells were mechanically stimulated on a Stuart rocking platform for 1 h, 5 days per week from day 3 at room temperature. Metabolic activity was assessed with RR. Data represents mean ± SD n=9.

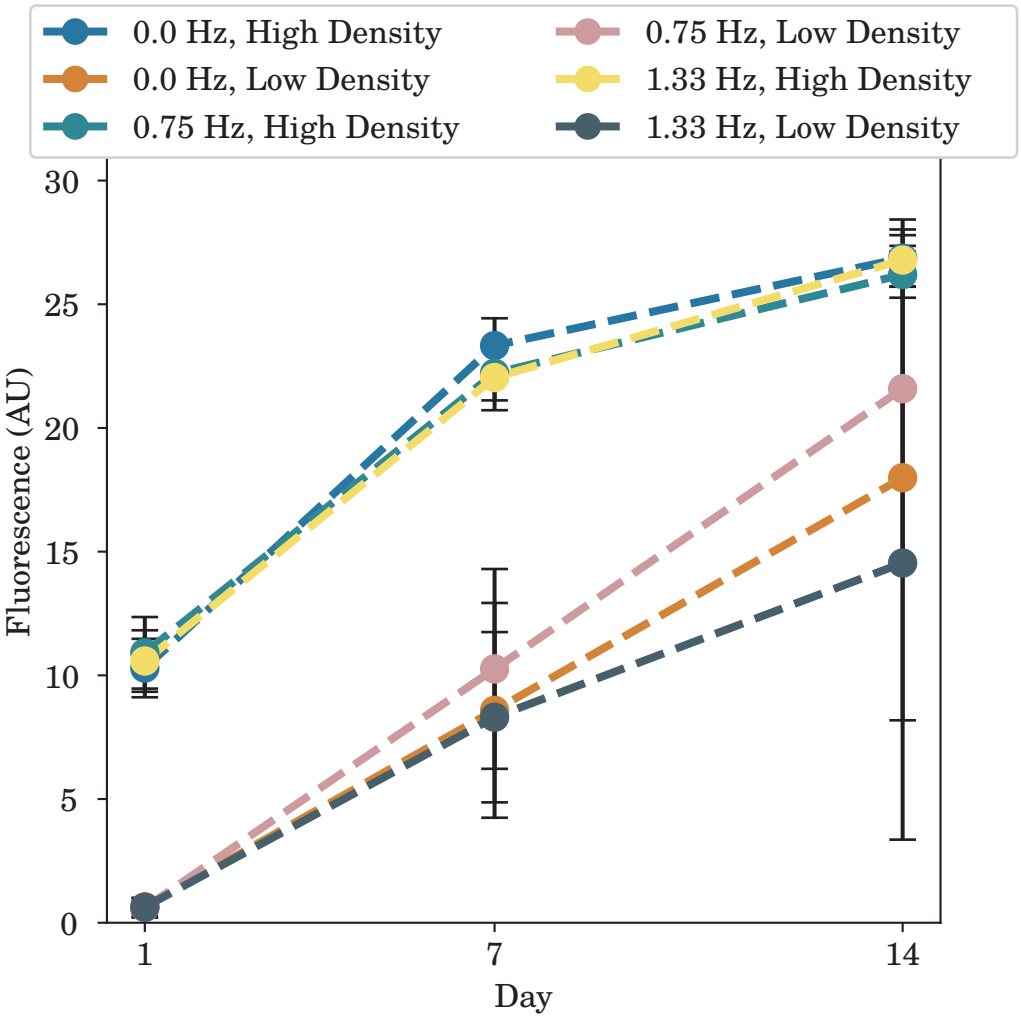


**Figure 6.4:** Effect of FSS on MLO-A5 metabolic activity over 14 days of monolayer culture at a high and low seeding density. Cells were mechanically stimulated on a IKA rocking platform for 1 h, 5 days per week from day 3 in an incubator. Metabolic activity was assessed with RR. Data represents mean ± SD n=9. Fluorescence was measured at $\lambda_{ex}$: 540 nm and $\lambda_{em}$: 590 nm.

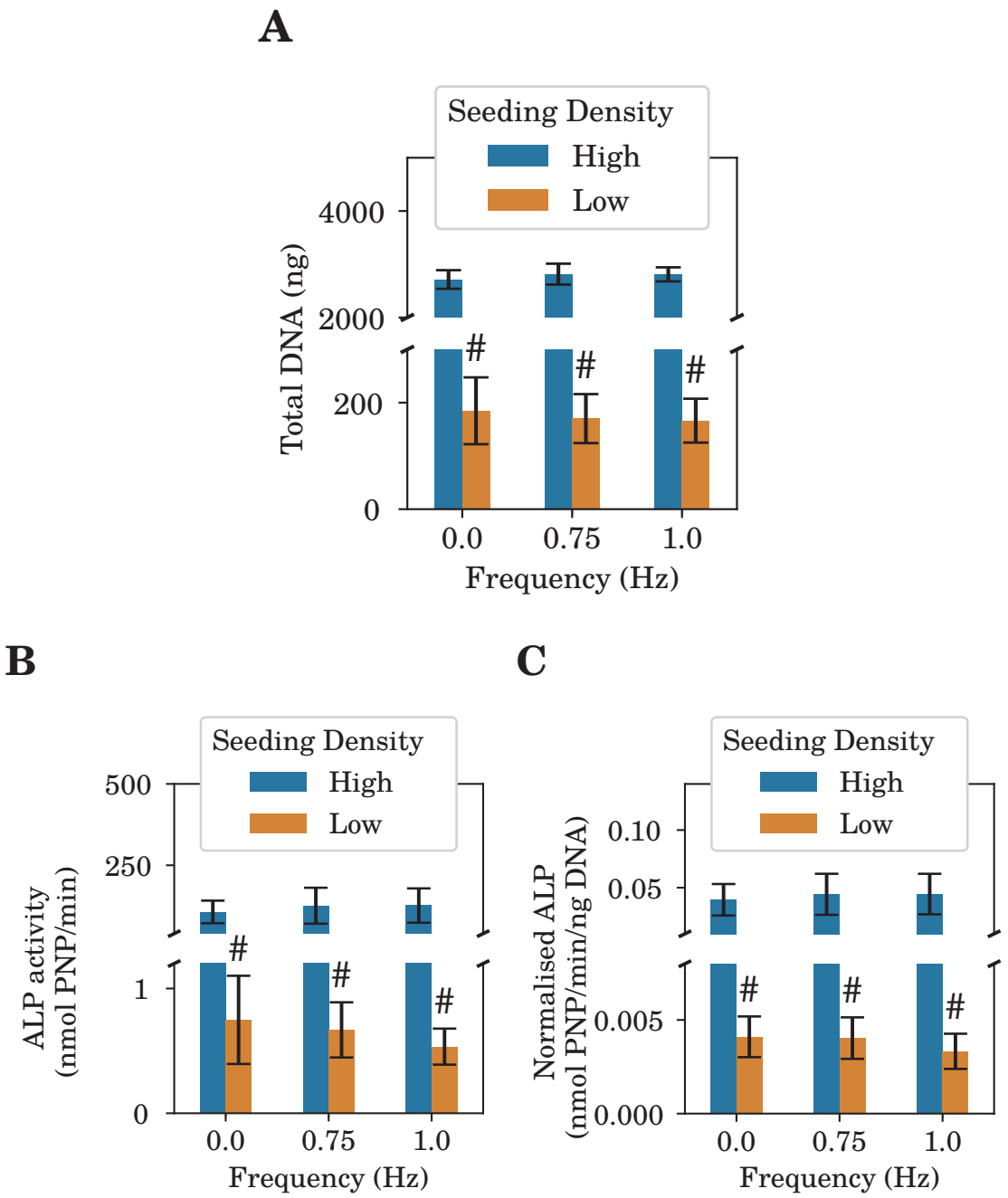


**Figure 6.5:** Effect of FSS on MLO-A5 day 7 cell number and ALP activity in monolayer culture at a high and low seeding density. Cells were mechanically stimulated on a Stuart rocking platform for 1 h, 5 days per week from day 3 at room temperature. (A) Total DNA. (B) ALP activity. (C) ALP activity normalised to total DNA. Data represents mean ± SD n=9. # = $p<0.05$ compared to the high seeding density.

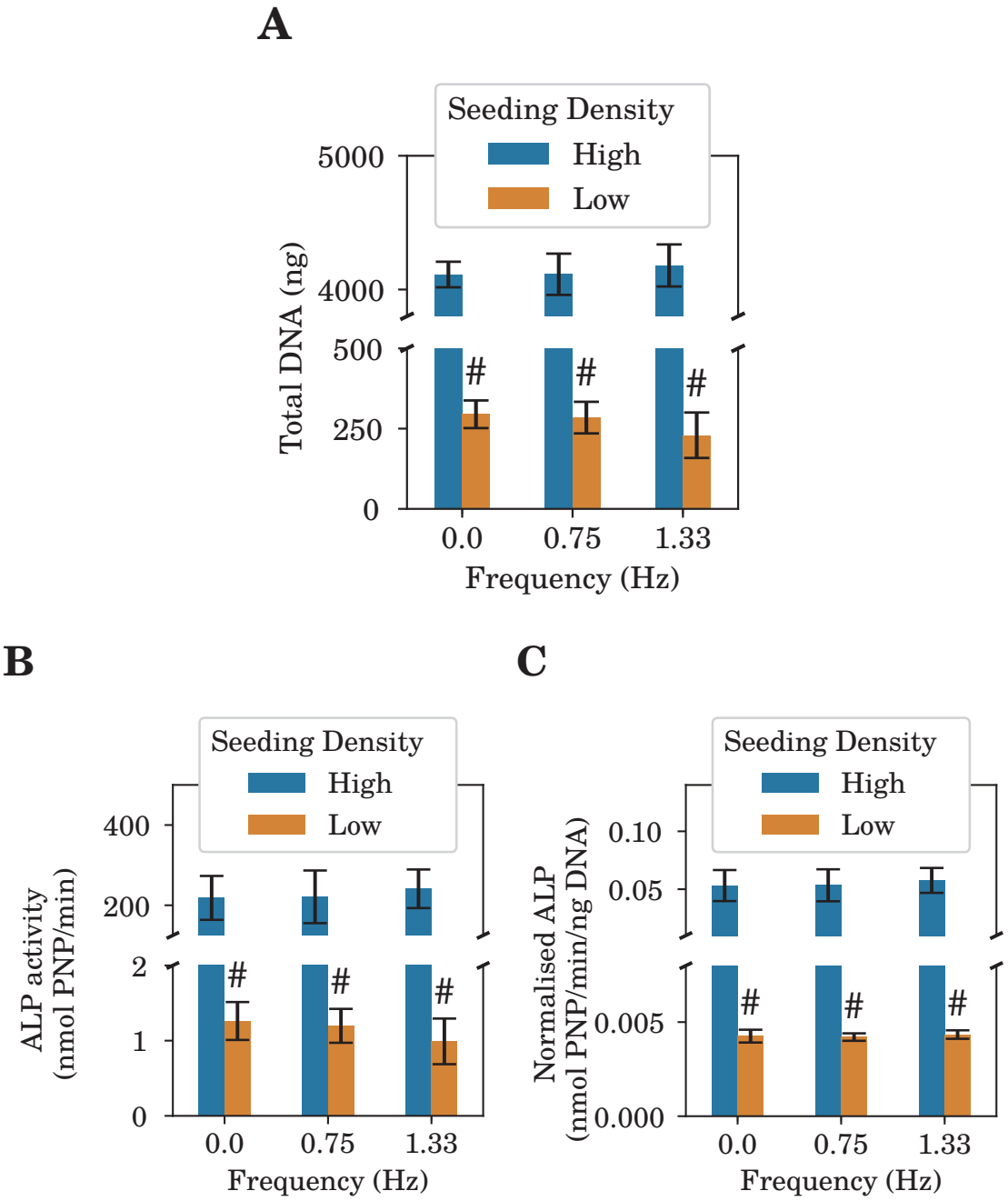


**Figure 6.6:** Effect of FSS on MLO-A5 day 7 cell number and ALP activity in monolayer culture at a high and low seeding density. Cells were mechanically stimulated on an IKA rocking platform for 1 h, 5 days per week from day 3 in an incubator. (A) Total DNA. (B) ALP activity. (C) ALP activity normalised to total DNA. Data represents mean ± SD n=9. # = $p<0.05$ compared to the high seeding density.

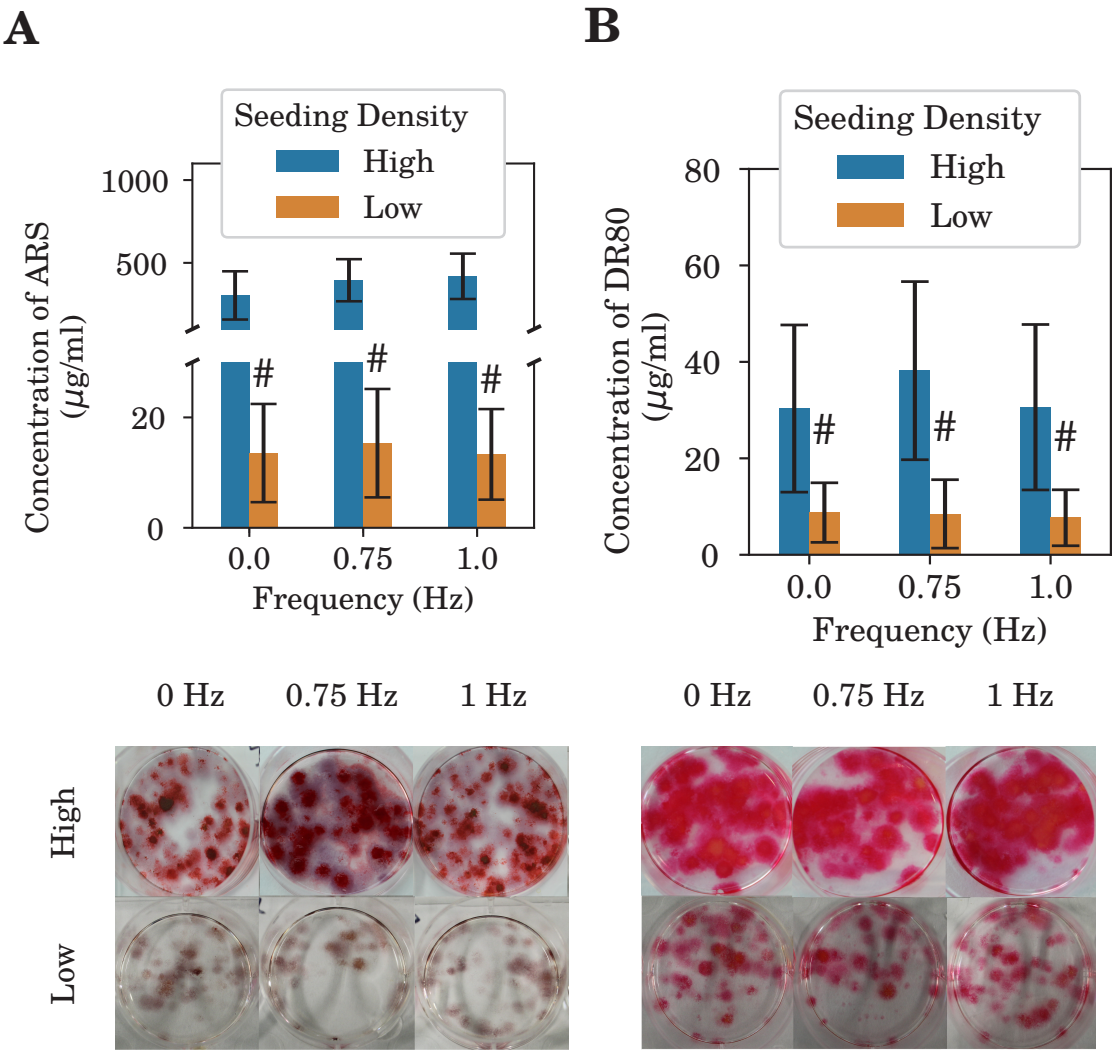


**Figure 6.7:** Effect of FSS on MLO-A5 matrix formation in monolayer culture at a high and low seeding density. Cells were mechanically stimulated on a Stuart rocking platform for 1 h, 5 days per week from day 3 at room temperature. (A) Day 14 matrix calcium quantified by ARS. (B) Day 14 matrix collagen quantified by DR80. Data represents mean ± SD n=9. # = $p<0.05$ compared to the high seeding density. Representative photographs of stained wells are shown below their corresponding graphs.

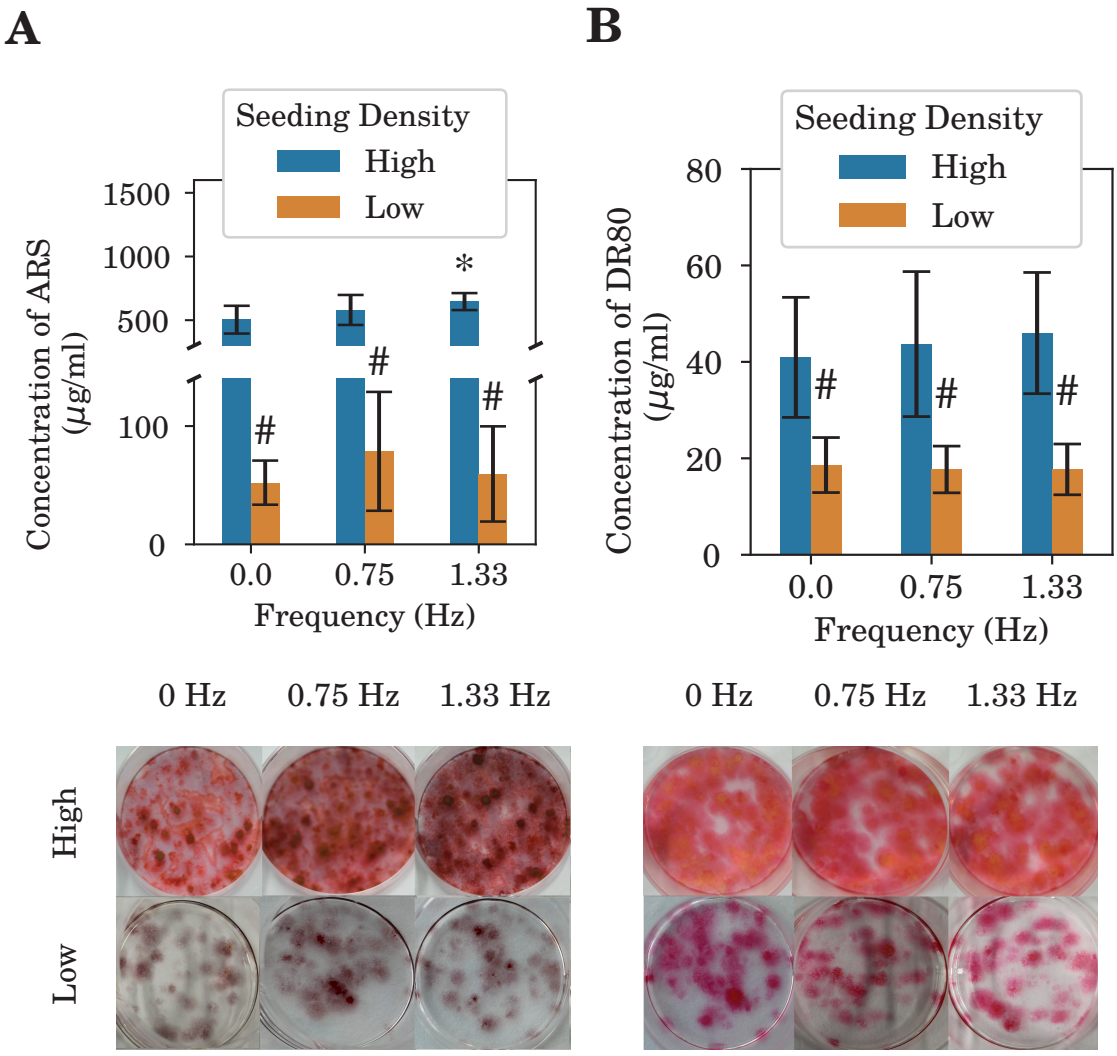


**Figure 6.8:** Effect of FSS on MLO-A5 matrix formation in monolayer culture at a high and low seeding density. Cells were mechanically stimulated on an IKA rocking platform for 1 h, 5 days per week from day 3 in an incubator. (A) Day 14 matrix calcium quantified by ARS. (B) Day 14 matrix collagen quantified by DR80. Data represents mean ± SD n=9. # = $p<0.05$ compared to the high seeding density. Representative photographs of stained wells are shown below their corresponding graphs.

### 6.4.3 Rocker culture of MC-3T3 cells

Metabolic activity significantly increased from day 1 to day 21 of culture increasing between each day except between day 14 and day 21 (Figure 6.9). No significant differences were found between static and rocked samples at any time point over the 21 day culture period. Similarly, day 14 DNA levels also showed no differences between groups (Figure 6.10).

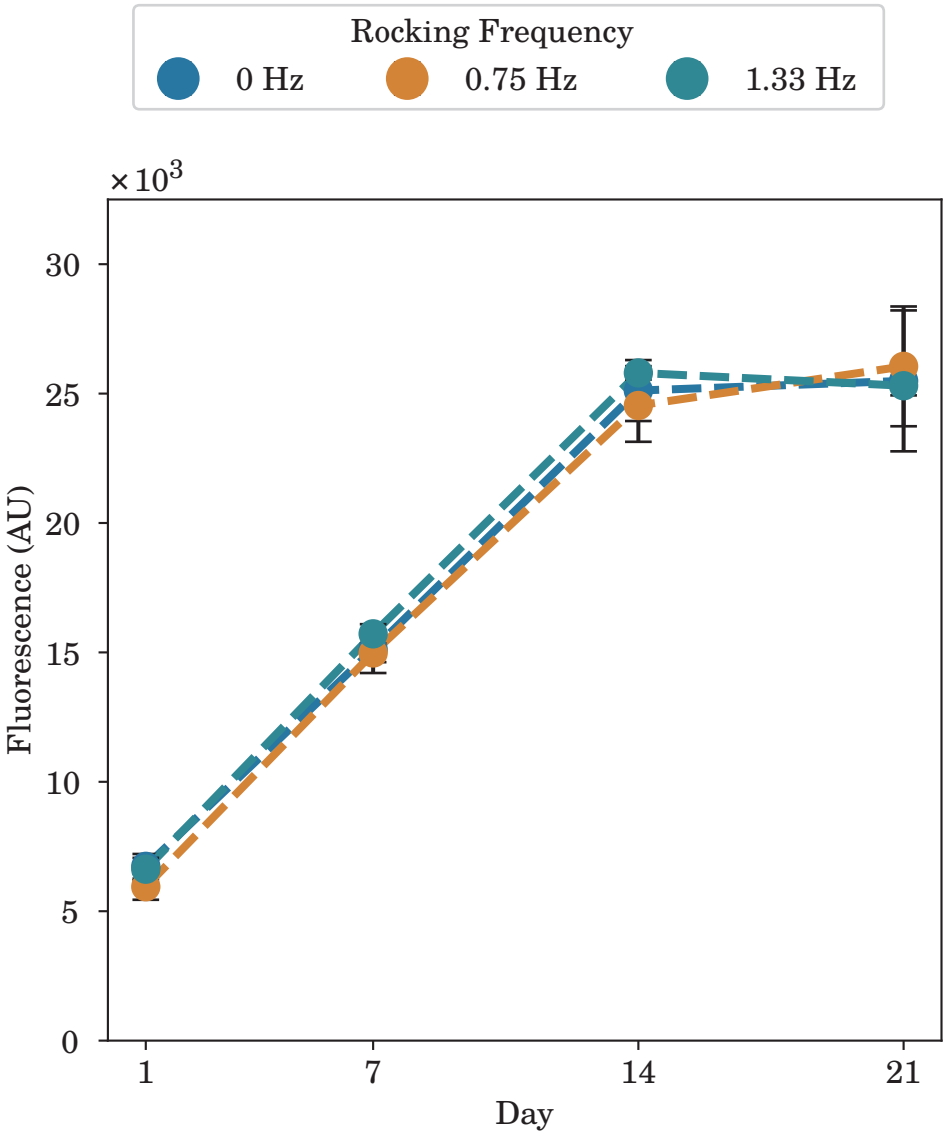


**Figure 6.9:** Effect of FSS on MC3T3-E1 metabolic activity over 21 days of monolayer culture. Cells were mechanically stimulated on an IKA rocking platform for 1 h, 5 days per week from day 7 in an incubator. Metabolic activity was assessed with RR. Data represents mean ± SD n=9. Fluorescence was measured at $\lambda_{ex}$: 540 nm and $\lambda_{em}$: 590 nm.

There were no significant differences between total ALP activity of stati-

cally cultured or rocked groups (Figure 6.10). This remained true when ALP activity was normalised to total DNA content in each well. Normalised ALP activity levels of MC3T3-E1 cells were similar to that of MLO-A5 cells.

ARS staining was evenly distributed over the surface of the well plate (Figure 6.11). ARS staining was significantly less intense than in MLO-A5 cells and unlike in MLO-A5 cells, mineralised matrix was not nodular in appearance. ARS levels in samples subjected to rocking did not differ from the statically cultured samples. Collagen staining was found to be uniformly spread across the majority of the well surface and when assessed quantitatively there were no significant differences in collagen production found in cells subjected to rocking, although 1.33 Hz levels were lower.

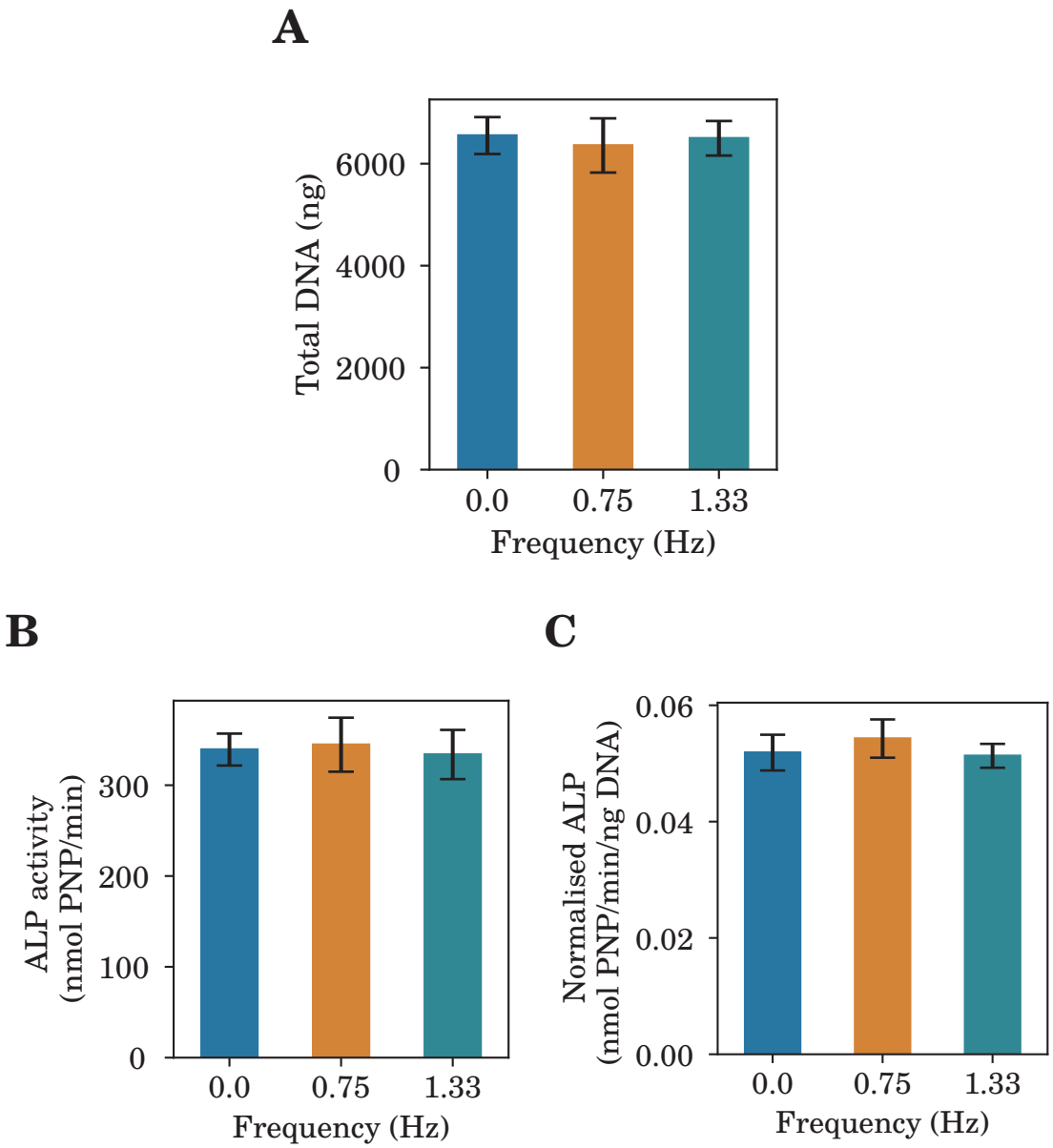


**Figure 6.10:** Effect of FSS on MC3T3-E1 day 14 cell number and ALP activity in monolayer culture. Cells were mechanically stimulated on an IKA rocking platform for 1 h, 5 days per week from day 7 in an incubator. (A) Total DNA. (B) ALP activity. (C) ALP activity normalised to total DNA. Data represents mean ± SD n=9.

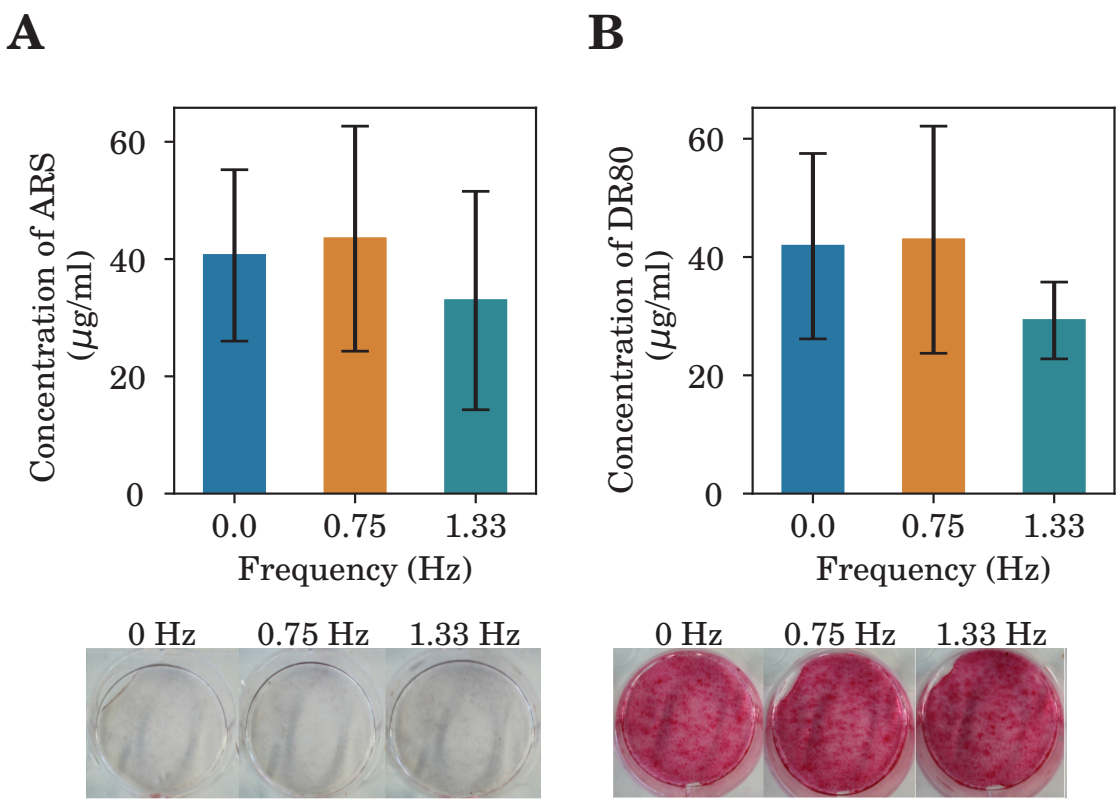


**Figure 6.11:** Effect of FSS on MC3T3-E1 matrix formation in monolayer culture. Cells were mechanically stimulated on an IKA rocking platform for 1 h, 5 days per week from day 7 in an incubator. (A) Day 21 matrix calcium quantified by ARS. (B) Day 21 matrix collagen quantified by DR80. Data represents mean ± SD n=9. Representative photographs of stained wells are shown below their corresponding graphs.

### 6.4.4 Rocker culture of hE-SMP cells

Rocking was initially performed at room temperature to more closely follow the method developed by Delaine-Smith et al. [82]. However, due to the greater control of variables offered by rocking within an incubator, subsequent experiments were performed using an incubator.

#### Influence of seeding density on osteogenic responses to FSS

To assess the influence of seeding density on osteogenesis in response to FSS stimulation, hES-MP cells were seeded at a low and high density and subjected to rocking in OIM. Cell metabolic activity increased from day 1 to day 21 in all groups with no significant difference between high and low seeding densities on day 21 (Figure 6.12). Rocking had no adverse effects on cell metabolic activity at 0.75 Hz or 1.33 Hz in either low or high density seeded cells.

Although RR showed no significant differences between static and rocked groups on day 14 of culture, day 14 DNA was higher in the static group compared to the 0.75 Hz rocked group (Figure 6.13). However, similarly to the RR results, DNA was significantly lower in all low-density groups compared to high density groups. There were no significant differences between static and rocked groups at low-density. Total ALP activity was significantly lower in all low-density groups compared to high density groups. There were no significant differences between static and rocked groups at low-density. At high density cells subjected to 0.75 Hz had significantly less total ALP activity compared to statically cultured cells. However, when normalised to total DNA there was no difference between static and rocked groups at high density.

HES-MP cells seeded at low-density showed very faint and patchy ARS staining (Figure 6.14). ARS staining was inconsistent in cells subjected to 1.33 Hz rocking with some wells showing very faint staining similar to statically cultured cells and other wells showing more intense staining as shown in Figure 6.14. Qualitatively there were no significant differences between statically cultured and cells rocked at 0.75 Hz at low seeding density. Cells seeded at low-density and subjected to 1 Hz had significantly higher ARS compared to statically cultured cells. Matrix mineralisation staining at high density was more intense but still patchy. Staining was more intense at the edges of rocked wells compared to statically cultured cells where staining intensity was more even throughout the well. Both 0.75 Hz and 1 Hz rocked cells had significantly

higher ARS levels compared to statically cultured cells. Collagen staining was patchy throughout the well plate in low seeding density groups with no differences between static and rocked samples. In high seeding density samples collagen staining was more intense at the edge of the wells in both static and rocked cells and patchy in the centre. There were no significant differences between static and rocked samples.

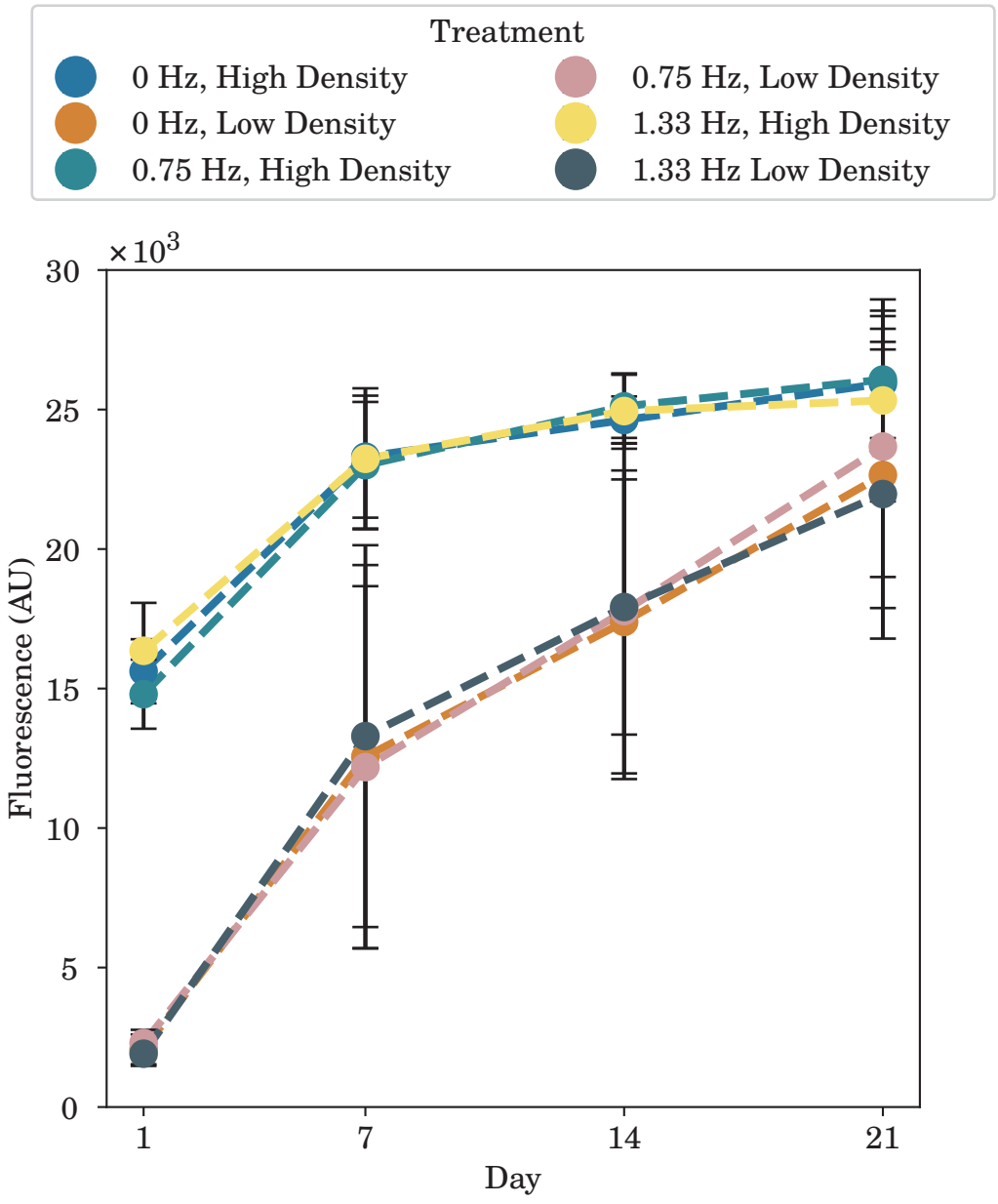


**Figure 6.12:** Effect of FSS on hES-MP metabolic activity over 21 days of monolayer culture. Cells were mechanically stimulated on an IKA rocking platform for 1 h, 5 days per week from day 7 at room temperature. Metabolic activity was assessed with RR. Data represents mean ± SD n=9. Fluorescence was measured at $\lambda_{ex}$: 540 nm and $\lambda_{em}$: 590 nm.

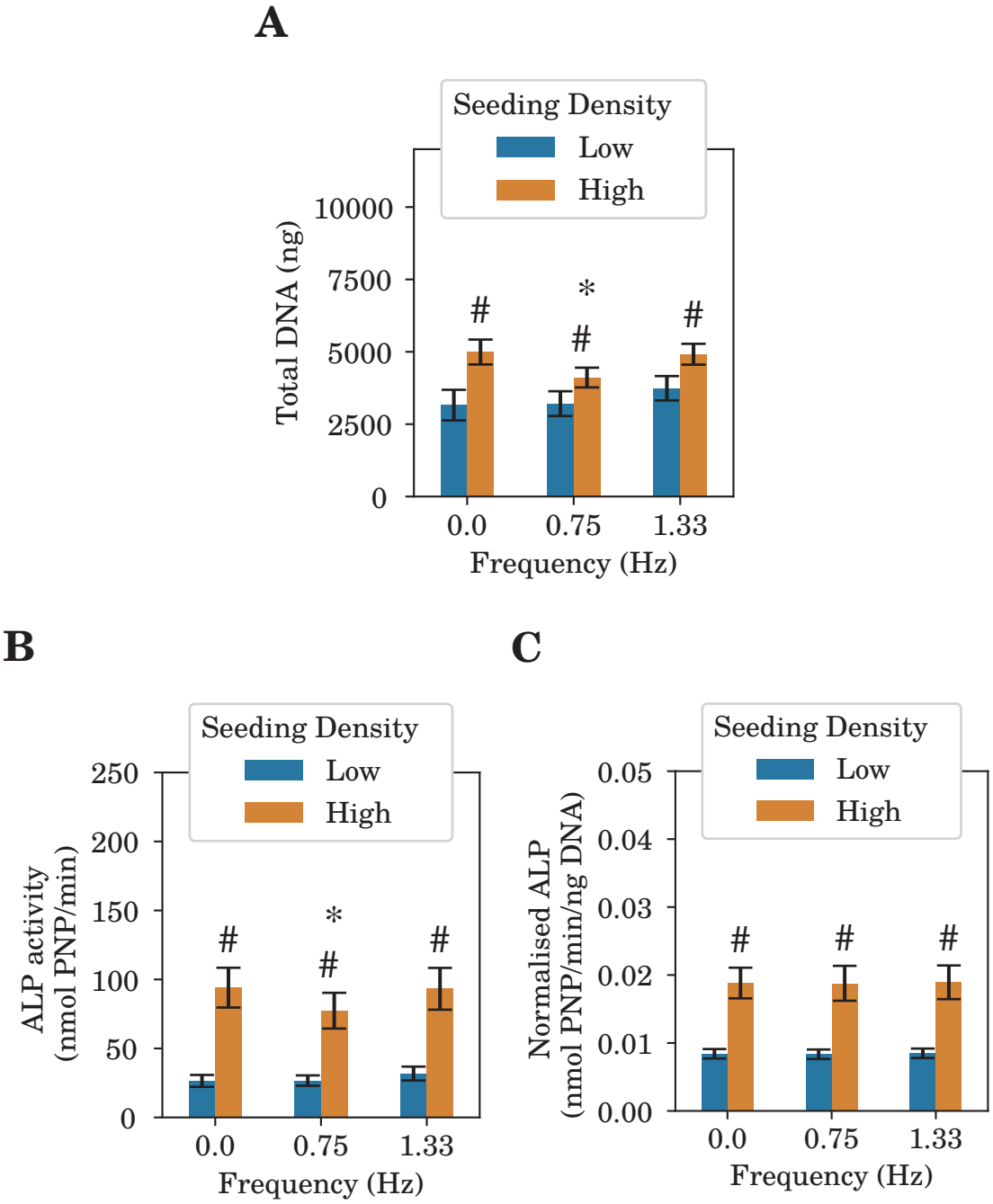


**Figure 6.13:** Effect of FSS on hES-MP day 14 cell number and ALP activity in monolayer culture. Cells were mechanically stimulated on an IKA rocking platform for 1 h, 5 days per week from day 7 at room temperature. (A) Total DNA. (B) ALP activity. (C) ALP activity normalised to total DNA. Data represents mean ± SD n=9. * = $p<0.05$ compared to the static control. # = $p<0.05$ compared to the high seeding density.

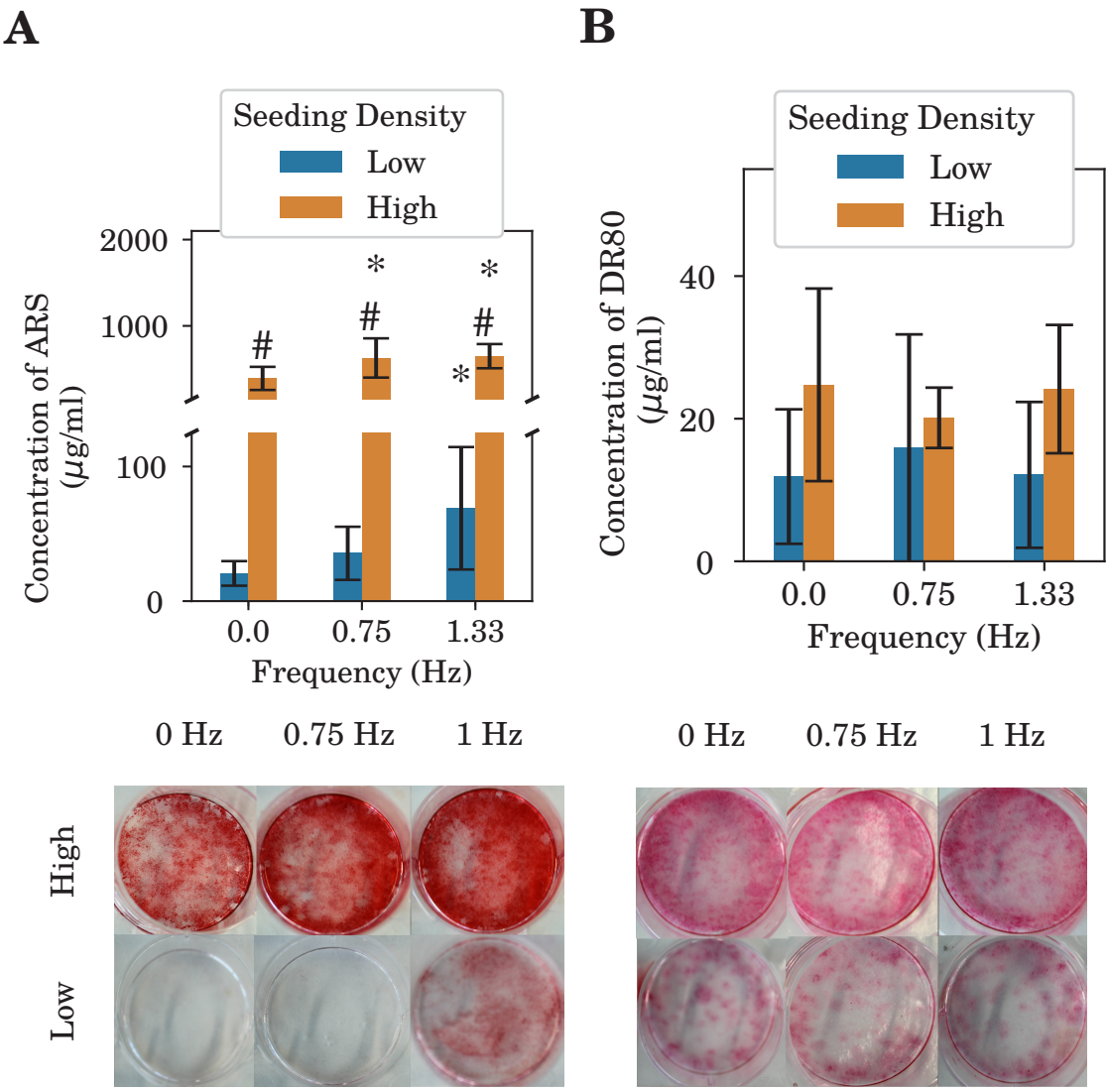


**Figure 6.14:** Effect of FSS on hES-MP matrix formation in monolayer culture. Cells were mechanically stimulated on an IKA rocking platform for 1 h, 5 days per week from day 7 at room temperature. (A) Day 21 matrix calcium quantified by ARS. (B) Day 21 matrix collagen quantified by DR80. Data represents mean ± SD n=9. * = $p<0.05$ compared to the static control. # = $p<0.05$ compared to the high seeding density. Representative photographs of stained wells are shown below their corresponding graphs.

**Influence of temperature on osteogenic responses to FSS**

To have further control of variables during mechanical stimulation, such as media pH and temperature, rocking was performed in standard conditions in an incubator (5% $CO_2$, 37 °C). There were no differences in culture conditions between seeding and day 7 of culture. Cell metabolic activity increased at the same rates between day 1 and day 7 of culture in all groups (Figure 6.15). From day 7 of culture, cells were subjected to rocking at either room temperature or in an incubator. The differences in temperature, humidity and $CO_2$ had no significant effects on metabolic activity levels at day 14 or day 21.

Although there were no significant differences found in terms of metabolic activity, day 14 total DNA was found to be significantly lower in samples subjected to 0.75 Hz at room temperature compared to samples cultured statically and samples subjected to rocking at 0.75 Hz in an incubator (Figure 6.16). There were no significant differences in total DNA between static and rocked samples when stimulated in an incubator. Samples stimulated in an incubator had significantly higher ALP activity both in terms of total ALP activity and when normalised to total DNA. There were no significant differences in ALP activity between static and rocked samples at either temperature.

Under static conditions matrix mineralisation was significantly higher in incubated samples compared to samples subjected to room temperature conditions (Figure 6.17). In rocked samples, at both frequencies there were no significant differences between incubated and room temperature samples. At both room temperature and when stimulated in an incubator, only samples subjected to 1.33 Hz had significantly greater matrix mineralisation compared to statically cultured cells. Similarly to ARS samples cultured at room temperature had significantly lower collagen staining compared to cells continuously cultured in an incubator. Staining in cells stimulated at room temperature was less evenly distributed throughout the well and often less intense. There were no significant differences in collagen production between static and rocked samples at either temperature.

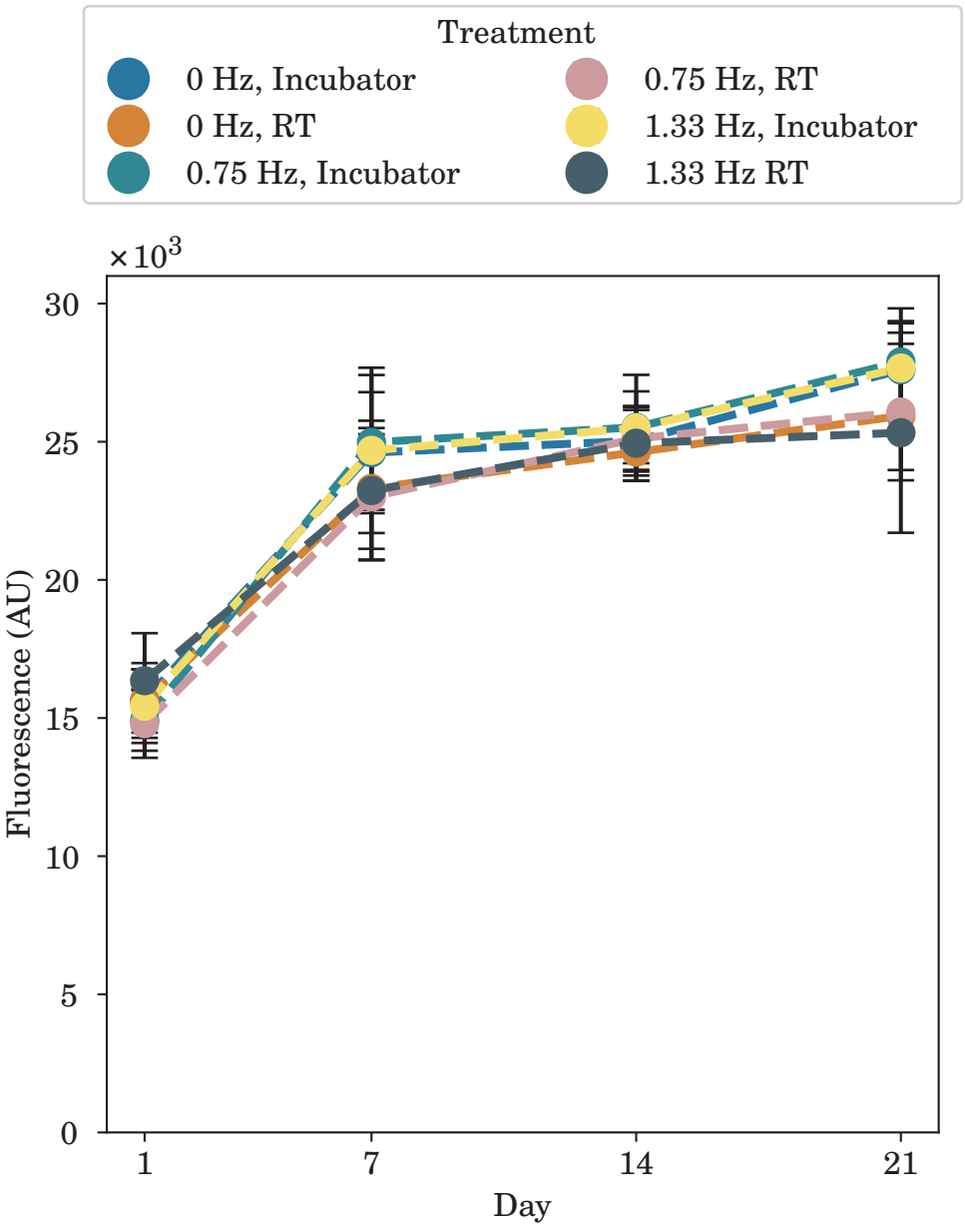


**Figure 6.15:** Effect of FSS on hES-MP metabolic activity over 21 days of monolayer culture. Cells were mechanically stimulated on an IKA rocking platform for 1 h, 5 days per week from day 7 in an incubator. Metabolic activity was assessed with RR. Data represents mean ± SD n=9. Fluorescence was measured at $\lambda_{ex}$: 540 nm and $\lambda_{em}$: 590 nm.

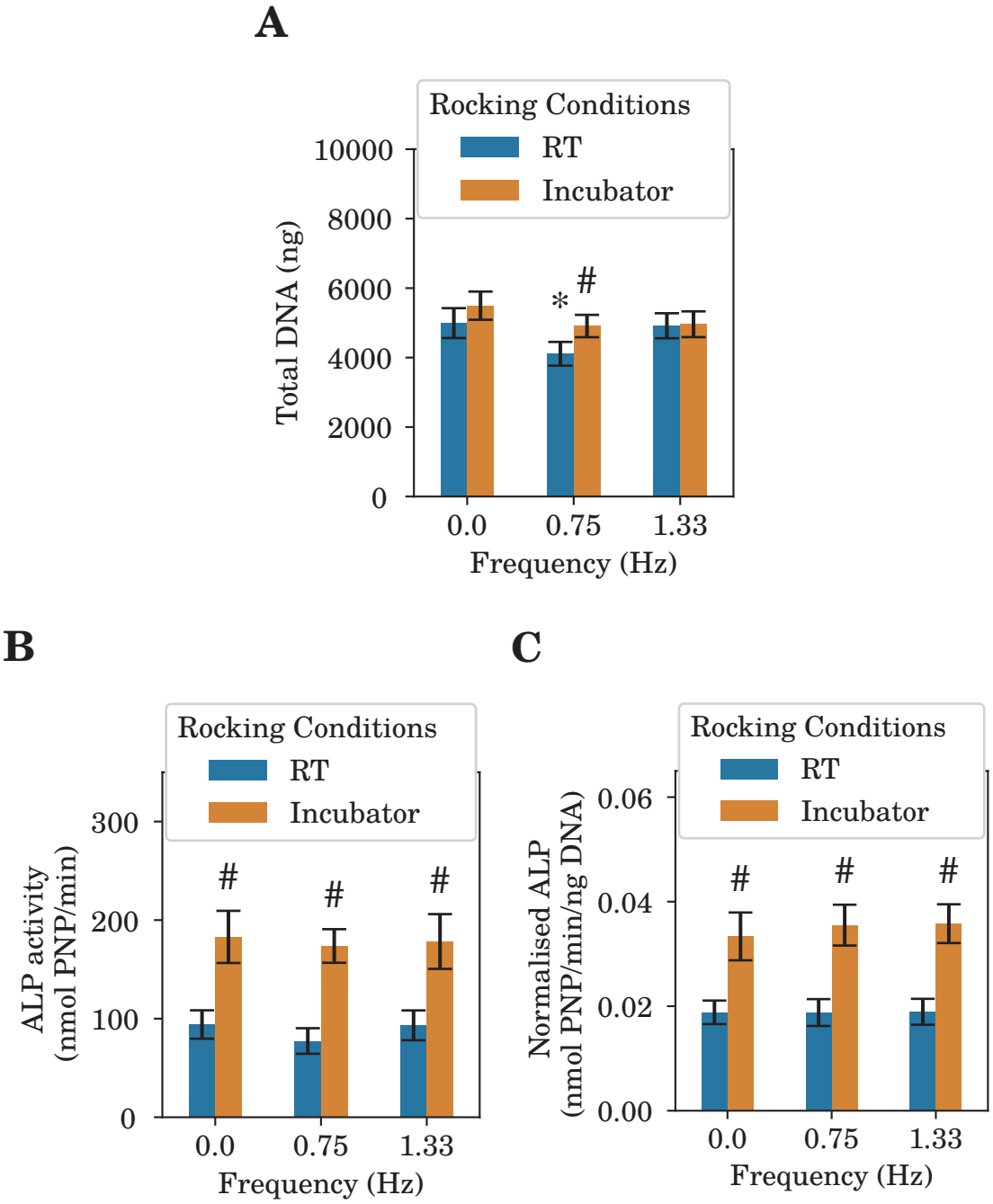


**Figure 6.16:** Effect of FSS on hES-MP day 14 cell number and ALP activity in monolayer culture. Cells were mechanically stimulated on an IKA rocking platform for 1 h, 5 days per week from day 7 in an incubator. (A) Total DNA. (B) ALP activity. (C) ALP activity normalised to total DNA. Data represents mean ± SD n=9. * = $p<0.05$ compared to the static control. # = $p<0.05$ compared to the room temperature stimulated group.

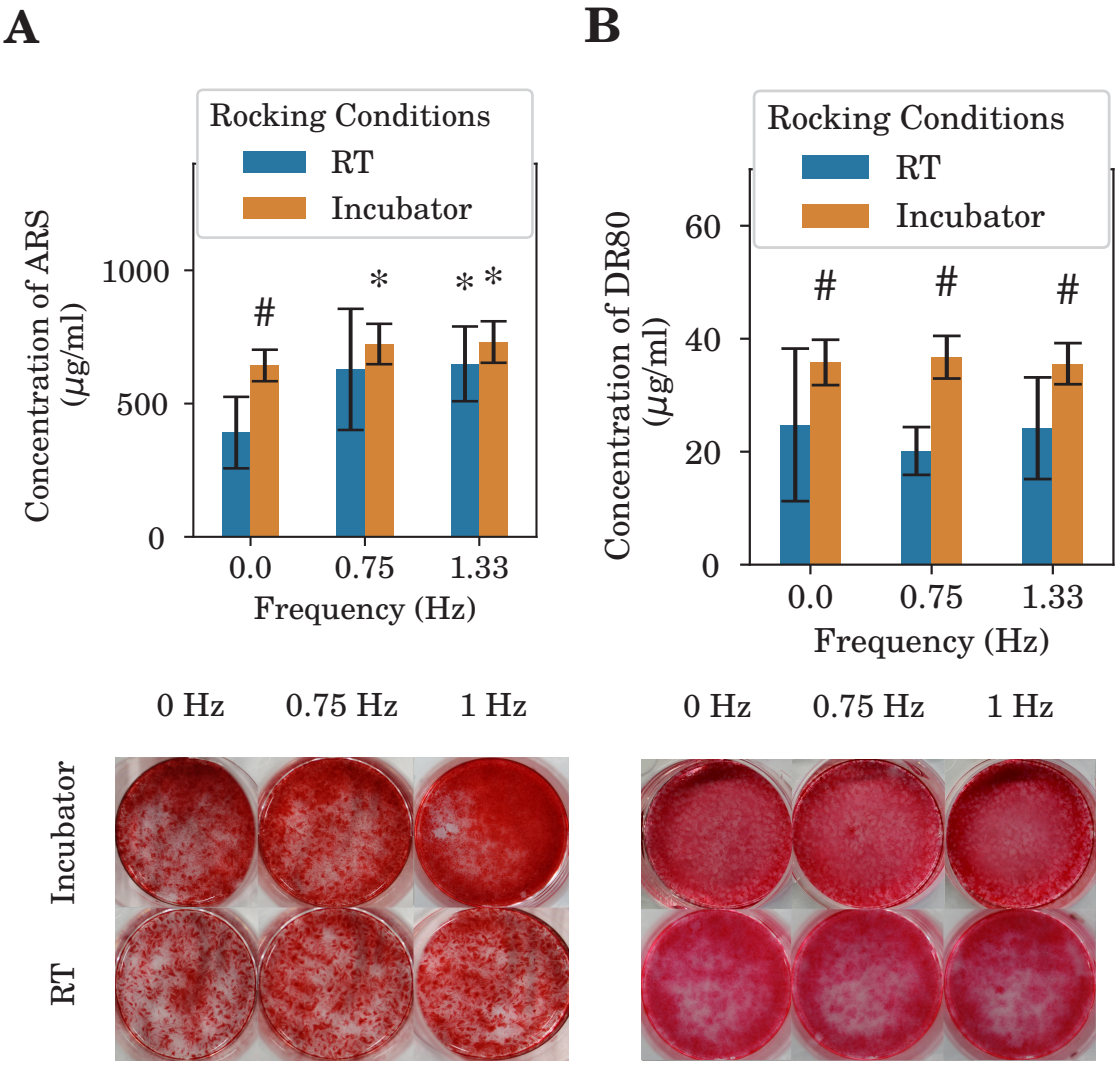


**Figure 6.17:** Effect of FSS on hES-MP matrix formation in monolayer culture. Cells were mechanically stimulated on an IKA rocking platform for 1 h, 5 days per week from day 7 in an incubator. (A) Day 21 matrix calcium quantified by ARS. (B) Day 21 matrix collagen quantified by DR80. Data represents mean ± SD n=9. * = $p<0.05$ compared to the static control. # = $p<0.05$ compared to the room temperature stimulated group. Representative photographs of stained wells are shown below their corresponding graphs.

### Influence of stimulus duration on osteogenic responses to FSS

Longer durations of rocking at 1.33 Hz had no detrimental effects on metabolic activity over 21 days of culture (Figure 6.18). Both static and rocked samples metabolic activity increased from day 1 to day 7 with no further significant increase between day 7 and day 21.

Increased rocking duration had no significant effect on matrix mineralisation or collagen production (Figure 6.19). Samples subjected to 1, 2 or 3 h of rocking all showed significantly higher matrix mineralisation compared to statically cultured cells. Collagen production levels were similar between static and rocked groups at all durations tested.

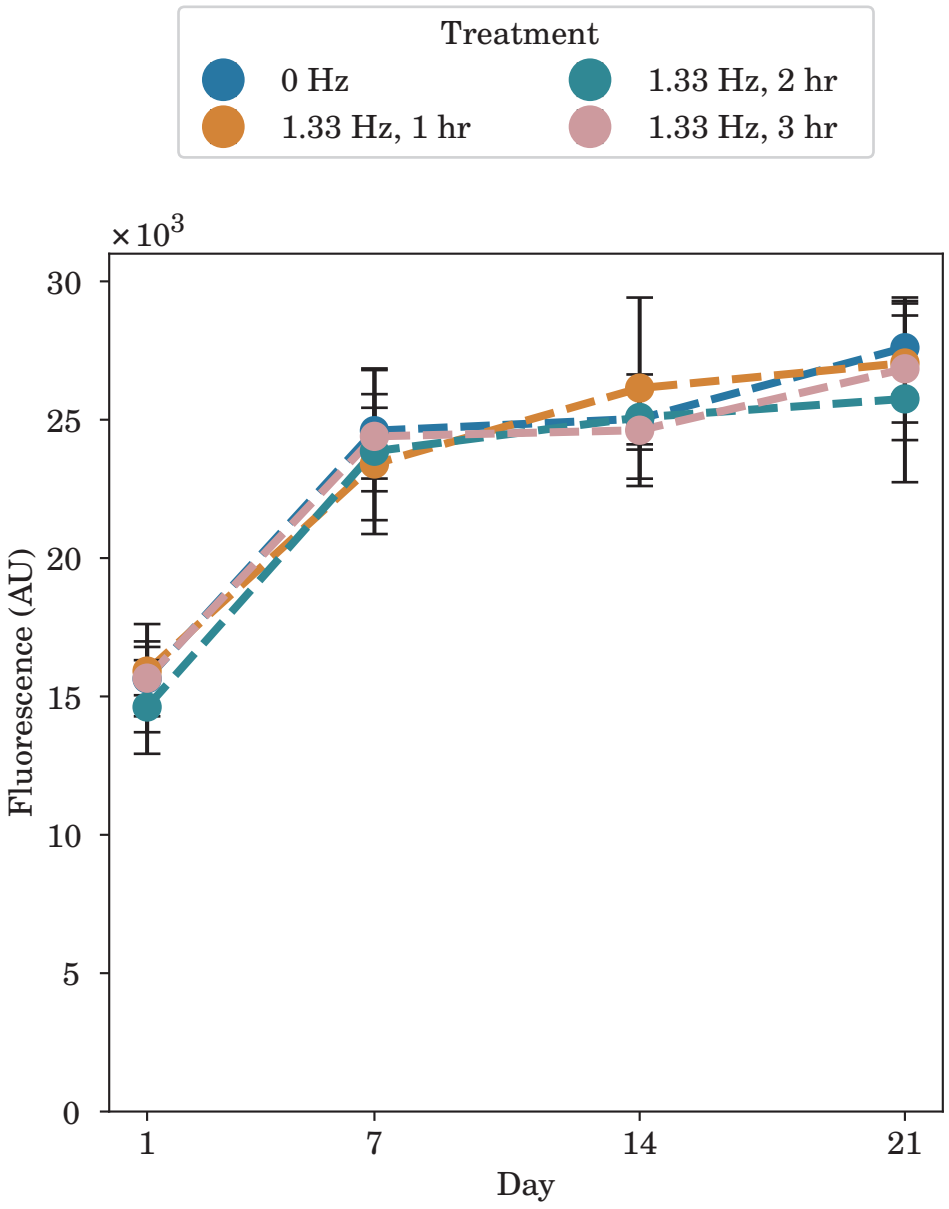


**Figure 6.18:** Effect of rocking duration on hES-MP metabolic activity in monolayer culture over 21 days of monolayer culture. Cells were mechanically stimulated on an IKA rocking platform for 1 h, 2 h or 3 h 5 days per week from day 7 in an incubator. Metabolic activity was assessed with RR. Data represents mean ± SD n=9.

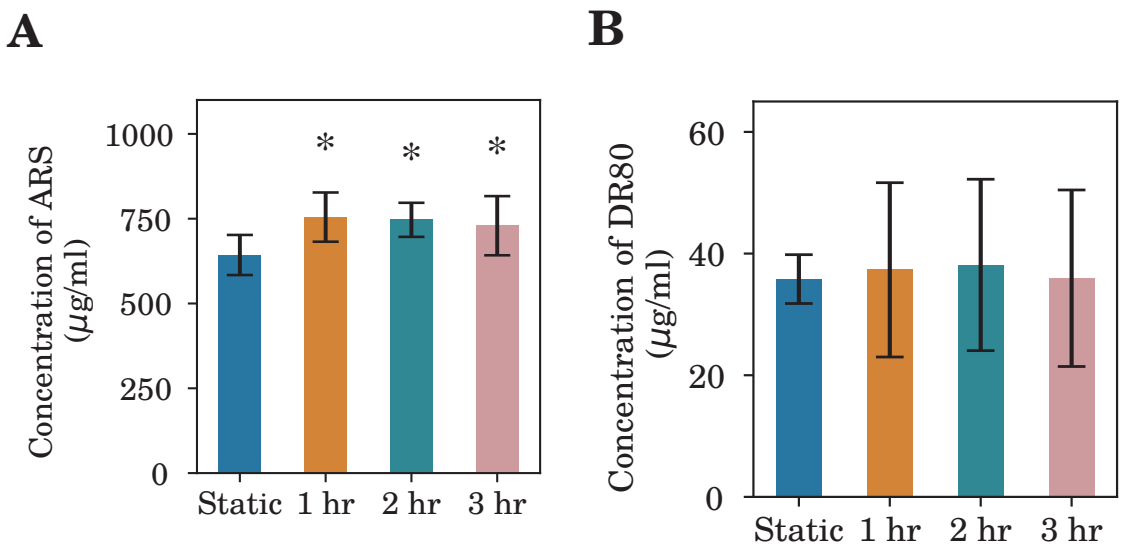


**Figure 6.19:** Effect rocking duration on hES-MP matrix formation in monolayer culture. Cells were mechanically stimulated on an IKA rocking platform for 1 h, 5 days per week from day 7 in an incubator. (A) Day 21 matrix calcium quantified by ARS. (B) Day 21 matrix collagen quantified by DR80. Data represents mean ± SD n=9. * = $p<0.05$ compared to the static control.

### Influence of media composition on osteogenic responses to FSS

Withdrawal of Dex from culture media had no significant effects on metabolic activity at any subsequent RR assay days (Figure 6.20). Cells in both DW and OIM samples showed similar increases in metabolic activity between day 1 and day 7 and remained at similar levels between day 7 and day 21.

Although RR showed no differences in metabolic activity between groups,

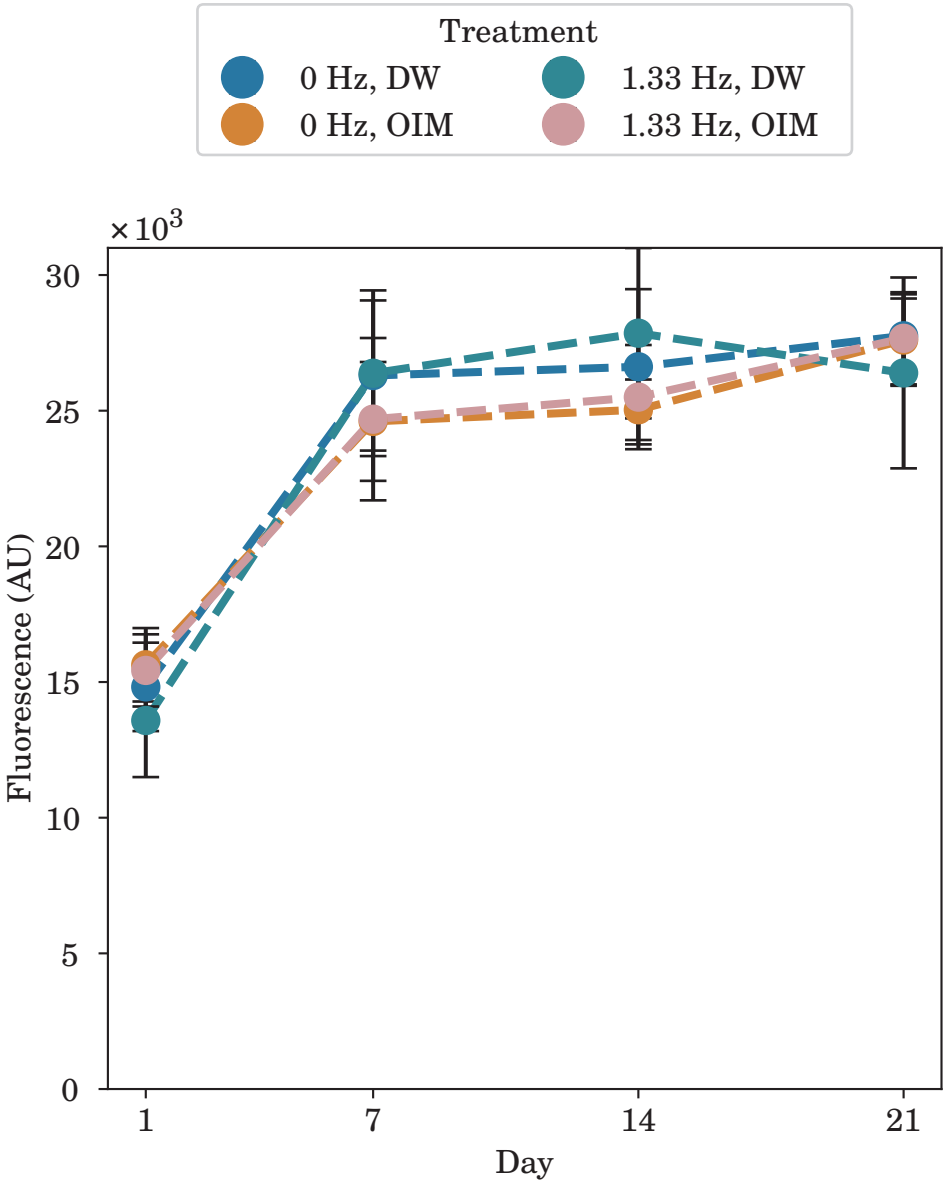


**Figure 6.20:** Effect of Dex withdrawal on hES-MP metabolic activity over 21 days in response to rocking in monolayer culture. Cells were mechanically stimulated on a rocking platform for 1 h, 5 days per week from day 7 in an incubator. Metabolic activity was assessed with RR. Data represents mean ± SD n=9. Fluorescence was measured at $\lambda_{ex}$: 540 nm and $\lambda_{em}$: 590 nm.

day 14 total DNA was significantly lower in cells continually cultured in OIM both when statically cultured and when subjected to rocking (Figure 6.21). There were no significant differences between static and rocked samples whether Dex was withdrawn or not. In statically cultured samples ALP activity was significantly lower in samples that had Dex withdrawn, both when normalised to DNA and total levels. In samples subjected to rocking and DW, ALP activity was only significantly lower when normalised to total DNA. There were no significant differences in total or normalised ALP activity between static and rocked groups whether Dex was withdrawn or not.

In static conditions Dex withdrawal resulted in significantly lower matrix mineralisation compared to OIM cultured samples (Figure 6.22). However, in Dex withdrawn samples, rocking stimulated matrix mineralisation to similar levels to OIM cultured samples. Matrix mineralisation was significantly higher in both OIM and DW samples when rocked compared to statically cultured. Samples that had Dex withdrawn had significantly higher collagen matrix compared to OIM cultured samples. Rocking had no significant effect on collagen production whether Dex was withdrawn or not.

Metabolic activity increased between day 1 and day 7 in all sera when statically cultured and rocked (Figure 6.23). Serum B had the lowest increase in metabolic activity between day 1 and day 7 and was significantly lower than both serum A and C. On day 14 of culture rocked samples cultured in serum B had significantly lower metabolic activity compared to all other samples except statically cultured samples in serum A and rocked samples in serum B. On day 21 of culture metabolic activity was similar in all serum types.

Similarly to metabolic activity there was no significant differences in total DNA on day 14 of culture between serum A and C (Figure 6.24). Total DNA was also lower in samples cultured in serum B compared to both serum A and C. Cells cultured in serum C also had significantly lower total and normalised ALP activity compared to cells cultured in serum B and C. There was no difference in ALP activity in samples cultured in serum A compared to serum C. Additionally, rocking had no effect on ALP activity in any of the sera tested.

Serum B cultured samples had significantly lower mineralised matrix and collagen production compared to both serum A and C cultured samples (Figure 6.25). Rocking only had a significant effect on matrix mineralisation in

samples cultured in serum A, where samples subjected to rocking had significantly more mineralised matrix compared to statically cultured samples. Collagen production was not affected by rocking in any of the tested sera.

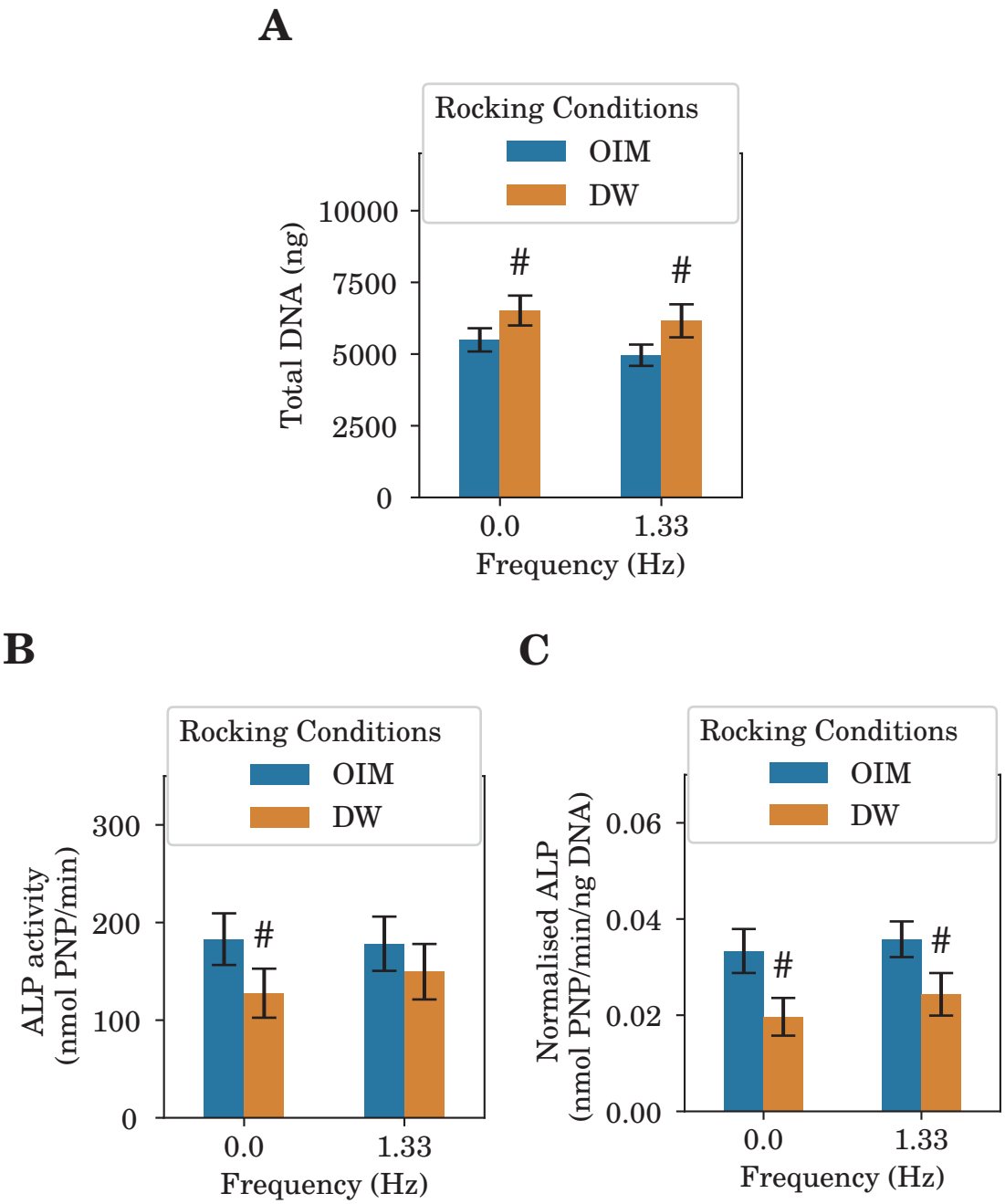


**Figure 6.21:** Effect of Dex withdrawal on hES-MP day 14 cell number and ALP activity in monolayer culture. Cells were mechanically stimulated on an IKA rocking platform for 1 h, 5 days per week from day 7 in an incubator. (A) Total DNA. (B) ALP activity. (C) ALP activity normalised to total DNA. Data represents mean ± SD n=9.# = $p<0.05$ compared to the OIM cultured group.

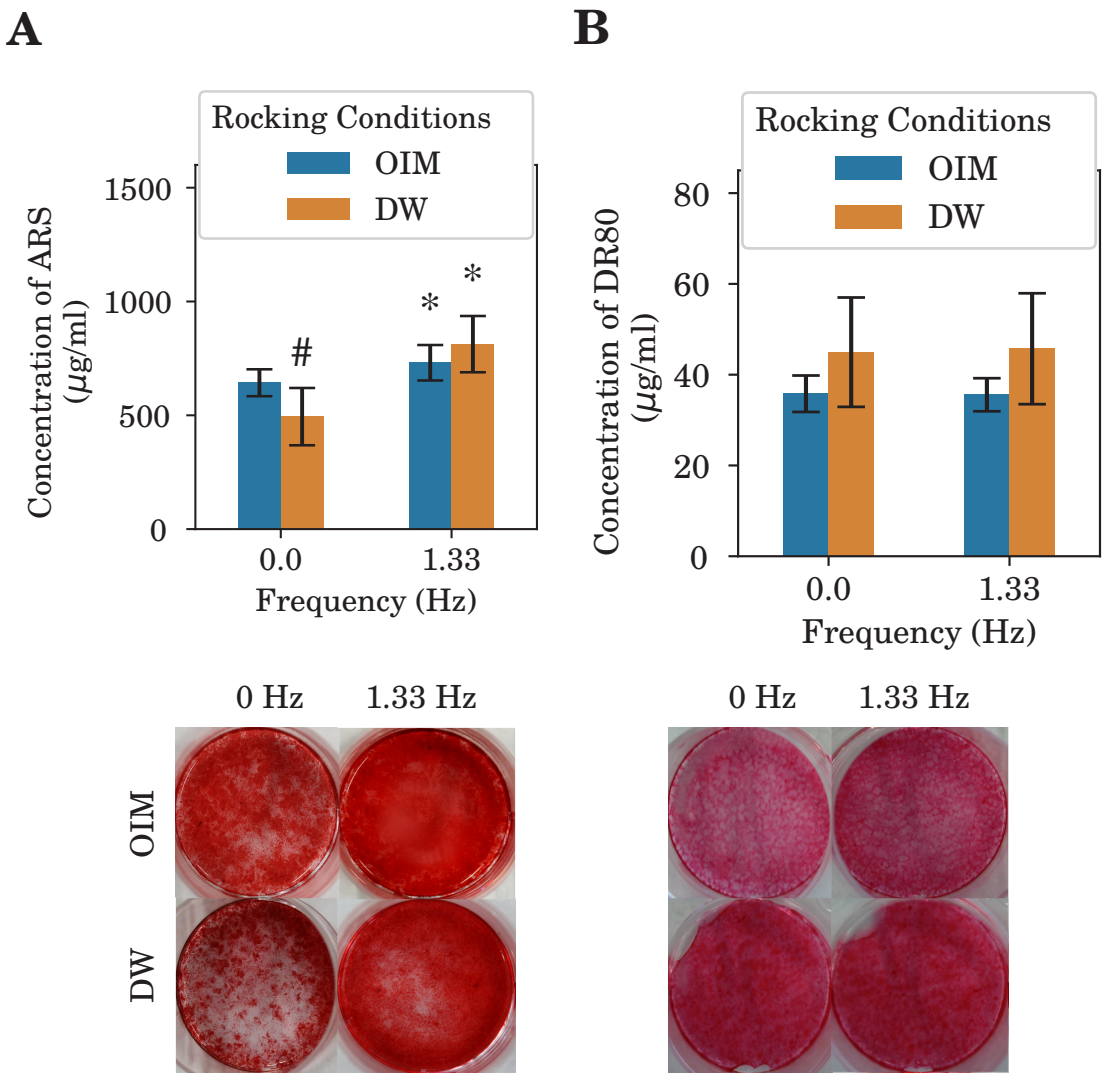


**Figure 6.22:** Effect of Dex withdrawal on hES-MP matrix formation in monolayer culture. Cells were mechanically stimulated on an IKA rocking platform for 1 h, 5 days per week from day 7 in an incubator. (A) Day 21 matrix calcium quantified by ARS. (B) Day 21 matrix collagen quantified by DR80. Data represents mean ± SD n=9. * = $p<0.05$ compared to the static control. # = $p<0.05$ compared to the OIM cultured group. Representative photographs of stained wells are shown below their corresponding graphs.

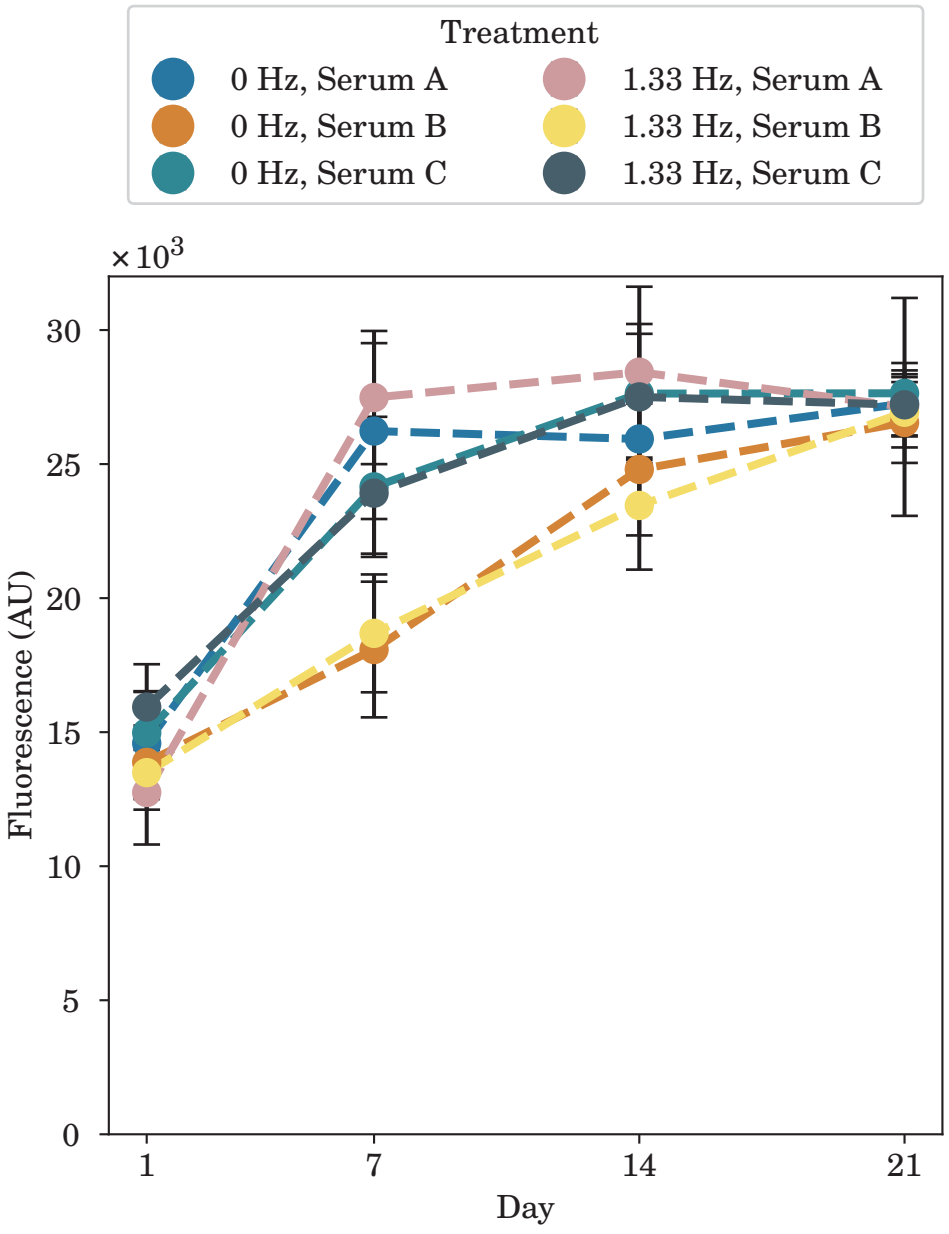


**Figure 6.23:** Effect of different sera on hES-MP metabolic activity over 21 days in response to rocking in monolayer culture. Cells were mechanically stimulated on a rocking platform for 1 h, 5 days per week from day 7 in an incubator. Metabolic activity was assessed with RR. Data represents mean ± SD n=6. Fluorescence was measured at $\lambda_{ex}$: 540 nm and $\lambda_{em}$: 590 nm.

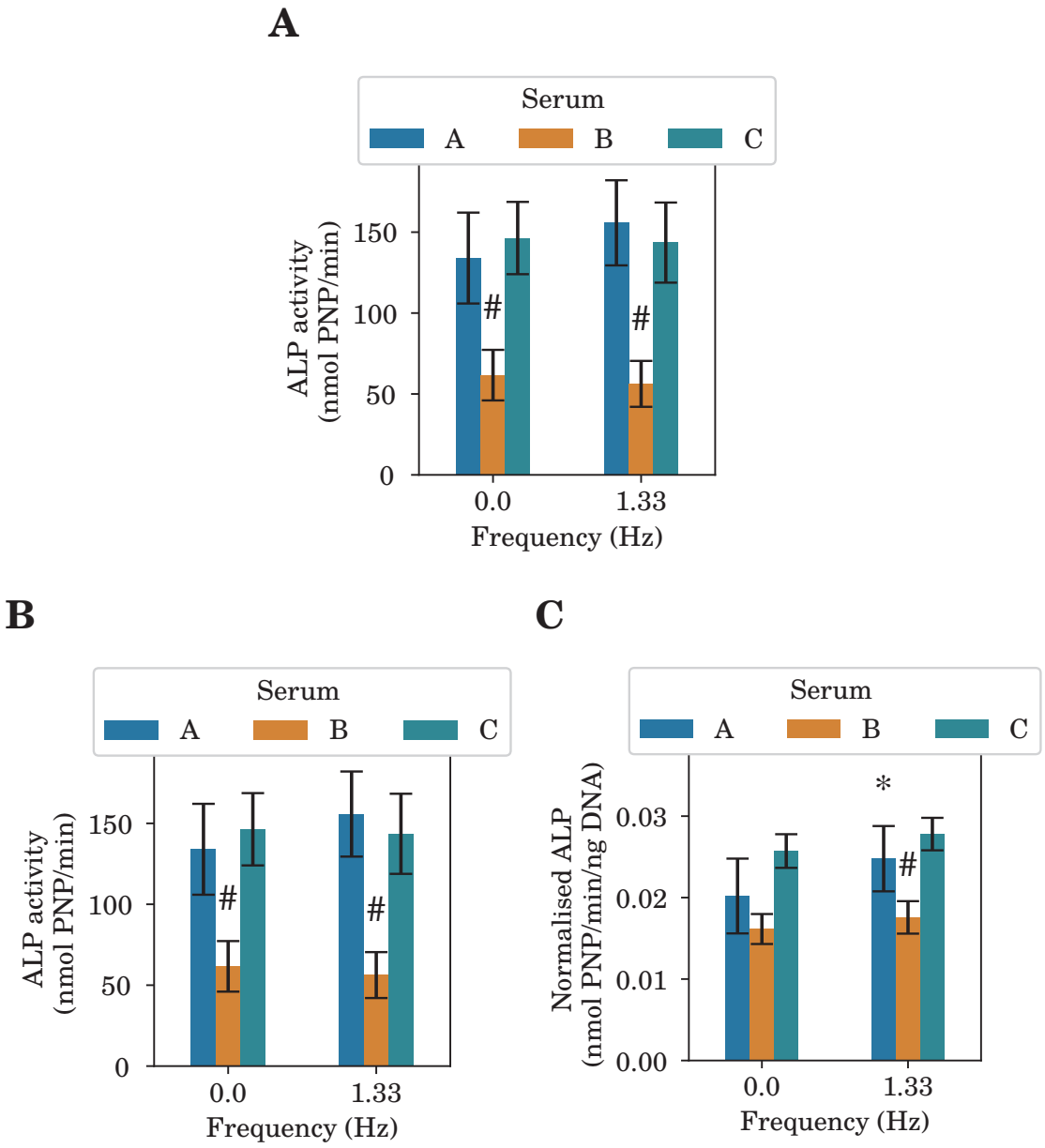


**Figure 6.24:** Effect of different sera on hES-MP day 14 cell number and ALP activity in monolayer culture. Cells were mechanically stimulated on an IKA rocking platform for 1 h, 5 days per week from day 7 in an incubator. (A) Total DNA. (B) ALP activity. (C) ALP activity normalised to total DNA. Data represents mean ± SD n=6. * = $p<0.05$ compared to the static control. # = $p<0.05$ compared to serum A.

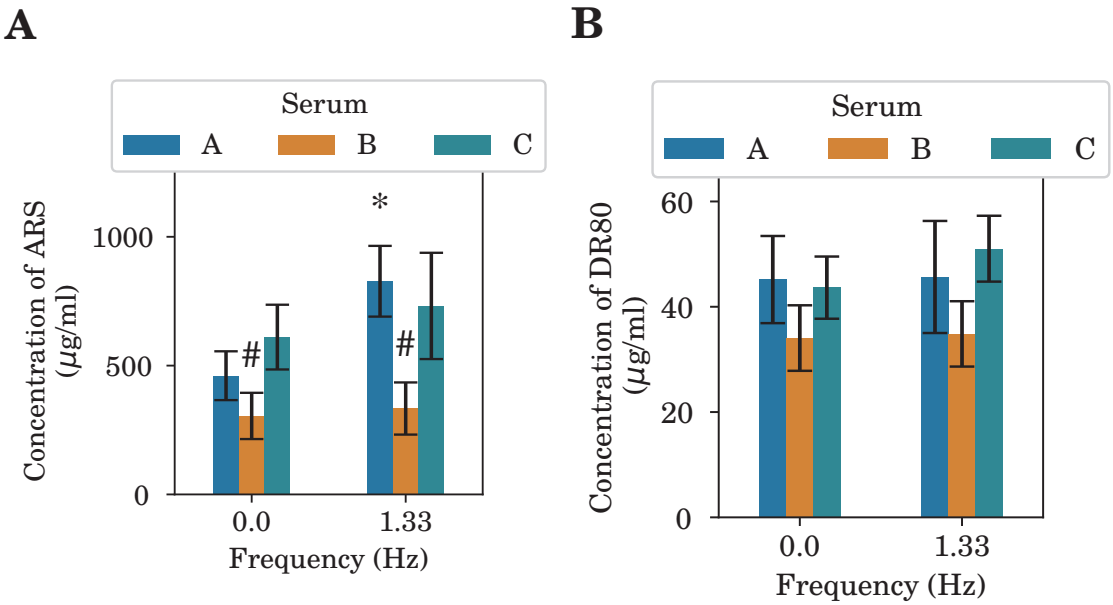


**Figure 6.25:** Effect of different sera on hES-MP matrix formation in monolayer culture. Cells were mechanically stimulated on an IKA rocking platform for 1 h, 5 days per week from day 7 in an incubator. (A) Day 21 matrix calcium quantified by ARS. (B) Day 21 matrix collagen quantified by DR80. Data represents mean ± SD n=6. * = $p<0.05$ compared to the static control. # = $p<0.05$ compared to serum A.

## 6.5 Discussion

This chapter investigated the response of osteogenic progenitors (hES-MP) and osteoblast (MLO-A5, MC3T3-E1) cell lines to low-level FSS. Following the protocol developed by Delaine-Smith et al., MLO-A5 cells were not found to respond to low-level FSS [132]. When the protocol was modified by performing the stimulation in an incubator, cells were found to respond to the FSS. However, the increase in mineralised matrix production was of a lesser extent to that reported by Delaine-Smith et al. Another osteoblast cell line, MC3T3-E1, also did not respond to low-level FSS. The osteogenic progenitor cell line, hES-MP was found to respond to low-level FSS following a similar protocol to that developed by Delaine-Smith et al. [240]. However, this was again to a lesser extent to that reported by Delaine-Smith et al where matrix mineralisation more than doubled. With further optimisation of the culture conditions the increase in matrix mineralisation due to FSS was increased but was still lower than double.

MLO-A5 cells are a fast-growing osteoblast-like cell line with doubling times of less than two days (data not shown). Initial experiments found that when seeded at 1,000 cells $cm^{-2}$ MLO-A5 cells detached resulting in cell apoptosis during long-term culture. The seeding density was therefore reduced to 50 cells $cm^{-2}$ to prevent this cell detachment and subsequent apoptosis. Although this prevented the problem it resulted in the formation of cell colonies rather than a confluent cell sheet at the bottom of the well. Additionally, ALP activity and matrix production were low and no apparent responses to the application of FSS at room temperature were observed. Since cell confluence is an important factor in matrix production and mineralisation, the low levels of osteogenesis and lack of response to FSS observed may be due to the lack of confluent cell sheet [343]. The issue of cell detachment may have been caused by a change in phenotype in the cells due to the high passage number. Cell phenotype, including osteogenic characteristics and cell growth are known to be influenced by passage number [344]. However, the passage numbers used (28-31) in this study were within the same 25-30 range used by Delaine-Smith et al. As no information was available as to any passage limit for this cell line, a new batch of MLO-A5 cells were purchased from Kerafast and used between passage 22-25 (cells were received as passage 21).

This batch of MLO-A5 cells did not have the same issues of detachment and death at higher density and had similar levels of ALP and matrix production (data not shown). When rocking was repeated at room temperature at the

higher seeding density with this batch of cells there was still no response to FSS observed.

It was also noted that the Stuart rocker that was used to stimulate the MLO-A5 cells did not seem to be functioning as designed. This was confirmed by measuring the rocking cycle using an inertial measurement unit. The Stuart rocking platform was found to have a higher tilt angle than designed on one half of the cycle. Surprisingly, although this resulted in a higher FSS being applied to the cells it had not resulted in any FSS stimulated osteogenic responses. This may have been due to the higher FSS being offset by the fact the higher tilt angle resulted in the platform passing the critical flip angle (the angle at which media no longer covers the entirety of the bottom of the well plate). As noted by Zhou et al., exceeding the critical flip angle results in a FSS discontinuity at regions where the media loses contact but also in a FSS singularity at two regions in the well plate [83]. The discontinuity of FSS during rocking would result in a loss of stimulus to those cells affected. Additionally, the FSS singularity may have been at a detrimentally high level further affecting the ability of the cells to respond to the stimulus. The use of this rocker was therefore discontinued and an IKA rocking platform was purchased and characterised. Characterisation of this rocker showed it did not surpass the critical flip angle and more closely adhered to its designed characteristics. An added benefit of the IKA rocking platform was that it was also rated for use in an incubator allowing further variables such as temperature and media pH to be more tightly controlled.

When rocking was performed in an incubator using the IKA rocking platform, increases in matrix mineralisation at 1.33 Hz were observed with MLO-A5 cells. This suggests that the environmental conditions provided by the incubator were more favourable to mechanotransduction in MLO-A5 cells. Cold stress and heat shock can be caused by a change in temperature of only a few degrees and results in a wide array of cellular responses. Performing rocking in the incubator thus prevented both cold stress when cells were removed from the incubator and heat shock when cells were reintroduced to the incubator. With hES-MP cells these changes in environmental conditions appeared to be less of an issue. However, Puwanun found that both hES-MP cells and primary human jaw periosteum cells mineralised differently in room temperature compared to incubator conditions [345]. This was dependent upon the supplements added to the media with higher mineralisation in room temperature conditions when cultured in SM and higher in incubator conditions when cultured in OIM.

Although metabolic activity was found to be affected, osteogenic responses were stimulated by FSS at both room temperature and in an incubator. However, the temperature of the room was not recorded during rocking and it was noted that during summer months, when the hES-MP experiments were conducted, temperatures ranged between 22-27 °C compared to the winter months, when MLO-A5 experiments were conducted, where temperatures ranged between 16-24 °C. These lower temperatures may therefore have had a greater influence in MLO-A5 cells. Furthermore, since the room temperatures of the rocking performed by Delaine-Smith et al. were not reported it is not possible to directly compare the results.

Cold stress has received little attention in the research community and to the authors knowledge there are no studies investigating its effects on mechanotransduction. The majority of studies investigating heat shock focus on the effects of increasing temperatures above the typical 37 °C. However, there are studies that have shown increasing temperatures from below 37 °C back to 37 °C causes similar heat shock responses in cells [346, 347]. Additionally, the responses of cells to both cold-stress and heat shock are themselves similar, causing reduced metabolic activity, cell cycle arrest and disassembly of the cytoskeleton [348–350]. In this study only cold stress could have had a direct effect on mechanotransduction since cells were stimulated after removal from the incubator. However, heat shock upon returning the cells to the incubator could also diminish any responses to FSS stimulation.

Although metabolic activity was not measured during room temperature conditions, metabolic activity and therefore cell growth was lower in cells subjected to rocking at room temperature compared to in an incubator at multiple time-points in the culture. Lower metabolic activity and activity of various enzymes within the cells would likely have a detrimental impact on a number of cellular processes, including cell signalling, which is required for mechanotransduction to occur. Many external cellular features that are thought to be involved in mechanotransduction, such as focal adhesions and the primary cilia are internally linked to the cytoskeleton. It is therefore not surprising that the cytoskeleton plays a central role in mechanotransduction or that its disruption alters mechanically induced responses [85, 351]. Another phenomenon that has been reported to occur with temperature shock is disassembly of the primary cilia. Prodromou et al., showed elevated temperatures in kidney, fibroblast and retinal cells resulted in rapid resorption of their primary cilium [352]. Although this was only reported with heat

shock this may also occur with cold stress since many other responses are similar. Removal of primary cilia has been shown in a number of studies to abbrogate cellular responses to mechanical stimuli [132, 139, 140, 201]. If this resorption of primary cilia also occurred here during cold-stress this would have had a negative effect on the cells ability to sense mechanical stimuli.

The FSS experienced by cells within bone has been estimated to be between 0.8-3 Pa for osteocytes and their processes and between 1-25 Pa for cells in trabecular bone marrow such as bone lining osteoblasts or osteogenic progenitor cells. Some studies have suggested the lower threshold of osteoblast mechanosensitivity to lie between 0.6-2 Pa which lies roughly within the range of FSS levels thought to occur *in vivo* [340, 353]. The results presented here suggest this threshold may be lower since the osteoblastic cell line MLO-A5 responded to the low-level FSS applied here (peak levels between 0.08-0.2 Pa).

MC3T3-E1 cells, the other osteoblastic cell line used here, did not show differences in any of the measured osteogenic responses. MC3T3-E1 cells have been shown to be mechanically sensitive to higher magnitudes of FSS [86, 341, 342]. This may suggest MLO-A5 cells are more sensitive to mechanical stimuli than other osteoblastic cells. However, to the authors knowledge, no studies have investigated the effects of mechanical stimulation on matrix mineralisation in MC3T3-E1 cells. Although no mechanically induced increase in matrix production was observed, the level of matrix mineralisation with MC3T3-E1 cells was extremely low. If any mechanically induced increases had occurred, they would also likely have been low. Therefore, due to the sensitivity of the ARS assay and the variability in the matrix mineralisation itself, this result does not necessarily suggest MC3T3-E1 cells are mechanically unresponsive. Furthermore, none of the cell lines tested showed increased ALP activity in response to FSS. Therefore, no conclusions on MC3T3-E1 mechanosensitivity can be drawn from these result. Other measurements that were not performed such as calcium signalling assays or gene upregulation may have shown the MC3T3-E1 cells to be mechanosensitive. However, since the aim of this chapter was to optimise a mechanical stimulation method that stimulated matrix production no further experiments with MC3T3-E1 cells were performed. Furthermore, there have been other studies that have shown mechanosensitivity to occur at similarly low FSS levels in osteoblastic cells [242, 354]. Which gives evidence to suggest that the mechanosensitivity of MLO-A5 cells may actually be more representative of other osteoblastic cell lines and primary cells.

Although both MLO-A5 cells and hES-MP cells were found to be mechanically sensitive in the form of increased matrix mineralisation, neither ALP activity or collagen production were affected. To the authors knowledge no studies have investigated the effects of low-level FSS on ALP activity or collagen production in MLO-A5 cells. However, other osteoblastic cell lines have been shown to upregulate both collagen production and ALP activity in response to low-level FSS [238, 355]. This suggests the lack of sensitivity in these areas to mechanical stimulation may be specific to MLO-A5 cells and not all osteoblastic cells. MLO-A5 cells were originally isolated by Kato et al. and were noted to have high ALP activity compared to other cells isolated from the same bone fragments [269]. This inherently high ALP activity may limit further increases in activity from mechanical stimulation.

Both collagen production and ALP activity have previously been shown by Delaine-Smith et al. to be upregulated by low-level FSS in hES-MP cells [240]. However, neither of these osteogenic markers were found to be upregulated in this study. A number of variables may have contributed towards these differences. When hES-MP cells were rocked in an incubator, both ALP activity and collagen production were higher compared to samples rocked at room temperature. The previously discussed points with regards to effects due to environmental conditions, such as cold and heat shock, are therefore also relevant here and may go some way to explain the observed differences. Additionally, serum batch variability is well known for having an influence on cell culture reproducibility [103, 356–358]. This was highlighted here where metabolic activity, ALP activity, collagen production and matrix mineralisation were all affected by the use of different batches of FBS.

Dex is commonly used to stimulate osteogenic differentiation in stem cells [317, 359, 360]. Despite this Dex and other glucocorticoids can have detrimental effects on cell growth, mineralisation and collagen formation [360–363]. To avoid these detrimental effects, it would therefore be beneficial to avoid the use of Dex. Delaine-Smith et al. found rocking without the use of Dex did not induce osteogenic differentiation [240]. Other studies have also found FSS alone is not a potent enough stimulator to induce osteogenic differentiation [240, 364]. Therefore, Dex was initially added to media of hES-MP cells to induce osteogenic differentiation and was subsequently withdrawn on day 5 of culture. Although no significant differences were observed in terms of metabolic activity, withdrawal of Dex resulted in higher total DNA per well on day 14 of culture suggesting greater cell growth. Dex withdrawal also beneficially increased

collagen production. Despite this, Dex withdrawal had a detrimental impact on both ALP activity and matrix mineralisation. However, matrix mineralisation was only lower in DW samples cultured under static conditions and ARS staining of rocked samples was indistinguishable from rocked OIM cultured samples.

The greater increase in matrix mineralisation with loaded cells that had Dex withdrawn could be due to Dex inhibiting mechanosensitivity. To the authors knowledge there are no direct studies investigating the effects of Dex withdrawal on osteogenic responses to FSS or mechanosensitivity. However, Dex treatment itself has been shown to affect multiple mechanisms involved in mechanotransduction. Xu et al. found Dex decreased expression of mechanosensitive micro ribonucleic acid (miRNA), which have been shown to be important in bone formation [365, 366]. Dex has also been shown to alter both the cytoskeleton itself, actin polymerization dynamics, and Wnt signalling which are all known to play a role in mechanotransduction. Alternatively, mechanical loading itself may have increased the sensitivity of the cells to the detrimental effects of Dex. Two isoenzymes of 11$\beta$-hydroxysteroid dehydrogenase (11$\beta$-HSD) modulate the actions of glucocorticoids such as Dex and have been shown to be stimulated by pro inflammatory cytokines such as interleukin-1 (IL-1) and tumor necrosis factor $\alpha$ (TNF-$\alpha$) [367, 368]. Proinflammatory cytokines have also been shown to be released in response to FSS in bone cells, although this is typically at high shear levels [369]. Furthermore, FSS has also been shown to activate the glucocorticoid receptor and its transcriptional signalling pathway which may further increase sensitivity of the cells to Dex [370].

The peak FSS profiles varied between different locations in the wells and this was more pronounced with the Stuart rocker. Despite this variation in peak FSS matrix production was typically consistent throughout the well in MLO-A5 cells and MC3T3-E1 cells. In hES-MP cells matrix mineralisation typically appeared stronger at the edges of the wells, where FSS was higher. However, it is not thought that this is due to the higher FSS but rather due to mineralisation progressing from the edge of the well towards the centre, as this was also observed under static conditions. The uniform matrix production suggests that either the different FSS profiles experienced by cells in different areas of the well have similar effects or that there is communication between cells. Communication between cells can either be direct, such as through gap junctions, or indirect, such as endocrine signalling [371, 372]. FSS has been shown to cause cell-cell signalling through gap junctions in a range of bone cell lines [373, 374]. Additionally, FSS has also been shown to cause the

release of nitric oxide, $PGE_2$ and other soluble signalling factors involved in cell-cell signalling [375–377]. It is therefore likely that a combination of these signalling pathways were stimulated by the FSS applied here.

In addition to the magnitude of the FSS, the duration of the loading and how often it is applied has also been shown to affect osteogenic responses to mechanical stimulation [378–380]. Other studies have shown longer durations of mechanical loading to be more stimulatory than shorter durations. Prodanov et al. found cells responded to 3 h of fluid flow but did not respond when only 1 h of loading was applied [379]. In this studyhES-MP cells were stimulated once per day, 5 days per week for 1, 2 or 3 h. All three durations resulted in an increase in matrix mineralisation but no increase in collagen production. Longer durations of rocking did not result in further increases in matrix mineralisation.

Extending the rocking duration further may have resulted in greater increases in osteogenic responses. However, continuous loading has been shown to decrease mechanosensitivity, although, this can be regained through the introduction of rest periods [381, 382]. Therefore, any further increases in loading duration would need to be split by rest periods to allow the cells to recover their sensitivity. Although the underlying mechanism behind this phenomenon is not entirely understood, it is thought the primary cilia plays a role. With continuous loading primary cilia have been shown to become shorter [195, 383]. In addition, shorter cilia have also been shown to be less mechanically sensitive [384]. It is therefore thought that primary cilia length regulation plays an important role in regulating mechanosensitivity.

## 6.6 Summary

To summarise, methods of mechanically stimulating long-term osteogenic responses in osteogenic progenitor and osteoblast cell lines was developed. Low-level FSS enhanced osteogenesis in MLO-A5 and hES-MP cells but not in MC3T3-E1 cells. However, enhanced osteogenic responses were only seen in matrix mineralisation and not in collagen production or ALP activity, which is in contrast to previously published results. In MLO-A5 cells only rocking at 1.33 Hz stimulated osteogenesis and in hES-MP cells both 0.75 and 1.33 Hz stimulated osteogenic responses. However, increasing the frequency also results in increasing shear stress it was not possible to conclude if these results were

due to frequency or shear stress levels. Increasing the duration of stimulation to 3 h had no effect on osteogenic responses. Seeding density and environmental conditions during rocking (temperature, $CO_2$ concentration) affected responses to FSS in hES-MP cells and MLO-A5 cells. Furthermore, media conditions (serum batch and Dex withdrawal) were also found to influence responses to FSS in hES-MP cells. These developed methods can be taken forward to study the effects of lithium on mechanically induced osteogenesis.

# 7. Osteogenic responses to lithium and fluid shear stress

## 7.1 Introduction

Mechanotransduction is a critical process in the development, maintenance and function of a variety of tissues. During embryonic development morphogenesis generates mechanical cues which activate mechanotransduction pathways involved in regulating cytoskeleton remodelling, cell differentiation and proliferation [385]. In the collecting duct of kidneys epithelial cells sense and respond to urine flow rates [386]. In bone, mechanotransduction is essential in regulating the balance between bone formation and resorption in response to the current levels of mechanical stimulation [387, 388]. Further understanding of the mechanisms behind how cells sense and transduce these mechanical cues into biochemical responses would therefore be of great use in the development of treatments for a wide variety of diseases, including skeletal disorders such as osteoporosis.

Mechanical regulation of cells occurs through a variety of mechanisms including, stretch activated ion channels, cytoskeletal mechanics, the glycocalyx and the primary cilium [131, 389–391]. Each of these mechanisms may have differing levels of involvement in mechanotransduction, dependent upon the type of mechanical force that is applied, such as matrix strain or fluid shear. When bone is loaded it has been predicted that interstitial fluid flows through the lacunae-canaliculae network where it may stimulate osteocytes residing in the lacunae and osteoblasts that line the bone surface [392, 393]. Additionally, modelling of trabecular bone marrow under load has shown fluid shear within the marrow to reach mechanostimulatory levels [340]. Fluid shear within bone can therefore affect both mature osteogenic cells and osteogenic precursors, where it can stimulate their differentiation towards osteogenic cells and the

formation of new bone. *In vitro* primary cilia are known to be present in both osteogenic lineage cells and precursor cells and have been shown to deflect in response to fluid flow, highlighting their potential as a fluid flow sensor [130, 131, 335]. Additionally, mechanically induced osteogenic responses to fluid flow are abrogated when primary cilia are removed, further highlighting their importance in mechanotransduction [94, 132, 201]. Primary cilia are also able to modulate their responsiveness to mechanical stimuli by triggering a reduction in primary cilia length through disassembly in response to mechanical stimuli [195, 383, 394]. This disassembly of primary cilia in response to mechanical stimuli results in a reduced mechanoresponse to the same magnitude of stimulus, this allows cells to modulate their sensitivity, preventing over stimulation [199]. This relationship between primary cilia length and magnitude of stimulus could therefore be manipulated to increase mechanosensitivity of cells.
As discussed in chapter 5 lithium can be used to elongate primary cilia without affecting the number of ciliated cells or osteogenesis itself when applied intermittently. Since primary cilia are thought to be mechanosensitive, with length playing a role in controlling sensitivity, it was hypothesised that lithium treatment may alter mechanosensitivity of cells. This chapter therefore investigates the effects of the LiCl treatment regime established in chapter 5 used in combination with the application of FSS on mechanoinduced osteogenic responses.

## 7.2 Aims and objectives

The aim of this chapter was to explore the mechanoresponse of osteogenic progenitor and osteoblast cells after treatment with LiCl. The following objectives were addressed in order to achieve this:

- Evaluate the effect LiCl treatment has on FSS induced osteogenesis in monolayer culture and in PU scaffolds.

- Evaluate the effect LiCl treatment has on FSS induced $Ca^{2+}$ and cAMP signalling

## 7.3 Methods

The following materials and methods are specific to the work presented in this chapter and expand upon the materials and methods presented in chapter 4, chapter 6 and chapter 5. hES-MP cells were cultured in DW media and MLO-A5 cells were cultured in SM.

### 7.3.1 Application of fluid shear stimuli

#### Monolayer stimulation

Mechanical stimulation in combination with LiCl treatment was applied following the rocking protocol optimised in chapter 6 and the LiCl treatment optimised in chapter 5, as shown in Figure 7.1.

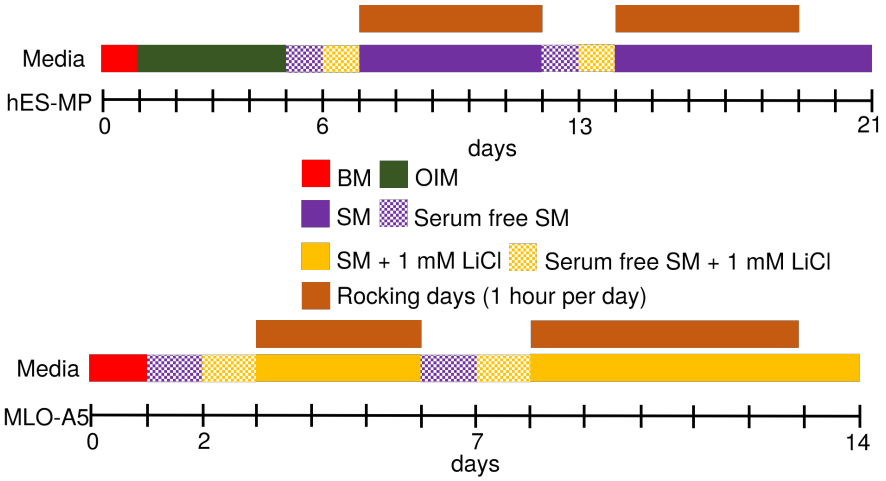


**Figure 7.1:** Timeline for rocking experiments showing the days LiCl and FSS stimulus was applied.

#### 3D stimulation

Scaffolds were treated with LiCl and subjected to oscillatory FSS generated by fluid flow in an Ibidi perfusion pump system (Ibidi GmbH, Germany) on day 5, 13 and 18 for hES-MPs and day 3 and 8 for MLO-A5s (Figure 7.2). This flow regime had previously been optimised by the author during their Master's degree research project. Fluid flow was applied at $8\,\mathrm{mm^3\,s^{-1}}$ ($0.63\,\mathrm{mm\,s^{-1}}$) at 1 Hz. Scaffolds were placed inside silicone tubing with an inside diameter of 4 mm, connected to the fluidic unit of the pump system and subjected to flow for 1 hour in an incubator. Statically cultured cells were also placed within tubing

for 1 hour but were not subjected to flow to control for scaffold manipulation and confinement. LiCl was applied following the the protocol optimised in chapter 5.

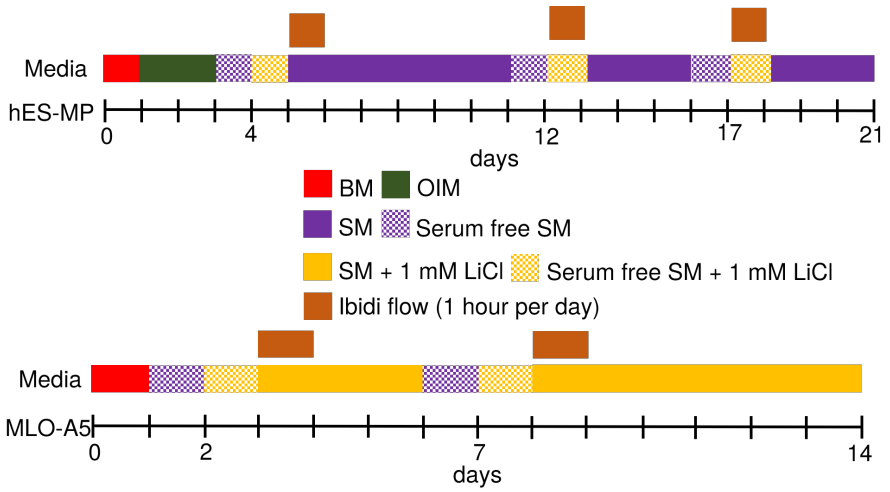


**Figure 7.2:** Timeline for Ibidi reactor fluid shear stress experiments showing the days LiCl and FSS stimulus was applied

### cAMP measurement

cAMP levels were measured using a cAMP ELISA (cAMP XP® assay kit #4339, Cell Signaling Technology Europe, Netherlands) following the manufacturer's instructions. Cells were rinsed twice with ice cold PBS, 900 µL of the supplied lysis buffer (10X lysis buffer diluted to 1X in di$H_2O$) with 1 mM phenylmethylsulfonyl fluoride was added and the samples were incubated on ice for 5 min. Well plates were scraped and the lystates transferred to 1.5 mL centrifuge tubes. The tubes were centrifuged at 6700 × g to remove cell debris. 50 µL of cell lysates and 50 µL of horseradish peroxidase (HRP) conjugated cAMP were added to the supplied microplate with anti-cAMP rabbit antibody immobilised on its surface and incubated for 3 h at room temperature on an orbital shaker. The cAMP in the cell lysates competes with the fixed amount of HRP conjugated cAMP for binding to the antibody. The wells were washed 4 times with 200 µL of the supplied wash buffer (20X wash buffer diluted to 1X in di$H_2O$) and 100 µL of 3,3',5,5'-tetramethylbenzidine (TMB) substrate added. After 30 min incubation at room temperature 100 µL stop solution was added. The optical density of each well was measured at $\lambda_{abs}$: 450 nm. The absorbance at 570 nm was subtracted from the absorbance at 450 nm to correct for optical aberrations in the plate. To determine the concentration of cAMP in the samples, a four-parameter logistic curve, fit to the absorbance of the known standards was

used.

### cAMP signalling in response to FSS

Measurement of cAMP signalling was only performed in monolayer culture. cAMP signalling was assessed on the first application of rocking (day 7). hES-MP cells were treated with 1 mM LiCl for 24 h following 24 h serum free media culture. Baseline cAMP levels were evaluated before the application of FSS for both 1 mM LiCl treated cells and untreated controls. cAMP levels were then measured 15 min, 30 min and 60 min after the initiation of FSS.

### Adenylyl cyclase inhibition

Although LiCl is a known inhibitor of adenylyl cyclase it also affects other pathways within the cell. Therefore, to assess the role of adenylyl cyclase in mechanotransduction, MDL-12330A hydrochloride (MDL) (Sigma Aldrich - M182) was employed as a more specific inhibitor of AC. To determine the optimum MDL concentration to inhibit AC without affecting basal cAMP levels, a dose response study of MDL was performed. MDL was dissolved in DMSO and added to culture medium to give a final concentration of 1, 10 or 100 mM MDL and a final concentration of 0.1% DMSO. hES-MP cells were cultured in MDL containing media or vehicle control for 60 min on day 7 of culture, matching the duration of time FSS would be applied. hES-MP cells were then treated with 10 mM MDL during the application of FSS to assess if it inhibited an increase in cAMP due to AC activity. 10 mM was chosen as it was the highest concentration that did not affect basal cAMP levels.

### Calcium signalling

Mechanical stimulation is known to induce calcium signalling. This calcium signalling occurs within seconds after the initiation of the stimulus. Due to this rapid response and the inability to visualise cells on the rocking platform, a different method to apply FSS in monolayer culture was required. For this 0.1% gelatin coated Ibidi $\mu$-slide VI 0.4 (Ibidi GmbH, Germany) were used as they allowed simultaneous application of FSS and microscopic imaging. Cells were seeded at 10,000 cells $cm^{-2}$ and cultured to day 6 following the culture regime outlined in Figure 7.1. On day 7 of culture cells were subjected to FSS using an Ibidi perfusion pump and calcium signalling observed through the use of a

fluorogenic calcium-sensitive dye Fluo-4 acetoxymethyl ester (Fluo-4) (Thermo Fisher Scientific, UK). The acetoxymethyl ester of the Fluo-4 is membrane-permeant, once inside a cell esterases cleave the acetoxymethyl group which renders the Fluo-4 membrane-impermeant. Fluo-4 exhibits an increase in fluorescence upon $Ca^{2+}$ binding and can therefore be used to monitor changes in intracellular $Ca^{2+}$ concentrations. On day 7 of culture hES-MP cells were rinsed with hanks balanced salt solution (HBSS) and incubated with 5 µM Fluo-4 in serum free BM containing 0.02% Pluronic F-127 and 25 mM 4-(2-hydroxyethyl)-1-piperazineethanesulfonic acid (HEPES) for 30 min at 37 °C. After loading cells were rinsed twice with HBSS to remove any extracellular dye. Oscillatory FSS was applied for 1 min at 1.33 Hz with a shear stress of 0.3 Pa or 1.5 Pa. Fluorescent images were captured every second, with 10 images captured before the initiation of flow. ImageJ was used for post-processing of the captured images. 25 cells were randomly selected per field of view and the baseline intensity calculated by measuring the average intensity of each cell over the 10 images captured before flow initiation. The maximum fluorescence intensity of each of the cells during flow was measured and the relative change in intensity was calculated by subtracting the baseline intensity from the maximum intensity. Peaks in fluorescence caused by floating cell debris were excluded from analysis.

## 7.4 Results

### 7.4.1 Effects of lithium chloride on hES-MP flow induced osteogenesis in monolayer

hES-MP cells were mechanically stimulated after treatment with LiCl. 1 mM LiCl was applied on day 6 and day 13 for 24 h and rocking was performed at 1.33 Hz for 1 h 5 days per week from day 7. Cell viability was measured on day 1, 7, 14 and 21 with RR (Figure 7.3). Metabolic activity increased from day 1 to day 7 in all groups with no significant differences between groups. There was no significant increase in metabolic activity between day 7 and day 21 in any group. There were also no significant differences in metabolic activity at any time point between groups. Total DNA and ALP activity was measured on day 14 (Figure 7.4). Similarly to the day 14 RR results, there was no significant difference in total DNA between any of the groups. In static culture, LiCl had no effect on ALP activity. Additionally, rocking alone

without LiCl treatment had no effect on ALP activity. However, when rocking was performed after LiCl treatment, ALP activity was significantly higher compared to both the static control and the untreated rocked group. The amount of mineralised matrix and collagen produced was analysed on day 21 of culture by ARS and DR80 respectively (Figure 7.5). Despite no increase in day 14 ALP activity with rocking alone, there was a significant increase in the amount of mineralised matrix produced by day 21 of culture compared to the static control. LiCl treatment in statically cultured cells had no significant effect on matrix mineralisation. However, when rocking was performed after LiCl treatment, the amount of mineralised matrix produced over 21 days of culture was significantly higher compared to both statically cultured controls and rocked cells without LiCl treatment. The amount of collagen produced over 21 days of culture was not significantly different between any of the experimental groups.

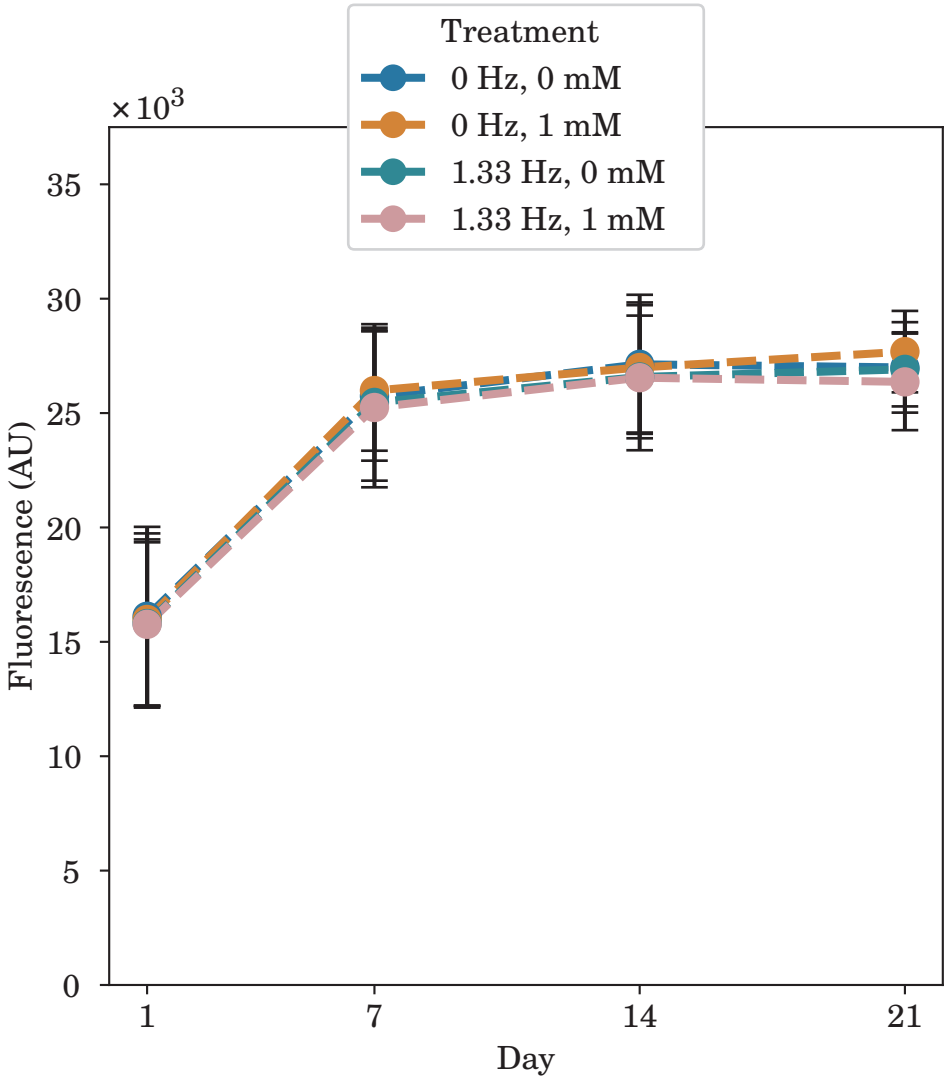


**Figure 7.3:** Effect of FSS and LiCl exposure on hES-MP metabolic activity over 21 days of monolayer culture. LiCl was applied on day 6 and day 13 for 24 hours and cells were mechanically stimulated on a rocking platform for 1 h, 5 days per week from day 7. Metabolic activity was assessed with RR. Data represents mean ± SD n=9. Fluorescence was measured at $\lambda_{ex}$: 540 nm and $\lambda_{em}$: 590 nm.

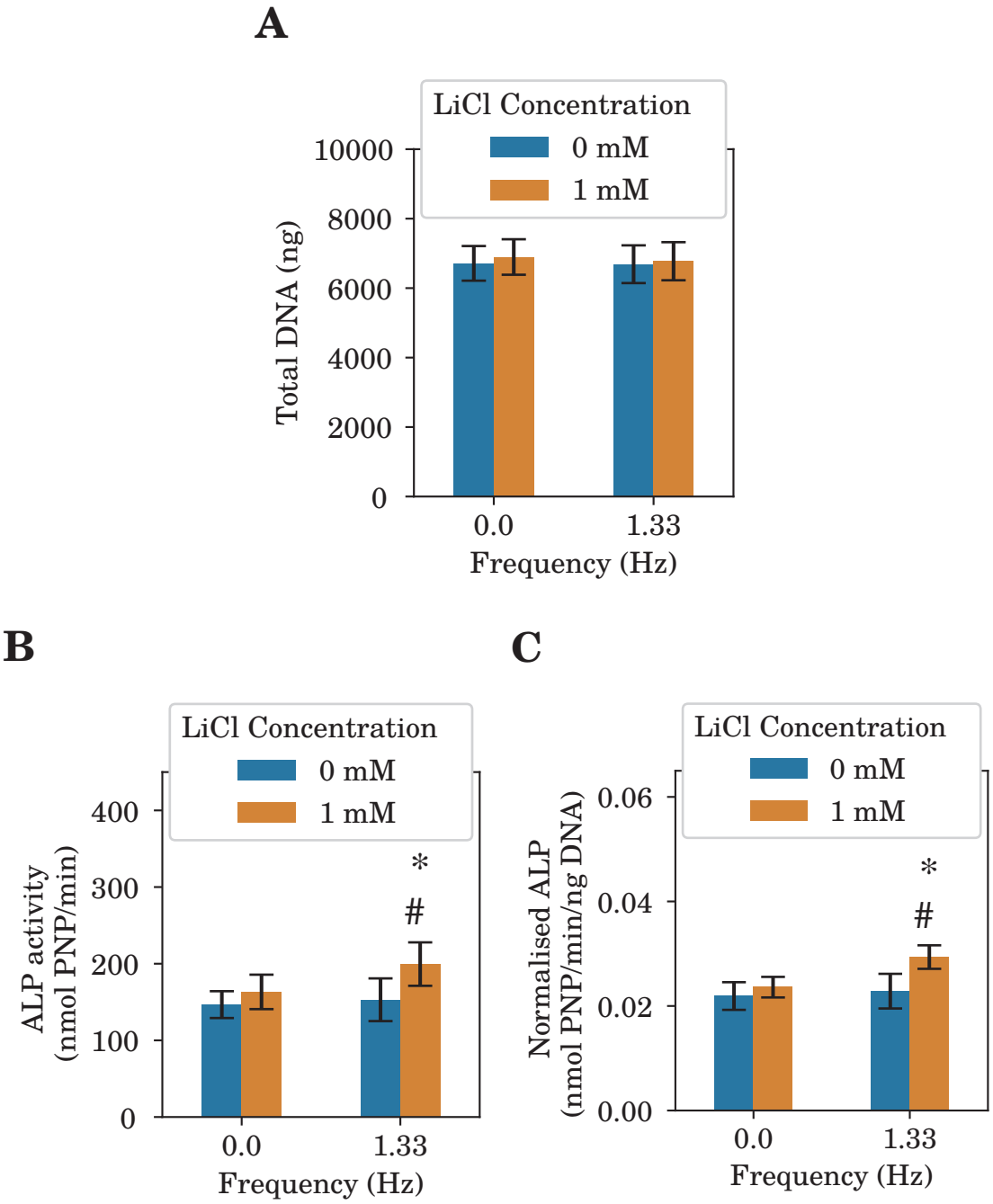


**Figure 7.4:** Effect of FSS and LiCl exposure on hES-MP day 14 cell number and ALP activity in monolayer culture. LiCl was applied on day 6 and day 13 for 24 hours and cells were mechanically stimulated on a rocking platform for 1 h, 5 days per week from day 7. (B) Total DNA. (A) ALP activity. (C) ALP activity normalised to total DNA. Data represents mean ± SD n=9. * = $p<0.05$ compared to the static control. # = $p<0.05$ compared to 0 mM LiCl.

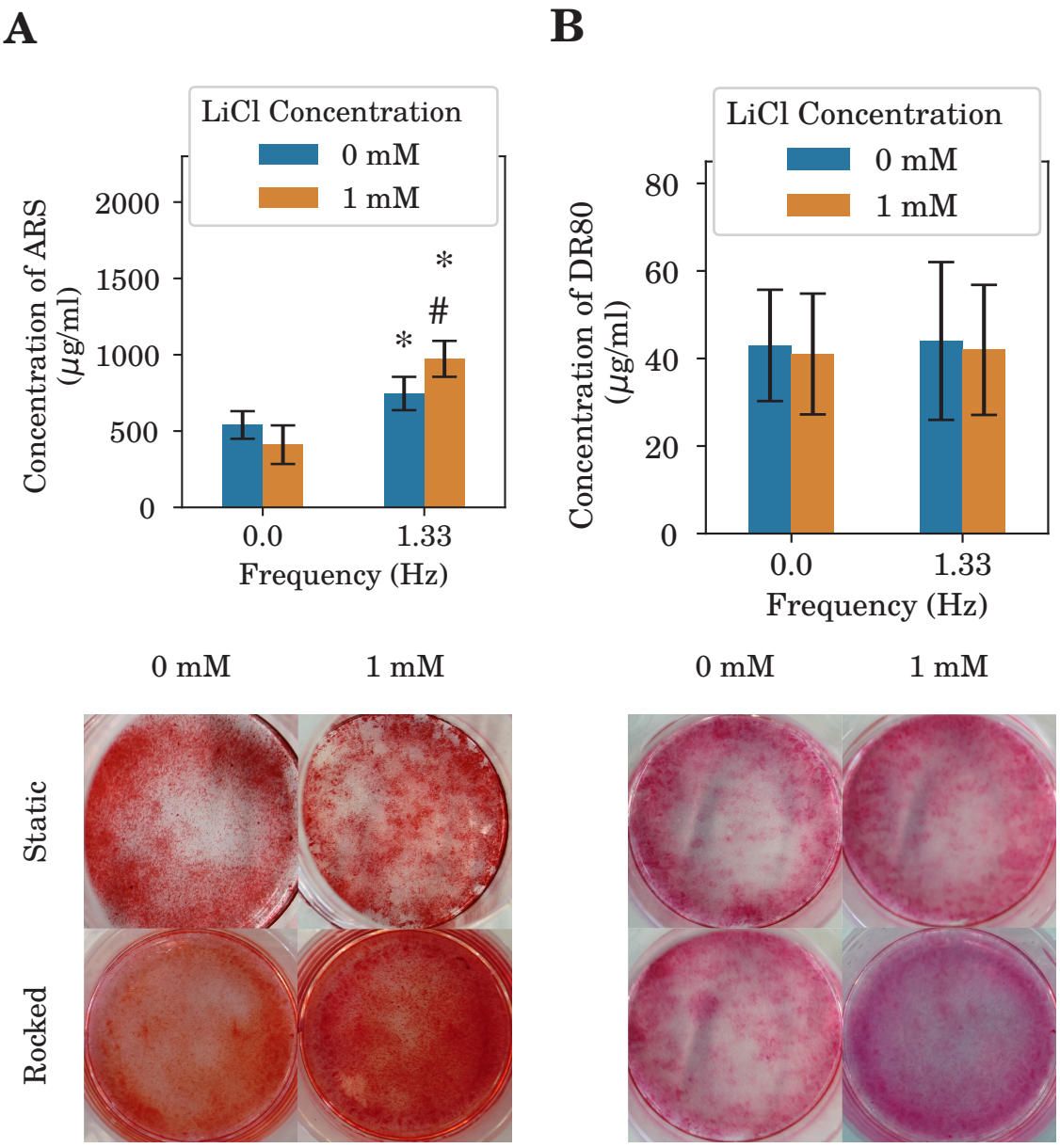


**Figure 7.5:** Effect of FSS and LiCl exposure on hES-MP matrix formation in monolayer culture. LiCl was applied on day 6 and day 13 for 24 hours and cells were mechanically stimulated on a rocking platform for 1 h, 5 days per week from day 7. (A) Day 21 matrix calcium quantified by ARS. (B) Day 21 matrix collagen quantified by DR80. Data represents mean ± SD n=9. * = $p<0.05$ compared to the static control. # = $p<0.05$ compared to 0 mM LiCl. Representative photographs of stained wells are shown below their corresponding graphs.

### 7.4.2 Effects of lithium chloride on MLO-A5 flow induced osteogenesis in 2D

MLO-A5 cells were mechanically stimulated after LiCl treatment. 1 mM LiCl was applied on day 2 and day 7 for 24 h and rocking was performed at 1.33 Hz for 1 h 5 days per week from day 7. Cell viability was measured on day 1, 7 and 14 with RR (Figure 7.6). Metabolic activity increased from day 1 to day 7 in all groups with no significant differences between groups. There was no significant increase in metabolic activity between day 7 and day 14 in any group. There were also no significant differences in metabolic activity at any time point between groups. Total DNA and ALP activity was measured on day 7 (Figure 7.7). Similarly to the day 7 RR results, there was no significant difference in total DNA between any of the groups. In static culture, LiCl had no effect on ALP activity. Additionally, rocking alone without LiCl treatment had no effect on ALP activity. However, when rocking was performed after LiCl treatment, ALP activity was significantly higher compared to both the static control and the untreated rocked group. The amount of mineralised matrix and collagen produced was analysed on day 14 of culture by ARS and DR80 respectively (Figure 7.8). Despite no increase in day 7 ALP activity with rocking alone, there was a significant increase in the amount of mineralised matrix produced by day 14 of culture compared to the static control. LiCl treatment in statically cultured cells had no significant effect on matrix mineralisation. However, when rocking was performed after LiCl treatment, the amount of mineralised matrix produced over 14 days of culture was significantly higher compared to both statically cultured controls and rocked cells without LiCl treatment. The amount of collagen produced over 14 days of culture was not significantly different between any of the experimental groups.

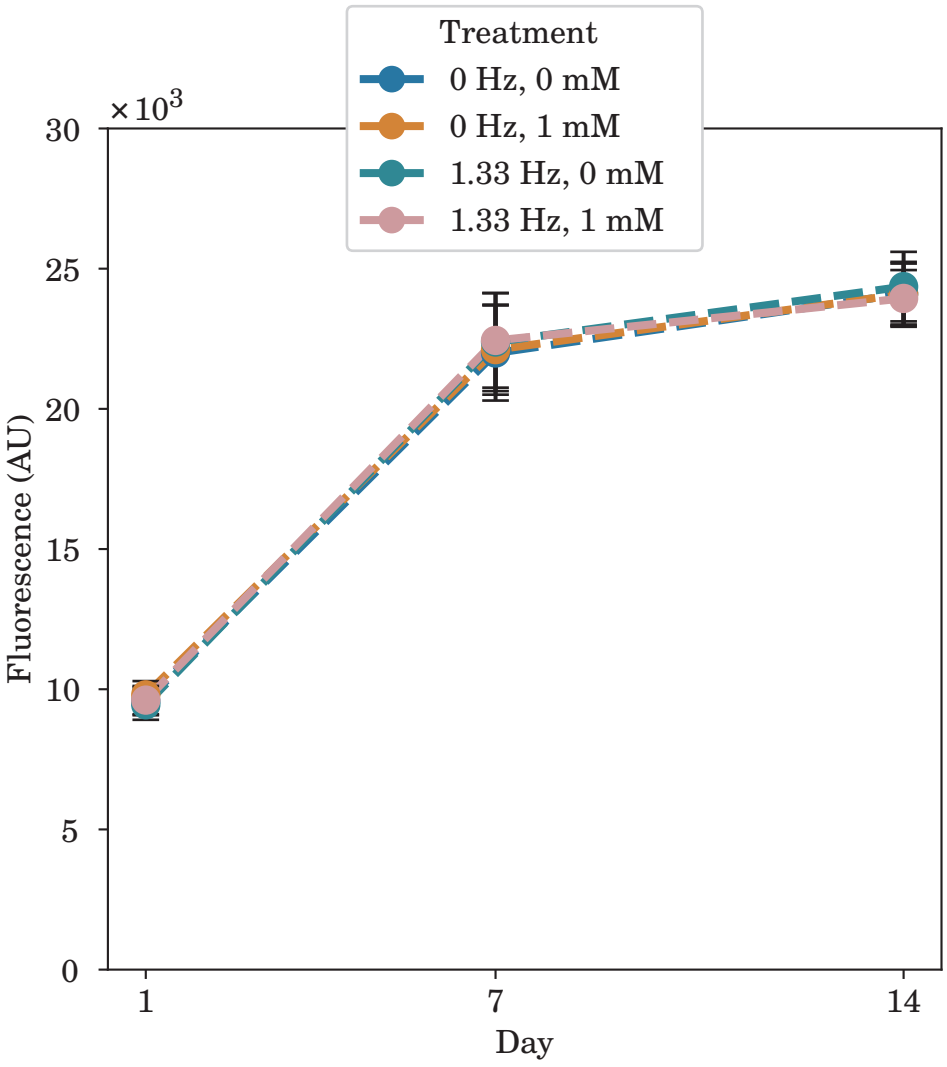


**Figure 7.6:** Effect of FSS and LiCl exposure on MLO-A5 metabolic activity over 14 days of monolayer culture. LiCl was applied on day 2 and day 7 for 24 hours and cells were mechanically stimulated on a rocking platform for 1 h, 5 days per week from day 3. Metabolic activity was assessed with RR. Data represents mean ± SD n=9. Fluorescence was measured at $\lambda_{ex}$: 540 nm and $\lambda_{em}$: 590 nm.

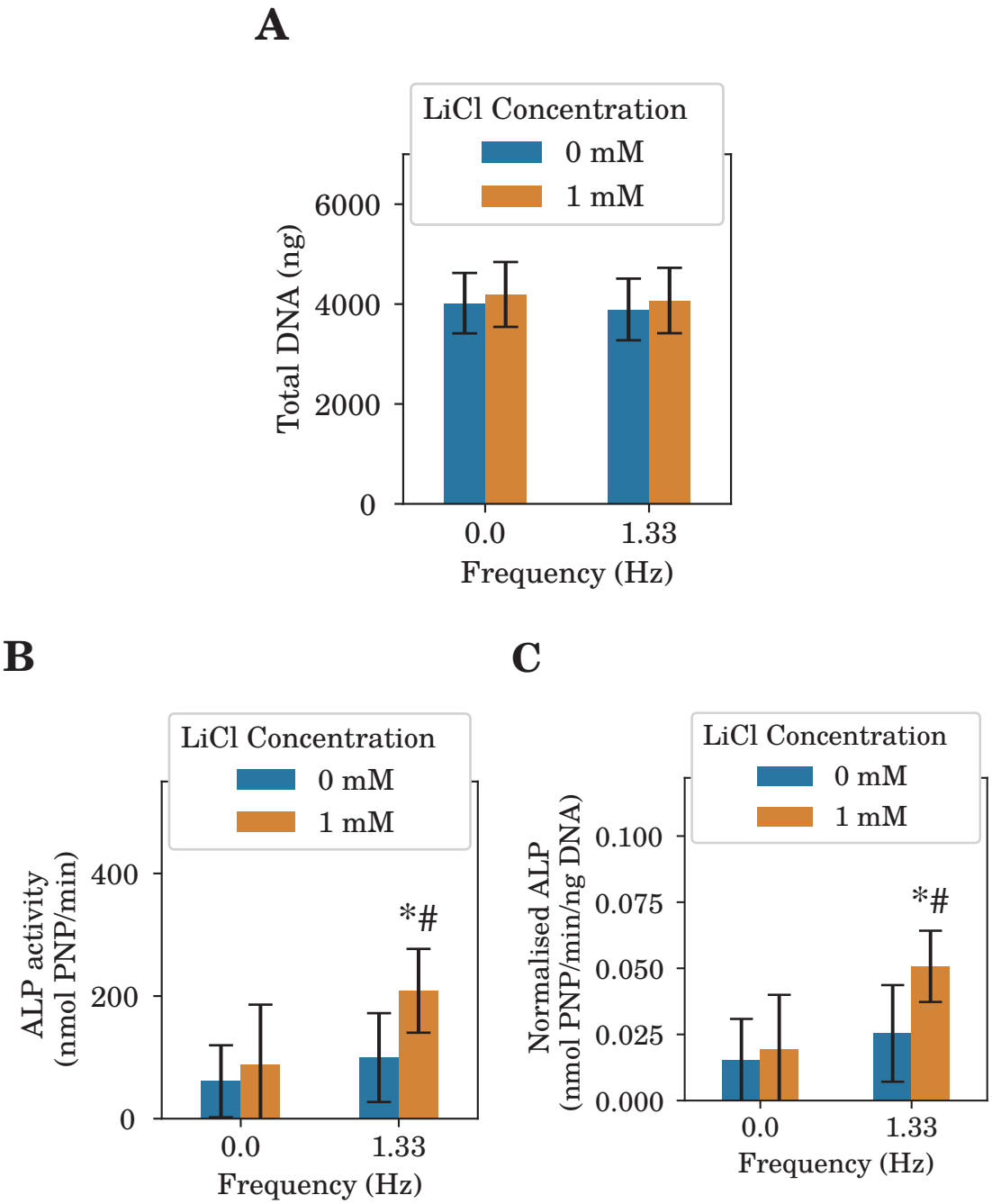


**Figure 7.7:** Effect of FSS and LiCl exposure on MLO-A5 day 7 cell number and ALP activity in monolayer culture. LiCl was applied on day 2 for 24 hours and cells were mechanically stimulated on a rocking platform for 1 h, 5 days per week from day 3. (A) Total DNA. (B) ALP activity. (C) ALP activity normalised to total DNA. Data represents mean ± SD n=9. * = $p<0.05$ compared to the static control. # = $p<0.05$ compared to 0 mM LiCl.

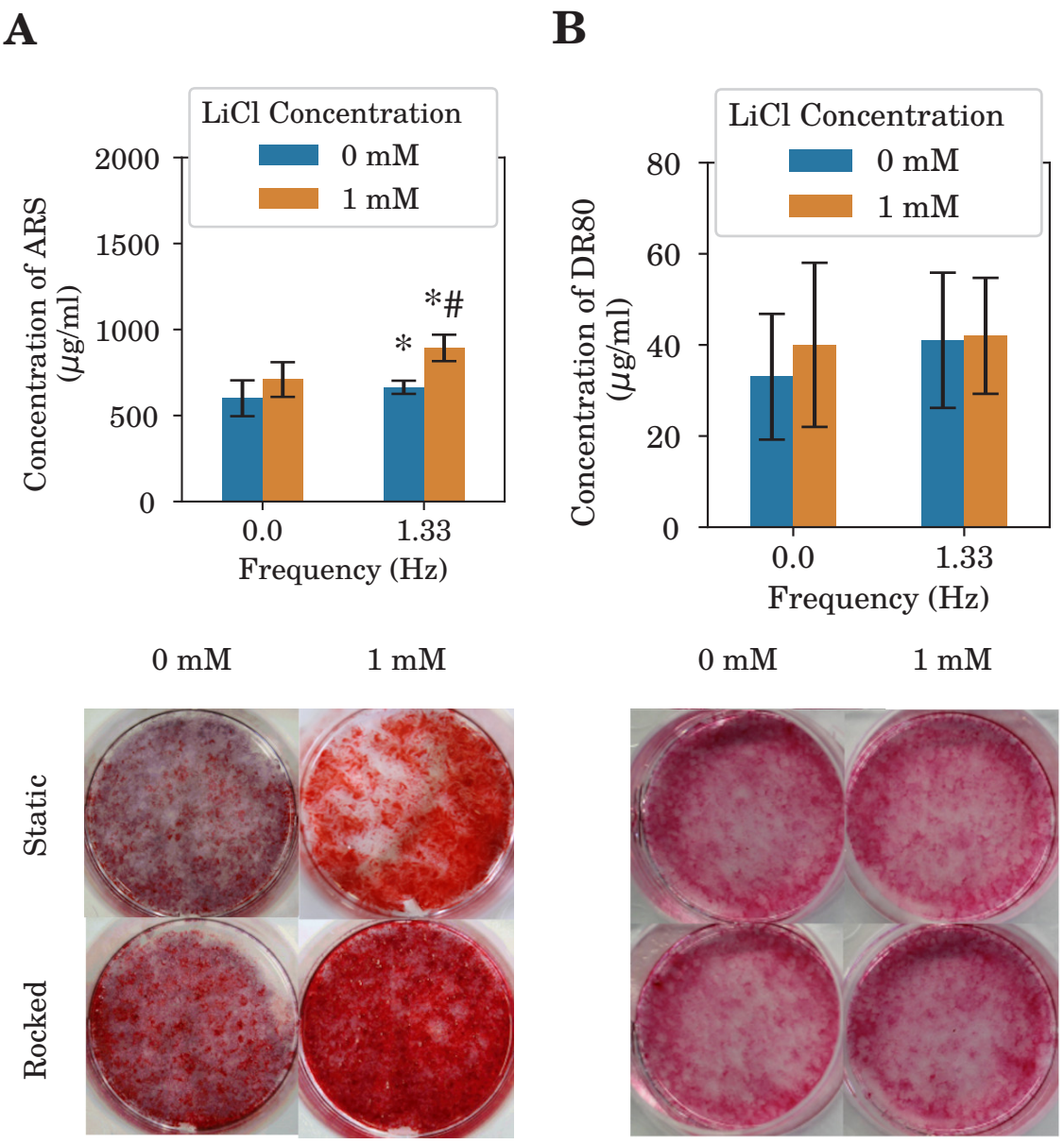


**Figure 7.8:** Effect of FSS and LiCl exposure on MLO-A5 matrix formation in monolayer culture. LiCl was applied on day 2 for 24 hours and cells were mechanically stimulated on a rocking platform for 1 h, 5 days per week from day 3. (A) Day 14 matrix calcium quantified by ARS. (B) Day 14 matrix collagen quantified by DR80. Data represents mean ± SD n=9. * = $p<0.05$ compared to the static control. # = $p<0.05$ compared to 0 mM LiCl. Representative photographs of stained wells are shown below their corresponding graphs.

### 7.4.3 Effects of lithium chloride on hES-MP flow induced osteogenesis in 3D

To assess if the increased osteogenic responses found when mechanically stimulating cells after LiCl treatment in 2D culture translates to 3D culture, hES-MPs were cultured in DW media in PU scaffolds and mechanically stimulated after LiCl treatment. 1 mM LiCl was applied following the intermittent treatment regime, as this regime was shown to not affect osteogenesis itself, and the cells were subjected to FSS in an Ibidi bioreactor (Figure 7.2). Cell viability was measured on day 1, 7, 14 and 21 with RR (Figure 7.9), ALP and total DNA was measured on day 14 (Figure 7.10) and total matrix calcium and collagen production was assessed with ARS and DR80 staining respectively on day 21 (Figure 7.11). DR80 stained samples were also imaged with light-sheet microscopy to visualise the collagen matrix (Figure 7.12).
Cell viability was higher in all groups on day day 21 compared to day 1. Between day 14 and day 21 viability decreased in the LiCl treated cells subjected to flow. However, despite this reduction viability remained higher than the control on day 21. Additionally, all other groups had significantly higher viability compared to the control on day 21. FSS stimulus alone did not have an osteogenic effect, showing no significant changes in ALP activity or total mineralised matrix or collagen production. However, when FSS was applied after using LiCl, there was an osteogenic effect. ALP activity and total mineralised matrix production was significantly higher compared to the static controls. Total DNA was also significantly higher in the LiCl treated cells subjected to flow compared to the untreated static control. No other treatment had an effect on total DNA. Collagen production was not affected by LiCl treatment or FSS in terms of the amount of collagen produced. However, light-sheet microscopy images of DR80 stained samples show the collagen in samples not treated with LiCl to be more fibrous compared to the LiCl treated samples.

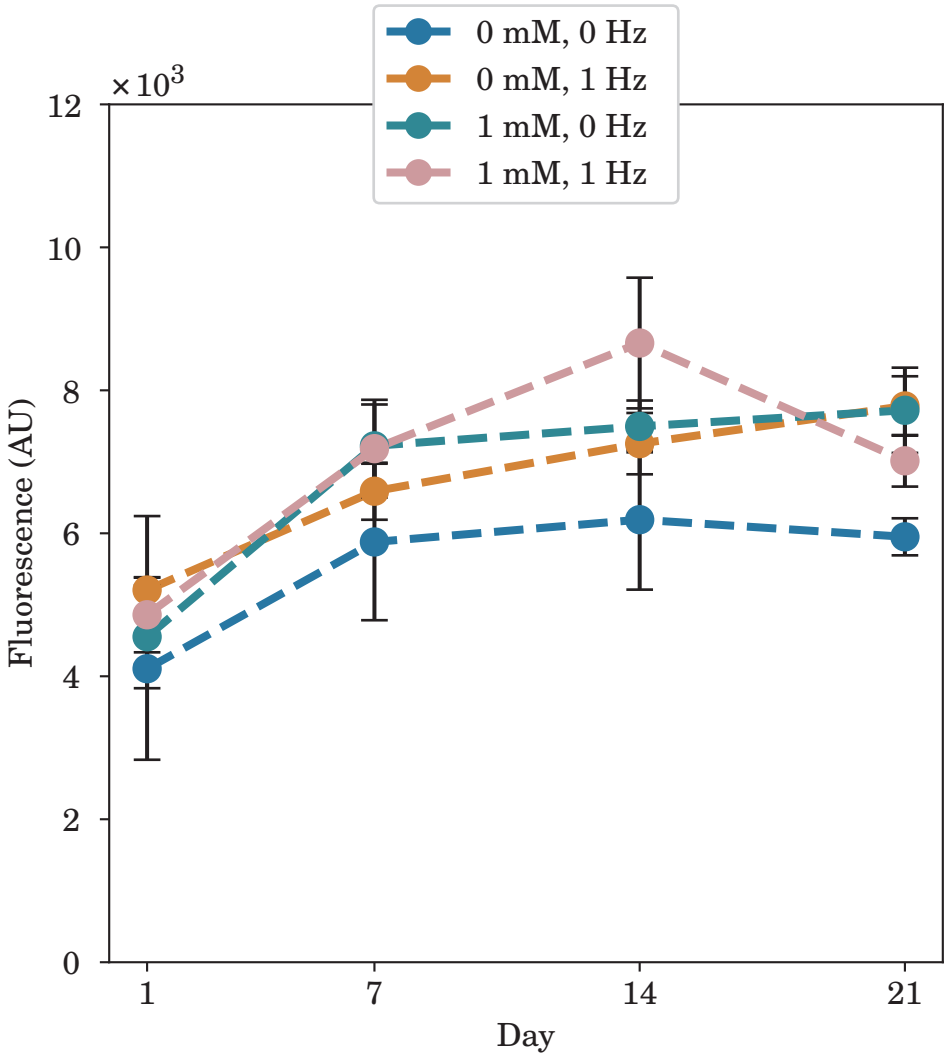


**Figure 7.9:** Effect of FSS and LiCl exposure on hES-MP metabolic activity over 21 days of 3D culture. LiCl was applied on day 4, day 12 and day 17 for 24 hours and cells were mechanically stimulated for 1 h using an Ibidi perfusion pump on day 5, day 13 and day 18. Metabolic activity was assessed with RR. Data represents mean ± SD n=9. Fluorescence was measured at $\lambda_{ex}$: 540 nm and $\lambda_{em}$: 590 nm.

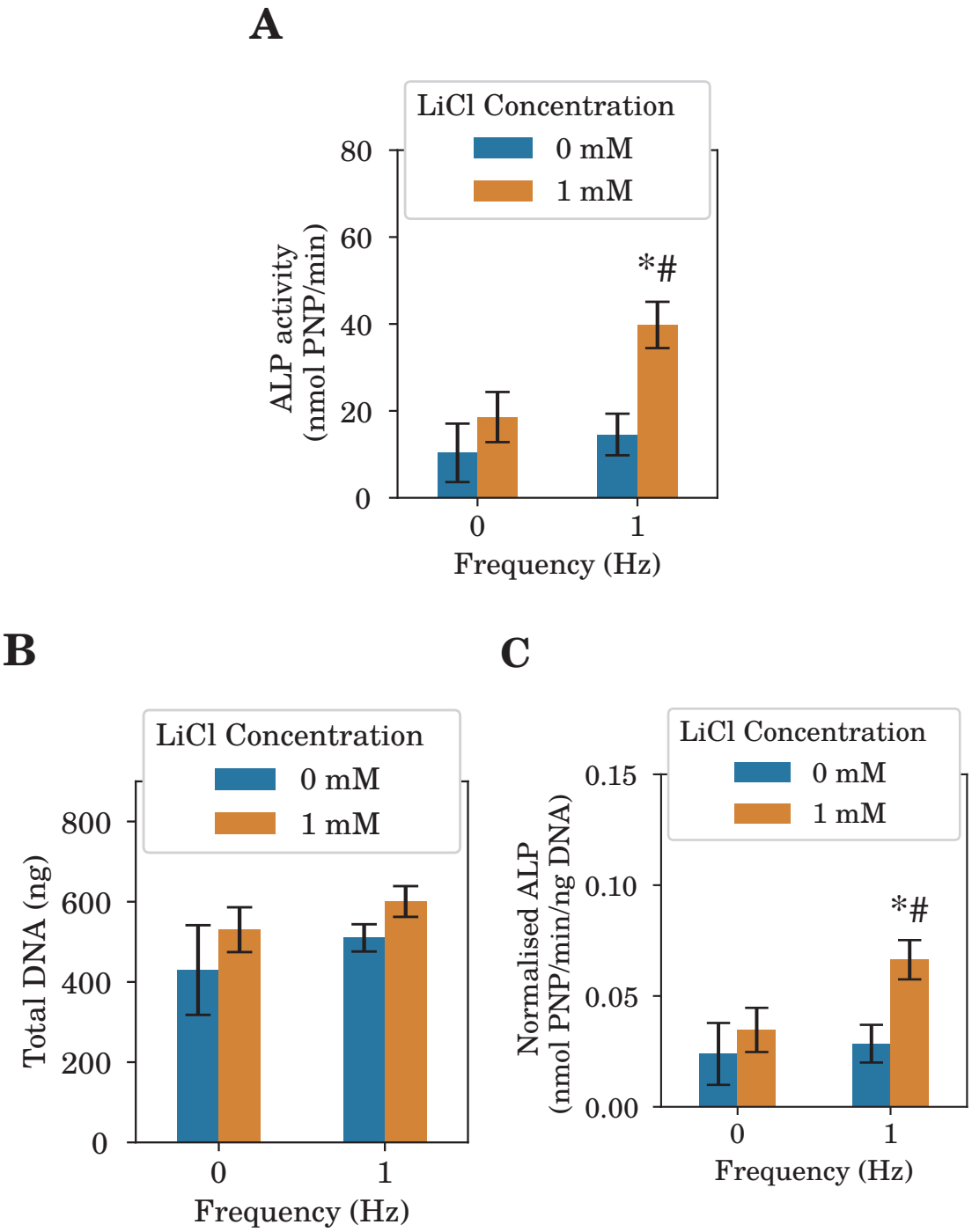


**Figure 7.10:** Effect of FSS and LiCl exposure on hES-MP day 14 cell number and ALP activity in 3D culture. LiCl was applied on day 4, day 12 and day 17 for 24 hours and cells were mechanically stimulated for 1 h using an Ibidi perfusion pump on day 5, day 13 and day 18. (A) ALP activity. (B) Total DNA. (C) ALP activity normalised to total DNA. Data represents mean ± SD n=9. * = $p<0.05$ compared to the static control. # = $p<0.05$ compared to 0 mM LiCl.

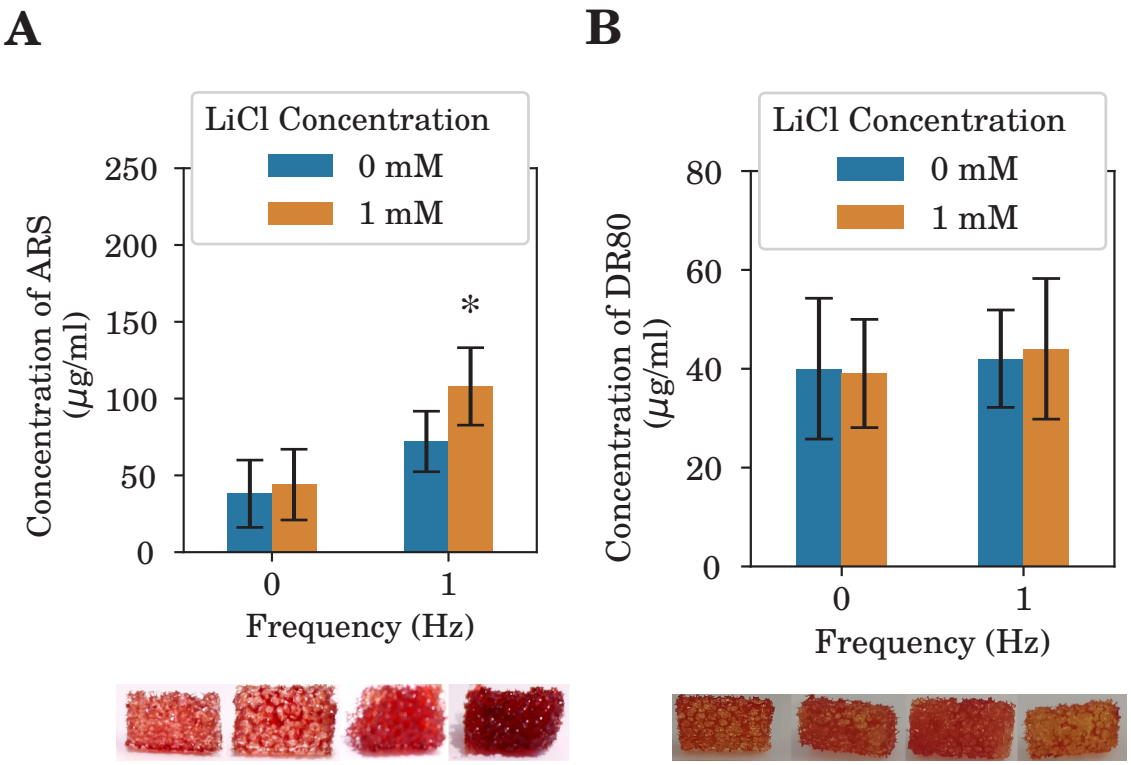


**Figure 7.11:** Effect of FSS and LiCl exposure on hES-MP matrix formation in 3D culture. LiCl was applied on day 4, day 12 and day 17 for 24 hours and cells were mechanically stimulated for 1 h using an Ibidi perfusion pump on day 5, day 13 and day 18. (A) Day 21 matrix calcium quantified by ARS. (B) Day 21 matrix collagen quantified by DR80. Data represents mean ± SD n=9. * = $p<0.05$ compared to the static control. Representative photographs of stained scaffolds are shown below their corresponding graphs. (left to right) 0 Hz 0 mM, 0 Hz 1 mM, 1 Hz 0 mM and 1 Hz 1 mM.

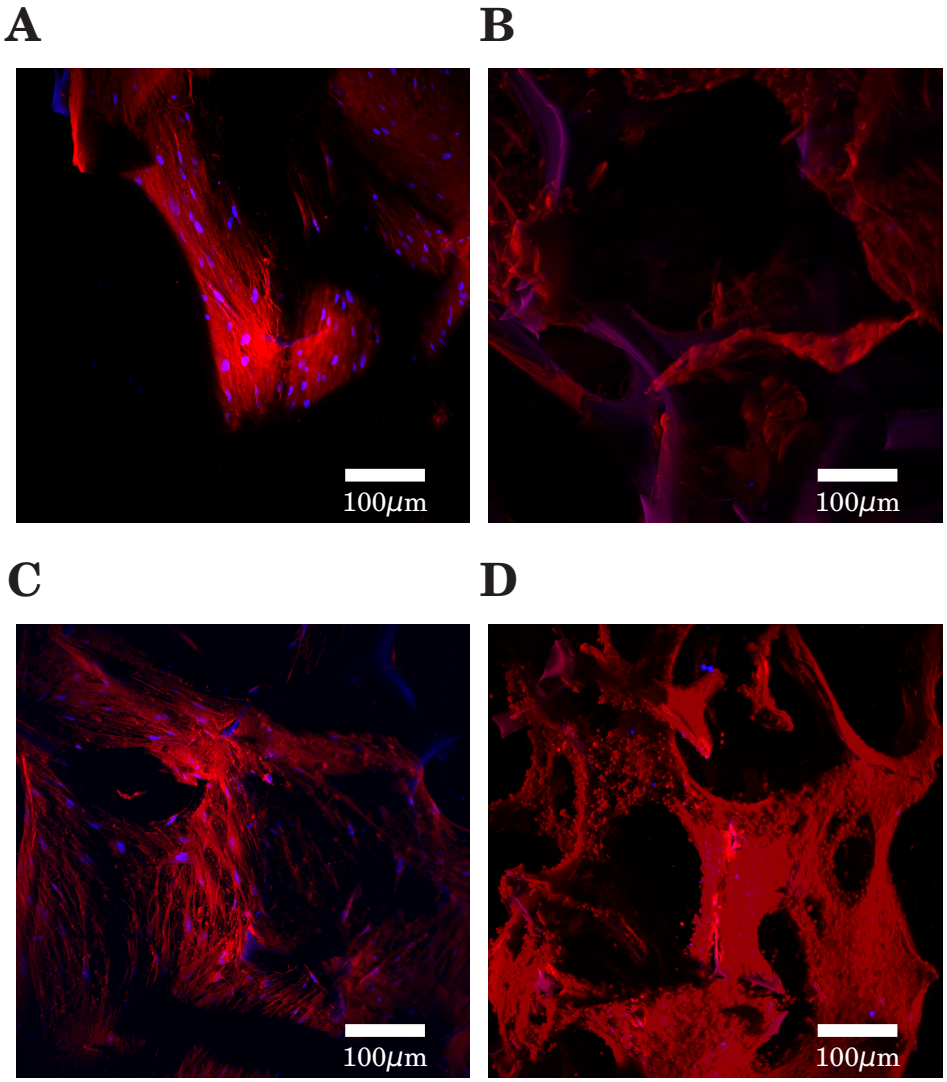


**Figure 7.12:** Day 21 Light-sheet images of DR80 (red) and DAPI (blue) stained scaffolds showing collagen matrix formation in response to LiCl exposure and FSS on hES-MPs. (A) 0 Hz 0 mM LiCl (B) 0 Hz 1 mM LiCl (C) 1 Hz 0 mM LiCl and (D) 1 Hz 1 mM LiCl.

### 7.4.4 Effects of lithium chloride on MLO-A5 flow induced osteogenesis in 3D

MLO-A5s were mechanically stimulated after treatment with LiCl. 1 mM LiCl was applied following the intermittent treatment regime and the cells were subjected to FSS in an Ibidi bioreactor (Figure 7.2). The intermittent treatment regime was used as it did not affect osteogenesis itself. Cell viability was measured on day 1, 7 and 14 with RR (Figure 7.13), ALP and total DNA was measured on day 7 (Figure 7.14) and total matrix calcium and collagen production was assessed with ARS and DR80 staining respectively on day 14 (Figure 7.15). DR80 stained samples were also imaged with light-sheet microscopy to visualise the collagen matrix (Figure 7.16). Cell viability increased in all groups between day 1 and day 14. Day 7 viability was significantly lower in LiCl treated cells subjected to FSS compared to the control. However, this was still significantly greater than day 1 viability and by day 14 all groups showed similar viability. FSS significantly increased ALP activity compared to the static controls. With the addition of LiCl treatment the FSS induced increase in ALP activity was increased further. However, when normalised to total DNA, FSS alone was not significantly different to the static control but FSS in conjunction with LiCl treatment was. LiCl treatment alone did not affect ALP activity. FSS and LiCl treatment alone or in combination did not have an effect on total DNA. FSS significantly increased mineralised matrix deposition compared to the static controls, which similarly to ALP activity was further increased with the addition of LiCl treatment. Total collagen production was not affected by FSS and LiCl treatment alone or in combination.

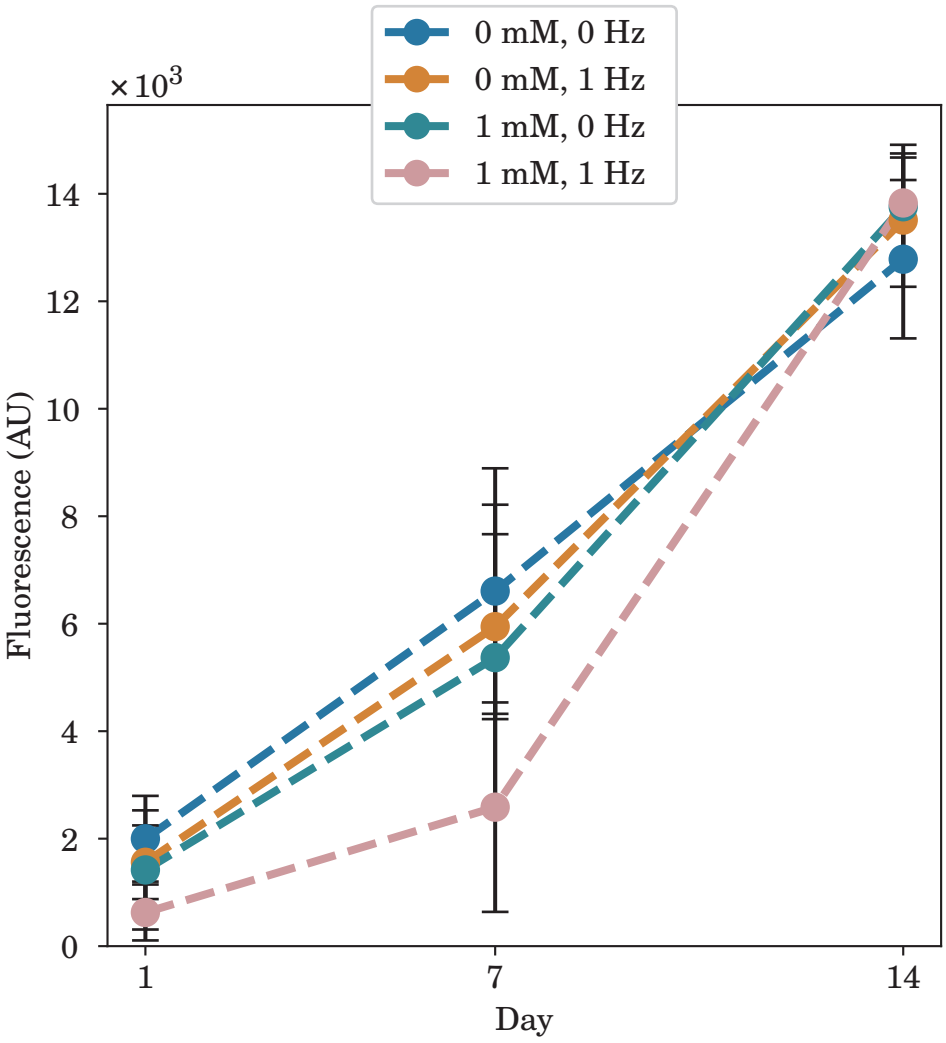


**Figure 7.13:** Effect of FSS and LiCl exposure on MLO-A5 metabolic activity over 14 days of 3D culture. LiCl was applied on day 2 and day 7 for 24 h and cells were mechanically stimulated for 1 h using an Ibidi perfusion pump on day 3 and day 8. Metabolic activity was assessed with RR. Data represents mean ± SD n=9. Fluorescence was measured at $\lambda_{ex}$: 540 nm and $\lambda_{em}$: 590 nm.

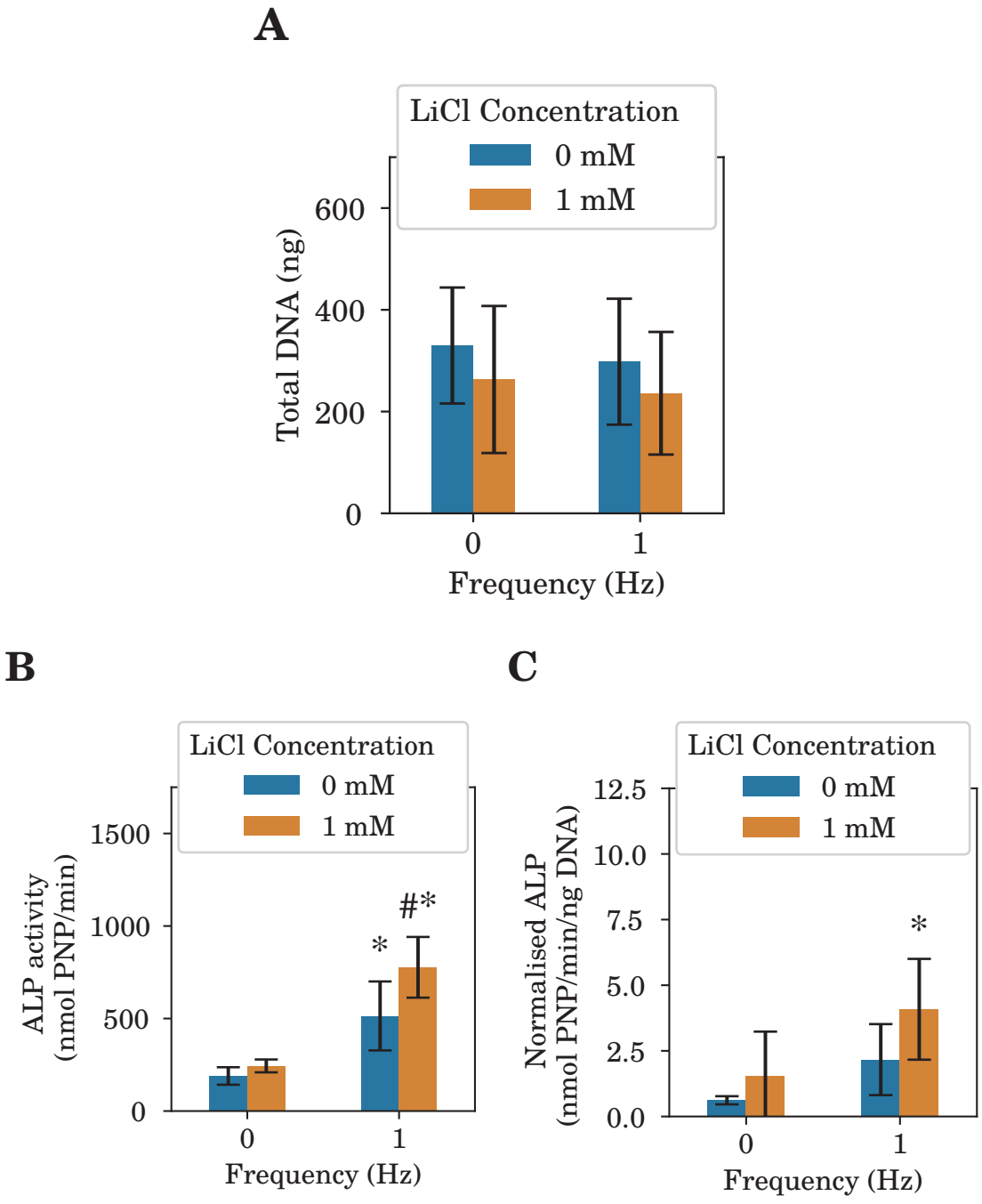


**Figure 7.14:** Effect of FSS and LiCl exposure on MLO-A5 day 7 cell number and ALP activity in 3D culture. LiCl was applied on day 2 and day 7 for 24 h and cells were mechanically stimulated for 1 h using an Ibidi perfusion pump on day 3 and day 8. (A) Total DNA. (B) ALP activity. (C) ALP activity normalised to total DNA. Data represents mean ± SD n=9. * = $p<0.05$ compared to the static control. # = $p<0.05$ compared to 0 mM LiCl.

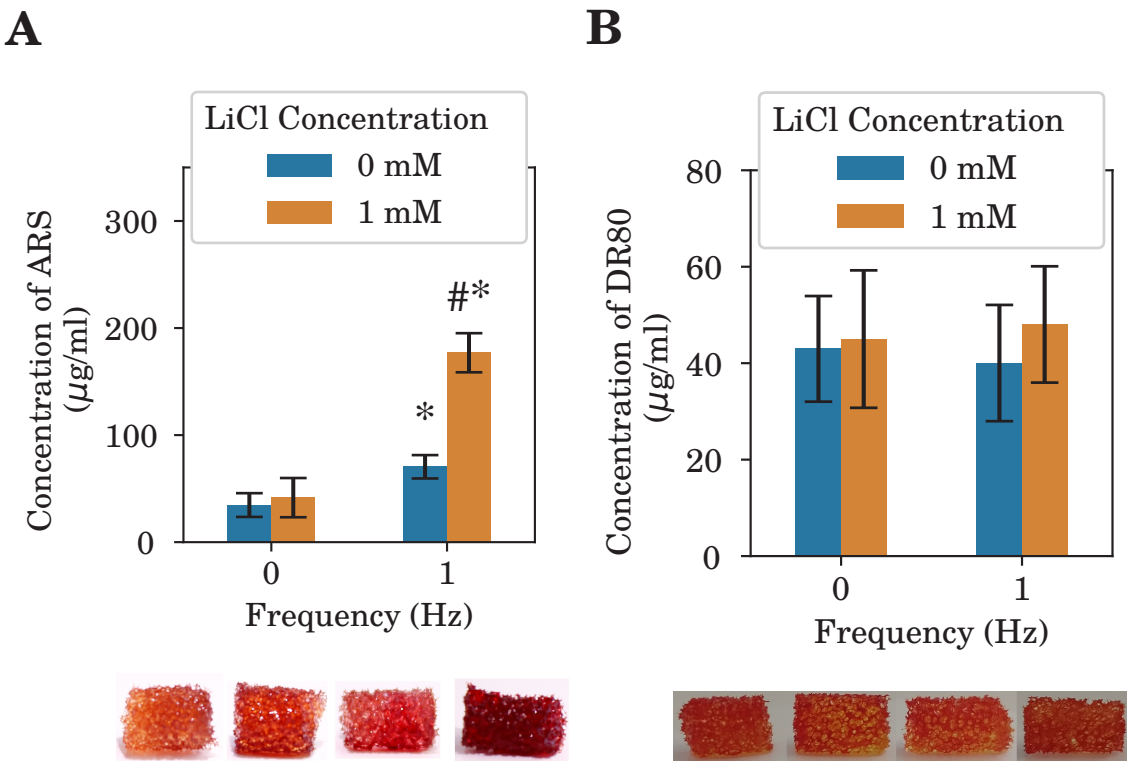


**Figure 7.15:** Effect of FSS and LiCl exposure on MLO-A5 matrix formation in 3D culture. LiCl was applied on day 2 and day 7 for 24 h and cells were mechanically stimulated for 1 h using an Ibidi perfusion pump on day 3 and day 8. (A) Day 14 matrix calcium quantified by ARS. (B) Day 14 matrix collagen quantified by DR80. Data represents mean ± SD n=9. * = $p<0.05$ compared to the static control. # = $p<0.05$ compared to 0 mM LiCl. Representative photographs of stained scaffolds are shown below their corresponding graphs. (left to right) 0 Hz 0 mM, 0 Hz 1 mM, 1 Hz 0 mM and 1 Hz 1 mM

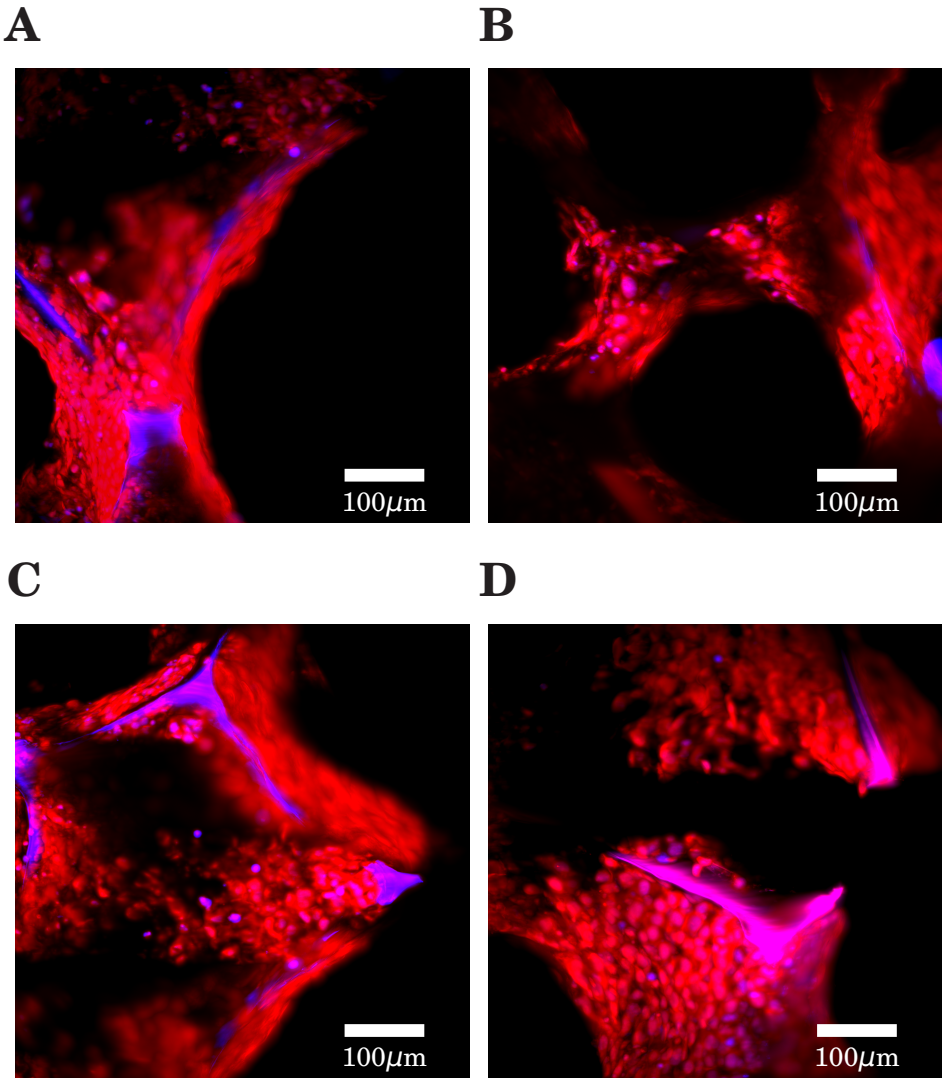


**Figure 7.16:** Day 21 Light-sheet images of DR80 (red) and DAPI (blue) stained scaffolds showing collagen matrix formation in response to LiCl exposure and FSS on MLO-A5s. (A) 0 Hz 0 mM LiCl (B) 0 Hz 1 mM LiCl (C) 1 Hz 0 mM LiCl and (D) 1 Hz 1 mM LiCl

### 7.4.5 Adenylyl cyclase activity is required for mechanotransduction

LiCl is a known inhibitor of AC, a key enzyme in the production of cAMP. cAMP is an important second messenger involved in many biological processes including mechanotransduction, although its role in mechanotransduction is not well understood. Therefore, to determine if cAMP signalling is utilised as a second messenger in hES-MP cells and how LiCl affects this, cAMP levels were measured after cells were exposed to FSS with and without LiCl treatment. Basal levels of cAMP were higher in cells treated with LiCl (Figure 7.17). cAMP levels peaked after 15 min of FSS exposure in both untreated and LiCl treated cells. However, the peak cAMP levels were significantly higher in untreated cells compared to the LiCl treated cells. After the initial peak in cAMP levels at 15 min, cAMP levels in cells not treated with LiCl decreased between 15 and 30 min but was not different between 30 and 60 min. In the LiCl treated cells this reduction in cAMP levels after the initial peak was not observed and at 15 and 30 min of FSS cAMP levels were not significantly different to the non-LiCl treated cells. cAMP levels remained higher than the static basal levels at all time points after the initiation of FSS in both LiCl treated and untreated cells.

Since LiCl treated cells had previously shown increased osteogenic responses but had shown a reduced response in terms of peak cAMP levels, a general adenylyl cyclase inhibitor, MDL, was employed to asses if adenylyl cyclase activity and cAMP signalling is required for osteogenic responses to mechanical stimulation. MDL was applied at 1, 10 and 100 µM to determine a concentration that did not affect basal cAMP levels. 100 mM MDL resulted in a significant decrease in cAMP levels compared to the vehicle control (Figure 7.17). Neither 1 nor 10 µM MDL affected basal cAMP levels.

To assess whether MDL inhibited the mechanically induced increase in cAMP 10 µM MDL was applied during the application of FSS and cAMP levels were measured at 15 min. 10 µM MDL blocked the mechanically induced increase in cAMP levels in both LiCl treated and untreated cells (Figure 7.17). To assess if this AC dependant cAMP increase was required for the mechanically induced osteogenic responses observed, rocking with and without LiCl treatment was performed in conjunction with 10 µM MDL. When cAMP signalling was inhibited with MDL there was no longer a mechanically induced increase in ALP activity as there was when cAMP signalling was not inhibited (Figure 7.18).

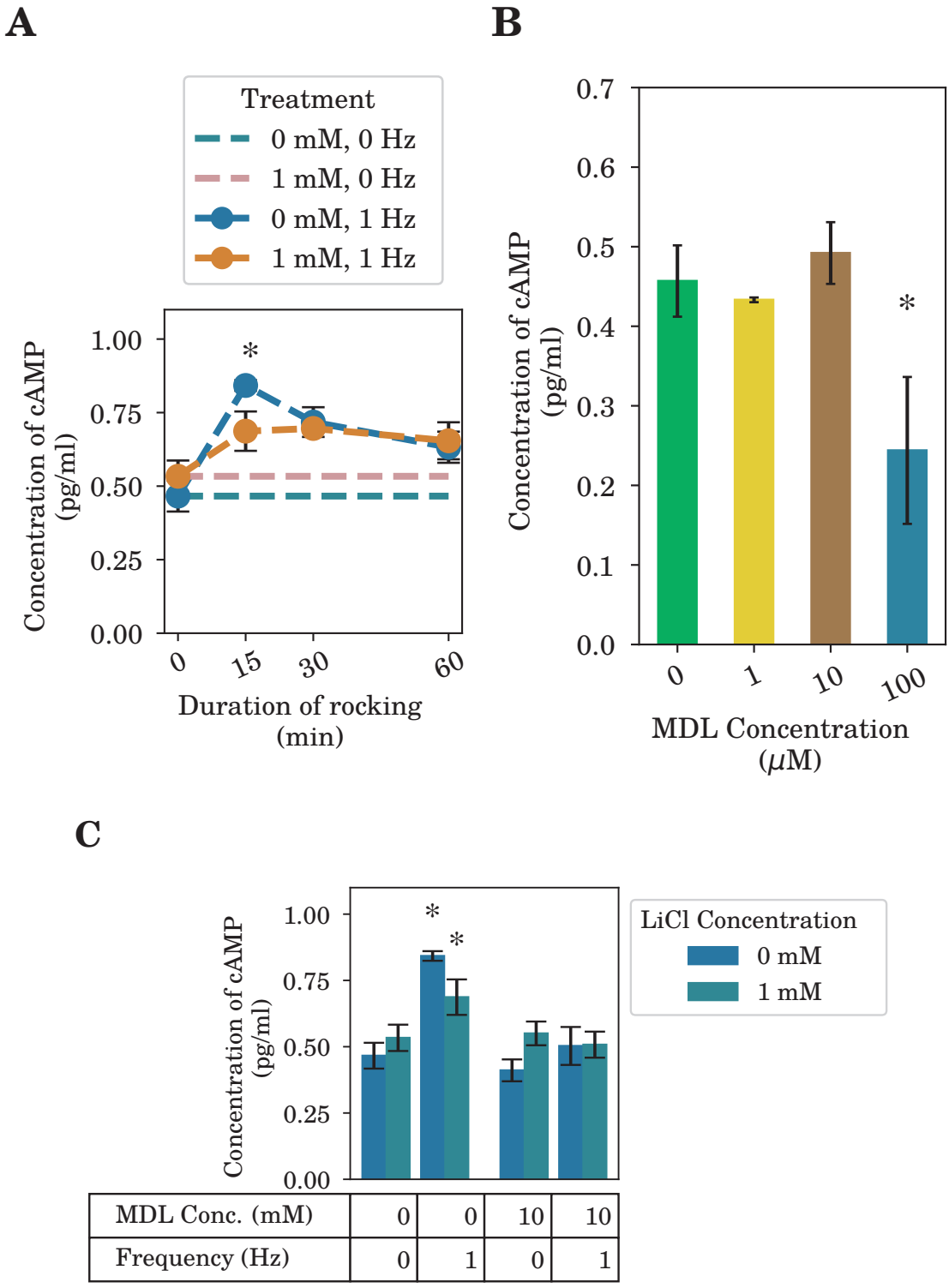


**Figure 7.17:** cAMP signalling in response to FSS and LiCl exposure. (A) Effect of FSS and LiCl exposure on hES-MP cAMP signalling at 15, 30 and 60 minutes after flow initiation in monolayer culture. (B) Dose response of the adenylyl cyclase inhibitor MDL on cAMP signalling at 15 min. (C) cAMP signalling in response to FSS and LiCl when adenylyl cyclase is inhibited with 10 μM MDL. Data represents mean ± SD n=4. * = $p<0.05$ compared to the untreated control.

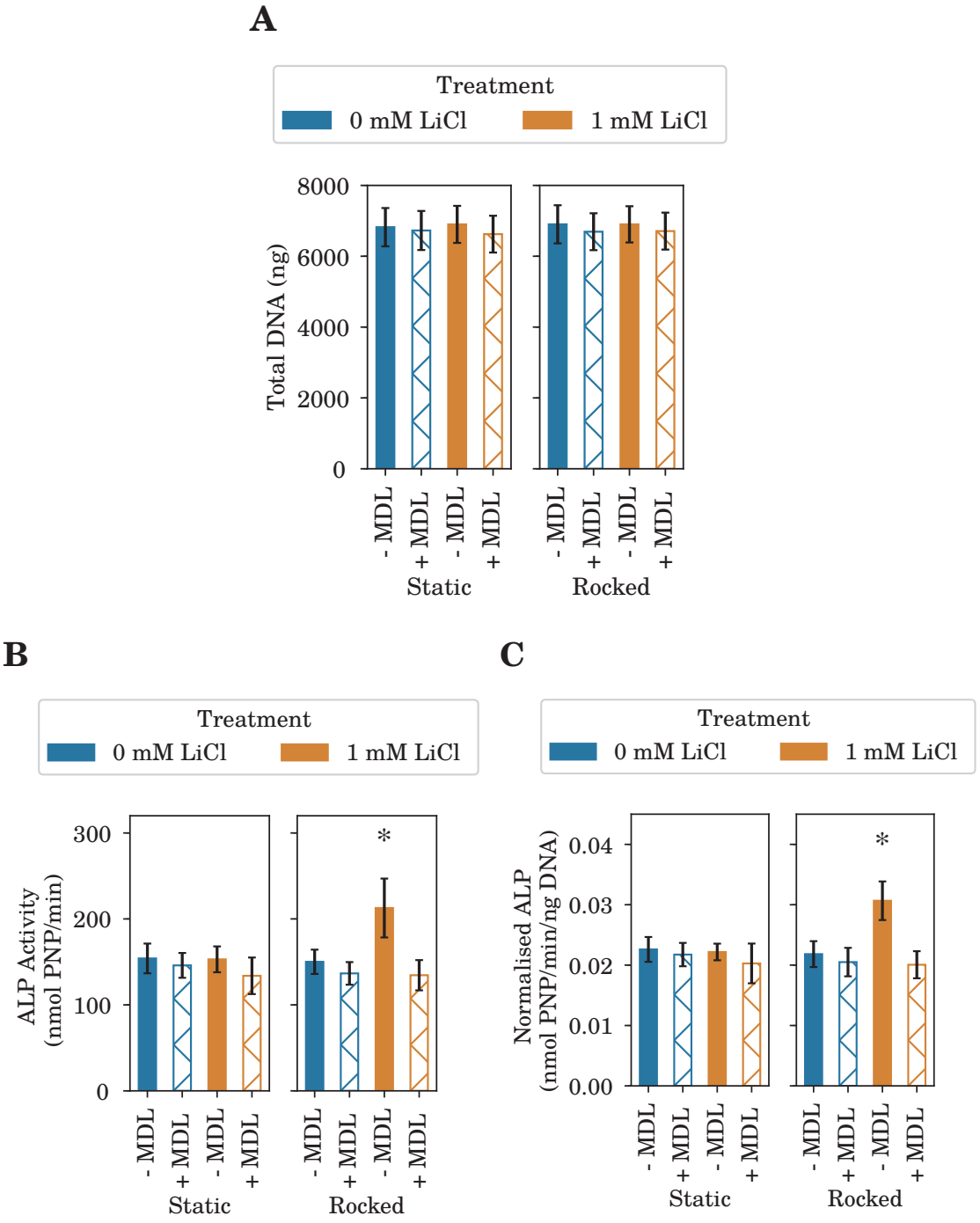


**Figure 7.18:** Day 14 ALP activity and total DNA in response to FSS and LiCl treatment when adenylyl cyclase activity is inhibited with MDL. LiCl was applied on day 6 and day 13 for 24 h and cells were mechanically stimulated on a rocking platform for 1 h 5 days per week from day 7. 10 µM MDL was added to culture media for the 1 h of rocking. (A) Total DNA. (B) ALP activity. (C) ALP activity normalised to total DNA. Data represents mean ± SD n=6. * = $p<0.05$ compared to the 0 mM control.

### 7.4.6 Mechanically induced calcium signalling is increased with LiCl treatment

$Ca^{2+}$ signalling in response to oscillatory FSS at 1.33 Hz was assessed at a low (0.3 Pa) and a high (1 Pa) shear stress in monolayer culture (Figure 7.19). A higher percentage of cells responded to the high fluid shear stress (1 Pa) compared to low fluid shear stress (0.3 Pa) in both LiCl treated and untreated hES-MP cells. At low fluid shear stress, a higher percentage of cells responded when treated with LiCl compared to untreated. However, at high fluid shear stress there was no difference. The maximum response was detected between 15 and 20 s after the initiation of flow at high fluid shear stress. At low fluid shear stress, the maximum response was detected between 15 and 20 s for LiCl treated cells but between 30 and 50 s for untreated cells. The increase in fluorescence intensity from the baseline was greater in LiCl treated cells at both fluid shear stress levels compared to untreated cells. However, this was less pronounced at the high fluid shear stress. The increase in fluorescence was also greater in both high fluid shear stress groups compared to low fluid shear stress groups.

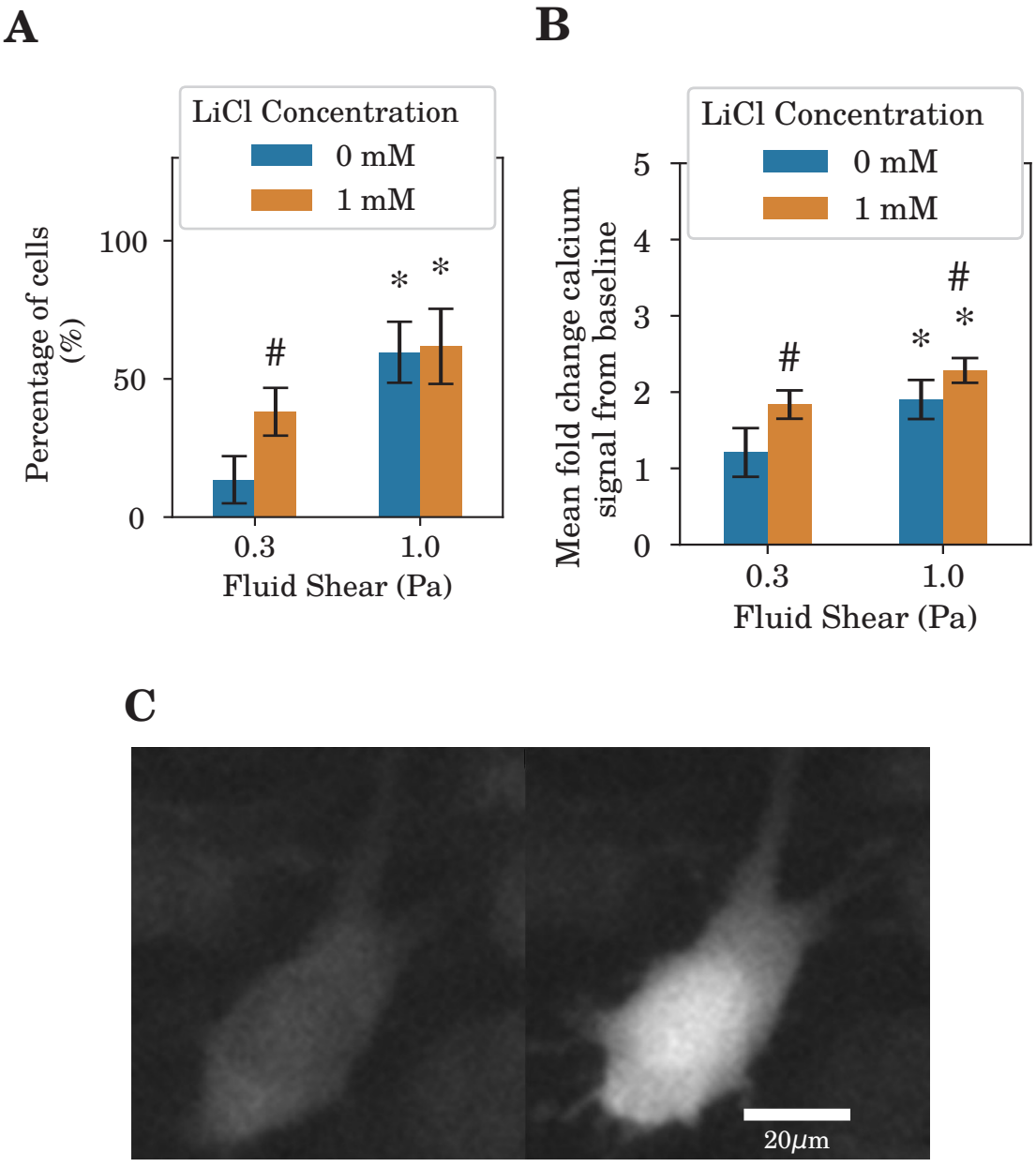


**Figure 7.19:** $Ca^{2+}$ signalling in response to fluid shear stress and LiCl exposure. Data represents mean ± SD n=55. * = $p<0.05$ compared to the 0.3 Pa stimulated control. # = $p<0.05$ compared to 0 mM LiCl control. (A) Percentage of cells responding to FSS. (B) Fold increase in calcium at first peak following application of FSS. Data represents mean ± SD $n\geqslant 9$). (C) Basal and peak intensity fluorescence images of hES-MP cells subjected to 1 Pa FSS.

## 7.5 Discussion

This chapter investigates the effects of FSS on osteogenesis when used in combination with LiCl treatment. This chapter highlights the potential of LiCl for use as a drug to stimulate bone formation in both monolayer culture and tissue engineered constructs. The LiCl treatment regime developed in chapter 5 was used in combination with FSS to evaluate if mechanically induced osteogenesis can be pharmacologically manipulated.

Promoting osteogenic differentiation in progenitor cells and promoting new bone matrix formation in mature bone cells would be highly beneficial in the treatment of osteoporosis. The traditional approach for treating osteoporosis has been through the use of pharmaceuticals that are either inhibitors of bone resorption, such as bisphosphonates, hormone replacement therapy or selective oestrogen receptor modulators, or stimulate bone formation directly, such as strontium renelate or parathyroid hormone (PTH) [395–398]. However, the majority of these treatments come with increased risks of developing other diseases. Bisphosphonates can result in bisphosphate-related necrosis of the jaw, hormone replacement therapy, selective oestrogen receptor modulators and strontium renelate can increase the risk of venous thromboembolisms and PTH may increase the risk of developing osteosarcoma, although this has not been observed in humans [399–403]. Since bone is a mechanically sensitive organ that upregulates bone formation in response to bone loading, an alternative method of treatment could be through targeting mechanotransduction. The primary cilia, a hair like protrusion present on bone cells, is thought to play a mechanotrandsuctory role and could therefore be a target for manipulating mechanotransduction in bone.

The effects LiCl treatment on mechanotransduction was first evaluated in monolayer culture as a proof-of-concept due to its simplicity and higher throughput compared to 3D culture. However, it was important to conduct the experiments in 3D culture due to differences in 3D culture compared to monolayer culture that may influence any responses.

Metabolic activity of hES-MP and MLO-A5 cells was not influenced by the application of fluid shear stress with or without LiCl treatment in monolayer culture. In 3D culture, MLO-A5 cells treated with LiCl and subjected to fluid shear stress had significantly lower metabolic activity on day 7 compared to the controls. LiCl can downregulate E-cadherin and integrins through

GSK3-$\beta$ inhibition and the subsequent $\beta$-catenin accumulation [404, 405]. Downregulation of these cell adhesion molecules may cause reduced cell-cell and cell-matrix attachment which could result in an increase in cell detachment cause by fluid shear. However, in 3D culture hES-MP cells treated with LiCl and subjected to fluid shear stress had higher metabolic activity on day 14 and day 21 suggesting higher cells numbers were present. Additionally, the concentration used by studies investigating the effects of LiCl on cell adhesion molecules used 10-fold higher concentrations compared to the 1 mM LiCl used here. The influence of LiCl on cell attachment is therefore either different in stem cells compared to mature bone cells or at the 1 mM concentration used, is likely to be minimal. The differences between monolayer and 3D culture may be due to differences in the applied shear stress. Although in 3D culture the shear stress was not calculated it is likely to be higher than the low magnitude applied in monolayer culture and could therefore have a greater effect on cell attachment.

In monolayer culture, both early and late stage indicators of osteogenesis were increased when treated with LiCl and mechanically stimulated compared to both statically cultured cells treated with LiCl and untreated mechanically stimulated cells. As progenitor cells differentiate towards an osteogenic lineage, ALP levels increase and it is therefore often used as a marker of early osteogenic differentiation. With mechanical stimulation alone ALP activity was not affected, however with LiCl treatment and mechanical stimulation ALP activity was higher compared to all other groups. Of the late stage osteogenic differentiation indicators only matrix calcium was affected. Similarly, other studies have found no changes in collagen matrix formation in response to mechanical stimulation and this suggests mechanical stimulation may preferentially upregulate mineralisation of the existing collagen matrix, rather than stimulating collagen matrix formation [250]. Although mechanical stimulation alone did enhance osteogenic differentiation, as indicated by increased matrix mineralisation, it did so at a delayed rate, or less prominently compared to mechanical stimulation in cells treated with LiCl. The earlier osteogenic differentiation with LiCl treatment could be due to a combinatorial effect of LiCl and mechanical stimulation upregulating osteogenic pathways or may be due to enhanced mechanotransduction due to LiCl with primary cilia elongation being one potential mechanism behind this.

It is theorised that primary cilia mediated mechanotransduction involves bending of primary cilia and this has been shown to occur in kidney epithelial

cells [130, 139]. However, it is not known if this occurs in bone cells *in vivo* and in osteocytes in particular, the available space within lacunae may limit primary cilia length, potentially making primary cilia bending unlikely at the shear levels experienced by the cells. In order for primary cilia to bend *in vitro* they must be exposed to fluid flow. The majority of primary cilia of both hES-MP and MLO-A5 cells presented themselves on the apical surface of the cells, meaning primary cilia would be presented to the fluid flow. However, this is complicated by the fact that the experiments performed were long term experiments and both cell types produce high levels of extracellular matrix over this time. It was observed that in monolayer culture this matrix was produced primarily at the apical surface of the cells, which could have resulted in primary cilia becoming covered and potentially embedded in matrix. Collagen matrix production was measurable by day 10 in hES-MP cells and day 5 in MLO-A5 cells. By the end time point for each cell type collagen matrix covered the majority of the well plate area. This would undoubtedly alter the shear stress the cells and therefore the primary cilia and other mechanotransducers are exposed to and could possible prevent primary cilia from bending, either through spatially constraining them or by completely blocking them from being exposed to fluid flow. Therefore, the forces applied to the cells by rocking in monolayer culture are likely to vary from the calculated 0.05 Pa and over the course of the culture may change from predominantly fluid shear forces to varying levels of matrix strain and fluid shear.

If primary cilia and other mechanotransducers were shielded from fluid flow at later time points, this would suggest the enhanced matrix production stimulated by fluid shear is a result of mechanical stimulation at earlier time points. The importance of earlier time points of mechanical loading has been highlighted by Delaine-Smith, where applying mechanical loading in the first half of culture was more stimulatory than in the second half of culture [82]. The production of matrix and resultant shielding of primary cilia and other mechanotransducers from fluid flow may explain the reduction in stimulatory responses seen by Delaine-Smith. When cells were not treated with LiCl, early osteogenic responses, measured through ALP activity, were not observed in response to fluid shear. However, when cells were treated with LiCl, ALP activity was upregulated in response to loading. This indicates whatever mechanism is behind the lithium induced increase in sensitivity occurs before day 7 and day 14 for MLO-A5 and hES-MP cells respectively.

An alternative mechanism to direct detection of shear stress could be through

the detection of matrix strain. Cells embedded in extracellular matrix would be subjected to matrix strain from matrix deformation caused by fluid shear forces acting upon it. However, any matrix strain resulting from rocking induced shear stress would be minimal due to the low level of shear stress applied (0.05 Pa). It would therefore be unlikely that any matrix deformation caused would be a high enough magnitude to be stimulatory. In 3D culture the production of matrix over the duration of culture would have different effects to that in monolayer culture. Firstly, in 3D culture the cells were not confined to a monolayer, they were able to bridge pores and grow on top of each other and the produced matrix. Therefore, at any given time there could be cells present on the surface that could be exposed to fluid flow. Secondly, as the cells produce more matrix the pore sizes would decrease and since the volumetric flow rate was kept constant, the shear stress applied to cells would increase. For these reasons, in 3D culture the earlier applications of fluid flow may be be less important than in monolayer and each application of loading over the culture period may have been as stimulatory or more stimulatory than the previous due to increased shear stress resulting from reduced pore size.

In 3D culture, cells were treated with LiCl before each fluid flow application. However, in monolayer culture 1 application of LiCl preceded 5 applications of fluid flow. Although the duration that primary cilia remained elongated was not investigated thoroughly, observations suggested that it was less than 24 h. Therefore, any increase in mechanosensitivity caused by primary cilia elongation in monolayer culture would potentially be limited to the single application of fluid flow directly following LiCl treatment. In 3D culture however, increased mechanosensitivity would have occurred with all fluid flow applications. The observed upregulation of osteogenic responses are therefore due to as little as 1 h of enhanced mechanosensitivity to fluid shear stress with regards to ALP activity or 2 h for matrix calcium. Enhanced osteogenic responses from this limited duration of LiCl exposure would be beneficial if translatable to an *in vivo* treatment. Treatment of mental disorders with lithium salts require continuous dosing that can result in adverse effects such as impaired concentration and vision, polyuria and with extended use can result in renal failure [411–413]. Since only short and intermittent LiCl exposure was required to enhance mechanosensitivity this is beneficial for its potential application *in vivo* for enhancing bone matrix deposition in response to mechanical loading.

In 3D culture primary cilia were of a more representative length to those

observed by Coughline et al. *in vivo* in bone [335]. Coughlin et al. attributed the shorter lengths compared to those typical observed *in vitro* to the spatial constraints within lacunae. However, the cells cultured here did not have these same spatial constraints applied to them yet had similar length primary cilia. Therefore, these shorter lengths may not be due to spatial constraints as has been suggested, and may instead be due to other environmental differences between monolayer culture and 3D. Due to the more representative primary cilia lengths with 3D culture the 3D culture results may more accurately reflect what may occur *in vivo* compared to monolayer culture. It may still not accurately reflect what would occur *in vivo*. Despite this, the 3D culture results do highlight the potential for using LiCl to enhance osteogenesis in bone tissue engineered scaffolds.

There have been two other studies that have investigated the effects of chemicals on mechanotransduction where primary cilia elongation also occurs [205, 414]. Both studies utilised LiCl and fenoldopam. Spasic et al., found primary cilia elongated with either chemical and resulted in upregulation of mechanically induced osteogenic gene expression compared to mechanical stimulation alone. Since the two chemicals have affect different pathways but both resulted in primary cilia elongation and increased mechanosensitivity. It suggest the primary cilia elongation is playing a role in the increased mechanosensitvity. Although, Corrigan et al., found only fenoldopam induced primary cilia elongation resulted in increases in osteogenic markers with mechanical stimulation. However, the study by Corrigan et al., used a higher concentration of LiCl (100 mM compared to 0.5 mM) and was performed with a murine stem cell line whereas the study by Spasic et al. used a murine osteocyte cell line. The use of such a high concentration by Corrigan et al. is unusual as unsurprisingly they found it was cytotoxic, resulted in further cell death when used in combination with mechanical stimulation and down-regulated osteogenic gene expression when applied alone. Conversely, the study by Spasic et al. showed no cytotoxicity with 0.5 mM LiCl application, however, it is not clear if there was any cytotoxicity when used in combination with mechanical stimulation or if it affected osteogenic markers itself as this was not reported. Here, cell viability, indicated by metabolic activity, was not affected by LiCl treatment alone or in combination with mechanical stimulation in either hES-MP or MLO-A5 cells. Since *in vitro* matrix formation typically requires cells to be at or near confluence, reductions in cell viability would be likely to reduce or prevent matrix production and mask any effects primary cilia elongation may have, as was seen by Corrigan et al. This may explain the differences between these

studies and the findings presented here [415].

Whether elongating primary cilia increases their mechanical sensitivity and the mechanism that may be behind it is still not known. However, there are a number of potential mechanisms that could be responsible. When primary cilia are elongated, the amount of primary cilia membrane and primary cilia compartment size is increased. This in turn may result in increases in primary cilia membrane proteins, as well as primary cilia specific proteins and signalling molecules within the primary cilia microdomain [416, 417]. Many proteins and signalling molecules that have been shown to be needed for mechanically induced cellular responses can be found in the primary cilia. Therefore, increasing the total number of ciliary proteins could enhance primary cilia mediated signalling. Additionally, longer primary cilia may also be subjected to greater membrane strain when fluid flow is applied as hypothesised by Schwartz et al. [129]. This greater membrane strain could result in greater opening of stretch-activated ion channels on the ciliary membrane and if there were more stretch-activated ion channels present this effect could be amplified further.

Second messengers such as cAMP and $Ca^{2+}$ signalling play an important role in mechanotransduction and they were both altered with LiCl treatment, with mechanically induced cAMP signalling being diminished and $Ca^{2+}$ signalling being enhanced. For some time, the prevailing thought has been that primary cilia are $Ca^{2+}$ responsive mechanosensors. With advances in calcium indicators, genetically encoded cilia-localised calcium indicators have been used to show mechanically induced $Ca^{2+}$ signalling to occur within primary cilia [94, 130, 418]. Additionally, Resnick and Hopfer have shown the magnitude of $Ca^{2+}$ signalling is directly proportional to the length of primary cilia [199]. This would suggest the enhanced $Ca^{2+}$ signalling responses observed here are a result of increased sensitivity of the elongated primary cilia. However, most recently, Delling et al. have used genetically encoded calcium indicators and found no changes in ciliary calcium in response to fluid flow, which suggests $Ca^{2+}$ signalling does not originate in the primary cilia. The discrepancy between their study and others was attributed to potential imaging artefacts resulting from the lower temporal resolution of previous studies and subsequent errors in their examination [137]. Delling at el., only subjected the cells to 2 s of flow, where other studies used longer durations and examined peak calcium influx. Nevertheless, these results suggest mechanically induced calcium signalling may not originate in the primary cilia and has raised interest in the role of alternative second messengers in cilia mediated mechanotransduction,

such as cAMP.

cAMP levels within the primary cilia microdomain have been found to be fivefold higher than cytostolic levels in fibroblasts and IMCD3 cells [419]. Furthermore, cAMP levels are regulated by adenylyl cyclases and some, such as adenylyl cyclase 6, have been shown to localise to the primary cilium and be required for mechanically induced cellular responses [140, 143, 420]. However, it is unclear exactly how mechanical stimulation affects cAMP signalling and the role it plays in mechanotransduction. For example, there are conflicting findings with regards to how cAMP levels are altered in response to mechanical stimulation. Kwon et al., have shown the mechanoresponse of cAMP signalling to be temporal, initially decreasing before increasing in osteocytes [140]. This decrease was not observed here, cAMP levels rose with mechanical stimulation in both control and LiCl treated cells before decreasing back towards basal levels. Since the reduction in cAMP was seen 2 min after the initiation of fluid flow this decrease may have been missed as the earliest time point measured was 15 min. However, Johnson et al. measured cAMP levels in stem cells in response to fluid flow at 2 min and did not observe a decrease at this earlier time point. This may suggest that the cAMP response varies between stem cells and mature bone cells. cAMP responses have also been shown to be dependent on the magnitude of the fluid shear applied, increasing in a dose dependant manner, giving further evidence to support the hypothesis that cAMP levels rise in response to mechanical stimulation [421].

A magnitude dependant cAMP response would suggest if the mechanosensitivity of cells was enhanced the cAMP response would be greater for a given magnitude of stimulation. However, the cAMP response to mechanical stimulation was diminished with LiCl treatment despite the apparent increase in mechanosensitivity indicated by increased mechanically induced osteogenic responses. The diminished cAMP response is likely due to the inhibitory effect LiCl is known to have on adenylyl cyclase activity and suggests peak cAMP levels may not influence osteogenic mechanoresponses [219, 422]. cAMP signalling regulated through adenylyl cyclase activity was however required for mechanically induced increases in osteogenesis to occur, as when mechanically induced cAMP signalling was abrogated with MDL treatment, osteogenic responses to mechanical stimulation no longer occurred.

Counter-intuitively, basal levels of cAMP were higher in LiCl treated cells compared to controls, despite the fact LiCl inhibits adenylyl cyclase activity.

Other studies have shown LiCl treatment decreases cAMP levels [423–425]. However, these studies were performed in neuronal cells which may respond differently. Furthermore, lithium's inhibitory effects on adenylyl cyclase that cause the decreased cAMP have been shown to be specific to the adenylyl cyclase V and VII isoforms in neuronal cells [426]. The increase observed here could therefore be due to an increase in different adenylyl cyclase isoform expression as a compensatory mechanism to LiCl's inhibitory action as has been observed by Colin et al. [427]. Additionally, the expression levels of each of the different adenylyl cyclase isoforms is likely to be different between neuronal cells and the hES-MP cells used here. Changes in cAMP levels are known to alter primary cilia length, Besschetnova et al. have shown increased cAMP levels result in primary cilia elongation through higher anterograde intraflagellar transport speeds [195]. The primary cilia elongation caused by LiCl treatment may therefore be due to this increase in basal cAMP.

Clearly both cAMP and $Ca^{2+}$ signalling are important and required for mechotransduction to occur, since, when either of these are inhibited mechanically induced responses are attenuated or abrogated [133, 140, 428]. However, neither of these work in strict isolation. Adenylyl cyclases can either be activated by or inhibited by $Ca^{2+}$ signalling and cAMP through its downstream effector, protein kinase A (PKA), can affect $Ca^{2+}$ signalling at every level from its generation to termination [429–433]. This coupled with the fact LiCl affects both of these pathways makes it difficult to pinpoint the role each of these second messengers plays in the increased mechanosensitivity observed here.

## 7.6 Summary

To summarise, the previously optimised LiCl treatment regime and mechanical loading regime were combined to assess the effects of LiCl on mechanosensitivity. LiCl treatment resulted in increased sensitivity to FSS stimulation in osteogenic progenitors and osteoblast cell lines. This increased mechanosensitivity occurred in both monolayer culture and 3D culture. LiCl was found to increase basal levels of cAMP but also inhibited FSS stimulated cAMP signalling. Although cAMP signalling was reduced in LiCl treated cells, cAMP signalling was required for FSS stimulated increases in ALP activity to occur. $Ca^{2+}$ signalling in response to FSS after LiCl treatment was found to increase the number of $Ca^{2+}$ responding cells at low FSS but not at high FSS. Addition-

ally, intracellular $Ca^{2+}$ levels increased more in LiCl treated cells compared to untreated cells in response to both levels of FSS.

# 8. General discussion and future work

Mechanotransduction is a critical process in the development, maintenance and function of a variety of tissues, including bone. Bone itself is a complex tissue that contains multiple cell types, each playing an essential role in regulating the balance between bone formation and resorption in response to the habitual levels of mechanical stimulation [387, 388]. Diseases such as osteoporosis can cause imbalances in this bone remodelling cycle, resulting in reduced bone density and quality and subsequent increases to the risk of bone fractures. In order to restore the balance of resorption and deposition current therapies focus on the inhibition of bone resorption. However, with many of these treatments over a quarter of patients respond poorly and in rare circumstances serious and debilitating side-effects can occur [434]. Alternatives to these treatments would therefore be highly beneficial. High impact physical activity is well known to increase bone deposition; however, the amount of exertion elderly and osteoporotic patients can tolerate can be limited. Therapeutically enhancing the sensitivity of bone cells to lower levels of physical stimuli could form an alternative treatment.

In addition to applications for treating osteoporosis, increased mechanosensitivity in osteogenic cells could be used to enhance matrix deposition in tissue engineered bone. One method for creating tissue engineered bone involves initial culture of the scaffold *in vitro* to allow cells to deposit natural matrix onto the scaffold. This is often performed in bioreactors to increase mass transport into the core of the scaffold but also to mechanically stimulate the cells. Enhancing the osteogenic responses to this mechanical stimulation would therefore be beneficial.

The main aim of this thesis was to investigate the use of lithium in enhancing

osteogenic responses to FSS.

Lithium, in the form of lithium salts such as LiCl, have previously been shown to elongate primary cilia [208, 209, 211]. Primary cilia are one organelle thought to play a role in mechanotransduction. They have been shown to regulate their length in response to mechanical loading, becoming shorter in response to continuous loading leading to a subsequent decrease in mechanical sensitivity of the cells [195, 383, 384]. Lithium is also safe for use in humans and has been used clinically for many years to treat psychiatric disorders, although it is not without its side effects. Due to these reasons it was a promising candidate for investigating its effects on mechanosensitivity. However, lithium has also been shown to directly affect osteogenesis, although there are also conflicting studies that have found it to have no effects [287–290]. If the lithium treatment used to enhance mechano-induced osteogenesis also enhanced osteogenesis itself, this would make analysis of the effects of lithium on FSS driven osteogenesis more difficult. Therefore, in addition to investigating the effects of lithium on mechanotransduction and primary cilia length, it was necessary to optimise a treatment regime that did this without affecting osteogenesis. To this end, continuous LiCl treatment, at a therapeutically used concentration, was found to promote osteogenic markers. When used intermittently this same concentration of LiCl was found to increase primary cilia length without affecting primary cilia prevalence or osteogenic markers. For this study the use of continuous LiCl treatment was therefore excluded. Despite this, in the future it would be interesting to investigate if these osteogenic effects are combinatorial with increased osteogenic responses due to enhanced mechanosensitivity. If this were to be the case this would have greater potential as a treatment for bone disorders such as osteoporosis.

Although the cells used in this study did respond to mechanical stimulation, collagen production was not affected. Previous studies have shown collagen production to be increased in response to mechanical loading in bone cells [82, 266, 342]. Specifically, Delaine-Smith et al., showed increased collagen production in response to low magnitude FSS in hES-MP cells [82]. This cell type is therefore responsive to mechanical loading in terms of collagen production. Different batches of serums can contain different levels and types of hormones and other proteins, which can greatly influence the way cells grow and respond to treatments [435–437]. This was highlighted here where different batches of serum were found to alter cell growth, collagen production, matrix mineralisation and responses to FSS. Although the serum composition

may have played a role in the differences in responses observed it is not known at which point in culture the serum influences the cellular responses. For example, the FSS applied may have upregulated collagen type 1 $\alpha$ 1 (COL-1$\alpha$1) gene expression but downstream of this each different serum may alter translation of COL-1$\alpha$1 into collagen or the expression of other genes that may alter collagen expression. Future studies should focus on the use of chemically defined media to avoid these problems and also to allow comparison between studies. Additionally, it would be beneficial to assess both short-term (such as gene expression) and long-term responses in the future to gain a better understanding of what is occurring throughout the culture period.

There is growing evidence Wnt/$\beta$-catenin signalling plays an important regulatory role in bone formation and controlling stem cell proliferation and differentiation [292, 307, 312]. When Wnt/$\beta$-catenin signalling is inhibited or highly stimulated it results in reduced bone formation or reduced bone remodelling and reduced bone strength [438]. In contrast, with only a slight activation of Wnt/$\beta$-catenin signalling, bone formation increases resulting in improved bone strength [438]. The extent at which Wnt/$\beta$-catenin signalling is stimulated is therefore important and may explain some of the contrasting conclusions from studies investigating the role of Wnt/$\beta$-catenin signalling in bone formation. LiCl is well known to inhibit GSK3-$\beta$ activity and therefore increase $\beta$-catenin levels [321]. With regards to this it is likely the LiCl treatment applied here altered $\beta$-catenin levels. Only continuous LiCl treatment affected osteogenesis and this only occurred when hES-MP cells were cultured in DW media. The LiCl treatment therefore did not stimulate osteogenic differentiation alone but did enhance osteogenic differentiation through increased matrix mineralisation when osteogenic differentiation was pre-stimulated with Dex. It would therefore be interesting to explore how the LiCl treatments effected $\beta$-catenin levels in non-differentiated compared to differentiated hES-MP cells and what differences there were between continuous compared to intermittent treatments.

In 3D culture primary cilia were found to be shorter than in monolayer culture and of a more similar length to those reported to occur *in vivo* in bone. Cells with shorter primary cilia have been shown to be less mechanically sensitive [195]. This would suggest that when cultured in 3D the cells would be less mechanically sensitive than in monolayer culture. Since the FSS magnitude applied to the cells in monolayer and 3D culture were not matched it is not possible to conclude this from the results presented in this study. In the future

modelling the FSS within the PU scaffold would allow a flow regime to be used that matches the FSS applied by the rocking platform, allowing comparisons of osteogenic responses to the same magnitude of FSS.

The shorter primary cilia of bone cells observed *in vivo* has previously been attributed to spatial constrains of bone surrounding the cells such as osteocytes within the lacunae [335]. However, the pore size of the PU scaffold used here was greater than 100 µm and therefore the scaffold does not apply significant spatial constraints to the cells. Furthermore, bone lining osteoblasts and osteogenic progenitors within bone marrow have also been shown to have similarly short primary cilia despite these cell types not being surrounded by bone matrix and therefore not having the same spatial constraints [335].

If the elongation of primary cilia is part of the mechanism behind the increased mechanosensitivity, it would be important to know if spatial constraints would limit the amount of primary cilia elongation that is achievable. If primary cilia elongation is limited by spatial constraints *in vivo* it could limit the potential for the use of lithium in elongating primary cilia which may limit any enhancement in mechnosensitivity due to increased primary cilia length *in vivo*. This would be more of a limiting factor in osteocytes within lacunae where cells are surrounded by bone matrix and less of a limiting factor in both bone lining osteoblasts and osteogenic progenitor cells within the bone marrow which have less spatial constraints applied to them. The work presented here highlights lithium induced primary cilia elongation in both osteoblasts and osteogenic progenitor cells. As these cells are less spatially constrained primary cilia elongation in these cell types may be less limited. This suggests primary cilia elongation may still have beneficial effects in these cell types *in vivo*. To investigate if spatial constraints may limit primary cilia elongation and whether this would prevent enhanced mechanoresponses to FSS an alternative scaffold with smaller pores could be employed. A possible alternative scaffold could be polyHIPE scaffolds, where median pore size can be controlled in the range of 8-21 µm diameter [439].

The mechanism by which lithium increases primary cilia length is still unclear. Nakakura et al., proposed lithium induced primary cilia elongation occurs through an increase in acetylated $\alpha$-tubulin due to GSK3-$\beta$ inhibition [208]. If there was an increase in acetylated $\alpha$-tubulin there would likely be an increase in fluorescence intensity of the stained primary cilia here. This was not the case as there was no increases in fluorescence intensity of anti-acetylated

$\alpha$-tubulin stained primary cilia observed. However, a more in-depth analysis through measuring acetylated and non-acetylated $\alpha$-tubulin levels by ELISA and measuring $\alpha$-tubulin N-acetyltransferase expression levels would be required to assess if this were the case.

Studies have shown LiCl as well as other GSK3-$\beta$ inhibitors elongate primary cilia [208, 212]. However, other studies have contradicted these findings, suggesting primary cilia elongation, due to lithium, is independent of GSK3-$\beta$ inhibition and that other GSK3-$\beta$ inhibitors did not cause primary cilia elongation [209, 210]. Instead of GSK3-$\beta$ inhibition Ou et al., found LiCl inhibited adenylyl cyclase and suggested the subsequent decrease in cAMP levels caused primary cilia elongation [209]. However, Besschetnova et al., found activation of adenylyl cyclase and subsequent increases in cAMP levels caused primary cilia elongation [195]. Interestingly, this study found basal levels of cAMP were higher after LiCl treatment. It should be noted however that these measurements were taken after the removal of LiCl from the media and by this time-point primary cilia elongation had already occurred. Since lithium itself affects multiple pathways, including both cAMP and $Ca^{2+}$ signalling, it may be that lithium causes primary cilia elongation through multiple mechanisms. Furthermore, due to these many conflicting findings it is clear further work in this area is necessary and a more specific drug to elongate primary cilia would be more beneficial moving forwards.

Although LiCl treatment did elongate primary cilia, it may not have been the only mechanosensitive organelle of the cell that was altered. There may therefore be other factors involved in the increased mechanosensitivity observed here. For example, the cytoskeleton is known to play an important role in mechanotransduction and in osteoblasts lithium has been shown to increase focal adhesions and F-actin stress fibres, altering cell spreading and shape [316]. Other studies have also shown lithium affects focal adhesion turnover rates which may also alter mechanotransduction [440]. Furthermore, lithium inhibits inositol enzymes resulting in reduced Phosphatidylinositol 4,5-bisphosphate ($PIP_2$), which are a required cofactor in many ion channels including mechanosensitive ion channels [226]. However, since the mechanical stimulation was applied after LiCl was removed from the media some of these effects may have been minimised, such as the inhibition of inositol and subsequent alterations in $PIP_2$ levels. Nevertheless, it is possible the increased mechanosensitivity observed here is due to a combination of these effects and not due to primary cilia elongation alone or at all. To further elucidate how

much of an impact primary cilia elongation played in the increased osteogenic responses observed, these experiments could be repeated after primary cilia are elongated with other chemicals or either removed through chloral hydrate treatment or prevented from forming through knockdown of intraflagellar transport (IFT) 88 with small interfering ribonucleic acid (siRNA). If enhanced responses to stimulation still occurred this would indicate either other mechanosensors are playing a role or that the increase is due to other effects lithium has.

Primary cilia are known to reduce their length in response to continuous mechanical loading and these cells become less mechanically sensitive after their primary cilia become shorter [384, 441]. To the authors knowledge there have been no studies investigating if drugs can prevent this shortening from occurring or if their length can be quickly recovered. It is thought that this phenomenon also occurs *in vivo* as cells in areas of higher loading have been shown to have shorter primary cilia than those in areas of lower loading [383]. Future studies could apply this LiCl treatment regime developed here after shortening primary cilia through mechanical loading and also assess if primary cilia shortening occurs due to continuous mechanical loading while LiCl is also applied.

One limitation of this study may be the use of only osteogenic progenitor and osteoblast/pre-osteocyte cell lines. Osteocytes are thought to play an important role in mechanotransduction and directing bone resorption and deposition in response to loading. As this study focused on long term effects such as matrix production and osteocytes themselves do not produce bone matrix they were not used for this study. However, it would be important to see how lithium treatment affects the function of osteocytes, including how it alters osteoblast recruiting signalling such as $PGE_2$ and nitric oxide (NO). The previously discussed point on spatial constraints limiting primary cilia elongation is also particularly relevant to osteocytes. It would therefore be important to assess if primary cilia elongation is also possible in osteocytes given the spatial constraints applied by the lacunae.

The FSS applied in this study through rocking was of a low magnitude and is lower than what is theorised to occur *in vivo* when bones are loaded. With increasing levels of loading stimulus cellular responses such as calcium signalling also increase [442]. However, this only occurs until responses become saturated, after which further increases in stimulus magnitude do not result in increased responses [443–445]. This may mean that increased mechanosensitivity

observed here is limited to low magnitudes of loading and that at higher magnitudes responses may already be saturated. However, increasing responses to low level stimuli would be beneficial in older people who are less able to perform high impact activities such as running that stimulates bone deposition.

Lithium treatment has been shown to reduce the risk of fracture in osteoporotic patients being treated with lithium for mental disorders [281–283]. However, its use as a bone anabolic agent is limited by its side effects which can range from excessive thirst and urination to mental impairment and kidney, thyroid and parathyroid gland problems with continuous use. Previous investigations into lithium's bone anabolic effects have only focused on its direct effects on bone formation and not on its potential to increase mechanosensitivity. This study therefore highlights a second potential mechanism by which lithium treatment may reduce bone fracture risk through increased bone density. Furthermore, only intermittent lithium treatment was required in order to induce increases in osteogenic responses to FSS. Only requiring intermittent treatment could mean only taking lithium before bouts of exercise, this would be beneficial as many of the side effects from lithium treatment occur due to its continuous use.

The exact mechanism by which lithium caused increases in mechanoresponses was not fully elucidated in this study. There are numerous signalling pathways involved in mechanotransduction and second messengers such as cAMP and $Ca^{2+}$ play an important role in the transduction of mechanical stimuli to biochemical responses. When adenylyl cyclase activity, the enzyme which catalyses adenosine triphosphate (ATP) to cAMP, was inhibited with MDL ALP activity was no longer increased with lithium treatment and FSS application. This suggests adenylyl cyclase and cAMP signalling is required for osteogenic mechanoresponses to occur. Interestingly although adenylyl cyclase was found to be required, cAMP signalling was actually found to be lower in LiCl treated cells subjected to FSS than control cells. Since cAMP signalling is temporal, it may be that cAMP signalling was not lower and instead peaked at a different time point. Certain isoforms of adenylyl cyclase have been shown to be concentrated in or specific to primary cilia [133, 140, 446]. Elongation of primary cilia could potentially also result in an increase in adenylyl cyclase expression. Due to these reasons further work is required in both assessing the temporal cAMP response to FSS and also whether lithium treatment alters the distribution of adenylyl cyclase within the cell or increases or its levels or alters the isoforms in the primary cilium.

# 9. Conclusion

This thesis explored the feasibility of pharmacologically enhancing osteogenic responses to mechano-stimulation in osteogenic progenitor and osteoblast cells. Cells were established to be mechanically sensitive to an optimised low-level FSS stimulus, where they showed enhanced osteogenesis in response to FSS. Lithium, in the form of LiCl was applied to cells in monolayer culture and in a 3D porous PU scaffold. LiCl treatment was found to increase osteogenesis when applied continuously. In order to assess the effects of LiCl on mechanoresponses, a treatment regime that did not stimulate osteogenesis in static conditions was optimised. Osteogenic responses to FSS were found to be enhanced with the established LiCl treatment regime compared to stimulation without LiCl treatment. One mechanism that may have played a role in the enhanced mechanoresponses observed is through lithium's effects on primary cilia. Primary cilia length is thought to play a role in regulating mechanosensitivity and the LiCl treatment used here was found to elongate primary cilia. However, this would require further work to fully elucidate whether primary cilia elongation was involved in the increases in mechanoinduced osteogenic responses observed here. In 3D culture primary cilia were shown to be shorter than in monolayer culture and were found to be of similar lengths to those reported to occur *in vivo*. As primary cilia were able to be elongated it suggests the shorter lengths were not due to physical confinement.

Due to the complex and multifaceted pharmacological actions of lithium, the exact mechanisms behind how it induced primary cilia elongation and the exact mechanism behind the enhancement in mechanosensitivity were not established. However, two pathways that lithium effects, namely cAMP and $Ca^{2+}$ signalling, were found to be altered in LiCl treated cells subjected to FSS. Furthermore, when AC activity was inhibited mechanically induced increases in ALP activity no longer occurred, suggesting AC activity and

cAMP signalling are required for mechanotransduction to occur. Further work should aim to elucidate the exact mechanisms behind both the LiCl induced primary cilia elongation and the enhanced mechanosensitivity and if possible, to find a pharmacological agent that more specifically targets this mechanism. Despite the exact mechanisms behind these responses not being known, this thesis highlights a novel therapeutic option that could be used to enhance mechanosensitivity in bone cells in order to treat diseases that cause reduced bone density, such as osteoporosis.

# References


[1] R. S. Taichman, "Blood and bone: two tissues whose fates are intertwined to create the hematopoietic stem-cell niche." *Blood*, vol. 105, no. 7, pp. 2631–9, 2005.

[2] D. Sommerfeldt and C. Rubin, "Biology of bone and how it orchestrates the form and function of the skeleton," *European Spine Journal*, vol. 10, no. 0, pp. S86–S95, 2001.

[3] C. Anderson, "Bone histomorphometry," *Bone and Mineral*, vol. 26, no. 2, p. 191, 1994.

[4] C. Engine and L. Gibson, "The mechanical behaviour of cancellous bone," *Journal of Biomechanics*, vol. 18, no. 5, pp. 317–328, 1985.

[5] B. Clarke, "Normal Bone Anatomy and Physiology," *Clinical Journal of the American Society of Nephrology*, vol. 3, no. Supplement 3, pp. S131–S139, 2008.

[6] C. A. Squier, S. Ghoneim, and C. R. Kremenak, "Ultrastructure of the periosteum from membrane bone," *Journal of anatomy*, vol. 171, pp. 233–9, 1990.

[7] A. Islam, C. Glomski, and E. S. Henderson, "Bone lining (endosteal) cells and hematopoiesis: a light microscopic study of normal and pathologic human bone marrow in plastic-embedded sections." *The Anatomical record*, vol. 227, no. 3, pp. 300–6, 1990.

[8] S. Weiner and H. D. Wagner, "The materials bone: Structure-Mechanical Function Relations," *Annual Review of Materials Science*, vol. 28, pp. 271–298, 1998.

[9] D. R. Keene, L. Y. Sakai, R. E. Burgeson, O. Article, and E. Burgeson, "Bone Contains Type III Collagen , Type VI Collagen , and Fibrillin : Type

III Collagen is Present on Specific Fibers That May Mediate Attachment of Tendons , Ligaments , and Periosteum to Calcified Bone Cortex ',"
*The journal of histochemistry and cytochemistry : official journal of the Histochemistry Society*, vol. 39, no. 1, pp. 59–69, 1991.

[10] J. Sodek and M. D. McKee, "Molecular and cellular biology of alveolar bone," *Periodontology 2000*, vol. 24, pp. 99–126, 2000.

[11] P. G. Robey, "The biochemistry of bone," *Endocrinology and Metabolism Clinics*, vol. 18, no. 4, pp. 858–902, 1989.

[12] V. I. Sikavitsas, J. S. Temenoff, and A. G. Mikos, "Biomaterials and bone mechanotransduction," *Biomaterials*, vol. 22, no. 19, pp. 2581–2593, 2001.

[13] I. J. Lorch, "Alkaline phosphatase and the mechanism of ossification," *The Journal of bone and joint surgery. British volume*, vol. 31B, no. 1, pp. 94–9, 1949.

[14] J. M. Roudsari and S. Mahjoub, "Quantification and comparison of bone-specific alkaline phosphatase with two methods in normal and paget's specimens," *Caspian Journal of Internal Medicine*, vol. 3, no. 3, pp. 478–483, 2012.

[15] J.-Y. Rho, L. Kuhn-Spearing, and P. Zioupos, "Mechanical properties and the hierarchical structure of bone," *Medical Engineering & Physics*, vol. 20, no. 2, pp. 92–102, 1998.

[16] C. D. Hoemann, H. El-Gabalawy, and M. D. McKee, "In vitro osteogenesis assays: Influence of the primary cell source on alkaline phosphatase activity and mineralization," *Pathologie Biologie*, vol. 57, no. 4, pp. 318–323, 2009.

[17] R. Lakes, "Materials With Structural Hierarchy," *Nature*, vol. 361, no. 6412, pp. 511–15, 1993.

[18] T. Komori, "Functions of the osteocyte network in the regulation of bone mass," *Cell and tissue research*, vol. 352, no. 2, pp. 191–8, 2013.

[19] F. Long, "Building strong bones: Molecular regulation of the osteoblast lineage," *Nature Reviews Molecular Cell Biology*, vol. 13, no. 1, pp. 27–38, 2012.

[20] W. J. Boyle, W. S. Simonet, and D. L. Lacey, "Osteoclast differentiation and Activation," *Nature*, vol. 423, pp. 337–342, 2003.

[21] S. C. Manolagas, “Birth and Death of Bone Cells : Basic Regulatory,” *Endocrine Reviews*, vol. 21, no. 2, pp. 115–137, 2000.

[22] A. D. Berendsen and B. R. Olsen, “Bone development,” *Bone*, vol. 80, pp. 14–8, 2015.

[23] J. Klein-Nulend, R. G. Bacabac, A. D. Bakker, M. B. Group, and C. City, “mechanical Loading And How It Affects Bone Cells: The Role Of The Osteocyte Cytoskeleton In Maintaining Our Skeleton,” *European cells and Materials*, vol. 24, pp. 2078–291, 2012.

[24] M. Hillsley and J. Frangos, “Review: Bone tissue engineering: The role of interstitial fluid flow,” *Biotechnology and Bioengineering*, vol. 43(7), no. 7, pp. 573–581, 1994.

[25] K. M. Kim, Y. J. Choi, J. H. Hwang, A. R. Kim, H. J. Cho, E. S. Hwang, J. Y. Park, S. H. Lee, and J. H. Hong, “Shear stress induced by an interstitial level of slow flow increases the osteogenic differentiation of mesenchymal stem cells through TAZ activation,” *PLoS ONE*, vol. 9, no. 3, 2014.

[26] L. J. Raggatt and N. C. Partridge, “Cellular and molecular mechanisms of bone remodeling,” *Journal of Biological Chemistry*, vol. 285, no. 33, pp. 25 103–25 108, 2010.

[27] I. Fernández-Tresguerres-Hernández-Gil, M. A. Alobera -Gracia, M. del Canto-Pingarrón, and L. Blanco-Jerez, “Physiological bases of bone regeneration II. The remodeling process,” *Medicina Oral, Patología Oral y Cirugía Bucal (Internet)*, vol. 11, no. 2, pp. 151–157, 2004.

[28] J. Bonjour, G. Theintz, F. Law, D. Slosman, and R. Rizzoli, “Osteoporosis International Peak Bone Mass Measurement of Bone Mass Development,” *Osteoporosis international*, vol. supp 1, pp. s7–s13, 1994.

[29] J. C. Prior, C. Berger, A. Tenenhouse, N. Kreiger, S. Jackson, L. Joseph, K. S. Davison, R. G. Josse, L. Langsetmo, D. Goltzman, and D. A. Hanley, “Peak bone mass from longitudinal data: Implications for the prevalence, pathophysiology, and diagnosis of osteoporosis,” *Journal of Bone and Mineral Research*, vol. 25, no. 9, pp. 1948–1957, 2010.

[30] D. Taylor, J. G. Hazenberg, and T. C. Lee, “Living with cracks: Damage and repair in human bone,” *Nature Materials*, vol. 6, pp. 263–268, 2007.

[31] A. Boyde and E. C. Firth, “Musculoskeletal responses of 2-year-old Thoroughbred horses to early training. 8. Quantitative back-scattered electron scanning electron microscopy and confocal fluorescence microscopy of

the epiphysis of the third metacarpal bone," *New Zealand Veterinary Journal*, vol. 53, no. 2, pp. 123–132, 2005.

[32] A. Parfitt, "Targeted and nontargeted bone remodeling: Relationship to basic multicellular unit origination and progression," *Bone*, vol. 30, no. 1, pp. 5–7, 2002.

[33] R. Owen and G. C. Reilly, "In vitro Models of Bone Remodelling and Associated Disorders," *Frontiers in Bioengineering and Biotechnology*, vol. 6, no. October, pp. 1–22, 2018.

[34] N. Rucci, "Molecular Biology of Bone Biology," *Clinical Cases in Mineral and Bone Metabolism*, vol. 5, no. 1, pp. 49–56, 2008.

[35] R. Tamma and A. Zallone, "Osteoblast and Osteoclast Crosstalks: From OAF to Ephrin," *Inflammation & Allergy-Drug Targets*, vol. 11, no. 3, pp. 196–200, 2012.

[36] S. Muruganandan, A. A. Roman, and C. J. Sinal, "Adipocyte differentiation of bone marrow-derived mesenchymal stem cells: Cross talk with the osteoblastogenic program," *Cellular and Molecular Life Sciences*, vol. 66, no. 2, pp. 236–253, 2009.

[37] A. Thiel, M. K. Reumann, A. Boskey, J. Wischmann, R. von Eisenhart-Rothe, and P. Mayer-Kuckuk, "Osteoblast migration in vertebrate bone," *Biological Reviews*, vol. 93, no. 1, pp. 350–363, 2018.

[38] Y. Tang, X. Wu, W. Lei, L. Pang, C. Wan, Z. Shi, L. Zhao, T. R. Nagy, X. Peng, J. Hu, X. Feng, W. Van Hul, M. Wan, and X. Cao, "TGF-$\beta$1-induced migration of bone mesenchymal stem cells couples bone resorption with formation," *Nature Medicine*, vol. 15, no. 7, pp. 757–765, 2009.

[39] U. Kini and B. N. Nandeesh, *Physiology of Bone Formation, Remodeling, and Metabolism*. Berlin, Heidelberg: Springer Berlin Heidelberg, 2012, pp. 29–57.

[40] L. G. Raisz, "Pathogenesis of osteoporosis : concepts , conflicts , and prospects Find the latest version : Science in medicine Pathogenesis of osteoporosis : concepts , conflicts , and prospects," *The Journal of Clinical investigation*, vol. 115, no. 12, pp. 3318–3325, 2005.

[41] E. Hernlund, A. Svedbom, M. Ivergård, J. Compston, C. Cooper, J. Stenmark, E. V. McCloskey, B. Jönsson, and J. A. Kanis, "Osteoporosis in the European Union: Medical management, epidemiology and economic

burden: A report prepared in collaboration with the International Osteoporosis Foundation (IOF) and the European Federation of Pharmaceutical Industry Associations (EFPIA)," *Archives of Osteoporosis*, vol. 8, no. 1-2, 2013.

[42] G. Kaltsas and P. Makras, "Skeletal diseases in Cushing's syndrome: Osteoporosis versus arthropathy," *Neuroendocrinology*, vol. 92, no. SUPPL. 1, pp. 60–64, 2010.

[43] G. Haugeberg, T. Uhlig, J. A. Falch, J. I. Halse, and T. K. Kvien, "Bone mineral density and frequency of osteoporosis in female patients with rheumatoid arthritis: Results from 394 patients in the Oslo County rheumatoid arthritis register," *Arthritis and Rheumatism*, vol. 43, no. 3, pp. 522–530, 2000.

[44] E. Canalis, G. Mazziotti, A. Giustina, and J. P. Bilezikian, "Glucocorticoid-induced osteoporosis: Pathophysiology and therapy," *Osteoporosis International*, vol. 18, no. 10, pp. 1319–1328, 2007.

[45] R. O. Ritchie, M. J. Buehler, and P. Hansma, "Plasticity and toughness in bone," *Physics Today*, vol. 62, no. 6, pp. 41–7, 2009.

[46] J. R. Center, T. V. Nguyen, D. Schneider, P. N. Sambrook, and J. A. Eisman, "Morrtality after all major types of osteoporotic fracture in men and women: an observational study," *The Lancet*, vol. 353, no. 9156, pp. 878–82, 1999.

[47] International Osteoporosis Foundation, "Broken Bones , Broken Lives: A roadmap to solve the fragility crisis in the United Kingdom," International Osteoporosis Foundation, Tech. Rep., 2018. [Online]. Available: www.iofbonehealth.org

[48] F. J. A. Penning-van Beest, J. A. Erkens, M. Olson, and R. M. C. Herings, "Determinants of non-compliance with bisphosphonates in women with postmenopausal osteoporosis," *Current Medical Research and Opinion*, vol. 24, no. 5, pp. 1337–1344, 2008.

[49] T. Ikebe, "Pathophysiology of BRONJ: Drug-related osteoclastic disease of the jaw," *Oral Science International*, vol. 10, no. 1, pp. 1–8, 2013.

[50] S. Otto, M. H. Abu-Id, S. Fedele, P. H. Warnke, S. T. Becker, A. Kolk, T. Mücke, G. Mast, R. Köhnke, E. Volkmer, F. Haasters, O. Lieger, T. Iizuka, S. Porter, G. Campisi, G. Colella, O. Ploder, A. Neff, J. Wiltfang, M. Ehrenfeld, T. Kreusch, K. D. Wolff, S. R. Stürzenbaum, M. Schieker,

and C. Pautke, “Osteoporosis and bisphosphonates-related osteonecrosis of the jaw: Not just a sporadic coincidence - A multi-centre study,” *Journal of Cranio-Maxillofacial Surgery*, vol. 39, no. 4, pp. 272–277, 2011.

[51] J. Schilcher and K. Michaelsson, “Bisphosphonate Use and Atypical Fractures of the Femoral Shaft,” *The new england journal of medicine*, vol. 364, pp. 1728–37, 2011.

[52] H. Hamoda, N. Panay, R. Arya, and M. Savvas, “The British Menopause Society & Women’s Health Concern 2016 recommendations on hormone replacement therapy in menopausal women,” *Post Reproductive Health*, vol. 22, no. 4, pp. 165–183, 2016.

[53] D. B. Muchmore, “Raloxifene: A selective estrogen receptor modulator (SERM) with multiple target system effects,” *Oncologist*, vol. 5, no. 5, pp. 388–392, 2000.

[54] R. Rizzoli, J. Y. Reginster, S. Boonen, G. Bréart, A. Diez-Perez, D. Felsenberg, J. M. Kaufman, J. A. Kanis, and C. Cooper, “Adverse reactions and drug-drug interactions in the management of women with postmenopausal osteoporosis,” *Calcified Tissue International*, vol. 89, no. 2, pp. 91–104, 2011.

[55] M. Arlot, P. J. Meunier, G. Boivin, L. Haddock, J. Tamayo, R. Correa-Rotter, S. Jasqui, D. W. Donley, G. P. Dalsky, J. San Martin, and E. F. Eriksen, “Differential effects of teriparatide and alendronate on bone remodeling in postmenopausal women assessed by histomorphometric parameters,” *Journal of Bone and Mineral Research*, vol. 20, no. 7, pp. 1244–1253, 2005.

[56] R. Eastell, T. Nickelsen, F. Marin, C. Barker, P. Hadji, J. Farrerons, M. Audran, S. Boonen, K. Brixen, J. M. Gomes, B. Obermayer-Pietsch, A. Avramidis, G. Sigurdsson, and C. C. Glüer, “Sequential treatment of severe postmenopausal osteoporosis after teriparatide: final results of the randomized, controlled european study of forsteo (EUROFORS),” *Journal of Bone and Mineral Research*, vol. 24, no. 4, pp. 726–736, 2009.

[57] A. Sikon and P. Batur, “Profile of teriparatide in the management of postmenopausal osteoporosis,” *International Journal of Women’s Health*, vol. 2, no. 1, pp. 37–44, 2010.

[58] J. L. Vahle, M. Sato, G. G. Long, J. K. Young, P. C. Francis, J. A. Engelhardt, M. S. Westmore, Y. L. Ma, and J. B. Nold, “Skeletal Changes

in Rats Given Daily Subcutaneous Injections of Recombinant Human Parathyroid Hormone (1-34) for 2 Years and Relevance to Human Safety," *Toxicologic Pathology*, vol. 30, no. 3, pp. 312–321, 2002.

[59] H. M. Frost, "Bone "Mass" and the "Mechanostat": A Proposal," *The Anatomical record*, vol. 9, pp. 1–9, 1987.

[60] ——, "Bone's mechanostat: A 2003 update," *The Anatomical Record*, vol. 275A, no. 2, pp. 1081–1101, 2003.

[61] R. Al Nazer, J. Lanovaz, C. Kawalilak, J. D. Johnston, and S. Kontulainen, "Direct in vivo strain measurements in human bone-A systematic literature review," *Journal of Biomechanics*, vol. 45, no. 1, pp. 27–40, 2012.

[62] J. Klein-Nulend, A. van der Plas, C. M. Semeins, N. Ajubi, J. A. Frangos, P. J. Nijweide, and E. H. Burger, "Sensitivity of osteocytes to biomechanical stress in vitro," *The FASEB journal*, vol. 9, no. 5, pp. 441–445, 1995.

[63] J. You, C. Yellowley, H. J. Donahue, Y. Zhang, Q. Chen, and C. R. Jacobs, "Substrate Deformation Levels Associated With Routine Physical Activity Are Less Stimulatory to Bone Cells Relative to Loading-Induced Oscillatory Fluid Flow," *Journal of Biomechanical Engineering*, vol. 122, no. 4, pp. 387–393, 2000.

[64] A. R. Bonivtch, L. F. Bonewald, and D. P. Nicolella, "Tissue strain amplification at the osteocyte lacuna: A microstructural finite element analysis," *J Biomech*, vol. 40, no. 10, pp. 2199–2206, 2007.

[65] W. Yao, Y. Li, and G. Ding, "Interstitial fluid flow: The mechanical environment of cells and foundation of meridians," *Evidence-based Complementary and Alternative Medicine*, vol. 2012, 2012.

[66] R. M. Dillaman, R. D. Roer, and D. M. Gay, "Fluid movement in bone: Theoretical and empirical," *Journal of Biomechanics*, vol. 24, no. 1, pp. 163–177, 1991.

[67] J. Tavassoli, M. Yoffey, "Bone marrow: structure and function." *Scandinavian Journal of Haematology*, vol. 32, no. 3, p. 335, 1984.

[68] S. Kumar, P. R. Davis, and B. Pickles, "Bone-marrow pressure and bone strength," *Acta Orthopaedica*, vol. 50, no. 5, pp. 507–512, 1979.

[69] H. Winet, "A bone fluid flow hypothesis for muscle pump-driven capillary filtration: ii proposed role for exercise in erodible scaffold implant incorporation," *European cells amd Material*, vol. 6, pp. 1–11, 2016.

[70] M. Otter, V. Palmieri, and G. Cochran, "Transcortical streaming potentials are generated by circulatory pressure gradients in living canine tibia," *Journal of Orthopaedic Research*, vol. 8, no. 1, pp. 119–126, 1990.

[71] C. T. Rubin and L. E. Lanyon, "Regulation of Bone Mass by Mechanical Strain Magnitude," *Calcif Tissue Int*, vol. 37, pp. 411–7, 1985.

[72] S. Weinbaum, S. C. Cowin, and Y. Zeng, "A model for the excitation of osteocytes by mechanical loading-induced bone fluid shear stresses," *Journal of Biomechanics*, vol. 27, no. 3, pp. 339–360, 1994.

[73] L. F. Bonewald and M. L. Johnson, "Osteocytes mechanosensing and wnt signaling," *Bone*, vol. 42, no. 4, pp. 606–15, 2008.

[74] J. G. McGarry, J. Klein-Nulend, M. G. Mullender, and P. J. Prendergast, "A comparison of strain and fluid shear stress in stimulating bone cell responses—a computational and experimental study," *The FASEB Journal*, vol. 19, no. 3, pp. 482–484, 2005.

[75] A. Leblanc, V. S. Schneider, and J. M. Evans, H. J. Engelbretson, D. A. Krebs, "Bone mineral loss and recovery after 17 weeks of bed rest," *J Bone Miner Res*, vol. 5, pp. 843–850, 1990.

[76] M. Weinreb, G. A. Rodan, and D. D. Thompson, "Osteopenia in the immobilized rat hind limb is associated with increased bone resorption and decreased bone formation," *Bone*, vol. 10, no. 3, pp. 187–194, 1989.

[77] J. A. Calbet, J. S. Moysi, C. Dorado, and L. P. Rodriguez, "Bone mineral content and density in professional tennis players," *Calcified Tissue International*, vol. 62, no. 6, pp. 491–496, 1998.

[78] I. Westbroek, N. E. Ajubi, M. J. Alblas, C. M. Semeins, J. Klein-Nulend, E. H. Burger, and P. J. Nijweide, "Differential Stimulation of Prostaglandin G/H Synthase-2 in Osteocytes and Other Osteogenic Cells by Pulsating Fluid Flow," *Biochemical and Biophysical Research Communications*, vol. 268, no. 2, pp. 414–9, 2000.

[79] D. E. Ingber, "Cellular mechanotransduction: putting all the pieces together again," *The FASEB Journal*, vol. 20, no. 7, pp. 811–827, 2006.

[80] I. Kalajzic, B. G. Matthews, E. Torreggiani, M. A. Harris, P. Divieti Pajevic, and S. E. Harris, "In vitro and in vivo approaches to study osteocyte biology." *Bone*, vol. 54, no. 2, pp. 296–306, 2013.

[81] M. L. Knothe Tate, P. Niederer, and U. Knothe, "In Vivo Tracer Transport Through the Lacunocanalicular System of Rat Bone in an Environment Devoid of Mechanical Loading," *Bone*, vol. 22, no. 2, pp. 107–117, 1998.

[82] R. M. Delaine-smith, "Mechanical and physical guidance of osteogenic differentiation and matrix production Thesis submitted to the University of Sheffield for the degree of Doctor of Philosophy Engineering," Ph.D. dissertation, The University of Sheffield, 2013.

[83] X. Zhou, D. Liu, L. You, and L. Wang, "Quantifying fluid shear stress in a rocking culture dish," *Journal of Biomechanics*, vol. 43, no. 8, pp. 1598–1602, 2010.

[84] A. D. Bakker, K. Soejima, J. Klein-Nulend, and E. H. Burger, "The production of nitric oxide and prostaglandin E 2 by primary bone cells is shear stress dependent," *Journal of Biomechanics*, vol. 34, pp. 671–677, 2001.

[85] F. J. Alenghat and D. E. Ingber, "Mechanotransduction: All Signals Point to Cytoskeleton, Matrix, and Integrins," *Science Signaling*, vol. 2002, no. 119, pp. pe6–pe6, 2002.

[86] F. M. Pavalko, N. X. Chen, C. H. Turner, D. B. Burr, S. Atkinson, Y. F. Hsieh, J. Qiu, and R. L. Duncan, "Fluid shear-induced mechanical signaling in MC3T3-E1 osteoblasts requires cytoskeleton-integrin interactions." *The American journal of physiology*, vol. 275, no. 6, pp. 1591–601, 1998.

[87] H. Xu, J. Zhang, J. Wu, Y. Guan, Y. Weng, and P. Shang, "Oscillatory fluid flow elicits changes in morphology, cytoskeleton and integrin-associated molecules in MLO-Y4 cells, but not in MC3T3-E1 cells," *Biological Research*, vol. 45, no. 2, pp. 163–169, 2012.

[88] A. Liedert, D. Kaspar, R. Blakytny, L. Claes, and A. Ignatius, "Signal transduction pathways involved in mechanotransduction in bone cells," *Biochemical and Biophysical Research Communications*, vol. 349, no. 1, pp. 1–5, 2006.

[89] C. E. Larkins, G. D. G. Aviles, M. P. East, R. A. Kahn, and T. Caspary, "Arl13b regulates ciliogenesis and the dynamic localization of Shh signal-

ing proteins," *Molecular Biology of the Cell*, vol. 22, no. 23, pp. 4694–4703, 2011.

[90] R. J. Quinlan, J. L. Tobin, and P. L. Beales, "Modeling Ciliopathies: Primary Cilia in Development and Disease," *Current Topics in Developmental Biology*, vol. 84, pp. 249–310, 2008.

[91] B. Martinac, "Mechanosensitive ion channels: molecules of mechanotransduction," *Journal of Cell Science*, vol. 117, no. 12, pp. 2449–2460, 2004.

[92] S. Hughes, J. Magnay, M. Foreman, S. J. Publicover, J. P. Dobson, and A. J. El Haj, "Expression of the mechanosensitive 2PK+ channel TREK-1 in human osteoblasts," *Journal of Cellular Physiology*, vol. 206, no. 3, pp. 738–748, 2006.

[93] S. Temiyasathit and J. R. Christopher, "The osteocyte primary cilium and its role in bone mechanotransduction," *National Institute of Health*, vol. 1192, no. 212, pp. 422–428, 2014.

[94] K. L. Lee, M. D. Guevarra, A. M. Nguyen, M. C. Chua, Y. Wang, and C. R. Jacobs, "The primary cilium functions as a mechanical and calcium signaling nexus," *Cilia*, vol. 4, no. 1, p. 7, jul 2015.

[95] B. K. Yoder, "Role of Primary Cilia in the Pathogenesis of Polycystic Kidney Disease," *Journal of the American Society of Nephrology*, vol. 18, no. 5, pp. 1381–1388, 2007.

[96] J. B. Freund, J. G. Goetz, K. L. Hill, and J. Vermot, "Fluid flows and forces in development: functions, features and biophysical principles." *Development*, vol. 139, no. 7, pp. 1229–45, 2012.

[97] D. N. Wheatley, A. M. Wang, and G. E. Strugnell, "Expression of primary cilia in mammalian cells." *Cell biology international*, vol. 20, no. 1, pp. 73–81, 1996.

[98] A. Heydemann and E. M. McNally, "Consequences of Disrupting the Dystrophin-Sarcoglycan Complex in Cardiac and Skeletal Myopathy," *Trends in Cardiovascular Medicine*, vol. 17, no. 2, pp. 55–59, 2007.

[99] A. Franco and J. B. Lansman, "Calcium entry through stretch-inactivated ion channels in mdx myotubes," *Nature*, vol. 344, no. 6267, pp. 670–673, 1990.

[100] M. Driscol and M. Chalfie, "The met-4 gene is a member of a family of Caenorhabditis elegans genes that can mutate to induce neuronal degeneration," *Nature*, vol. 349, pp. 588–593, 1991.

[101] M. R. Franz, R. Cima, D. Wang, D. Profitt, and R. Kurz, "Electrophysiological effects of myocardial stretch and mechanical determinants of stretch-activated arrhythmias." *Circulation*, vol. 86, no. 3, pp. 968–78, 1992.

[102] R. Köhler, A. Distler, and J. Hoyer, "Increased mechanosensitive currents in aortic endothelial cells from genetically hypertensive rats," *Journal of Hypertension*, vol. 17, no. 3, pp. 365–371, 1999.

[103] C. Tekkatte, G. P. Gunasingh, K. M. Cherian, and K. Sankaranarayanan, ""Humanized" Stem Cell Culture Techniques: The Animal Serum Controversy," *Stem Cells International*, vol. 2011, pp. 1–14, 2011.

[104] K. Gardner, S. P. Arnoczky, and M. Lavagnino, "Effect of in vitro stress-deprivation and cyclic loading on the length of tendon cell cilia in situ," *Journal of Orthopaedic Research*, vol. 29, no. 4, pp. 582–587, apr 2011.

[105] A. Pitaval, Q. Tseng, M. Bornens, and M. Théry, "Cell shape and contractility regulate ciliogenesis in cell cycle–arrested cells," *The Journal of Cell Biology*, vol. 191, no. 2, pp. 303–312, 2010.

[106] G. Albercht-Buehler and A. Bushnell, "The ultrastructure of primary cilia in quiescent 3t3 cells," *Experimental Cell Research*, vol. 126, pp. 427–437, 1980.

[107] P. Satir, L. B. Pedersen, and S. T. Christensen, "The primary cilium at a glance," *Journal of Cell Science*, vol. 123, no. 4, pp. 499–503, 2010.

[108] S. C. Goetz and K. V. Anderson, "The primary cilium: A signalling centre during vertebrate development," *Nature Reviews Genetics*, vol. 11, no. 5, pp. 331–344, 2010.

[109] J. L. Tobin and P. L. Beales, "Bardet-Biedl syndrome: Beyond the cilium," *Pediatric Nephrology*, vol. 22, no. 7, pp. 926–936, 2007.

[110] B. K. Yoder, X. Hou, and L. M. Guay-Woodford, "The polycystic kidney disease proteins, polycystin-1, polycystin-2, polaris, and cystin, are co-localized in renal cilia," *Journal of the American Society of Nephrology*, vol. 13, no. 10, pp. 2508–2516, 2002.

[111] P. Satir and S. T. Christensen, "Overview of structure and function of mammalian cilia." *Annual review of physiology*, vol. 69, pp. 377–400, 2007.

[112] C. Jensen, C. Poole, S. McGlashan, M. Marko, Z. Issa, K. Vujcich, and S. Bowser, "Ultrastructural, tomographic and confocal imaging of the chondrocyte primary cilium in situ," *Cell Biology International*, vol. 28, no. 2, pp. 101–110, 2004.

[113] N. A. Zaghloul and N. Katsanis, "Mechanistic insights into Bardet-Biedl syndrome, a model ciliopathy," *Journal of Clinical Investigation*, vol. 119, no. 3, pp. 428–437, 2009.

[114] S. M. Nauli, F. J. Alenghat, Y. Luo, E. Williams, P. Vassilev, X. Li, A. E. Elia, W. Lu, E. M. Brown, S. J. Quinn, D. E. Ingber, and J. Zhou, "Polycystins 1 and 2 mediate mechanosensation in the primary cilium of kidney cells," *Nature Genetics*, vol. 33, no. 2, pp. 129–137, 2003.

[115] J. A. Deane, D. G. Cole, E. S. Seeley, D. R. Diener, and J. L. Rosenbaum, "Localization of intraflagellar transport protein IFT52 identifies basal body transitional fibers as the docking site for IFT particles," *Current Biology*, vol. 11, pp. 1586–1590, 2001.

[116] X. Pan, G. Ou, G. Civelekoglu-Scholey, O. E. Blacque, N. F. Endres, L. Tao, A. Mogilner, M. R. Leroux, R. D. Vale, and J. M. Scholey, "Mechanism of transport of IFT particles in C. elegans cilia by the concerted action of kinesin-II and OSM-3 motors," *Journal of Cell Biology*, vol. 174, no. 7, pp. 1035–1045, 2006.

[117] G. J. Pazour, C. G. Wilkerson, and G. B. Witman, "A dynein light chain is essential for the retrograde particle movement of intraflagellar transport (IFT)," *Journal of Cell Biology*, vol. 141, no. 4, pp. 979–992, 1998.

[118] C. Wood, K. Huang, D. Diener, and J. Rosenbaum, "The Cilium Secretes Bioactive Ectosomes CR," *Current Biology*, vol. 23, no. 110, pp. 1–14, 2013.

[119] H. R. Dawe, H. Farr, and K. Gull, "Centriole/basal body morphogenesis and migration during ciliogenesis in animal cells," *Journal of Cell Science*, vol. 120, no. 1, pp. 7–15, 2006.

[120] C. L. Rieder, C. G. Jensen, L. C. W. Jensen, H. Voltage, E. Microscope, A. S. Building, O. Drive, and P. Bag, "The resorption of primary cilia

during mitosis in a vertebrate (PtK1) cell line," *Journal of Ultrasructure Research*, vol. 68, no. 2, pp. 173–185, 1979.

[121] C. G. Jensen, E. A. Davison, S. S. Bowser, and C. L. Rieder, "Primary cilia cycle in PtK1 cells: Effects of colcemid and taxol on cilia formation and resorption," *Cell Motility*, vol. 7, no. 3, pp. 187–197, 1987.

[122] S. Sorokin, "Centrioles and the formation of rudimentary cilia by fibroblasts and smooth muscle cells." *The Journal of cell biology*, vol. 15, no. 10, pp. 363–377, 1962.

[123] ——, "Reconstructions of centriole formation and ciliogenesis in mammalian lungs." *Journal of cell science*, vol. 3, no. 2, pp. 207–30, 1968.

[124] K. Szymanska and C. A. Johnson, "The transition zone: An essential functional compartment of cilia," *Cilia*, vol. 1, 2012.

[125] J. M. Scholey, "Intraflagellar transport," *Annual Review of Cell and Developmental Biology*, vol. 19, no. 1, pp. 423–43, 2003.

[126] J. L. Rosenbaum and G. B. Witman, "Intraflagellar transport," *Nature Reviews Molecular Cell Biology*, vol. 3, no. 11, pp. 813–825, 2002.

[127] W. F. Marshall and J. L. Rosenbaum, "Intraflagellar transport balances continuous turnover of outer doublet microtubules: Implications for flagellar length control," *Journal of Cell Biology*, vol. 155, no. 3, pp. 405–414, 2001.

[128] K. E. Roth, C. L. Rieder, and S. S. Bowser, "Flexible-substratum technique for viewing cells from the side: some in vivo properties of primary (9+0) cilia in cultured kidney epithelia." *Journal of cell science*, vol. 89, pp. 457–466, 1988.

[129] E. A. Schwartz, L. Leonard, R. Bizios, A. Eric, L. Leonard, R. Bizios, S. S. Bowser, M. L. Leonard, R. Bizios, S. S. Bowser, L. Leonard, R. Bizios, A. Eric, L. Leonard, R. Bizios, and S. S. Bowser, "Analysis and modeling of the primary cilium bending response to fluid shear," *Modeling in Physiology*, vol. 272, no. 1 Pt 2, pp. 132–138, 1997.

[130] H. A. Praetorius and K. R. Spring, "Bending the MDCK cell primary cilium increases intracellular calcium," *Journal of Membrane Biology*, vol. 184, no. 1, pp. 71–79, 2001.

[131] A. M. D. Malone, C. T. Anderson, P. Tummala, R. Y. Kwon, T. R. Johnston, R. Zhang, D. H. Dowhan, Y. R. Miao, M. Gewirtz, S. C. Barry, R. G. Ram-

say, J. Thomas, F. Depreux, N. Kraeva, R. E. Loy, A. Sanjeewa, S. Boncompagi, A. Kraev, O. Anthony, R. T. Dirksen, C. Franzini-armstrong, C. E. Seidman, J. G. Seidman, D. H. Maclennan, E. Zvaritch, F. Depreux, N. Kraeva, E. Ryan, S. A. Goonasekera, S. Boncompagni, A. Kraev, A. O. Gramolini, T. Robert, C. Franzini-armstrong, C. E. Seidman, J. G. Seidman, D. H. Maclennan, A. M. D. Malone, C. T. Anderson, P. Tummala, R. Y. Kwon, T. R. Johnston, T. Stearns, and C. R. Jacobs, "Primary cilia mediate mechanosensing in bone cells by a calcium-independent mechanism," *Proceedings of the National Academy of Sciences*, vol. 104, no. 33, pp. 13 325—-13 330, 2008.

[132] R. M. Delaine-Smith, A. Sittichokechaiwut, and G. C. Reilly, "Primary cilia respond to fluid shear stress and mediate flow-induced calcium deposition in osteoblasts," *The FASEB Journal*, vol. 28, no. 1, pp. 430–439, 2014.

[133] G. P. Johnson, E. Stavenschi, K. F. Eichholz, M. A. Corrigan, S. Fair, and D. A. Hoey, "Mesenchymal stem cell mechanotransduction is cAMP dependent and regulated by Adenylyl Cyclase 6 and the Primary Cilium," *Journal of Cell Science*, vol. 131, no. 21, pp. 1–11, 2018.

[134] A. Masyuk, T. Masyuk, and N. LaRusso, "Cholangiocyte Primary Cilia in Liver Health and Disease," *Dev Dyn*, vol. 237, no. 8, pp. 2007–12, 2008.

[135] S. Low, S. Vasanth, C. Larson, S. Mukherjee, N. Sharma, M. Kinter, M. Kane, T. Obara, and T. Weimbs, "Polycystin-1, STAT6, and P100 Function in a Pathway that Transduces Ciliary Mechanosensation and Is Activated in Polycystic Kidney Disease," *Developmental Cell*, vol. 10, pp. 57–69, 2006.

[136] M. Köttgen, B. Buchholz, M. A. Garcia-Gonzalez, F. Kotsis, X. Fu, M. Doerken, C. Boehlke, D. Steffl, R. Tauber, T. Wegierski, R. Nitschke, M. Suzuki, A. Kramer-Zucker, G. G. Germino, T. Watnick, J. Prenen, B. Nilius, E. W. Kuehn, and G. Walz, "TRPP2 and TRPV4 form a polymodal sensory channel complex," *Journal of Cell Biology*, vol. 182, no. 3, pp. 437–447, 2008.

[137] M. Delling, A. A. Indzhykulian, X. Liu, Y. Li, T. Xie, D. P. Corey, and D. E. Clapham, "Primary cilia are not calcium-responsive mechanosensors," *Nature*, vol. 531, no. 7596, pp. 656–660, 2016.

[138] M. Spasic and C. R. Jacobs, "Primary cilia: Cell and molecular mechanosensors directing whole tissue function," *Semin Cell Dev Biol*,

vol. 71, pp. 42–52, 2017.

[139] H. Praetorius and K. Spring, "Removal of the MDCK Cell Primary Cilium Abolishes Flow Sensing," *Journal of Membrane Biology*, vol. 191, no. 1, pp. 69–76, 2003.

[140] R. Y. Kwon, S. Temiyasathit, P. Tummala, C. C. Quah, and C. R. Jacobs, "Primary cilium-dependent mechanosensing is mediated by adenylyl cyclase 6 and cyclic AMP in bone cells," *FASEB journal : official publication of the Federation of American Societies for Experimental Biology*, vol. 24, no. 8, pp. 2859–68, 2010.

[141] G. Bishop, N. F. Berbari, J. Lewis, and K. Mykytyn, "Functional Ionotropic Glutamate Receptors on Tangentially Dispersed Cells in the Developing Mouse Retina," *The journal of comparative neurology*, vol. 505, pp. 562–71, 2007.

[142] J. L. Guillou, H. Nakata, and D. M. Cooper, "Inhibition by calcium of mammalian adenylyl cyclases," *Journal of Biological Chemistry*, vol. 274, no. 50, pp. 35 539–35 545, 1999.

[143] E. Moore, H. S. Ryu, Y. X. Zhu, and C. R. Jacobs, "Adenylyl cyclases and TRPV4 mediate Ca2+/ cAMP dynamics to enhance fluid flow-induced osteogenesis in osteocytes," *Journal of Molecular Biochemistry*, vol. 7, pp. 48–59, 2018.

[144] V. Locatelli and V. E. Bianchi, "Effect of GH/IGF-1 on Bone Metabolism and Osteoporsosis," *International Journal of Endocrinology*, vol. 2014, 2014.

[145] D. Zhu, S. Shi, H. Wang, and K. Liao, "Growth arrest induces primary-cilium formation and sensitizes IGF-1-receptor signaling during differentiation induction of 3T3-L1 preadipocytes," *Journal of Cell Science*, vol. 122, no. 15, pp. 2760–2768, 2009.

[146] M. T. Dalbay, S. D. Thorpe, J. T. Connelly, J. P. Chapple, and M. M. Knight, "Adipogenic differentiation of hMSCs is mediated by recruitment of IGF-1r onto the primary cilium associated with cilia elongation," *Stem Cells*, vol. 33, no. 6, pp. 1952–1961, 2015.

[147] H. Wang, X. Zou, Z. Wei, Y. Wu, R. Li, R. Zeng, Z. Chen, and K. Liao, "Hsp90 forms a stable complex at the cilium neck for the interaction of signalling molecules in IGF-1 receptor signalling," *Journal of Cell Science*, vol. 128, no. 1, pp. 100–108, 2015.

[148] C. Yeh, A. Li, J. Chuang, M. Saito, A. Caceres, and C. Sung, "IGF-1 activates a cilium-localized non-canonical G$\beta\gamma$ signaling pathway that regulates cell cycle progression," *Developmental Cell*, vol. 26, no. 4, pp. 358–68, 2013.

[149] D. Huangfu, A. Liu, A. S. Rakeman, N. S. Murcia, L. Niswander, and K. V. Anderson, "Hedgehog signalling in the mouse requires intraflagellar transport proteins," *Nature*, vol. 426, no. 6962, pp. 83–87, 2003. [Online]. Available: https://doi.org/10.1038/nature02061

[150] J. Cayuso, F. Ulloa, B. Cox, J. Briscoe, and E. Marti, "The Sonic hedgehog pathway independently controls the patterning, proliferation and survival of neuroepithelial cells by regulating Gli activity," *Development*, vol. 133, no. 3, pp. 517–528, 2006.

[151] F. Bangs and K. V. Anderson, "Primary cilia and Mammalian Hedgehog signaling," *Cold Spring Harbor Perspectives in Biology*, vol. 9, no. 5, pp. 1–21, 2017.

[152] J. K. Chen, J. Taipale, M. K. Cooper, and P. A. Beachy, "Inhibition of Hedgehog signaling by direct binding of cyclopamine to Smoothened," *Genes & Dev*, vol. 16, pp. 2743–2748, 2002.

[153] P. Kogerman, T. Grimm, L. Kogerman, D. Krause, A. B. Undén, R. Toftgård, and P. G. Zaphiropoulos, "Mammalian Suppressor-of-Fused modulates nuclear – cytoplasmic shuttling of GLI-1," *Nature Cell Biology*, vol. 1, pp. 312–9, 1999.

[154] E. H. Villavicencio, D. O. Walterhouse, and P. M. Iannaccone, "The Sonic hedgehog-Patched-Gli pathway in human development and disease," *American Journal of Human Genetics*, vol. 67, no. 5, pp. 1047–1054, 2000.

[155] D. Huangfu and K. Anderson, "Signaling from Smo to Ci/Gli: conservation and divergence of Hedgehog pathways from Drosophila to vertebrates," *Development*, vol. 133, no. 1, pp. 3–14, 2006.

[156] H. Tukachinsky, L. V. Lopez, and A. Salic, "A mechanism for vertebrate Hedgehog signaling: Recruitment to cilia and dissociation of SuFu-Gli protein complexes," *Journal of Cell Biology*, vol. 191, no. 2, pp. 415–428, 2010.

[157] X. Yuan, J. Cao, X. He, R. Serra, J. Qu, X. Cao, and S. Yang, "Ciliary IFT80 balances canonical versus non-canonical hedgehog signalling for

osteoblast differentiation," *Nature Communications*, vol. 7, pp. 1–13, 2016. [Online]. Available: http://dx.doi.org/10.1038/ncomms11024

[158] D. Huangfu and K. V. Anderson, "Cilia and Hedgehog responsiveness in the mouse," *Proceedings of the National Academy of Sciences*, vol. 102, no. 32, pp. 11 325–11 330, 2005.

[159] C. J. Haycraft, B. Banizs, Y. Aydin-Son, Q. Zhang, E. J. Michaud, and B. K. Yoder, "Gli2 and Gli3 Localize to Cilia and Require the Intraflagellar Transport Protein Polaris for Processing and Function," *PLoS Genetics*, vol. preprint, no. 2005, p. e53, 2005.

[160] R. R. Damerla, C. Cui, G. C. Gabriel, X. Liu, B. Craige, B. C. Gibbs, R. Francis, Y. Li, B. Chatterjee, J. T. San Agustin, T. Eguether, R. Subramanian, G. B. Witman, J. L. Michaud, G. J. Pazour, and C. W. Lo, "Novel Jbts17 mutant mouse model of joubert syndrome with cilia transition zone defects and cerebellar and other ciliopathy related anomalies," *Human Molecular Genetics*, vol. 24, no. 14, pp. 3994–4005, 2015.

[161] C. Hui and A. L. Joyner, "A mouse model of Greig cephalo- polysyndactyly syndrome : the extra-toes-I mutation contains an intragenic deletion of the Gli3 gene," *Nature Genetics*, vol. 3, pp. 241–246, 1993.

[162] D. Warburton, M. Schwarz, D. Tefft, G. Flores-delgado, K. D. Anderson, and W. V. Cardoso, "The molecular basis of lung morphogenesis," *Mechanisms of Development*, vol. 92, pp. 55–81, 2000.

[163] L. A. Schimmenti, J. D. Cruz, R. A. Lewis, J. D. Karkera, G. S. Manligas, E. Roessler, and M. Muenke, "Novel Mutation in Sonic Hedgehog in Non-Syndromic Colobomatous Microphthalmia," *American Journal of Medical Genetics*, vol. 116A, pp. 215–221, 2003.

[164] J. Kim, S. Dabiri, and E. S. Seeley, "Primary Cilium Depletion Typifies Cutaneous Melanoma In Situ and Malignant Melanoma," *PLoS ONE*, vol. 6, no. 11, pp. 1–7, 2011.

[165] S. Y. Wong, A. D. Seol, P.-l. So, A. N. Ermilov, C. K. Bichakjian, E. H. E. Jr, A. A. Dlugosz, and J. F. Reiter, "Primary cilia can both mediate and suppress Hedgehog pathway – dependent tumorigenesis," *Nature Medicine*, vol. 15, no. 9, pp. 1055–62, 2009.

[166] Y.-g. Han, H. J. Kim, A. A. Dlugosz, D. W. Ellison, R. J. Gilbertson, and A. Alvarez-buylla, "Dual and opposing roles of primary cilia in medul-

loblastoma development," *Nature Medicine*, vol. 15, no. 9, pp. 1062–6, 2009.

[167] P. J. R. Ocbina, M. Tuson, and K. V. Anderson, "Primary Cilia Are Not Required for Normal Canonical Wnt Signaling in the Mouse Embryo," *PLoS ONE*, vol. 4, no. 8, pp. 1–8, 2009.

[168] G. Schulte and V. Bryja, "The Frizzled family of unconventional G-protein-coupled receptors," *Trends in Pharmacological Sciences*, vol. 28, no. 10, pp. 518–25, 2007.

[169] J. R. K. Seifert and M. Mlodzik, "Frizzled / PCP signalling : a conserved mechanism regulating cell polarity and directed motility," *Nature Reviews Genetics*, vol. 8, pp. 126–138, 2007.

[170] B. T. Macdonald and X. He, "Frizzled and LRP5 / 6 Receptors for Wnt / b -Catenin Signaling," *Cold Spring Harbor Perspectives in Biology*, vol. 4, pp. 1–23, 2012.

[171] D. V. F. Tauriello, I. Jordens, K. Kirchner, J. W. Slootstra, and T. Kruitwagen, "Wnt / $\beta$ -catenin signaling requires interaction of the Dishevelled DEP domain and C terminus with a discontinuous motif in Frizzled," *Proceedings of the National Academy of Sciences*, vol. 109, no. 14, pp. E812–E820, 2012.

[172] G. Wu, H. Huang, J. G. Abreu, and X. He, "Inhibition of GSK3 Phosphorylation of b -Catenin via Phosphorylated PPPSPXS Motifs of Wnt Coreceptor LRP6," *PLoS ONE*, vol. 4, no. 3, pp. 1–11, 2009.

[173] S. Amit, A. Hatzubai, Y. Birman, J. S. Andersen, E. Ben-shushan, M. Mann, Y. Ben-neriah, and I. Alkalay, "Axin-mediated CKI phosphorylation of beta-catenin at Ser 45 : a molecular switch for the Wnt pathway," *Genes and Development*, vol. 16, pp. 1066–1076, 2002.

[174] J. Mao, J. Wang, B. Liu, W. Pan, G. H. Farr, C. Flynn, H. Yuan, S. Takada, D. Kimelman, L. Li, D. Wu, and N. York, "Low-Density Lipoprotein Receptor-Related Protein-5 Binds to Axin and Regulates the Canonical Wnt Signaling Pathway," *Molecular Cell*, vol. 7, pp. 801–809, 2001.

[175] J. L. Stamos and W. I. Weis, "The beta-Catenin Destruction Complex," *Cold Spring Harbor Perspectives in Biology*, vol. 5, pp. 1–16, 2013.

[176] T. Valenta, G. Hausmann, and K. Basler, "The many faces and functions of beta-catenin," *The EMBO Journal*, vol. 31, pp. 2714–36, 2012.

[177] M. Kieslinger, S. Folberth, G. Dobreva, T. Dorn, L. Croci, R. Erben, G. G. Consalez, and R. Grosschedl, "EBF2 Regulates Osteoblast-Dependent Differentiation of Osteoclasts," *Developmental Cell*, vol. 9, pp. 757–767, 2005.

[178] R. Zhang, B. O. Oyajobi, S. E. Harris, D. Chen, C. Tsao, H.-w. Deng, and M. Zhao, "Wnt / $\beta$ -catenin signaling activates bone morphogenetic protein 2 expression in osteoblasts," *Bone*, vol. 52, no. 1, pp. 145–156, 2013.

[179] Y. Araki, S. Okamura, S. P. Hussain, M. Nagashima, P. He, M. Shiseki, K. Miura, and C. C. Harris, "Regulation of Cyclooxygenase-2 Expression by the Wnt and Ras Pathways 1," *Cancer Research*, vol. 63, pp. 728–734, 2003.

[180] V. Krishnan, H. U. Bryant, A. Ormond, J. C. Invest, V. Krishnan, H. U. Bryant, and O. A. Macdougald, "Regulation of bone mass by Wnt signaling," *Journal of Clinical Investigation*, vol. 116, no. 5, pp. 1202–1209, 2006.

[181] G. J. Spencer, J. C. Utting, S. L. Etheridge, T. R. Arnett, and P. G. Genever, "Wnt signalling in osteoblasts regulates expression of the receptor activator of NFkB ligand and inhibits osteoclastogenesis in vitro," *Journal of Cell Science*, vol. 119, pp. 1283–96, 2006.

[182] R. Habas, Y. Kato, and X. He, "Wnt / Frizzled Activation of Rho Regulates Vertebrate Gastrulation and Requires a Novel Formin Homology Protein Daam1," *Cell*, vol. 107, pp. 843–854, 2001.

[183] M. Amano, M. Nakayama, and K. Kaibuchi, "Rho-Kinase/ROCK: A Key Regulator of the Cytoskeleton and Cell Polarity," *Cytoskeleton*, vol. 67, pp. 545–554, 2010.

[184] L. Li, H. Yuan, W. Xie, J. Mao, A. M. Caruso, A. Mcmahon, D. J. Sussman, and D. Wu, "Dishevelled Proteins Lead to Two Signaling Pathways," *The Journal of Biological Chemistry*, vol. 274, no. 1, pp. 129–134, 1999.

[185] M. Misheva and M. A. Bogoyevitch, "JNK Signaling : Regulation and Functions Based on Complex Protein- Protein Partnerships," *Microbiol Mol Biol Rev*, vol. 80, pp. 793–835, 2016.

[186] C. Jones, V. C. Roper, I. Foucher, D. Qian, B. Banizs, C. Petit, B. K. Yoder, and P. Chen, "Ciliary proteins link basal body polarization to planar cell polarity regulation," *Nature Genetics*, vol. 40, no. 1, pp. 69–77, 2008.

[187] M. Simons, J. Gloy, A. Ganner, A. Bullerkotte, M. Bashkurov, C. Kro, B. Schermer, T. Benzing, O. A. Cabello, A. Jenny, M. Mlodzik, B. Polok, W. Driever, T. Obara, and G. Walz, "Inversin , the gene product mutated in nephronophthisis type II , functions as a molecular switch between Wnt signaling pathways," *Nature Genetics*, vol. 37, no. 5, pp. 537–543, 2005.

[188] M. Lancaster, J. Schroth, and J. Gleeson, "Subcellular Spatial Regulation of Canonical Wnt Signaling at the Primary Cilium," *Nature Cell Biology*, vol. 13, no. 6, pp. 700–707, 2011.

[189] A. Dummer, C. Poelma, M. C. Deruiter, M. T. H. Goumans, and B. P. Hierck, "Measuring the primary cilium length: improved method for unbiased high-throughput analysis," *Cilia*, vol. 5, no. 7, 2016.

[190] J. Kim, J. E. Lee, S. Heynen-Genel, E. Suyama, K. Ono, K. Lee, T. Ideker, P. Aza-Blanc, and J. G. Gleeson, "Functional genomic screen for modulators of ciliogenesis and cilium length," *Nature*, vol. 464, no. 7291, pp. 1048–1051, 2010.

[191] N. Sharma, Z. A. Kosan, J. E. Stallworth, N. F. Berbari, and B. K. Yoder, "Soluble levels of cytosolic tubulin regulate ciliary length control," *Molecular Biology of the Cell*, vol. 22, no. 6, pp. 806–816, 2011.

[192] R. E. Stephens, "Synthesis and turnover of embryonic sea urchin ciliary proteins during selective inhibition of tubulin synthesis and assembly," *Molecular biology of the cell*, vol. 8, no. 11, pp. 2187–98, 1997.

[193] B. D. Engel, W. B. Ludington, and W. F. Marshall, "Intraflagellar transport particle size scales inversely with flagellar length: revisiting the balance-point length control model," *The Journal of cell biology*, vol. 187, no. 1, pp. 81–9, 2009.

[194] J. Pan and W. J. Snell, "Chlamydomonas shortens its flagella by activating axonemal disassembly, stimulating IFT particle trafficking, and blocking anterograde cargo loading," *Developmental Cell*, vol. 9, no. 3, pp. 431–438, 2005.

[195] T. Y. Besschetnova, E. Kolpakova-Hart, Y. Guan, J. Zhou, B. R. Olsen, and J. V. Shah, "Identification of Signaling Pathways Regulating Primary Cilium Length and Flow-Mediated Adaptation," *Current Biology*, vol. 20, no. 2, pp. 182–187, 2010.

[196] Z. Xiao and L. Quarles, "Role of the polycytin-primary cilia complex in bone development and mechanosensing," *Annals of the New York Academy of Sciences*, vol. 1192, no. 1, pp. 410–421, 2010.

[197] G. Dalagiorgou, C. Piperi, U. Georgopoulou, C. Adamopoulos, E. K. Basdra, and A. G. Papavassiliou, "Mechanical stimulation of polycystin-1 induces human osteoblastic gene expression via potentiation of the calcineurin/NFAT signaling axis." *Cellular and molecular life sciences : CMLS*, vol. 70, no. 1, pp. 167–180, 2013.

[198] H. Wang, W. Sun, J. Ma, Y. Pan, L. Wang, and W. Zhang, "Polycystin-1 Mediates Mechanical Strain-Induced Osteoblastic Mechanoresponses via Potentiation of Intracellular Calcium and Akt/b-Catenin Pathway," *PLoS ONE*, vol. 9, no. 3, 2014.

[199] A. Resnick and U. Hopfer, "Force-response considerations in ciliary mechanosensation." *Biophysical journal*, vol. 93, no. 4, pp. 1380–90, 2007.

[200] A. Chakrabarti, H. Schatten, K. D. Mitchell, M. Crosser, and M. Taylor, "Chloral hydrate alters the organization of the ciliary basal apparatus and cell organelles in sea urchin embryos." *Cell and tissue research*, vol. 293, no. 3, pp. 453–62, 1998.

[201] M. E. Deren, X. Yang, Y. Guan, and Q. Chen, "Biological and Chemical Removal of Primary Cilia Affects Mechanical Activation of Chondrogenesis Markers in Chondroprogenitors and Hypertrophic Chondrocytes." *International journal of molecular sciences*, vol. 17, no. 2, p. 188, 2016.

[202] S.-I. Yoshimura, J. Egerer, E. Fuchs, A. K. Haas, and F. A. Barr, "Functional dissection of Rab GTPases involved in primary cilium formation." *The Journal of cell biology*, vol. 178, no. 3, pp. 363–9, 2007.

[203] H. Husson, S. Moreno, L. A. Smith, M. M. Smith, R. J. Russo, R. Pitstick, M. Sergeev, S. R. Ledbetter, N. O. Bukanov, M. Lane, K. Zhang, K. Billot, G. Carlson, J. Shah, L. Meijer, D. R. Beier, and O. Ibraghimov-Beskrovnaya, "Reduction of ciliary length through pharmacologic or genetic inhibition of CDK5 attenuates polycystic kidney disease in a model of nephronophthisis." *Human molecular genetics*, vol. 25, no. 11, pp. 2245–2255, 2016.

[204] Y. Fukata, T. J. Itoh, T. Kimura, C. C. Ménager, T. Nishimura, T. Shiromizu, H. Watanabe, N. Inagaki, A. Iwamatsu, H. Hotani, and

K. Kaibuchi, “CRMP-2 binds to tubulin heterodimers to promote microtubule assembly,” *Nature Cell Biology*, vol. 4, no. 8, pp. 583–591, 2002.

[205] M. Spasic and C. R. Jacobs, “Lengthening primary cilia enhances cellular mechanosensitivity,” *European Cells and Materials*, vol. 33, pp. 158–168, 2017.

[206] S. H. Kathem, A. M. Mohieldin, S. Abdul-Majeed, S. H. Ismail, Q. H. Altaei, I. K. Alshimmari, M. M. Alsaidi, H. Khammas, A. M. Nauli, B. Joe, and S. M. Nauli, “Ciliotherapy: a novel intervention in polycystic kidney disease.” *Journal of geriatric cardiology : JGC*, vol. 11, no. 1, pp. 63–73, 2014.

[207] V. S. Upadhyay, B. S. Muntean, S. H. Kathem, J. J. Hwang, W. A. Aboualaiwi, and S. M. Nauli, “Roles of dopamine receptor on chemosensory and mechanosensory primary cilia in renal epithelial cells.” *Frontiers in physiology*, vol. 5, p. 72, 2014.

[208] T. Nakakura, A. Asano-Hoshino, T. Suzuki, K. Arisawa, H. Tanaka, Y. Sekino, Y. Kiuchi, K. Kawai, and H. Hagiwara, “The elongation of primary cilia via the acetylation of alpha-tubulin by the treatment with lithium chloride in human fibroblast KD cells,” *Medical Molecular Morphology*, vol. 48, no. 1, pp. 44–53, 2015.

[209] Y. Ou, Y. Ruan, M. Cheng, J. J. Moser, J. B. Rattner, and F. A. van der Hoorn, “Adenylate cyclase regulates elongation of mammalian primary cilia,” *Experimental Cell Research*, vol. 315, no. 16, pp. 2802–2817, 2009.

[210] C. L. Thompson, A. Wiles, C. A. Poole, and M. M. Knight, “Lithium chloride modulates chondrocyte primary cilia and inhibits Hedgehog signaling,” *FASEB Journal*, vol. 30, no. 2, pp. 716–726, 2016.

[211] K. Miyoshi, K. Kasahara, I. Miyazaki, and M. Asanuma, “Lithium treatment elongates primary cilia in the mouse brain and in cultured cells,” *Biochemical and Biophysical Research Communications*, vol. 388, no. 4, pp. 757–762, 2009.

[212] Y. Ou, Y. Zhang, M. Cheng, J. B. Rattner, I. Dobrinski, and F. A. van der Hoorn, “Targeting of CRMP-2 to the Primary Cilium Is Modulated by GSK-3$\beta$,” *PLoS ONE*, vol. 7, no. 11, p. e48773, 2012.

[213] P. E. Stokes, J. H. Kocsis, and O. J. Arcuni, “Relationship of Lithium Chloride Dose to Treatment Response in Acute Mania,” *Archives of general psychiatry*, vol. 33, no. 9, pp. 1080–4, 1976.

[214] A. Jaeger, "Lithium," *Medicine*, vol. 31, no. 10, p. 58, 2003.

[215] D. S. Reddy and M. S. Reddy, "Serum lithium levels: Ideal time for sample collection! Are we doing it right?" *Indian Journal of Psychological Medicine*, vol. 36, no. 3, p. 346, 2014.

[216] J. Birch, "Lithium and magnesium-dependent enzymes," *Lancet*, vol. 2, pp. 965–966, 1974.

[217] S. Avissar, D. L. Murphy, and G. Schreiber, "Magnesium Reversal of Lithium Inhibition of P-Adrenergic and Muscarinic Receptor Coupling to G Proteins," *Biochemical Pharmacology*, vol. 41, no. 2, pp. 171–175, 1991.

[218] S. J. Pollack, J. R. Atack, M. R. Knowles, G. Mcallister, C. I. A. N. Ragan, R. Bakert, S. R. Fletchert, L. L. Iversen, and H. B. Broughtont, "Mechanism of inositol monophosphatase, the putative target of lithium therapy," *Proc Natl Acad Sci*, vol. 91, pp. 5766–5770, 1994.

[219] L. Mann, E. Heldman, Y. Bersudsky, S. F. Vatner, Y. Ishikawa, O. Almog, R. H. Belmaker, and G. Agam, "Inhibition of specific adenylyl cyclase isoforms by lithium and carbamazepine, but not valproate, may be related to their antidepressant effect," *Bipolar Disorders*, vol. 11, no. 8, pp. 885–896, 2009.

[220] B. D. Spiegelberg, J. Cruz, T.-h. Law, and J. D. York, "Alteration of Lithium Pharmacology through Manipulation of Phosphoadenosine Phosphate Metabolism," *The Journal of Biological Chemistry*, vol. 280, no. 7, pp. 5400–5405, 2005.

[221] L. Freland and J.-M. Beaulieu, "Inhibition of GSK3 by lithium, from single molecules to signaling networks." *Frontiers in molecular neuroscience*, vol. 5, p. 14, 2012.

[222] E. Jakobsson, O. Arguello-Miranda, S.-W. Chiu, Z. Fazal, J. Kruczek, S. Nunez-Corrales, S. Pandit, and L. Pritchet, "Towards a Unified Understanding of Lithium Action in Basic Biology and its Significance for Applied Biology," *Journal of Membrane Biology*, vol. 250, pp. 587–604, 2017.

[223] R. S. Jope, "Lithium and GSK-3: one inhibito , two inhibitory actions, multiple outcomes," *Trends in Pharmacological Sciences*, vol. 24, no. 9, pp. 441–443, 2003.

[224] C. Mendes, F. Mury, E. de Sá Moreira, F. Alberto, O. Forlenza, E. Dias-Neto, and W. Gattaz, "Lithium reduces Gsk3b mRNA levels: implications for Alzheimer Disease," *Eur Arch Psychiatry Clin Neurosci*, vol. 259, pp. 16–22, 2009.

[225] P. S. Klein and D. A. Meltont, "A molecular mechanism for the effect of lithium on development," *Developmental Biology*, vol. 93, pp. 8455–8459, 1996.

[226] K. M. Brown and D. K. Tracy, "Lithium: The pharmacodynamic actions of the amazing ion," *Therapeutic Advances in Psychopharmacology*, vol. 3, no. 3, pp. 163–176, 2013.

[227] G. L. Galea, L. B. Meakin, C. M. Williams, S. L. Hulin-curtis, L. E. Lanyon, A. W. Poole, and J. S. Price, "Protein Kinase C alpha ( KC alpha) Regulates Bone Architecture and Osteoblast Activity," *The Journal of biological chemistry*, vol. 289, no. 37, pp. 25 509–25 522, 2014.

[228] P. B. Daniel, W. H. Walker, and J. F. Habener, "Cyclic Amp Signalling and Gene Regulation," *Annu Rev Nutr*, vol. 18, pp. 353–83, 1998.

[229] M. P. Delghandi, M. Johannessen, and U. Moens, "The cAMP signalling pathway activates CREB through PKA , p38 and MSK1 in NIH 3T3 cells," *Cellular Signalling*, vol. 17, pp. 1343–1351, 2005.

[230] R. Zhang, J. R. Edwards, S.-y. Ko, S. Dong, H. Liu, O. Babatunde, C. Papasian, H.-w. Deng, and M. Zhao, "Transcriptional Regulation of BMP2 Expression by the PTH-CREB Signaling Pathway in Osteoblasts," *PLoS ONE*, vol. 6, no. 6, p. e20780, 2011.

[231] A. Zamani, G. R. Omrani, and M. M. Nasab, "Lithium's effect on bone mineral density," *Bone*, vol. 44, no. 2, pp. 331–334, 2009.

[232] M. Arioka, F. Takahashi-Yanaga, M. Sasaki, T. Yoshihara, S. Morimoto, A. Takashima, Y. Mori, and T. Sasaguri, "Acceleration of bone development and regeneration through the Wnt/$\beta$-catenin signaling pathway in mice heterozygously deficient for GSK-3$\beta$," *Biochemical and Biophysical Research Communications*, vol. 440, no. 4, pp. 677–682, 2013.

[233] N. Tatsumoto, M. Arioka, S. Yamada, F. Takahashi-Yanaga, M. Tokumoto, K. Tsuruya, T. Kitazono, and T. Sasaguri, "Inhibition of GSK-3$\beta$ increases trabecular bone volume but not cortical bone volume in adenine-induced uremic mice with severe hyperparathyroidism." *Physiological reports*, vol. 4, no. 21, 2016.

[234] F. Kugimiya, H. Kawaguchi, S. Ohba, N. Kawamura, M. Hirata, H. Chikuda, Y. Azuma, J. R. Woodgett, K. Nakamura, and U.-i. Chung, "GSK-3$\beta$ Controls Osteogenesis through Regulating Runx2 Activity," *PLoS ONE*, vol. 2, no. 9, p. e837, 2007.

[235] D. Genetos, D. Geist, D. Liu, H. Donahue, and R. Duncan, "Fluid Shear-Induced ATP Secretion Mediates Prostaglandin Release in MC3T3-E1 Osteoblasts," *Journal of Bone and Mineral Research*, vol. 20, no. 1, pp. 41–9, 2004.

[236] J. Klein-Nulend, E. H. Burger, C. M. Semeins, L. G. Raisz, and C. C. Pilbeam, "Pulsating Fluid Flow Stimulates Prostaglandin Release and Inducible Prostaglandin G / H Synthase mRNA Expression," *Journal of Bon*, vol. 12, no. 1, pp. 45–51, 1997.

[237] X. L. Lu, B. Huo, M. Park, and X. E. Guo, "Calcium response in osteocytic networks under steady and oscillatory fluid flow," *Bone*, vol. 51, no. 3, pp. 466–473, 2012.

[238] W. Yu, H. Qu, G. Hu, Q. Zhang, K. Song, H. Guan, T. Liu, and J. Qin, "A microfluidic-based multi-shear device for investigating the effects of low fluid-induced stresses on osteoblasts," *PLoS ONE*, vol. 9, no. 2, pp. 1–7, 2014.

[239] R. P. Tucker, P. Henningsson, S. L. Franklin, D. Chen, Y. Ventikos, R. J. Bomphrey, and M. S. Thompson, "See-saw rocking : an in vitro model for mechanotransduction research," *Journal of the Royal Society, Interface*, vol. 11, pp. 1–9, 2014.

[240] R. M. Delaine-Smith, S. MacNeil, and G. C. Reilly, "Matrix Production and Collagen Structure Are Enhanced In Two Types Of Osteogenic Progenitor Cells By A Simple Fluid Shear Stress Stimulus," *European Cells and Materials*, vol. 24, no. 0, pp. 162–174, 2012.

[241] K. T. Lim, J. Hexiu, J. Kim, H. Seonwoo, P. H. Choung, and J. H. Chung, "Synergistic effects of orbital shear stress on in vitro growth and osteogenic differentiation of human alveolar bone-derived mesenchymal stem cells," *BioMed Research International*, vol. 2014, 2014.

[242] A. R. For, T. H. E. Primary, C. In, P. Signaling, B. Mechanically, S. Osteocytes, and M. S. Cells, "A Role for the Primary Cilium in Paracrine Signaling Between Mechanically Stimulated Osteocytes and Mesenchy-

mal Stem Cells," *Biochem Biophys Res Commun*, vol. 412, no. 1, pp. 182–187, 2011.

[243] M. Babincová, D. Leszczynska, P. Sourivong, and P. Babinec, "Selective treatment of neoplastic cells using ferritin-mediated electromagnetic hyperthermia," *Medical hypotheses*, vol. 54, no. 2, pp. 177–9, 2000.

[244] J. L. Kirschvink, A. Kobayashi-Kirschvink, and B. J. Woodford, "Magnetite biomineralization in the human brain," *Proceedings of the National Academy of Sciences*, vol. 89, no. 16, pp. 7683–7687, 1992.

[245] M. Yu, S. Huang, K. J. Yu, and A. M. Clyne, "Dextran and polymer polyethylene glycol (PEG) coating reduce both 5 and 30 nm iron oxide nanoparticle cytotoxicity in 2D and 3D cell culture," *International Journal of Molecular Sciences*, vol. 13, no. 5, pp. 5554–5570, 2012.

[246] S. H. Cartmell, J. Dobson, S. B. Verschueren, and A. J. El Haj, "Development of magnetic particle techniques for long-term culture of bone cells with intermittent mechanical activation," *IEEE Transactions on Nanobioscience*, vol. 1, no. 2, pp. 92–97, 2002.

[247] S. Hughes, J. Dobson, and A. J. El Haj, "Magnetic targeting of mechanosensors in bone cells for tissue engineering applications," *Journal of Biomechanics*, vol. 40, pp. S96–S104, 2007.

[248] S. Hughes, S. Mcbain, J. Dobson, A. J. E. Haj, and A. J. El Haj, "Selective activation of mechanosensitive ion channels using magnetic particles." *Journal of the Royal Society, Interface / the Royal Society*, vol. 5, no. 25, pp. 855–63, 2008.

[249] D. Kim and A. E. Herr, "Protein immobilization techniques for microfluidic assays." *Biomicrofluidics*, vol. 7, no. 4, p. 41501, 2013.

[250] S. Puwanun, R. M. Delaine-Smith, H. E. Colley, J. M. Yates, S. MacNeil, and G. C. Reilly, "A simple rocker-induced mechanical stimulus upregulates mineralization by human osteoprogenitor cells in fibrous scaffolds," *Journal of Tissue Engineering and Regenerative Medicine*, vol. 12, no. 2, pp. 370–381, 2018.

[251] J. V. D. Stok, E. M. M. V. Lieshout, Y. El-massoudi, G. H. V. Kralingen, and P. Patka, "Acta Biomaterialia Bone substitutes in the Netherlands – A systematic literature review," *Acta Biomaterialia*, vol. 7, no. 2, pp. 739–750, 2011.

[252] C. Laurencin, Y. Khan, and S. F. El-amin, "Bone graft substitutes," *Expert Rev. Med. Devices*, vol. 3, no. 1, pp. 49–57, 2006.

[253] T. W. Bauer, "Bone graft substitutes," *Skeletal Radiol.*, vol. 36, pp. 1105–1107, 2007.

[254] K. E. Follmar, H. L. Prichard, F. C. Decroos, H. T. Wang, L. S. Levin, B. Klitzman, and K. C. Olbrich, "Combined Bone Allograft and Adipose-Derived Stem Cell Autograft in a Rabbit Model," *Annals of Plastic Surgery*, vol. 58, no. 5, pp. 561–565, 2007.

[255] A. Griesemer, K. Yamada, and M. Sykes, "Xenotransplantation: Immunological hurdles and progress toward tolerance," *Immunol Rev.*, vol. 258, no. 1, pp. 241–258, 2014.

[256] D. W. Hutmacher, "Scaffolds in tissue engineering bone and cartilage," *Biomaterials*, vol. 21, pp. 2529–2543, 2000.

[257] K. J. L. Burg, S. Porter, and J. F. Kellam, "Biomaterial developments for bone tissue engineering," *Biomaterials*, vol. 21, pp. 2347–58, 2000.

[258] M. F. Pittenger, A. M. Mackay, S. C. Beck, R. K. Jaiswal, R. Douglas, J. D. Mosca, M. A. Moorman, D. W. Simonetti, S. Craig, and D. R. Marshak, "Multilineage Potential of Adult Human Mesenchymal Stem Cells," *Science*, vol. 284, pp. 143–148, 1999.

[259] L. Solchaga, K. Penick, and J. Welter, "Chondrogenic Differentiation of Bone Marrow-Derived Mesenchymal Stem Cells: Tips and Tricks," *Methods Mol Biol*, vol. 698, no. 12, pp. 253–278, 2011.

[260] S.-l. Cheng, J. W. Yang, S.-f. Zhang, and L. V. Avioli, "Differentiation of Human Bone Marrow Osteogenic Stromal Cells In Vitro : Induction of the Osteoblast by Dexamethasone," *Endocrinology*, vol. 134, no. 1, pp. 277–86, 2014.

[261] L. Meinel, V. Karageorgiou, R. Fajardo, B. Snyder, V. Shinde-Patil, L. Zichner, D. Kaplan, R. Langer, and G. Vunjak-Novakovic, "Bone Tissue Engineering Using Human Mesenchymal Stem Cells : Effects of Scaffold Material and Medium Flow," *Annals of Biomedical Engineering*, vol. 32, no. 1, pp. 112–122, 2004.

[262] A. Amini, C. Laurencin, and S. Nukavarapu, "Bone Tissue Engineering: Recent Advances and Challenges," *Crit Rev Biomed Eng*, vol. 40, no. 5, pp. 363–408, 2012.

[263] I. Martin, D. Wendt, and M. Heberer, “The role of bioreactors in tissue engineering,” *Trends in Biotechnology*, vol. 22, no. 2, pp. 10–12, 2004.

[264] D. Li, T. Tang, J. Lu, and K. Dai, “Effects of Flow Shear Stress and Mass Transport on the Construction of a Large-Scale Tissue-Engineered Bone in a Perfusion Bioreactor,” *Tissue Engineering Part A*, vol. 15, no. 10, pp. 2773–83, 2009.

[265] H. Schliephake, N. Zghoul, V. Jager, M. V. Griensven, J. Zeichen, M. Gelinsky, and T. Wulfing, “Effect of seeding technique and scaffold material on bone formation in tissue-engineered constructs,” *Journal of Biomedical Materials Research - Part A*, vol. 90, no. 20, pp. 429–37, 2009.

[266] H. L. Morris, C. I. Reed, J. W. Haycock, and G. C. Reilly, “Mechanisms of fluid-flow-induced matrix production in bone tissue engineering.” *Proceedings of the Institution of Mechanical Engineers. Part H, Journal of engineering in medicine*, vol. 224, no. 12, pp. 1509–1521, 2010.

[267] H.-a. Kodama, Y. Amagai, H. Sudo, S. Kasai, and S. Yamamoto, “Establishment of a clonal osteogenic cell line from newborn mouse calvaria,” *Japanese Journal of Oral Biology*, vol. 23, no. 1, pp. 899–901, 1981.

[268] D. Wang, K. Christensen, K. Chawla, G. Xiao, P. H. Krebsbach, and R. T. Franceschi, “Isolation and Characterization of MC3T3-E1 Vivo Differentiation / Mineralization Potential,” *Journal of Bone and Mineral Research*, vol. 14, no. 6, pp. 893–903, 1999.

[269] Y. Kato, A. Boskey, L. Spevak, M. Dallas, M. Hori, and L. F. Bonewald, “Establishment of an osteoid preosteocyte-like cell MLO-A5 that spontaneously mineralizes in culture.” *Journal of bone and mineral research : the official journal of the American Society for Bone and Mineral Research*, vol. 16, no. 9, pp. 1622–33, 2001.

[270] A. R. Stern, M. M. Stern, M. E. Van Dyke, K. Jahn, M. Prideaux, and L. F. Bonewald, “Isolation and culture of primary osteocytes from the long bones of skeletally mature and aged mice,” *Biotechiques*, vol. 52, no. 6, pp. 361–373, 2013.

[271] J. O’Brien, I. Wilson, T. Orton, and F. Pognan, “Investigation of the Alamar Blue (resazurin) fluorescent dye for the assessment of mammalian cell cytotoxicity,” *European Journal of Biochemistry*, vol. 267, no. 17, pp. 5421–5426, 2000.

[272] M. J. Pead and L. E. Lanyon, "Indomethacin modulation of load-related stimulation of new bone formation in vivo," *Calcified Tissue International*, vol. 45, pp. 34–40, 1989.

[273] K. M. Holtz and E. R. Kantrowitz, "The mechanism of the alkaline phosphatase reaction: insights from NMR , crystallography and site-specific mutagenesis," *Federation of European Biochemical Societies*, vol. 462, pp. 7–11, 1999.

[274] H. Puchtler, S. N. Meloan, M. S. Terry, and S. Terry, "On the history and mechanism of alizarin and alizarin red S stains for calcium," *Journal of Histochemistry & Cytochemistry*, vol. 17, no. 2, pp. 110–124, 1969.

[275] P. Virtanen and K. Isotupa, "Staining properties of alizarin red S for growing bone in vitro," *Acta Anatomica*, vol. 108, pp. 202–207, 1980.

[276] L. F. Nielsen, D. Moe, S. Kirkeby, and C. Garbarsch, "Sirius Red and Acid Fuchsin Staining Mechanisms," *Biotechnic & Histochemistry*, vol. 73, no. 2, pp. 71–77, 1997.

[277] G. S. Montes and L. C. U. Junqueira, "The use of the picosirius-polarization method for the study of the biopathology of collagen," *Memórias do Instituto Oswaldo Cruz*, vol. 86, no. 3, pp. 1–11, 1991.

[278] J. R. Geddes, S. Burgess, K. Hawton, K. Jamison, and G. M. Goodwin, "Long-Term Lithium Therapy for Bipolar Disorder: Systematic Review and Meta-Analysis of Randomized Controlled Trials," *American Journal of Psychiatry*, vol. 161, no. 2, pp. 217–222, 2004.

[279] F. K. Goodwin, B. Fireman, G. E. Simon, E. M. Hunkeler, J. Lee, and D. Revicki, "Suicide Risk in Bipolar Disorder during Treatment with Lithium and Divalproex," *Journal of the American Medical Association*, vol. 290, no. 11, pp. 1467–1473, 2003.

[280] T. Suppes, R. J. Baldessarini, G. L. Faedda, and M. Tohen, "Risk of Recurrence Following Discontinuation of Lithium Treatment in Bipolar Disorder," *Archives of General Psychiatry*, vol. 48, no. 12, pp. 1082–1088, 1991.

[281] P. Vestergaard, L. Rejnmark, and L. Mosekilde, "Reduced relative risk of fractures among users of lithium," *Calcified Tissue International*, vol. 77, no. 1, pp. 1–8, 2005.

[282] I. Wilting, F. de Vries, B. M. Thio, C. Cooper, E. R. Heerdink, H. G. Leufkens, W. A. Nolen, A. C. Egberts, and T. P. van Staa, "Lithium use and the risk of fractures," *Bone*, vol. 40, no. 5, pp. 1252–1258, 2007.

[283] J. M. Bolton, C. Metge, L. Lix, H. Prior, J. Sareen, and W. D. Leslie, "Fracture risk from psychotropic medications: a population-based analysis," *Journal of Clinical Psychopharmacology*, vol. 28, no. 4, pp. 384–391, 2008.

[284] P. C. Souverein, D. J. Webb, J. G. Weil, T. P. Van Staa, and A. C. Egberts, "Use of antiepileptic drugs and risk of fractures: Case-control study among patients with epilepsy," *Neurology*, vol. 66, no. 9, pp. 1318–1324, 2006.

[285] J. Gagne, A. Patrick, H. Mogun, and D. Solomon, "Comparative safety of antidepressants on fracture risk in older adults," *Clin Pharmacol Ther*, vol. 89, no. 6, pp. 880–887, 2011.

[286] S. Drost and A. Massicotte, "Are selective serotonin reuptake inhibitors associated with fractures?" *Canadian Pharmacists Journal*, vol. 149, no. 6, pp. 332–336, 2016.

[287] O. Cohen, T. Rais, E. Lepkifker, and I. Vered, "Lithium carbonate therapy is not a risk factor for osteoporosis," *Hormone and Metabolic Research*, vol. 30, no. 9, pp. 594–597, 1998.

[288] B. M. Harvey, M. Eschbach, E. A. Glynn, S. Kotha, M. Darre, D. J. Adams, R. Ramanathan, R. Mancini, and K. E. Govoni, "Effect of daily lithium chloride administration on bone mass and strength in growing broiler chickens," *Poultry Science*, vol. 94, no. 2, pp. 296–301, 2015.

[289] P. Clement-Lacroix, M. Ai, F. Morvan, S. Roman-Roman, B. Vayssiere, C. Belleville, K. Estrera, M. L. Warman, R. Baron, and G. Rawadi, "Lrp5-independent activation of Wnt signaling by lithium chloride increases bone formation and bone mass in mice," *Proceedings of the National Academy of Sciences*, vol. 102, no. 48, pp. 17 406–17 411, 2005.

[290] A. E. Loiselle, S. A. J. Lloyd, E. M. Paul, G. S. Lewis, and H. J. Donahue, "Inhibition of GSK-3$\beta$ rescues the impairments in bone formation and mechanical properties associated with fracture healing in osteoblast selective connexin 43 deficient mice," *PLoS ONE*, vol. 8, no. 11, pp. 1–10, 2013.

[291] N. K. Satija, D. Sharma, F. Afrin, R. P. Tripathi, and G. Gangenahalli, "High Throughput Transcriptome Profiling of Lithium Stimulated Human Mesenchymal Stem Cells Reveals Priming towards Osteoblastic Lineage," *PLoS ONE*, vol. 8, no. 1, p. e55769, 2013.

[292] V. J. Armstrong, M. Muzylak, A. Sunters, G. Zaman, L. K. Saxon, J. S. Price, and L. E. Lanyon, "Wnt/$\beta$-catenin signaling is a component of osteoblastic bone cell early responses to load-bearing and requires estrogen receptor $\alpha$," *Journal of Biological Chemistry*, vol. 282, no. 28, pp. 20 715–20 727, 2007.

[293] C. Galli, M. Piemontese, S. Lumetti, E. Manfredi, G. M. MacAluso, and G. Passeri, "The importance of WNT pathways for bone metabolism and their regulation by implant topography," *European Cells and Materials*, vol. 24, pp. 46–59, 2012.

[294] X. Liu, J. H. Kim, J. Wang, X. Chen, H. Zhang, S. H. Kim, J. Cui, L. Ruidong, W. Zhang, Y. Kong, J. Zhang, W. Shui, J. Lamplot, M. R. Rogers, C. Zhao, N. Wang, J. Tomal, J. Statz, N. Wang, H. H. Luu, R. C. Haydon, T. C. He, and P. Rajan, "Wnt signaling in bone formation and its therapeutic potential for bone diseases," *Therapeutic Advances in Musculoskeletal Disease*, vol. 5, no. 1, pp. 13–31, 2013.

[295] M. A. Kamel, J. L. Picconi, N. Lara-Castillo, and M. l. Johnson, "Activation of $\beta$–catenin Signaling in MLO-Y4 Osteocytic Cells versus 2T3 Osteoblastic Cells by Fluid Flow Shear Stress and PGE2: Implications for the Study of Mechanosensation in Bone," *Bone*, vol. 47, no. 5, pp. 872–881, 2010.

[296] I. Kramer, C. Halleux, H. Keller, M. Pegurri, J. H. Gooi, P. B. Weber, J. Q. Feng, L. F. Bonewald, and M. Kneissel, "Osteocyte Wnt/beta-Catenin Signaling Is Required for Normal Bone Homeostasis," *Molecular and Cellular Biology*, vol. 30, no. 12, pp. 3071–3085, 2010.

[297] J. A. Robinson, M. Chatterjee-Kishore, P. J. Yaworsky, D. M. Cullen, W. Zhao, C. Li, Y. Kharode, L. Sauter, P. Babij, E. L. Brown, A. A. Hill, M. P. Akhter, M. L. Johnson, R. R. Recker, B. S. Komm, and F. J. Bex, "Wnt/$\beta$-catenin signaling is a normal physiological response to mechanical loading in bone," *Journal of Biological Chemistry*, vol. 281, no. 42, pp. 31 720–31 728, 2006.

[298] A. Sittichockechaiwut, A. M. Scutt, A. J. Ryan, L. F. Bonewald, and G. C. Reilly, "Use of rapidly mineralising osteoblasts and short periods

of mechanical loading to accelerate matrix maturation in 3D scaffolds," *Bone*, vol. 44, no. 5, pp. 822–829, 2009.

[299] J. Edwards, "The effects of vibration as a mechanical stimulus on osteogenesis of mesenchymal progenitors," Ph.D. dissertation, University of Sheffield, 2013.

[300] W. S. Waring, "Management of lithium toxicity." *Toxicological reviews*, vol. 25, no. 4, pp. 221–230, 2006.

[301] S. B. Schleicher, J. J. Zaborski, R. Riester, N. Zenkner, R. Handgretinger, T. Kluba, F. Traub, and K. A. Boehme, "Combined application of arsenic trioxide and lithium chloride augments viability reduction and apoptosis induction in human rhabdomyosarcoma cell lines," *PLOS ONE*, vol. 12, no. 6, p. e0178857, 2017.

[302] V. Azimian-Zavareh, G. Hossein, and E. Janzamin, "Effect of lithium chloride and antineoplastic drugs on survival and cell cycle of androgen-dependent prostate cancer LNCap cells." *Indian journal of pharmacology*, vol. 44, no. 6, pp. 714–21, 2012.

[303] Z. Zhu, J. Yin, X. Niu, D. Jin, B. Hu, J. Guan, Y. Wang, and C. Zhang, "Lithium stimulates human bone marrow derived mesenchymal stem cell proliferation through GSK-3$\beta$-dependent $\beta$-catenin/Wnt pathway activation," *FEBS Journal*, vol. 281, no. 23, pp. 5371–5389, 2014.

[304] N. H. Holstein-Rathlou, "Lithium transport across biological membranes." *Kidney international. Supplement*, vol. 28, pp. S4–9, 1990.

[305] C. M. Hedgepeth, L. J. Conrad, J. Zhang, H. C. Huang, V. M. Lee, and P. S. Klein, "Activation of the Wnt signaling pathway: A molecular mechanism for lithium action," *Developmental Biology*, vol. 185, no. 1, pp. 82–91, 1997.

[306] T. Miki, S. ya Yasuda, and M. Kahn, "Wnt/$\beta$-catenin Signaling in Embryonic Stem Cell Self-renewal and Somatic Cell Reprogramming," *Stem Cell Reviews and Reports*, vol. 7, no. 4, pp. 836–846, 2011.

[307] T. Gaur, C. J. Lengner, H. Hovhannisyan, R. A. Bhat, P. V. Bodine, B. S. Komm, A. Javed, A. J. Van Wijnen, J. L. Stein, G. S. Stein, and J. B. Lian, "Canonical WNT signaling promotes osteogenesis by directly stimulating Runx2 gene expression," *Journal of Biological Chemistry*, vol. 280, no. 39, pp. 33 132–33 140, 2005.

[308] X. He, M. Semenov, K. Tamai, and X. Zeng, "LDL receptor-related proteins 5 and 6 in Wnt/beta-catenin signaling: Arrows point the way," *Development*, vol. 131, no. 8, pp. 1663–1677, 2004.

[309] M. D. Gordon and R. Nusse, "Wnt Signaling: Multiple Pathways, Multiple Receptors, and Multiple Transcription Factors," *Journal of Biological Chemistry*, vol. 281, no. 32, pp. 22 429–22 433, 2006.

[310] N. Zhang, P. Wei, A. Gong, W. Chiu, H. Lee, H. Colman, H. Huang, J. Xue, M. Liu, Y. Wang, R. Sawaya, K. Xie, A. W. K. Yung, R. H. Medema, X. He, and S. Huang, "FoxM1 Promotes $\beta$-Catenin Nuclear Localization and Controls Wnt Target-Gene Expression and Glioma Tumorigenesis," *Cancer Cell*, vol. 124, no. 17, pp. 1871–1881, 2012.

[311] M. B. Eslaminejad, M. Talkhabi, and B. Zeynali, "Effect of Lithium Chloride on Proliferation and Bone Differentiation of Rat Marrow-Derived Mesenchymal Stem Cells in Culture," *Iranian Journal of Basic Medical Sciences*, vol. 11, no. 3, pp. 143–151, 2008.

[312] J. de Boer, H. J. Wang, and C. van Blitterswijk, "Effects of Wnt Signaling on Proliferation and Differentiation of Human Mesenchymal Stem Cells," *Tissue Engineering*, vol. 10, no. 3-4, pp. 393–401, 2004.

[313] E. Smith, G. A. Coetzee, and B. Frenkel, "Glucocorticoids inhibit cell cycle progression in differentiating osteoblasts via glycogen synthase kinase-3$\beta$," *Journal of Biological Chemistry*, vol. 277, no. 20, pp. 18 191–18 197, 2002.

[314] K. Ohnaka, M. Tanabe, H. Kawate, H. Nawata, and R. Takayanagi, "Glucocorticoid suppresses the canonical Wnt signal in cultured human osteoblasts," *Biochemical and Biophysical Research Communications*, vol. 329, no. 1, pp. 177–181, 2005.

[315] G. Bain, T. Müller, X. Wang, and J. Papkoff, "Activated $\beta$-catenin induces osteoblast differentiation of C3H10T1/2 cells and participates in BMP2 mediated signal transduction," *Biochemical and Biophysical Research Communications*, vol. 301, no. 1, pp. 84–91, 2003.

[316] L. Li, X. Peng, Y. Qin, R. Wang, J. Tang, X. Cui, T. Wang, W. Liu, H. Pan, and B. Li, "Acceleration of bone regeneration by activating Wnt/$\beta$-catenin signalling pathway via lithium released from lithium chloride/calcium phosphate cement in osteoporosis," *Scientific Reports*, vol. 7, p. 45204, 2017.

[317] F. Langenbach and J. Handschel, “Effects of dexamethasone, ascorbic acid and $\beta$-glycerophosphate on the osteogenic differentiation of stem cells in vitro.” *Stem cell research & therapy*, vol. 4, no. 5, p. 117, 2013.

[318] L. Tang, Y. Chen, F. Pei, and H. Zhang, “Lithium chloride modulates adipogenesis and osteogenesis of human bone marrow-derived mesenchymal stem cells,” *Cellular Physiology and Biochemistry*, vol. 37, no. 1, pp. 143–152, 2015.

[319] L. Pasquali, C. L. Busceti, F. Fulceri, A. Paparelli, and F. Fornai, “Intracellular pathways underlying the effects of lithium,” *Behavioural Pharmacology*, vol. 21, no. 5-6, pp. 473–492, 2010.

[320] D. Veloso, R. W. Guynn, M. Oskarsson, and R. L. Veech, “The Concentrations of Free and Bound Magnesium in Rat Tissues,” *The Journal of biological chemistry*, vol. 248, no. 13, pp. 4811–9, 1973.

[321] W. J. Ryves and A. J. Harwood, “Lithium Inhibits Glycogen Synthase Kinase-3 by Competition for Magnesium,” *Biochemical and Biophysical Research Communications*, vol. 280, no. 3, pp. 720–725, 2001.

[322] K. Vachhani, C. Whyne, Y. Wang, D. M. Burns, and D. Nam, “Low-dose lithium regimen enhances endochondral fracture healing in osteoporotic rodent bone,” *Journal of Orthopaedic Research*, vol. 36, no. 6, pp. 1783–1789, 2018.

[323] X. Wang, S. Zhu, X. Jiang, Y. Li, D. Song, and J. Hu, “Systemic Administration of Lithium Improves Distracted Bone Regeneration in Rats,” *Calcified Tissue International*, vol. 96, no. 6, pp. 534–540, 2015.

[324] C. A. Gregory, A. S. Perry, E. Reyes, A. Conley, W. G. Gunn, and D. J. Prockop, “Dkk-1-derived Synthetic Peptides and Lithium Chloride for the Control and Recovery of Adult Stem Cells from Bone Marrow,” *Journal of Biological Chemistry*, vol. 280, no. 3, pp. 2309–2323, 2005.

[325] D. Li, X. Xie, Z. Yang, C. Wang, Z. Wei, and P. Kang, “Enhanced bone defect repairing effects in glucocorticoid-induced osteonecrosis of the femoral head using a porous nano-lithium-hydroxyapatite/gelatin microsphere/erythropoietin composite scaffold,” *Biomaterials Science*, vol. 6, no. 3, pp. 519–537, 2018.

[326] P. K. Khan, A. Mahato, B. Kundu, S. K. Nandi, P. Mukherjee, S. Datta, S. Sarkar, J. Mukherjee, S. Nath, V. K. Balla, and C. Mandal, “Influence of single and binary doping of strontium and lithium on in vivo biologi-

cal properties of bioactive glass scaffolds," *Scientific Reports*, vol. 6, no. September, pp. 1–18, 2016.

[327] W. Shi, Y. Xie, J. He, J. Zhou, Y. Gao, W. Wei, N. Ding, H. Ma, C. J. Xian, K. Chen, and J. Wang, "Microgravity induces inhibition of osteoblastic differentiation and mineralization through abrogating primary cilia," *Scientific Reports*, vol. 7, no. 1, pp. 1–12, 2017.

[328] N. Oliazadeh, K. F. Gorman, R. Eveleigh, G. Bourque, and A. Moreau, "Identification of Elongated Primary Cilia with Impaired Mechanotransduction in Idiopathic Scoliosis Patients," *Scientific Reports*, vol. 7, no. February, p. 44260, 2017.

[329] J. Zhang, M. T. Dalbay, X. Luo, E. Vrij, D. Barbieri, L. Moroni, J. D. de Bruijn, C. A. van Blitterswijk, J. P. Chapple, M. M. Knight, and H. Yuan, "Topography of calcium phosphate ceramics regulates primary cilia length and TGF receptor recruitment associated with osteogenesis," *Acta Biomaterialia*, vol. 57, pp. 487–497, 2017.

[330] M. A. Wozniak, K. Modzelewska, L. Kwong, and P. J. Keely, "Focal adhesion regulation of cell behavior," *Biochimica et Biophysica Acta - Molecular Cell Research*, vol. 1692, no. 2-3, pp. 103–119, 2004.

[331] G. F. Weber, M. A. Bjerke, and D. W. DeSimone, "Integrins and cadherins join forces to form adhesive networks," *Journal of Cell Science*, vol. 124, no. 8, pp. 1183–1193, 2011.

[332] O. V. Plotnikova, E. N. Pugacheva, and E. A. Golemis, "Primary Cilia and the Cell Cycle," *Methods Cell Biol*, vol. 94, pp. 137–160, 2009.

[333] A. Pitaval, Q. Tseng, M. Bornens, and M. Théry, "Cell shape and contractility regulate ciliogenesis in cell cycle-arrested cells," *Journal of Cell Biology*, vol. 191, no. 2, pp. 303–312, 2010.

[334] R. W. Tucker and A. Pardee, "Centriole Ciliation Is Related to Quiescence DNA Synthesis in 3T3 Cells," *Cell*, vol. 17, pp. 527–535, 1979.

[335] T. R. Coughlin, M. Voisin, M. B. Schaffler, G. L. Niebur, and L. M. McNamara, "Primary cilia exist in a small fraction of cells in trabecular bone and marrow," *Calcif Tissue Int*, vol. 96, no. 1, pp. 65–72, 2015.

[336] F. Wasserman and J. A. Yaeger, "Fine structure of the osteocyte capsule and of the wall of the lacunae in bone," *Zeitschrift für Zellforschung und Mikroskopische Anatomie*, vol. 67, pp. 636–652, 1965.

[337] L.-D. You, S. Weinbaum, S. C. Cowin, and M. B. Schauffler, "Ultrastructure of the Osteocyte Process and its Pericellular Matrix," *The Anatomical Record Part A*, vol. 278, pp. 505–13, 2004.

[338] L. M. McNamara, R. J. Majeska, S. Weinbaum, V. Friedrich, and M. B. Schaffler, "Attachment of osteocyte cell processes to the bone matrix," *Anatomical Record*, vol. 292, no. 3, pp. 355–363, 2009.

[339] G. C. Goulet, D. Coombe, R. J. Martinuzzi, and R. F. Zernicke, "Poroelastic evaluation of fluid movement through the lacunocanalicular system," *Annals of Biomedical Engineering*, vol. 37, no. 7, pp. 1390–1402, 2009.

[340] T. A. Metzger, S. A. Schwaner, A. J. LaNeve, T. C. Kreipke, and G. L. Niebur, "Pressure and shear stress in trabecular bone marrow during whole bone loading," *Journal of Biomechanics*, vol. 48, no. 12, pp. 3035–3043, 2015.

[341] A. Ogasawara, T. Arakawa, T. Kaneda, T. Takuma, T. Sato, H. Kaneko, M. Kumegawa, and Y. Hakeda, "Fluid Shear Stress-induced Cyclooxygenase-2 Expression is Mediated by C/ EBP $\beta$, cAMP-response Element-binding Protein, and AP-1 in Osteoblastic MC3T3-E1 Cells," *Journal of Biological Chemistry*, vol. 276, no. 10, pp. 7048–7054, 2001.

[342] Z. Mai, Z. Peng, S. Wu, J. Zhang, L. Chen, H. Liang, D. Bai, G. Yan, and H. Ai, "Single Bout Short Duration Fluid Shear Stress Induces Osteogenic Differentiation of MC3T3-E1 Cells via Integrin $\beta$1 and BMP2 Signaling Cross-Talk," *PLoS ONE*, vol. 8, no. 4, pp. 1–10, 2013.

[343] G. S. Stein and J. B. Lian, "Molecular mechanisms mediating proliferation/differentiation interrelationships during progressive development of the osteoblast phenotype," *Endocrine Reviews*, vol. 14, no. 4, pp. 424–442, 1993.

[344] K. Kwist, W. C. Bridges, and K. J. Burg, "The effect of cell passage number on osteogenic and adipogenic characteristics of D1 cells," *Cytotechnology*, vol. 68, no. 4, pp. 1661–1667, 2016.

[345] S. Puwanun, "Developing a tissue engineering strategy for cleft palate repair," Ph.D. dissertation, University of Sheffield, 2014.

[346] A. Y. Liu, H. Bian, L. E. Huangi, and Y. K. Lee, "Transient cold shock induces the heat shock response upon recovery at 37 °C in human cells," *Journal of Biological Chemistry*, vol. 269, no. 20, pp. 14 768–14 775, 1994.

[347] A. Roobol, M. J. Carden, R. J. Newsam, and C. M. Smales, "Biochemical insights into the mechanisms central to the response of mammalian cells to cold stress and subsequent rewarming," *FEBS Journal*, vol. 276, no. 1, pp. 286–302, 2009.

[348] J. Fujita, "Cold Shock Response in Mammalian Cells JMMB Symposium," *J. Mol. Microbiol. Biotechnol*, vol. 1, no. 2, pp. 243–255, 1999.

[349] L. A. Sonna, J. Fujita, S. L. Gaffin, and C. M. Lilly, "Effects of heat and cold stress on mammalian gene expression," *J Appl Physiol*, vol. 92, pp. 1725–42, 2002.

[350] I. M. Shapiro and E. I. Lubennikova, "Population kinetics of cells in tissue culture incubated at low temperature," *Experimental Cell Research*, vol. 49, no. 2, pp. 305–316, 1968.

[351] J. W. Shim, D. A. Wise, and S. H. Elder, "Effect of Cytoskeletal Disruption on Mechanotransduction of Hydrostatic Pressure by C3H10T1/2 Murine Fibroblasts," *The Open Orthopaedics Journal*, vol. 2, pp. 155–62, 2008.

[352] N. V. Prodromou, C. L. Thompson, D. P. S. Osborn, K. F. Cogger, R. Ashworth, M. M. Knight, P. L. Beales, and J. P. Chapple, "Heat shock induces rapid resorption of primary cilia," *Journal of Cell Science*, vol. 125, no. 18, pp. 4297–4305, 2012.

[353] J. Williams, J. Iannotti, A. Ham, J. Bleuit, and J. Chen, "Effects of fluid shear stress on bone cells," *Biorheology*, vol. 31, no. 2, pp. 163–70, 1994.

[354] M. R. Kreke, W. R. Huckle, and A. S. Goldstein, "Fluid flow stimulates expression of osteopontin and bone sialoprotein by bone marrow stromal cells in a temporally dependent manner." *Bone*, vol. 36, no. 6, pp. 1047–55, 2005.

[355] J. Xing, Y. Li, M. Lin, J. Wang, J. Wu, Y. Ma, Y. Wang, L. Yang, and Y. Luo, "Surface chemistry modulates osteoblasts sensitivity to low fluid shear stress," *Journal of Biomedical Materials Research - Part A*, vol. 102, no. 11, pp. 4151–4160, 2014.

[356] C. Mason, N. L. Davie, J. A. Rowley, D. W. Smith, E. J. Culme-Seymour, and D. A. Brindley, "Peak serum: implications of serum supply for cell therapy manufacturing," *Regenerative Medicine*, vol. 7, no. 1, pp. 7–13, 2011.

[357] S. N. Usta, C. D. Scharer, J. Xu, T. K. Frey, and R. J. Nash, "Chemically defined serum-free and xeno-free media for multiple cell lineages." *Annals of translational medicine*, vol. 2, no. 10, p. 97, 2014.

[358] J. van der Valk, K. Bieback, C. Buta, B. Cochrane, W. G. Dirks, J. Fu, J. J. Hickman, C. Hohensee, R. Kolar, M. Liebsch, F. Pistollato, M. Schulz, D. Thieme, T. Weber, J. Wiest, S. Winkler, and G. Gstraunthaler, "Fetal Bovine Serum (FBS): Past - Present - Future," *Altex*, vol. 35, no. 1, pp. 99–118, 2018.

[359] M. Yuasa, T. Yamada, T. Taniyama, T. Masaoka, W. Xuetao, T. Yoshii, M. Horie, H. Yasuda, T. Uemura, A. Okawa, and S. Sotome, "Dexamethasone enhances osteogenic differentiation of bone marrow-and muscle-derived stromal cells and augments ectopic bone formation induced by bone morphogenetic protein-2," *PLoS ONE*, vol. 10, no. 2, pp. 1–23, 2015.

[360] Y. Zhang, D. Khan, J. Delling, and E. Tobiasch, "Mechanisms Underlying the Osteo- and Adipo-Differentiation of Human Mesenchymal Stem Cells," *The Scientific World Journal*, vol. 2012, pp. 1–14, 2012.

[361] M.-F. F. Iu, H. Kaji, H. Sowa, J. Naito, T. Sugimoto, and K. Chihara, "Dexamethasone suppresses Smad3 pathway in osteoblastic cells," *Journal of Endocrinology*, vol. 185, no. 1, pp. 131–138, 2005.

[362] S. Xu, R. Guo, P. Z. Li, K. Li, Y. Yan, J. Chen, G. Wang, B. Brand-Saberi, X. Yang, and X. Cheng, "Dexamethasone interferes with osteoblasts formation during osteogenesis through altering IGF-1-mediated angiogenesis," *Journal of Cellular Physiology*, no. January, pp. 1–15, 2019.

[363] S. Walsh, G. R. Jordan, C. Jefferiss, K. Stewart, and J. N. Beresford, "High concentrations of dexamethasone suppress the proliferation but not the differentiation or further maturation of human osteoblast precursors in vitro: Relevance to glucocorticoid-induced osteoporosis," *Rheumatology*, vol. 40, no. 1, pp. 74–83, 2001.

[364] J. R. Mauney, S. Sjostorm, J. Blumberg, R. Horan, J. P. O'Leary, G. Vunjak-Novakovic, V. Volloch, and D. L. Kaplan, "Mechanical Stimulation Promotes Osteogenic Differentiation of Human Bone Marrow Stromal Cells on 3-D Partially Demineralized Bone Scaffolds in Vitro," *Calcified Tissue International*, vol. 74, no. 5, pp. 458–468, 2004.

[365] D. Xu, Y. Gao, N. Hu, L. Wu, and Q. Chen, "miR-365 ameliorates dexamethasone-induced suppression of osteogenesis in MC3T3-E1 cells

by targeting HDAC4," *International Journal of Molecular Sciences*, vol. 18, no. 5, pp. 1–10, 2017.

[366] Z. Chen, Y. Zhang, C. Liang, L. Chen, G. Zhang, and A. Qian, "Mechanosensitive miRNAs and bone formation," *International Journal of Molecular Sciences*, vol. 18, no. 8, pp. 1–16, 2017.

[367] M. S. Cooper, A. Blumsohn, P. E. Goddard, W. A. Bartlett, C. H. Shackleton, R. Eastell, M. Hewison, and P. M. Stewart, "11$\beta$-Hydroxysteroid Dehydrogenase Type 1 Activity Predicts the Effects of Glucocorticoids on Bone," *Journal of Clinical Endocrinology and Metabolism*, vol. 88, no. 8, pp. 3874–3877, 2003.

[368] M. S. Cooper, I. Bujalska, E. Rabbitt, E. A. Walker, R. Bland, M. C. Sheppard, M. Hewison, P. M. Stewart, and C. E. T. Al, "Isozymes by Proinflammatory Cytokines in Osteoblasts : An Autocrine Switch from Glucocorticoid Inactivation to Activation," *Journal of Bone and Mineral Research*, vol. 16, no. 6, pp. 1037–1044, 2001.

[369] K. Sakai, M. Mohtai, J. I. Shida, K. Harimaya, S. Benvenuti, M. L. Brandi, T. Kukita, and Y. Iwamoto, "Fluid shear stress increases interleukin-11 expression in human osteoblast-like cells: Its role in osteoclast induction," *Journal of Bone and Mineral Research*, vol. 14, no. 12, pp. 2089–2098, 1999.

[370] J. Y. Ji, H. Jing, and S. L. Diamond, "Shear stress causes nuclear localization of endothelial glucocorticoid receptor and expression from the GRE promoter," *Circulation Research*, vol. 92, no. 3, pp. 279–285, 2003.

[371] G. A. Zimmerman, D. E. Lorant, T. M. McIntyre, and S. M. Prescott, "Juxtacrine Intercellular Signaling: Another Way to Do It," *American Journal of Respiratory Cell and Molecular Biology*, vol. 9, no. 5, pp. 573–7, 1993.

[372] M. Mullender, A. J. El Haj, Y. Yang, M. A. van Duin, E. H. Burger, and J. Klein-Nulend, "Mechanotransduction of bone cells in vitro: Mechanobiology of bone tissue," *Medical and Biological Engineering and Computing*, vol. 42, no. 1, pp. 14–21, 2004.

[373] B. Cheng, S. Zhao, L. F. Luo, E. Sprague, L. F. Bonewald, and J. X. Jiang, "Expression of functional gap junctions and regulation by fluid flow in osteocyte-like MLO-Y4 cells," *Journal of Bone and Mineral Research*, vol. 16, no. 2, pp. 249–259, 2001.

[374] J. Li, D. Liu, H. Z. Ke, R. L. Duncan, and C. H. Turner, "The P2X7 nucleotide receptor mediates skeletal mechanotransduction," *Journal of Biological Chemistry*, vol. 280, no. 52, pp. 42 952–42 959, 2005.

[375] D. Genetos, D. Geist, D. Liu, H. J. Donahue, and R. L. Duncan, "Fluid Shear-Induced ATP Secretion Mediates Prostaglandin Release in MC3T3-E1 Osteoblasts," *Journal of Bone and Mineral Research*, vol. 20, no. 1, pp. 41–9, 2005.

[376] R. G. Bacabac, T. H. Smit, M. G. Mullender, S. J. Dijcks, J. J. Van Loon, and J. Klein-Nulend, "Nitric oxide production by bone cells is fluid shear stress rate dependent," *Biochemical and Biophysical Research Communications*, vol. 315, no. 4, pp. 823–829, 2004.

[377] M. M. Thi, S. O. Suadicani, and D. C. Spray, "Fluid flow-induced soluble vascular endothelial growth factor isoforms regulate actin adaptation in osteoblasts," *Journal of Biological Chemistry*, vol. 285, no. 40, pp. 30 931–30 941, 2010.

[378] M. R. Kreke, L. A. Sharp, Y. Woo Lee, and A. S. Goldstein, "Effect of Intermittent Shear Stress on Mechanotransductive Signaling and Osteoblastic Differentiation of Bone Marrow Stromal Cells," *Tissue Engineering Part A*, vol. 14, no. 4, pp. 529–537, 2008.

[379] L. Prodanov, C. M. Semeins, J. J. Van Loon, J. Te Riet, J. A. Jansen, J. Klein-Nulend, and X. F. Walboomers, "Influence of nanostructural environment and fluid flow on osteoblast-like cell behavior: A model for cell-mechanics studies," *Acta Biomaterialia*, vol. 9, no. 5, pp. 6653–6662, 2013.

[380] H. Yang, R. E. Embry, and R. P. Main, "Effects of loading duration and short rest insertion on cancellous and cortical bone adaptation in the mouse tibia," *PLoS ONE*, vol. 12, no. 1, pp. 1–20, 2017.

[381] A. G. Robling, D. B. Burr, and C. H. Turner, "Recovery periods restore mechanosensitivity to dynamically loaded bone." *The Journal of experimental biology*, vol. 204, no. Pt 19, pp. 3389–3399, 2001.

[382] S. Srinivasan, D. A. Weimer, S. C. Agans, S. D. Bain, and T. S. Gross, "Low-magnitude mechanical loading becomes osteogenic when rest is inserted between each load cycle," *Journal of Bone and Mineral Research*, vol. 17, no. 9, pp. 1613–1620, 2002.

[383] S. R. Mcglashan, M. M. Knight, T. T. Chowdhury, P. Joshi, C. G. Jensen, S. Kennedy, and C. A. Poole, "Mechanical loading modulates chondrocyte primary cilia incidence and length," *Cell Biology International*, vol. 34, pp. 441–446, 2010.

[384] C. L. Thompson, J. P. Chapple, and M. M. Knight, "Primary cilia disassembly down-regulates mechanosensitive hedgehog signalling: A feedback mechanism controlling ADAMTS-5 expression in chondrocytes," *Osteoarthritis and Cartilage*, vol. 22, no. 3, pp. 490–498, 2014.

[385] M. a. Wozniak and C. S. Chen, "Mechanotransduction in development: a growing role for contractility," *Nature Reviews Molecular Cell Biology*, vol. 10, no. 1, pp. 34–43, 2009.

[386] S. Weinbaum, Y. Duan, L. M. Satlin, T. Wang, and A. M. Weinstein, "Mechanotransduction in the renal tubule," *AJP: Renal Physiology*, vol. 299, no. 6, pp. F1220–F1236, 2010.

[387] S. C. Cowin, S. Weinbaum, and Y. Zeng, "A case for bone canaliculi As the anatomical Generated Potentials Site of strain generated potentials," *Journal of Biomechanics*, vol. 28, no. 11, pp. 1281–1297, 1995.

[388] R. L. Duncan and C. H. Turner, "Mechanotransduction and the Functional Response of Bone to Mechanical Strain," *Calcified tissue international*, vol. 57, pp. 344–358, 1995.

[389] R. M. Davidson, D. W. Tatakis, and A. L. Auerbach, "Multiple forms of mechanosensitive ion channels in osteoblast-like cells," *Pflügers Archiv European Journal of Physiology*, vol. 416, no. 6, pp. 646–651, 1990.

[390] A. M. D. Malone, N. N. Batra, G. Shivaram, R. Y. Kwon, L. You, C. H. Kim, J. Rodriguez, K. Jair, and C. R. Jacobs, "The role of actin cytoskeleton in oscillatory fluid flow-induced signaling in MC3T3-E1 osteoblasts," *American Journal of Physiology - Cell Physiology*, vol. 292, no. 5, pp. C1830–C1836, 2007.

[391] G. C. Reilly, T. R. Haut, C. E. Yellowley, H. J. Donahue, and C. R. Jacobs, "Fluid flow induced PGE2 release by bone cells is reduced by glycocalyx degradation whereas calcium signals are not," *Biorheology*, 2003.

[392] R. Steck, P. Niederer, and M. L. Knothe Tate, "A finite difference model of load-induced fluid displacements within bone under mechanical loading," *Medical Engineering and Physics*, vol. 22, no. 2, pp. 117–125, 2000.

[393] L. Wang, Y. Wang, Y. Han, S. C. Henderson, R. J. Majeska, S. Weinbaum, and M. B. Schaffler, "In situ measurement of solute transport in the bone lacunar-canalicular system," *Proceedings of the National Academy of Sciences*, vol. 102, no. 33, pp. 11 911–11 916, 2005.

[394] C. Iomini, K. Tejada, W. Mo, H. Vaananen, and G. Piperno, "Primary cilia of human endothelial cells disassemble under laminar shear stress," *Journal of Cell Biology*, vol. 164, no. 6, pp. 811–817, 2004.

[395] J. S. Chen and P. N. Sambrook, "Antiresorptive therapies for osteoporosis: A clinical overview," *Nature Reviews Endocrinology*, vol. 8, no. 2, pp. 81–91, 2012.

[396] R. G. Russell, N. B. Watts, F. H. Ebetino, and M. J. Rogers, "Mechanisms of action of bisphosphonates: Similarities and differences and their potential influence on clinical efficacy," *Osteoporosis International*, vol. 19, no. 6, pp. 733–759, 2008.

[397] A. Cranney, A. Papaioannou, N. Zytaruk, D. Hanley, J. Adachi, D. Goltzman, T. Murray, and A. Hodsman, "Parathyroid hormone for the treatment of osteoporosis: A systematic review," *Cmaj*, vol. 175, no. 1, pp. 52–59, 2006.

[398] P. J. Meunier, C. Roux, E. Seeman, S. Ortolani, J. E. Badurski, T. D. Spector, J. Cannata, A. Valogh, E. Lemmel, S. Pors-Nielsen, R. Rizzoli, H. K. Genant, and J. Reginster, "The Effects of Strontium Ranelate on the Risk of Vertebral Fracture in Women With Postmenopausal Osteoporosis," *The new england journal of medicine original*, vol. 350, pp. 459–68, 2004.

[399] N. B. Watts and L. M. Diab, "Long-Term use of bisphosphonates in osteoporosis," *Saudi Medical Journal*, vol. 95, no. 4, pp. 1555–65, 20172010.

[400] Y. Vinogradova, C. Coupland, and J. Hippisley-Cox, "Use of hormone replacement therapy and risk of venous thromboembolism: Nested case-control studies using the QResearch and CPRD databases," *BMJ*, vol. 364, pp. 1–14, 2019.

[401] L. Gennari, D. Merlotti, and R. Nuti, "Selective estrogen receptor modulator (SERM) for the treatment of osteoporosis in postmenopausal women: Focus on lasofoxifene," *Clinical Interventions in Aging*, vol. 5, no. 1, pp. 19–29, 2010.

[402] M. J. Bolland and A. Grey, "A comparison of adverse event and fracture efficacy data for strontium ranelate in regulatory documents and the publication record," *BMJ Open*, vol. 4, no. 10, pp. 1–8, 2014.

[403] P. D. Miller, "Safety of parathyroid hormone for the treatment of osteoporosis," *Curr Osteoporos Rep*, vol. 6, no. 1, pp. 12–6, 2008.

[404] P. Kumar, T. L. Thirkill, J. Ji, L. H. Monte, and G. C. Douglas, "Differential effects of sodium butyrate and lithium chloride on rhesus monkey trophoblast differentiation," *PLoS ONE*, vol. 10, no. 8, pp. 1–27, 2015.

[405] B. Yang, X.-Y. Wu, J. Ni, B.-H. Li, L.-H. Deng, and M.-J. Xiang, "Modulation of Wnt/$\beta$-catenin signaling affects the directional differentiation of hair follicle stem cells," *Plastic and Aesthetic Research*, vol. 3, no. 2, p. 39, 2016.

[406] C. A. Poole, M. Flint, and B. B.W., "Analysis of the morphology and function of primary cilia in connective tissue: a celluar cybernetic probe?" *Cell Motility*, vol. 5, pp. 175–93, 1985.

[407] S. R. McGlashan, C. G. Jensen, and C. A. Poole, "Localization of extracellular matrix receptors on the chondrocyte primary cilium," *Journal of Histochemistry and Cytochemistry*, vol. 54, no. 9, pp. 1005–1014, 2006.

[408] Z. He, D. J. Leong, Z. Zhuo, R. J. Majeska, L. Cardoso, D. C. Spray, M. B. Goldring, N. J. Cobelli, and H. B. Sun, "Strain-induced mechanotransduction through primary cilia, extracellular ATP, purinergic calcium signaling, and ERK1/2 transactivates CITED2 and downregulates MMP-1 and MMP-13 gene expression in chondrocytes," *Osteoarthritis and Cartilage*, vol. 24, no. 5, pp. 892–901, 2016.

[409] P. S. Mathieu, J. C. Bodle, and E. G. Loboa, "Primary Cilium Mechanotransduction of Tensile Strain in 3D Culture: Finite Element Analyses of Strain Amplification Caused by 10% Tensile Strain Applied to a Primary Cilium Embedded in a Collagen Matrix," *J Biomech*, vol. 47, no. 9, pp. 2211–2217, 2014.

[410] A. K. T. Wann, N. Zuo, C. J. Haycraft, C. G. Jensen, C. A. Poole, S. R. McGlashan, and M. M. Knight, " Primary cilia mediate mechanotransduction through control of ATP-induced Ca 2+ signaling in compressed chondrocytes ," *The FASEB Journal*, vol. 26, no. 4, pp. 1663–1671, 2012.

[411] B. Shine, R. F. Mcknight, L. Leaver, and J. R. Geddes, "Long-term effects of lithium on renal, thyroid, and parathyroid function: A retrospective

analysis of laboratory data," *The Lancet*, vol. 386, no. 9992, pp. 461–468, 2015.

[412] K. Movig, R. Baumgarten, H. Leufkens, J. Van Laarhoven, and A. Egberts, "Risk factors for the development of lithium-induced polyuria," *British Journal of Phsychiatry2*, vol. 182, pp. 319–323, 2003.

[413] S. L. Carney, C. Ray, and A. H. Gillies, "Mechanism of lithium-induced polyuria in the rat," *Kidney International*, vol. 50, no. 2, pp. 377–383, 1996.

[414] M. A. Corrigan, T. M. Ferradaes, M. Riffault, and D. A. Hoey, "Ciliotherapy Treatments to Enhance Biochemically- and Biophysically-Induced Mesenchymal Stem Cell Osteogenesis: A Comparison Study," *Cellular and Molecular Bioengineering*, vol. 12, no. 1, pp. 53–67, 2019.

[415] F. A. Abo-Aziza and A. A. Zaki, "The impact of confluence on bone marrow mesenchymal stem (BMMSC) proliferation and osteogenic differentiation," *International Journal of Hematology-Oncology and Stem Cell Research*, vol. 11, no. 2, pp. 121–132, 2017.

[416] D. K. Breslow, E. F. Koslover, F. Seydel, A. J. Spakowitz, and M. V. Nachury, "An in vitro assay for entry into cilia reveals unique properties of the soluble diffusion barrier." *The Journal of cell biology*, vol. 203, no. 1, pp. 129–47, 2013.

[417] H. L. Kee, J. F. Dishinger, T. Lynne Blasius, C.-J. Liu, B. Margolis, and K. J. Verhey, "A size-exclusion permeability barrier and nucleoporins characterize a ciliary pore complex that regulates transport into cilia," *Nature Cell Biology*, vol. 14, no. 4, pp. 431–437, 2012.

[418] X. Jin, A. M. Mohieldin, B. S. Muntean, J. A. Green, J. V. Shah, K. Mykytyn, and S. M. Nauli, "Cilioplasm is a cellular compartment for calcium signaling in response to mechanical and chemical stimuli," *Cell Mol Life Sci*, vol. 71, no. 11, pp. 2165–78, 2014.

[419] B. S. Moore, A. N. Stepanchick, P. H. Tewson, C. M. Hartle, J. Zhang, A. M. Quinn, T. E. Hughes, and T. Mirshahi, "Cilia have high cAMP levels that are inhibited by Sonic Hedgehog-regulated calcium dynamics," *Proceedings of the National Academy of Sciences*, vol. 113, no. 46, pp. 13 069–13 074, 2016.

[420] D. U. Mick, R. B. Rodrigues, R. D. Leib, C. M. Adams, A. S. Chien, S. P. Gygi, and M. V. Nachury, "Proteomics of Primary Cilia by Proximity Labeling," *Developmental Cell*, vol. 35, no. 4, pp. 497–512, 2015.

[421] K. M. Reich, C. V. Gay, and J. A. Frangos, "Fluid shear stress as a mediator of osteoblast cyclic adenosine monophosphate production," *Journal of Cellular Physiology*, vol. 143, no. 1, pp. 100–104, 1990.

[422] A. Mørk, "Actions of Lithium on the Cyclic AMP Signalling System in Various Regions of the Brain - Possible Relations to its Psychotropic Actions -: A Study on the Adenylate Cyclase in Rat Cerebral Cortex, Corpus Striatum and Hippocampus," *Pharmacology & Toxicology*, vol. 73, no. 3 S, pp. 1–47, 1993.

[423] T. Dousa and O. Hechter, "Lithium and brain adenylyl cyclase," *The Lancet*, vol. 295, no. 7651, pp. 834–835, 1970.

[424] R. P. Ebstein, M. Hermoni, and R. H. Belmaker, "The effect of lithium on noradrenaline-induced cyclic AMP accumulation in rat brain: inhibition after chronic treatment and absence of supersensitivity." *Journal of Pharmacology and Experimental Therapeutics*, vol. 213, no. 1, pp. 161 LP – 167, apr 1980.

[425] E. D. Risby, J. K. Hsiao, H. K. Manji, J. Bitran, F. Moses, D. F. Zhou, and W. Z. Potter, "The Mechanisms of Action of Lithium: II. Effects on Adenylate Cyclase Activity and $\beta$-Adrenergic Receptor Binding in Normal Subjects," *Archives of General Psychiatry*, vol. 48, no. 6, pp. 513–524, jun 1991.

[426] L. Mann, E. Heldman, G. Shaltiel, R. H. Belmaker, and G. Agam, "Lithium preferentially inhibits adenylyl cyclase V and VII isoforms," *International Journal of Neuropsychopharmacology*, vol. 11, no. 4, pp. 533–539, 2008.

[427] S. F. Colin, H.-C. C. Chang, S. Mollner, T. Pfeuffer, R. R. Reed, R. S. Duman, E. J. Nestler, S. Mollnert, T. Pfeuffert, R. R. Reeds, R. S. Duman, and E. J. Nestler, "Chronic lithium regulates the expression of adenylate cyclase and Gi-protein a subunit in rat cerebral cortex," *Proceedings of the National Academy of Sciences of the United States of America*, vol. 88, no. 23, pp. 10 634–7, 1991.

[428] M. A. Corrigan, G. P. Johnson, E. Stavenschi, M. Riffault, M. N. Labour, and D. A. Hoey, "TRPV4-mediates oscillatory fluid shear mechanotrans-

duction in mesenchymal stem cells in part via the primary cilium," *Scientific Reports*, vol. 8, no. 1, pp. 1–13, 2018.

[429] M. L. Halls and D. M. F. Cooper, "Regulation by Ca2þ-Signaling Pathways of Adenylyl Cyclases," *Cold Spring Harb Perspect Biol*, vol. 3, no. a004143, pp. 1–22, 2011.

[430] B. Hu, H. Nakata, C. Gu, T. De Beer, and D. M. F. Cooper, "A critical interplay between Ca2+ inhibition and activation by Mg2+ of AC5 revealed by mutants and chimeric constructs," *Journal of Biological Chemistry*, vol. 277, no. 36, pp. 33 139–33 147, 2002.

[431] J. I. Bruce, S. V. Straub, and D. I. Yule, "Crosstalk between cAMP and CA2+ signaling in non-excitable cells," *Cell Calcium*, vol. 34, no. 6, pp. 431–444, 2003.

[432] R. Schmidt, O. Baumann, and B. Walz, "cAMP potentiates InsP3-induced Ca2+ release from the endoplasmic reticulum in blowfly salivary glands," *BMC Physiology*, vol. 8, no. 1, pp. 1–11, 2008.

[433] G. Hajnóczky, E. Gao, T. Nomura, J. B. Hoek, and A. P. Thomas, "Multiple mechanisms by which protein kinase A potentiates inositol 1,4,5-trisphosphate-induced Ca 2+ mobilization in permeabilized hepatocytes," *Biochemical Journal*, vol. 293, no. 2, pp. 413–422, 1993.

[434] E. Cairoli, C. Eller-Vainicher, F. M. Ulivieri, V. V. Zhukouskaya, S. Palmieri, V. Morelli, P. Beck-Peccoz, and I. Chiodini, "Factors associated with bisphosphonate treatment failure in postmenopausal women with primary osteoporosis," *Osteoporosis International*, vol. 25, no. 4, pp. 1401–1410, 2014.

[435] J. van der Valk and G. Gstraunthaler, "Fetal Bovine Serum (FBS) — A Pain in the Dish?" *Alternatives to Laboratory Animals*, vol. 45, no. 6, pp. 329–332, 2019.

[436] G. Gstraunthaler, T. Lindl, and J. van der Valk, "A plea to reduce or replace fetal bovine serum in cell culture media," *Cytotechnology*, vol. 65, no. 5, pp. 791–793, 2013.

[437] F. D. Allen, C. T. Hung, S. R. Pollack, and C. T. Brighton, "Serum modulates the intracellular calcium response of primary cultured bone cells to shear flow," *Journal of Biomechanics*, vol. 33, no. 12, pp. 1585–1591, 2000.

[438] Q. Bao, S. Chen, H. Qin, J. Feng, H. Liu, D. Liu, A. Li, Y. Shen, Y. Zhao, J. Li, and Z. Zong, "An appropriate Wnt/$\beta$-catenin expression level during the remodeling phase is required for improved bone fracture healing in mice," *Scientific Reports*, vol. 7, no. 1, pp. 1–11, 2017.

[439] T. E. Paterson, G. Gigliobianco, C. Sherborne, N. H. Green, J. M. Dugan, S. MacNeil, G. C. Reilly, and F. Claeyssens, "Porous microspheres support mesenchymal progenitor cell ingrowth and stimulate angiogenesis," *APL Bioengineering*, vol. 2, no. 2, p. 026103, 2018.

[440] W. Xu, Y. Ge, Z. Liu, and R. Gong, "Glycogen synthase kinase 3$\beta$ dictates podocyte motility and focal adhesion turnover by modulating paxillin activity implications for the protective effect of low-dose lithium in podocytopathy," *American Journal of Pathology*, vol. 184, no. 10, pp. 2742–2756, 2014.

[441] D. T. Rowson, J. C. Shelton, H. R. Screen, and M. M. Knight, "Mechanical loading induces primary cilia disassembly in tendon cells via TGF$\beta$ and HDAC6," *Scientific Reports*, vol. 8, no. 1, pp. 1–12, 2018.

[442] D. Jing, A. D. Baik, X. L. Lu, B. Zhou, X. Lai, L. Wang, E. Luo, and X. E. Guo, "In situ intracellular calcium oscillations in osteocytes in intact mouse long bones under dynamic mechanical loading," *FASEB Journal*, vol. 28, no. 4, pp. 1582–1592, 2014.

[443] M. M. Maneshi, F. Sachs, and S. Z. Hua, "Heterogeneous Cytoskeletal Force Distribution Delineates the Onset Ca2+ Influx Under Fluid Shear Stress in Astrocytes," *Frontiers in Cellular Neuroscience*, vol. 12, no. March, pp. 1–9, 2018.

[444] F. Wei, X. Shi, J. Chen, and L. Zhou, "Fluid shear stress-induced cytosolic calcium signalling and degranulation dynamics in mast cells," *Cell Biology International Reports*, vol. 19, no. 2, pp. 45–51, 2012.

[445] M. M. Maneshi, F. Sachs, and S. Z. Hua, "A Threshold Shear Force for Calcium Influx in an Astrocyte Model of Traumatic Brain Injury," *Journal of Neurotrauma*, vol. 32, no. 13, pp. 1020–1029, 2014.

[446] X. Ma, R. Peterson, and J. Turnbull, "Adenylyl Cyclase type 3, a marker of primary cilia, is reduced in primary cell culture and in lumbar spinal cord in situ in G93A SOD1 mice," *BMC Neuroscience*, vol. 12, no. 1, p. 71, 2011.

# Appendix

## 9.1 Figure permissions

Figure 2.2[33] is licensed under CC BY 4.0. Figure 2.1 permissions were granted via RightsLink (Figure 9.1). Figure 2.4 permissions were confirmed in writing by Dr. James Weaver (Figure 9.2).

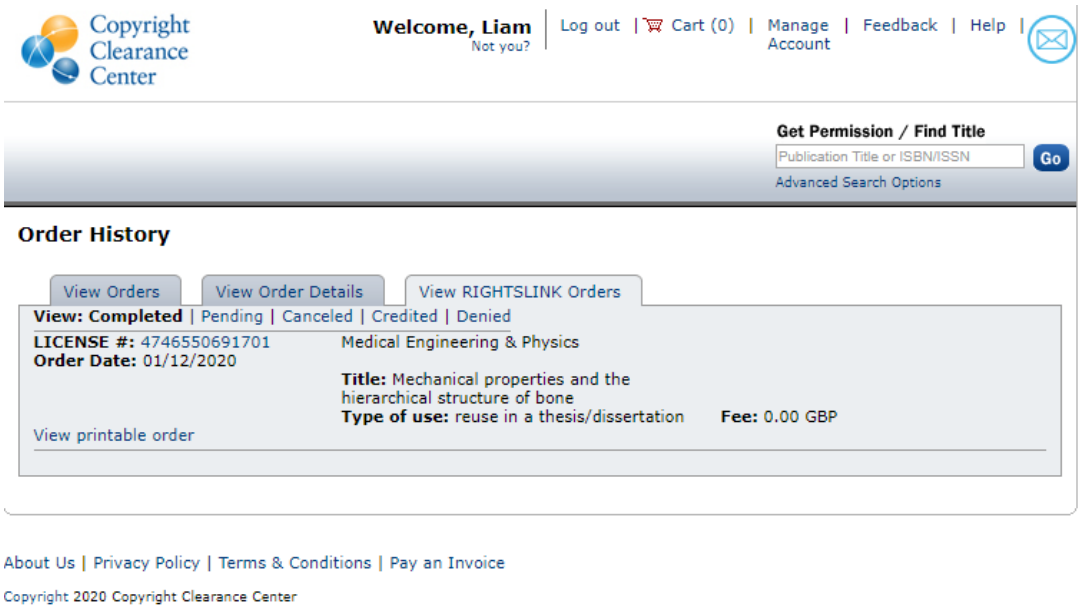


**Figure 9.1:** Reprint permissions.

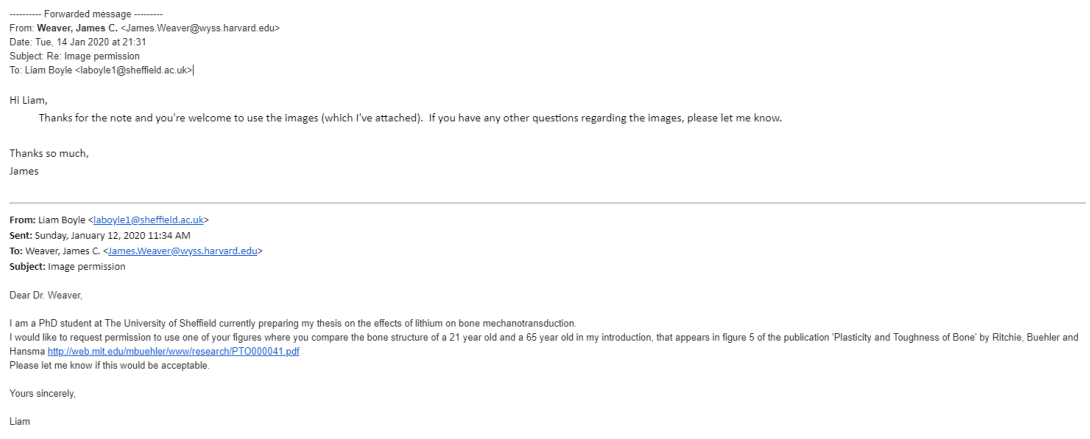

--------- Forwarded message ---------
From: **Weaver, James C.** <James.Weaver@wyss.harvard.edu>
Date: Tue, 14 Jan 2020 at 21:31
Subject: Re: Image permission
To: Liam Boyle <laboyle1@sheffield.ac.uk>

Hi Liam,

Thanks for the note and you're welcome to use the images (which I've attached). If you have any other questions regarding the images, please let me know.

Thanks so much,
James

---

**From:** Liam Boyle <laboyle1@sheffield.ac.uk>
**Sent:** Sunday, January 12, 2020 11:34 AM
**To:** Weaver, James C. <James.Weaver@wyss.harvard.edu>
**Subject:** Image permission

Dear Dr. Weaver,

I am a PhD student at The University of Sheffield currently preparing my thesis on the effects of lithium on bone mechanotransduction.
I would like to request permission to use one of your figures where you compare the bone structure of a 21 year old and a 65 year old in my introduction, that appears in figure 5 of the publication 'Plasticity and Toughness of Bone' by Ritchie, Buehler and Hansma http://web.mit.edu/mbuehler/www/research/PTO000041.pdf
Please let me know if this would be acceptable.

Yours sincerely,

Liam

**Figure 9.2:** Reprint permissions.